



UNIVERSIDADE ESTADUAL DE CAMPINAS  
INSTITUTO DE BIOLOGIA

LEONARDO LUIS ARTICO

MECHANISTIC INSIGHTS INTO IGFBP7-MEDIATED  
IGF1R ACTIVATION AND GLYCOLYTIC METABOLISM IN  
ACUTE LYMPHOBLASTIC LEUKEMIA

INSIGHTS MECANÍSTICOS SOBRE A ATIVAÇÃO DE  
IGF1R MEDIADA POR IGFBP7 E O METABOLISMO  
GLICOLÍTICO NA LEUCEMIA LINFOIDE AGUDA

CAMPINAS

2023

**LEONARDO LUIS ARTICO**

**MECHANISTIC INSIGHTS INTO IGFBP7-MEDIATED IGF1R  
ACTIVATION AND GLYCOLYTIC METABOLISM IN ACUTE  
LYMPHOBLASTIC LEUKEMIA**

**INSIGHTS MECANÍSTICOS SOBRE A ATIVAÇÃO DE IGF1R  
MEDIADA POR IGFBP7 E O METABOLISMO GLICOLÍTICO NA  
LEUCEMIA LINFOIDE AGUDA**

*Thesis presented to the Institute of  
Biology of the University of  
Campinas in partial fulfillment of the  
requirements for the degree of  
Doctor in Genetics and Molecular  
Biology, in the concentration area of  
Animal Genetics and Evolution.*

*Tese apresentada ao Instituto de  
Biologia da Universidade Estadual  
de Campinas como parte dos  
requisitos exigidos para a obtenção  
do Título de Doutor em Genética e  
Biologia Molecular, na área de  
Genética Animal e Evolução.*

*Orientador: DR. JOSÉ ANDRÉS YUNES*

ESTE ARQUIVO DIGITAL CORRESPONDE À  
VERSÃO FINAL DA TESE DEFENDIDA PELO  
ALUNO LEONARDO LUÍS ARTICO E  
ORIENTADA PELO DR. JOSÉ ANDRÉS YUNES.

**CAMPINAS**

**2023**



Ficha catalográfica  
Universidade Estadual de Campinas  
Biblioteca do Instituto de Biologia  
Mara Janaina de Oliveira - CRB 8/6972

Ar78m Artico, Leonardo Luis, 1994-  
Mechanistic insights into IGFBP7-mediated IGF1R activation and glycolytic metabolism in acute lymphoblastic leukemia / Leonardo Luis Artico. –  
Campinas, SP : [s.n.], 2023.

Orientador: José Andrés Yunes.  
Tese (doutorado) – Universidade Estadual de Campinas, Instituto de  
Biologia.

1. Gene IGFBP7. 2. Receptor IGF tipo 1. 3. Leucemia linfóide aguda. I.  
Yunes, José Andrés, 1967-. II. Universidade Estadual de Campinas. Instituto  
de Biologia. III. Título.

Informações Complementares

**Título em outro idioma:** *Insights* mecanísticos sobre a ativação de IGF1R mediada por IGFBP7 e o metabolismo glicolítico na leucemia linfóide aguda

**Palavras-chave em inglês:**

IGFBP7 gene

Receptor, IGF type 1

Acute lymphoblastic leukemia

**Área de concentração:** Genética Animal e Evolução

**Titulação:** Doutor em Genética e Biologia Molecular

**Banca examinadora:**

José Andrés Yunes [Orientador]

Carmen Veríssima Ferreira Halder

Céline Marques Pinheiro

Fabio Papes

Giselle Zenker Justo

**Data de defesa:** 18-08-2023

**Programa de Pós-Graduação:** Genética e Biologia Molecular

Identificação e informações acadêmicas do(a) aluno(a)

- ORCID do autor: <https://orcid.org/0000-0003-4691-2446>

- Currículo Lattes do autor: <http://lattes.cnpq.br/6658800337204378>

Campinas, 18 de agosto de 2023

### **COMISSÃO EXAMINADORA**

Prof. Dra Carmen Veríssima Ferreira Halder

Prof. Dra Céline Marques Pinheiro

Prof. Dr Fabio Papes

Prof. Dra Giselle Zenker Justo

Prof. Dr José Andrés Yunes

*Os membros da Comissão Examinadora acima assinaram a Ata de defesa, que se encontra no processo de vida acadêmica do aluno.*

A Ata da defesa com as respectivas assinaturas dos membros encontra-se no SIGA/Sistema de Fluxo de Dissertação/Tese e na Secretaria do Programa de Pós-graduação em Genética e Biologia Molecular do Instituto de Biologia.

## DEDICATION

*I offer this work as a heartfelt dedication to the patients of Boldrini Hospital. It is my sincere aspiration that the knowledge outlined in this Thesis may contribute, in some measure, to enhancing their quality of life and providing comfort and hope to their families.*

## **ACKNOWLEDGMENTS**

I would like to thank my family: my parents, Luizete Casali Artico and Enio Luiz Artico, for being my source of inspiration and support up to the present moment; my sister Maila Artico for being my greatest example of resilience and humility and my brother Eduardo Artico, for making me proud with his daily achievements.

I thank the family we have chosen throughout our lives, Cássio Roberto de Almeida, Natacha Azussa Migita and Jacinta Lupschinski.

Thank you to my research parents Dr. Ana Cristina Mazzocato and Dr. Juliano Lino Ferreira. Thanks to you, today I can carry out ethical and quality research. You are, without a doubt, my inspirational sources.

I am grateful to my current advisor, Dr. José Andrés Yunes, for believing in me, for the lessons learned and for the professional and personal development.

I would also like to thank Dr Ana Paula Arruda and Dr Gunes Parlakgul for all their support during my stay at the University of California, Berkeley and to all members of the ARRUDA Lab.

I would like to thank all my friends at the Boldrini Research Center who were so important to me and to my work. I would also like to thank all other colleagues at Hospital Boldrini who directly or indirectly contributed to this work. I would also like to thank Dr. Silvia Brandalise, Chancellor of Boldrini Hospital, for consenting to carry out this study and for providing me with such a learning opportunity.

Finally, I would like to thank Fundação de Amparo à Pesquisa do Estado de São Paulo (FAPESP) which provided funding for this project (process 2019/04943-3 and 2022/04464-0) through an agreement with Coordenação de Aperfeiçoamento de Pessoal de Nível Superior (CAPES).

This study was financed in part by the Coordenação de Aperfeiçoamento de Pessoal de Nível Superior - Brasil (CAPES) - Finance Code 001.

## RESUMO

A Leucemia Linfóide Aguda (LLA) é a principal neoplasia que acomete crianças e adolescentes. Embora as taxas de cura atingiram 90% na última década, 20 a 30% dos pacientes ainda apresentam recaída da doença e alguns apresentarão sequelas ao longo prazo, incluindo uma segunda malignidade. Logo, a descoberta de novos alvos e estratégias terapêuticas são ainda necessárias. Insulina e os fatores de crescimento semelhantes à insulina (IGFs) são fatores mitogênicos e de pró-sobrevivência para muitos tipos celulares, incluindo LLA. IGFs circulantes são ligados por *IGF Binding Proteins* (IGFBPs) que regulam sua ação. IGFBP7 é uma proteína relacionada ao IGFBP (IGFBP-rP) que, em contraste com outros IGFBPs/IGFBP-rPs, apresenta alta afinidade pela insulina comparada aos IGFs e demonstrou ligar-se também ao receptor de IGF1 (IGF1R). O papel do *IGFBP7* no câncer é controverso: em alguns tumores ele foi relatado como um oncogene, enquanto em outros como um supressor de tumor. Na LLA infantil, alta expressão de *IGFBP7* foi associada a um pior prognóstico. Aqui, primeiramente mostramos que IGFBP7 exerce efeitos mitogênicos autócrinos na LLA, que foram dependentes de insulina/IGF. O *knockdown* de IGFBP7 ou a neutralização mediada por anticorpo resultou em atenuação significativa da viabilidade celular da LLA *in vitro* e na progressão da leucemia *in vivo*. Ainda, mostramos que IGFBP7 prolonga a retenção de IGF1R na superfície das células sob estimulação com insulina/IGF1, resultando na fosforilação sustentada de IGF1R, IRS, AKT e ERK1/2. Em segundo lugar, comprovamos que a ativação sustentada do eixo IGF1R-PI3K-Akt, mediada por IGFBP7, coincide com a regulação positiva de GLUT1, melhorando o metabolismo glicolítico da LLA. A neutralização de IGFBP7 com um anticorpo monoclonal (clone C311) ou a inibição farmacológica da via PI3K-Akt demonstraram anular esse efeito, restaurando os níveis fisiológicos de GLUT1 na superfície celular. Em conclusão, destacamos que IGFBP7 desempenha um papel oncogênico na LLA, promovendo a permanência do IGF1R na superfície celular, prolongando a estimulação da insulina/IGFs e aumentando o metabolismo glicolítico através do eixo IGF1R-Akt-GLUT1. Os efeitos celulares e metabólicos descritos aqui revelam um papel até então desconhecido para IGFBP7 na LLA, abrindo portas para investigações futuras.

## ABSTRACT

Acute Lymphoblastic Leukemia (ALL) is the most common childhood cancer. Although survival rates for pediatric ALL have reached around 90% in the last decade, still approximately 20 to 30% of patient's relapse, and some experiencing long-term sequelae of therapy including a second malignancy. Therefore, new targets and therapeutic strategies are needed. Insulin and insulin-like growth factors (IGFs) are mitogenic and pro-survival factors for many different cell types, including ALL. Circulating IGFs are bound by IGF Binding Proteins (IGFBP) that regulate their action. IGFBP7 is an IGFBP-related protein (IGFBP-rP) that in contrast to other IGFBPs/IGFBP-rPs features higher affinity for insulin than IGFs and has been shown to bind the IGF1 receptor (IGF1R). The role of IGFBP7 in cancer is controversial: in some tumors it was related to oncogene while in others as a tumor suppressor. In childhood ALL, higher IGFBP7 expression levels were associated with worse prognosis. Here we first show that IGFBP7 exerts mitogenic and pro-survival autocrine effects on ALL, which is dependent on insulin/IGF. IGFBP7 knockdown or antibody-mediated neutralization resulted in significant attenuation of ALL cell viability *in vitro* and leukemia progression *in vivo*. Our data reveals that IGFBP7 prolongs the surface retention of the IGF1R under insulin/IGF1 stimulation, resulting in sustained phosphorylation of IGF1R, IRS, AKT, and ERK1/2. Second, we also show that sustained activation of the IGF1R-PI3K-Akt axis, mediated by IGFBP7, concurs to GLUT1 upregulation, which enhance energy metabolism and increases glycolytic metabolism in B-cell precursor ALL (BCP-ALL). Both IGFBP7 neutralization with a monoclonal antibody (clone C311) as well as pharmacological inhibition of PI3K-Akt pathway abrogates this effect, restoring the physiological levels of GLUT1 on the cell surface. In conclusion, IGFBP7 plays an oncogenic role in ALL by promoting the perdurance of IGF1R at the cell surface, prolonging insulin/IGFs stimulation and enhancing glycolytic metabolism through the IGF1R-Akt-GLUT1 axis. The cellular and metabolic effects described here may offer an additional mechanistic explanation for the strong negative impact seen in ALL cells *in vitro* and *in vivo* after the knockdown or antibody neutralization of IGFBP7, revealing a hitherto unknown role for IGFBP7 in ALL, and opening doors for future investigations.

## LIST OF FIGURES

<b>Figure 1.</b> Hallmarks of Cancer: New Dimensions	13
<b>Figure 2.</b> Estimated frequency of specific genotypes in ALL	15
<b>Figure 3.</b> BM microenvironment and HSC niches	17
<b>Figure 4.</b> Simplified diagram of insulin, IGF1 and IGF2 signaling pathways and their receptors	22
<b>Figure 5.</b> Expression of the different exons of the <i>INSR</i> gene in 93 samples of pediatric ALL	23
<b>Figure 6.</b> Amino acid sequence alignment of the N-terminal domains from human IGFBP1 to 6 and human IGFBP-rP1 to 10	26
<b>Figure 7.</b> PI3K-Akt signaling pathway	29

## TABLE OF CONTENTS

<b>1. INTRODUCTION</b> .....	12
1.1 Cancer: a global health challenge and its hallmarks.....	12
1.2 Pediatric ALL: classification and molecular mechanisms.....	15
1.3 Understanding the bone marrow microenvironment and leukemogenic process.....	18
1.4 The intersection of insulin and IGFs signaling pathways in cancer biology.....	21
1.5 IGF binding proteins.....	25
1.6 PI3K-Akt pathway and glycolytic metabolism.....	28
<b>2. JUSTIFICATION</b> .....	33
<b>3. OBJECTIVES</b> .....	34
3.1 General aim.....	34
3.2 Specific aims.....	34
<b>4. CHAPTER I – MANUSCRIPT “Physiologic IGFBP7 levels prolong IGF1R activation in Acute Lymphoblastic Leukemia”</b> .....	35
<b>5. SUPPLEMENTARY MATERIAL</b> .....	49
5.1 Supplementary figures.....	49
5.2 Supplementary tables.....	66
5.3 Supplementary references.....	69
<b>6. CHAPTER II – MANUSCRIPT “IGFBP7 fuels the glycolytic metabolism in B-cell Precursor Acute Lymphoblastic Leukemia by sustaining activation of the IGF1R-Akt-GLUT1 axis”</b> .....	70
<b>7. SUPPLEMENTARY MATERIAL</b> .....	84
7.1 Supplementary figures.....	84
7.2 Supplementary table.....	90
<b>8. GENERAL DISCUSSION</b> .....	91
<b>9. CONCLUSIONS</b> .....	95
<b>10. FINAL CONSIDERATIONS AND FUTURE DIRECTIONS</b> .....	96



<b>11. REFERENCES.....</b>	<b>98</b>
<b>12. ATTACHAMENTS .....</b>	<b>116</b>
<b>12.1</b> Activities Report BEPE – FAPESP 2019/4943-3).....	116
<b>12.2</b> List of publications (during PhD fellowship).....	141
<b>12.3</b> Ethics committee approval 1.....	143
<b>12.4</b> Ethics committee approval 2.....	145
<b>12.5</b> Animal ethics committee approval 1.....	148
<b>12.6</b> Animal ethics committee approval 2.....	149
<b>12.7</b> Authorization to reproduce chapter 1.....	150
<b>12.8</b> Authorization to reproduce chapter 2.....	158
<b>12.9</b> Copyright statement.....	159

## 1. INTRODUCTION

### 1.1 Cancer: a global health challenge and its hallmarks

Cancer is a broad term used to describe a multitude of diseases that result from abnormal and uncontrolled cell growth, mainly caused by genetic and epigenetic alterations. These changes lead to unique genetic profiles and morphological characteristics that vary among cancers, making universal clinical treatments difficult.<sup>1,2</sup> According to the World Health Organization, cancer is the second most common cause of death in the world, responsible for almost 10 million deaths in 2020<sup>3</sup> with about 70% of these deaths occurring in underdeveloped countries.<sup>4</sup>

During normal growth and development, cells undergo tightly regulated processes such as proliferation, differentiation, and apoptosis, which are controlled by complex signaling pathways. However, cancer cells have altered signaling pathways that allow them to bypass these regulatory mechanisms, leading to uncontrolled growth and progression.<sup>5,6</sup> Neoplastic transformation is directly related to lesions or genetic modifications that drive malignant cellular development. This complex process involves a set of characteristics that can be described as “*Hallmarks of Cancer*”.<sup>7</sup>

The Hallmarks of Cancer are a set of functional capabilities that human cells acquire as they transition from normal to malignant states. These capabilities were first defined over 20 years ago by Hanahan and Weinberg and are constantly being updated due to the advent of advanced genomic technologies.<sup>7-9</sup> The current set of Hallmarks of Cancer comprises 14 different sessions described below and shown in Figure 1.

- *Resisting cell death*: Cancer cells evade apoptosis or programmed cell death, which allows them to survive and accumulate genetic abnormalities.
- *Sustaining proliferative signaling*: Cancer cells acquire the ability to proliferate uncontrollably by activating oncogenes and inhibiting tumor suppressor genes.
- *Evading growth suppressors*: Cancer cells can evade the inhibitory signals from surrounding normal cells and escape growth control mechanisms.

- *Inducing angiogenesis*: Cancer cells secrete factors that promote the growth of new blood vessels, which supply the tumor with nutrients and oxygen.
- *Enabling replicative immortality*: Cancer cells maintain their telomeres, which are protective caps at the end of chromosomes, allowing them to divide indefinitely.
- *Activating invasion and metastasis*: Cancer cells acquire the ability to migrate and invade surrounding tissues, allowing them to spread to distant sites and form secondary tumors.
- *Reprogramming cellular metabolism*: Cancer cells alter their metabolism to support their growth and proliferation, even in conditions of nutrient deprivation.
- *Avoiding immune destruction*: Cancer cells can evade immune surveillance and attack by the immune system, allowing them to proliferate unchecked.
- *Genome instability and mutation*: Cancer cells accumulate genetic alterations that drive tumor progression and evolution.
- *Tumor-promoting inflammation*: Cancer cells can promote inflammation, which can contribute to tumor growth and progression.
- *Unlocking phenotypic plasticity*: Cancer cells can switch between different cell types or states, allowing them to adapt to changing environments and therapies.
- *Nonmutational epigenetic reprogramming*: Cancer cells can alter the expression of genes without changing their underlying DNA sequence, allowing them to regulate their behavior and promote tumor growth.
- *Polymorphic microbiomes*: The diverse communities of microorganisms in the tumor microenvironment can affect tumor growth and response to therapy.
- *Senescent cells*: Senescent cells accumulate in aging tissues and can promote inflammation and other cellular changes that contribute to cancer development.

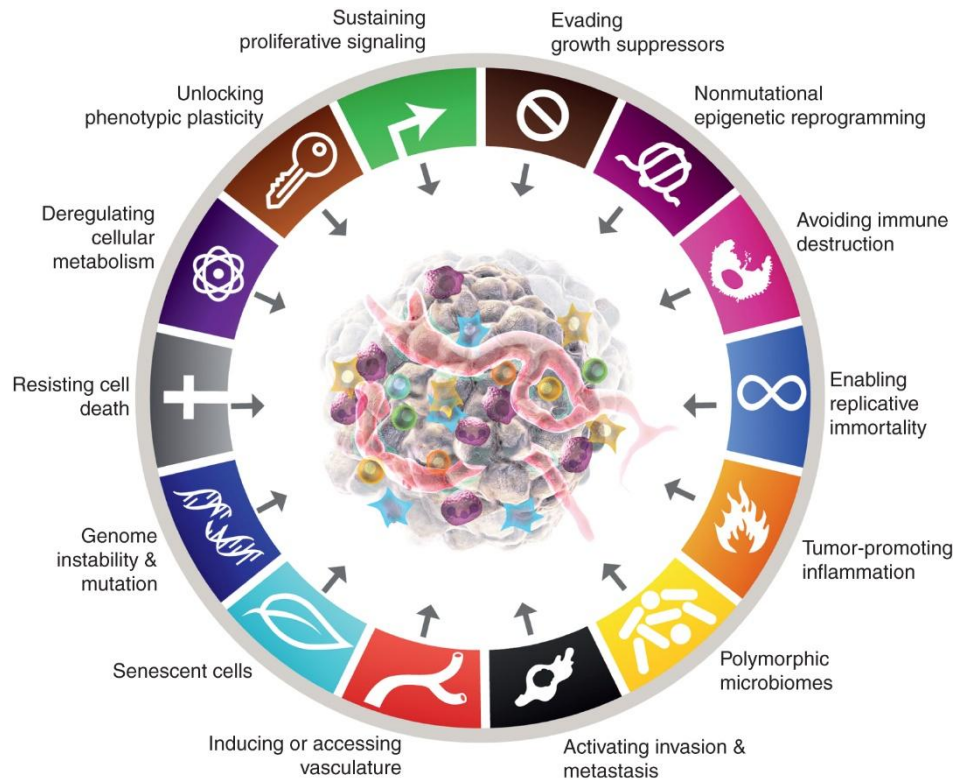


**Figure 1.** Hallmarks of Cancer: New Dimensions. The latest publication summarizing the Hallmarks of Cancer by Hanahan.<sup>9</sup>

The field of cancer biology has greatly contributed to the understanding of the genetics, specificities and variability of the disease. The development of precision medicine, which combines knowledge from basic sciences and clinical research with advances in diagnostic techniques, has led to a significant improvement in the diagnosis, treatment, management, prevention, survival and life quality of cancer patients. Childhood cancer, however, has distinct characteristics and differences when compared to adult cancers.

Pediatric cancer primarily affects undifferentiated embryonic cells, whereas in adult cancers differentiated cells are mostly affected. Leukemias, central nervous system tumors, lymphomas, neuroblastoma, sarcomas and Wilms' tumor are some of the most common pediatric cancers. Most childhood cancers have fewer genetic alterations when compared to adult cancers, and often do not benefit from target-specific drugs that have already been developed and approved for adult cancers. This presents a crucial need for the development of new therapies and treatment protocols that are less toxic and cause fewer adverse effects in children. Furthermore, the genetic heterogeneity of pediatric tumors presents another challenge in the

development of target-specific therapies. Genetic alterations that drive the growth of pediatric tumors include copy number alterations (CNAs), gene fusions, complex DNA rearrangements and chromosomal alterations.<sup>10,11</sup> A number of molecular studies and initiatives are underway with the objective of unraveling the genetic peculiarities and providing other treatment options for children.<sup>12-15</sup> In Brazil, childhood cancer is already the leading cause of death (8% of the total) among children and adolescents aged 1 to 19 years. According to data from the National Cancer Institute (INCA), it is estimated that more than 12,500 new cases of childhood cancer will be diagnosed in Brazil in 2022. Childhood cancer accounts for about 3% of all cancers in the country, and the most prevalent pediatric cancers in Brazil are leukemias, brain tumors, and lymphomas.<sup>16</sup>

Pediatric Acute Lymphoid Leukemia (ALL) is the most common type of childhood cancer worldwide.<sup>17</sup> In Brazil, pediatric ALL also represents the most frequent type of childhood cancer, comprising about 30% of all cases. According to the Brazilian National Cancer Register, between 2014 and 2018, 11,252 new cases of childhood ALL were diagnosed in Brazil, with an estimated incidence rate of 51.6 cases per million children per year. The survival rate for pediatric ALL in Brazil has improved in recent years with a five-year survival rate of around 80%, although the mortality rate remains significant, with an estimated 1,326 deaths due to childhood ALL in Brazil between 2014 and 2018.<sup>16</sup>

Therefore, the pursuit of novel target-specific therapeutics and the establishment of treatment regimens that exhibit reduced toxicity and minimal adverse effects in pediatric ALL still represent a foremost predicament in this field of research.

## **1.2 Pediatric ALL: classification and molecular mechanisms**

As described earlier, pediatric ALL is the most frequent hematological malignancy affecting children (<15 years old), accounting for 80% of all leukemias and 25% of cancer cases within this age group. ALL can be classified into two phenotypes based on the affected cell lineage: T-cell ALL, where the affected cells originate from T lymphocytes (15% of cases), and B-cell precursor ALL (BCP-ALL), which represents most cases (approximately 85%). Both phenotypes can be further subdivided based on chromosomal abnormalities, including aneuploidies and chromosomal translocations. Distinguishing and understanding these characteristics is essential for appropriate treatment and risk stratification of patients, as the prognosis varies

significantly among ALL subtypes (Figure 2). Prognosis can additionally be correlated to patient specific clinical and biological features, such as age, leukocyte count at diagnosis, and response to initial treatment.<sup>18-22</sup>

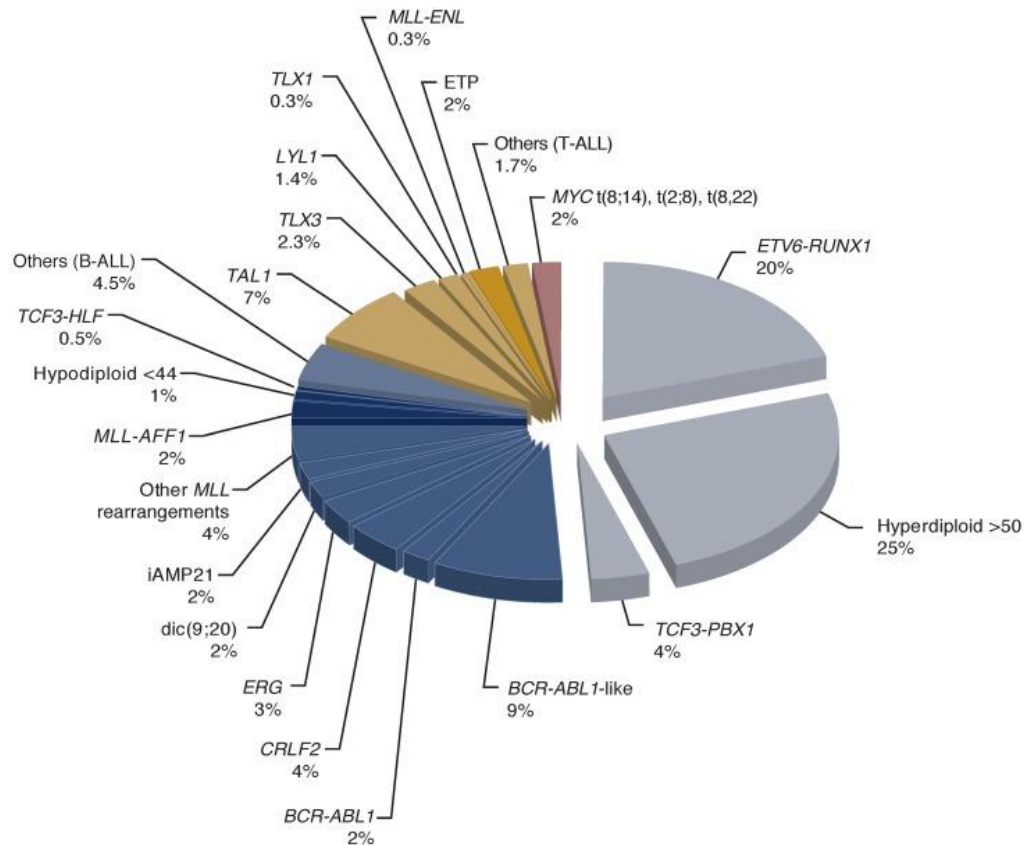


**Figure 2.** Estimated frequency of specific genotypes in ALL. The genetic lesions that are exclusively seen in cases of T-cell ALL are indicated in gold and those commonly associated with BCP-ALL in blue. The darker gold or blue color indicates those subtypes generally associated with poor prognosis. Adapted from Piu et al.<sup>18</sup>

Despite significant progress in the treatment of ALL, which has led to an 80% cure rate with combined drug therapy,<sup>23,24</sup> approximately 20% of patients still have leukemic cells resistant to chemotherapy, resulting in disease recurrence.<sup>24,25</sup> However, in the last two decades, advances have been made in understanding the molecular pathophysiology of ALL. For example, the identification and characterization of chromosomal translocations have revealed critical genes involved in the maintenance of this disease. Moreover, the occurrence of specific chromosomal translocations also plays a critical role in stratifying patients for more or less intensive therapies.<sup>26</sup>

In addition to chromosomal translocations, there are other molecular mechanisms that contribute to the development of pediatric ALL and disease maintenance. This includes the inhibition of tumor suppressor genes, upregulation of proto-oncogenes, ALL cells interactions with the tumor microenvironment, and autocrine interactions between leukemic cells.<sup>24,27</sup> Several studies suggest that ALL blasts' interaction with bone marrow stromal cells (BMSCs) enhances leukemic cell survival and chemotherapy resistance.<sup>28-32</sup> Interestingly, leukemic blasts can also function in an autocrine manner by secreting growth factors that enhance survival chances of the producer cells. Autocrine signaling is a cellular mechanism whereby a cell secretes signaling molecules that targets itself or cells of the same type.<sup>33</sup> In the context of tumor biology in ALL, autocrine signaling can have a pivotal role in leukemia cell growth and survival.<sup>34-37</sup>

The secretion of signaling molecules for ALL cells triggers the activation of multiple intracellular signaling pathways, predominantly including the Ras-MAPK pathway<sup>38</sup> the PI3K-Akt pathway<sup>39</sup> and the JAK-STAT pathway.<sup>40</sup> Cytokines and growth factors are the most important classes of signaling molecules secreted by leukemic cells that act through an autocrine mechanism, binding to specific receptors on the cells surface for self-advantageous purposes. Interleukin-3 (IL-3), interleukin-7 (IL-7) and insulin-like growth factors (IGFs) are prime examples of these molecules.<sup>41</sup> Although it is noteworthy to mention that the secretion or production of cytokines and growth factors are not exclusive to ALL cells. It has been previously elucidated that other cells, including BMSCs, can also secrete signaling molecules and gain benefits from leukemia cells via a paracrine mechanism.<sup>30,42,43</sup>

Overall, these signaling cascades facilitated by paracrine or autocrine mechanisms are crucial in triggering, promoting, and maintaining the leukemogenic process, which originates in the bone marrow microenvironment by leukemia-initiating cells (LICs).<sup>44</sup> Comprehending the autocrine and paracrine processes, discerning and characterizing signaling molecules, and interpreting the function of the ALL tumor microenvironment are essential steps in gaining a better understanding of the disease and developing more efficacious treatments.

### **1.3 Understanding the bone marrow microenvironment and leukemogenic process**

The bone marrow (BM) is a complex, vascularized, and innervated organ located within the bone. It hosts various hematopoietic and non-hematopoietic cell types, including osteoblasts, osteoclasts, adipocytes, reticular cells, endothelial cells, smooth muscle cells, mesenchymal stromal cells (MSCs), and cells of the sympathetic nervous system. These cells not only physically surround hematopoietic cells but also actively regulate hematopoietic processes through the secretion of cytokines, hormones, and growth factors, as well as the expression of receptors and adhesion molecules. The extracellular matrix, which comprises more than 200 proteins, is another critical factor in the BM microenvironment. Continuously secreted by the different cells, extracellular matrix proteins provide anchorage and regulate BM cellular functions.<sup>41</sup>

Furthermore, the BM microenvironment regulates the properties of healthy hematopoietic stem cells (HSCs) localized in specific niches. The fundamental understanding of the HSC niche was initially proposed in 1978 by Schofield, defining the microenvironment surrounding the HSCs.<sup>45</sup> The HSC niche provides critical signaling cues, growth factors, and extracellular matrix components that regulate HSC self-renewal and differentiation, allowing them to maintain their undifferentiated state. Since then, extensive research has been conducted to determine the anatomical location of the HSC niche. Until today, three distinct HSC niches have been widely described: endosteal, arteriolar, and sinusoidal (Figure 3).<sup>41,44,46,47</sup>

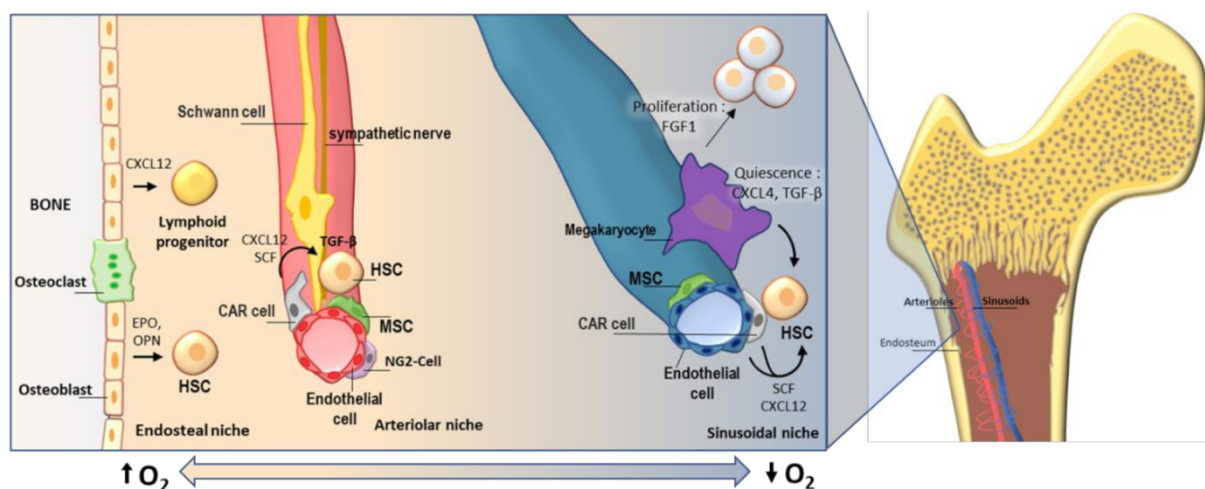


**Figure 3.** BM microenvironment and HSC niches. Graphical overview of the bone marrow components and cellular interactions taking place in the HSC niches: endosteal, arteriolar, and sinusoidal. SCF: stem cell factor. FGF1: fibroblast growth factor 1. OPN: osteopontin. EPO: erythropoietin. Image adapted from Congrains et al.<sup>47</sup>



The inner surface of the bone, called the endosteum, is lined by a thin cellular layer of osteoblasts and osteoclasts. The endosteal “osteoblastic” niche was the first putative HSC niche;<sup>48</sup> however, recent evidence has disputed the common assumption of HSCs’ direct contact with osteoblasts.<sup>49,50</sup> The endosteum is an important lymphopoietic site, and osteoblast secretion of CXCL12 (C-X-C motif chemokine ligand 12) is crucial for lymphoid differentiation. While CXCL12 expressed by osteoblasts seems to be responsible for early lymphoid progenitor maintenance, CXCL12 expressed by endothelial and stromal cells influences the maintenance of HSCs.<sup>55</sup> Osteoblasts are known to regulate HSC proliferation and erythroid differentiation by osteopontin<sup>52</sup> and erythropoietin<sup>53</sup> production. However, evidence shows that less than 20% of HSCs are in direct contact to the endosteum<sup>49</sup> and most recent studies suggest that the niche of HSCs is primarily perivascular, remarkably around the arterioles and sinusoids.<sup>50,51,54,56</sup>

Arterioles, which are close to the endosteum<sup>50</sup> are important HSC sites and are essential for HSC quiescence and maintenance.<sup>50,56</sup> The arteriole niche harbors several populations of stromal cells (particularly important, CXCL12-abundant reticular (CAR) perivascular stromal cells and neural–glial antigen 2 (NG2) periaarteriolar cells), endothelial cells, sympathetic nervous system (SNS) nerves and non-myelinating Schwann cells. They all contribute with chemical signals to HSC homeostasis. CAR cells are the main sources of CXCL12, where they localize to surrounding endothelial cells in the sinusoids and arterioles and are in direct contact to HSCs.<sup>57</sup> Schwann cells together with sympathetic nerves in the arteriole induce quiescence of HSCs through growth factor beta (TGF- $\beta$ ) activation and direct contact with a considerable number of HSCs.<sup>58</sup> In line with these findings, NG2+ stromal cells in the arteriole niche have been associated with lymphoid biased HSCs and megakaryocytes in the sinusoids have been linked to myeloid-biased HSCs.<sup>59</sup>

The sinusoidal niche, located near sinusoidal vessels, also plays a role in regulating HSC proliferation and differentiation through the secretion of cytokines and chemokines. Sinusoidal vessels promote HSC activation and serve as the location for the trafficking of leukocytes in and out of the BM. Megakaryocytes in the sinusoidal niche have been shown to regulate HSC quiescence through C-X-C motif ligand 4 (CXCL4), TGF- $\beta$  and expansion under stress through fibroblast growth factor 1 (FGF1). Arterial blood vessel endothelial cells maintain HSCs in a low reactive oxygen species

(ROS) state, promoting HSC quiescence and protecting them against genotoxic insults.<sup>60,61</sup>

Based on all of the described mechanisms above that are directly related to maintaining homeostasis in the BM microenvironment, we can postulate the following questions: What effects are caused by disruptions in the BM microenvironment? What are the impacts of these genetic and functional disturbances, and how do they contribute to a leukemogenic scenario?

It is known that the maintenance of HSCs in quiescence is crucial for their self-renewal and differentiation capacity, but also to prevent the accumulation of mutations that can lead to the development of hematologic malignancies, such as ALL. A key hallmark of ALL is the abnormal proliferation and accumulation of hematopoietic progenitor cells in the BM.<sup>41,47</sup> However, it is now known that the initiation of the leukemogenic process is mediated by leukemia-initiating cells (LIC).<sup>62</sup> LIC are a subpopulation of cells with stem-like properties that can initiate and sustain leukemia. In ALL, for example, these stem-like cell subsets have been described to have the ability of (i) propagating the tumor after transplantation into secondary mice, (ii) recreating the immunophenotypic heterogeneity of primary leukemia, and (iii) maintaining their self-renewing activity after serial transplantation.<sup>63,64</sup>

The molecular mechanisms that induce LIC outgrowth in the BM are not fully understood, but several factors have been implicated. One possible mechanism is the aberrant activation of signaling pathways that regulate HSC self-renewal and differentiation. For example, mutations in genes such as *NOTCH1*, *IKZF1*, and *PTEN* may impact LIC development and are known to affect signaling pathways involved in HSC homeostasis.<sup>62</sup>

Additionally, BM microenvironment also plays a critical role in LIC outgrowth. We know that BMSCs provide growth factors and cytokines to support normal hematopoiesis, but in the presence of LIC, they can provide a supportive niche for LIC to proliferate and establish disease. In the case of acute myeloid leukemia (AML), the identification of molecular pathways linked to LIC biology has led to the development of therapeutic strategies and compounds, including STAT3 inhibitors, which are currently in clinical trials.<sup>65,66</sup> On the other hand, PI3K/Akt/mTOR, IGFs, Wnt, and Notch signaling pathways have been recently reported as relevant pathways that functionally modulate LIC activity in ALL and may have a direct impact on disease maintenance.<sup>62</sup> Despite the numerous molecular pathways involved in pediatric ALL, our knowledge

regarding the involvement of the IGFs system in this disease remains limited. The signaling of this axis is governed by a diverse range of proteins and receptors, which add an additional level of complexity in comprehending the underlying mechanisms and identifying molecular targets capable of inhibiting the pathway, without eliciting adverse effects. The scientific community has recently developed a growing interest in understanding and characterizing specific aspects of the IGF system, as new proteins that control this pathway have been identified and present advantages when compared to the traditional molecular targets of the system.

#### **1.4 The intersection of insulin and IGFs signaling pathways in cancer biology**

The insulin-like growth factor (IGF) system comprises two polypeptides (IGF1 and IGF2), six high-affinity IGF binding proteins (IGFBP1 to -6), ten low-affinity IGF binding related proteins (IGFBP-rP1 to -10) and three cell surface tyrosine kinase receptors (RTKs): insulin receptor (INSR), IGF1 receptor (IGF1R) and IGF2 receptor (IGF2R).<sup>67,68</sup> Insulin, IGF1 and IGF2 are well-characterized mitogenic factors that promote cell survival in various cell types, including pediatric ALL.<sup>69</sup> Although these proteins have specific transmembrane tyrosine kinase receptors – RTKs (INSR, IGF1R and IGF2R, respectively), they can also share and/or compete for the same receptor, depending on the intended metabolic function.

It has been widely reported that upon activation and subsequent autophosphorylation, RTKs undergo swift internalization, predominantly through clathrin-mediated endocytosis. In addition to this mechanism, various other modulators may contribute to the internalization, recycling, and degradation of INSR, IGF1R and IGF2R, which have been extensively investigated and meticulously described by Girnita et al.<sup>70</sup> In brief, INSR harbors a C-terminal motif responsible for MAD2 binding, which, in turn, recruits BUBR1 and the clathrin adapter protein complex AP2. This recruitment facilitates clathrin-coated vesicle formation and subsequent endocytosis upon receptor activation.<sup>71</sup> Conversely, IGF1R lacks a MAD2-binding motif, leading to its prolonged retention on the cell surface, seemingly mediated by its interaction with insulin receptor substrate 1 (IRS-1) and the blockade of AP2.<sup>72</sup>

Insulin and IGFs proteins are involved in the regulation of cell proliferation and apoptosis. Studies have shown that high levels of circulating IGF1 is associated with an increased risk of several common cancers.<sup>73</sup> IGF1 is a 70 amino acid peptide encoded by a gene on chromosome 12q22-24.1.<sup>74</sup> Fetal growth is directly influenced

by the IGFs. However in children, the levels of IGFs are regulated by growth hormone, which controls liver IGF1 production.<sup>75</sup> High serum levels of IGF1 are associated with high birth weight and are correlated with the occurrence of pediatric ALL, a hypothesis that is termed Big Babies.<sup>76</sup>

Previous studies have demonstrated that insulin and IGF1, acting via INSR and IGF1R, promote the growth and proliferation of ALL cells in both an autocrine and paracrine manner.<sup>77-83</sup> IGF1 and insulin are both ligands for the IGF1R, activating intracellular signaling pathways that promote cell proliferation and survival. Upon binding to IGF1R, insulin receptor substrate proteins (IRS1-4) are phosphorylated, leading to downstream signaling of the PI3K/Akt/mTOR and Ras/Raf/MAPK pathways, which are involved in neoplastic cell mitogenic signals (see more in section 1.6).<sup>84</sup>

Initially thought to be a redundant receptor used only in the absence of insulin signaling, IGF1R has unique characteristics that distinguish it from INSR. IGF1R has an important role in cancer biology, including mitogenesis, transformation, and protection against apoptosis, ultimately contributing to sustained cell proliferation, a hallmark of cancer cells. Additionally, IGF1R contributes to cell adhesion and longevity.<sup>85</sup> IGF1R is a receptor tyrosine kinase with 70% homology to INSR. It is derived from a highly preserved ancestral gene in both vertebrates and invertebrates,<sup>86</sup> possessing 45-65% homology in the ligand binding site and 60-85% homology in the domains of tyrosine kinase and substrate recruitment.<sup>87</sup>

Both INSR and IGF1R are ligands for insulin, IGF1, and IGF2 (although IGF2 binds with the least affinity). The *INSR* gene is located on chromosome 19p13.2 and encodes INSR, a protein of 1370 amino acids with a molecular mass of ~100 kDa and includes 22 exons. Alternative splicing of exon 11 generates two structurally different isoforms, INSR-A and INSR-B. INSR-B, the mature isoform, contains the 12 amino acids derived from exon 11, whereas INSR-A, the fetal isoform, does not.<sup>88,89</sup> The two isoforms are differentially expressed: INSR-A is predominantly expressed in embryonic and fetal tissues, central nervous system, hematopoietic cells, and cancer cells, whereas INSR-B is expressed in insulin sensitive tissues (e.g., liver, fat, and muscle).<sup>89-92</sup>

INSR-B has a high affinity for insulin and low affinity for IGF1 and IGF2, whereas INSR-A has a high affinity for insulin and IGF2 and an approximately 10 times lower affinity for IGF1 (Figure 4).<sup>91-94</sup>

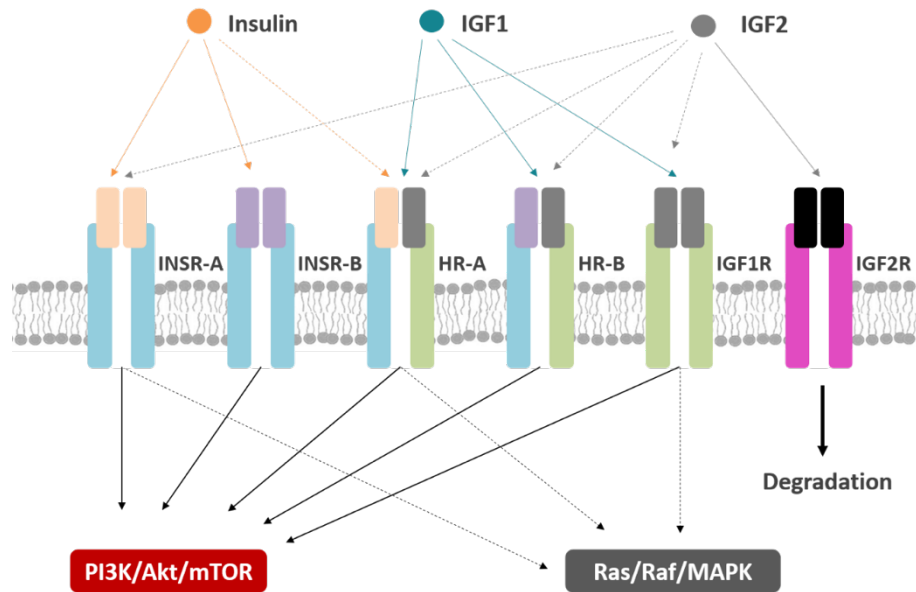


**Figure 4.** Simplified diagram of insulin, IGF1 and IGF2 signaling pathways and their receptors. The insulin receptor (INSR), the insulin-like growth factor 1 receptor (IGF1R), the insulin-like growth factor 2 receptor (IGF2R), and the hybrid receptors (HR-A and HR-B) are part of the RTKs family. The diagram demonstrates a certain level of functional overlap among them. Upon ligand binding, these receptors initiate the phosphorylation of tyrosine residues, subsequently leading to the phosphorylation of the insulin receptor substrate (IRS) and SHC. These proteins serve as docking points for activating the phosphatidylinositol 3-kinase (PI3K-Akt-mTOR) pathway or the Ras/Raf/MAPK pathway, respectively. The PI3K-Akt-mTOR pathway primarily participates in metabolic actions such as glucose uptake and insulin sensitivity, as well as cell proliferation. On the other hand, the Ras/Raf/MAPK pathway primarily contributes to mitogenic effects, including proliferation and growth. Modified from Genua et al.<sup>95</sup>

In addition to the classical isoforms of the INSR, hybrid receptors (HR) can also form through heterodimerization with IGF1R (Figure 4).<sup>96,97</sup> Two types of HR have been identified, INSR-A plus IGF1R (HR-A) and INSR-B plus IGF1R (HR-B), which have different affinities for insulin and IGFs (Figure 4). HR-A exhibits higher affinity for IGF1, IGF2, and insulin, whereas HR-B binds mainly to IGF1, but also has low affinity for IGF2. Notably, IGFs bind less efficiently to HR-B than to IGF1R and HR-A, which "attenuates" the mitogenic potential of IGF1R upon HR-B formation. Conversely, HR-A expression enhances sensitivity to the mitogenic effects of IGFs and insulin.<sup>98</sup>

INSR overexpression is commonly observed in several malignancies that exhibit abnormal responses to insulin and IGFs, and typically results in mitogenic effects.<sup>92,97-</sup>

<sup>99</sup> The biological role of overexpressed INSR in cancer remains poorly understood, although several studies have highlighted the significance of INSR-A isoform expression in cell proliferation and cancer.<sup>89,91,92</sup> Our microarray analyses of primary ALL samples corroborate these studies, since in ALL, INSR exon 11 is not expressed, indicating the prevalence of IR-A in these cell types (Figure 5).<sup>100</sup>

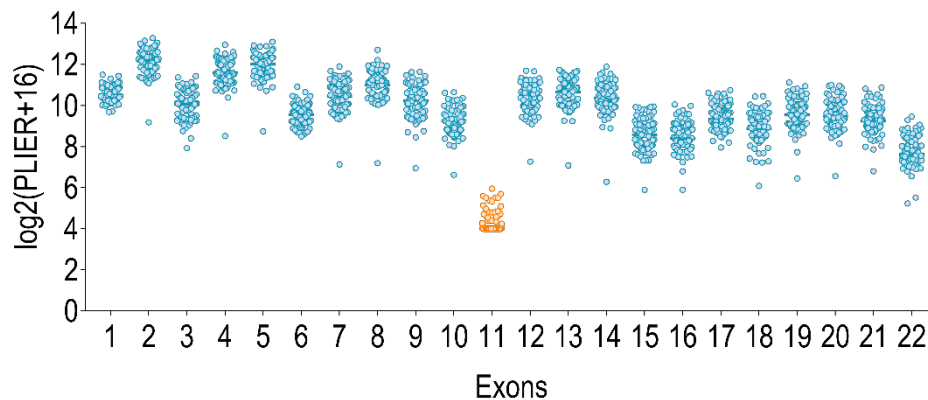


**Figure 5.** Expression of the different exons of the *INSR* gene in 93 samples of pediatric ALL. Each point corresponds to one patient's ALL. Results demonstrate that ALL cells predominantly express isoform A of the INSR (isoform that lacks exon 11). Modified from Laranjeira.<sup>100</sup>

IGF2 expression and regulation is complex, involving an untranslated mRNA called H19 and the silencing of one allele through gene imprinting.<sup>88</sup> The loss of imprinting or other regulatory failures that lead to increased H19 expression are the primary factors that confer an advantage to IGF2-dependent cell growth. Physiologically, IGF2 exhibits high affinity for IGF2R and lower affinity for IGF1R and INSR. Most studies suggest that IGF2R does not produce a metabolic signal when bound to IGF2; rather, its primary function is to sequester IGF2, as IGF2's biological effects (mitogenic and anti-apoptotic) occur through interactions with IGF1R. In this model, the reduction of IGF2R expression is related to an increase in IGF2-mediated activation of IGF1R.<sup>73</sup>

IGFs are distinguished from insulin by their interactions with high-affinity IGF binding proteins (IGFBP1 to -6) or low-affinity IGF binding related proteins (IGFBP-rP1 to -10), which modulate IGFs bioavailability and signaling by regulating their tissue distribution and receptor accessibility. Some preclinical studies suggest that IGFBPs may function as oncogenes depending on the cellular context, and there is evidence

that these proteins may serve as tissue biomarkers for assessing tumor progression and/or therapeutic resistance.<sup>101</sup>

### 1.5 IGF binding proteins

Circulating IGFs are bound by IGF binding proteins (IGFBPs), of which there are six different types (IGFBP1 to -6).<sup>102</sup> IGFBPs have a high affinity for IGFs and can either inhibit or potentiate the IGF signaling pathway. They do not bind to insulin but have a better affinity for IGFs than the IGF1Rs. In most cases, IGFBPs inhibit IGF action by preventing their binding to IGF receptors. This inhibition leads to downregulation of cellular proliferation, survival, differentiation and metabolism. However, in some instances, IGFBPs can increase IGF signaling through a process called proteolytic cleavage, which is one of the primary mechanisms involved in the release of IGFs from IGFBPs.<sup>103,104</sup>

IGFBPs are cysteine-rich proteins that share a high degree of similarity in their primary amino acid sequences. Structurally, IGFBPs have cysteines clustered at both the conserved N-terminal third (12 cysteines in IGFBP1 to 5; and 10 in IGFBP6) and the conserved C-terminal third (6 cysteines) of the proteins. Furthermore, 10 other extracellular proteins known as the IGFBP-related proteins (IGFBP-rP1 - 10) share the IGF-binding domain of IGFBPs. IGFBP-rPs carry the N-terminal domain of IGFBPs, as shown in Figure 6 with a blue box, but differ from IGFBPs mostly in the C-terminus region. While IGFBP-rPs can bind IGFs, its affinity is 100-1000 times lower than binding observed with IGFBPs. IGFBP-rPs also have multiple IGF-independent roles, and their physiological significance in the IGF pathway remains undefined.<sup>103-108</sup>

IGFBP-rP1, best known as IGFBP7, but also known as TAF (tumor-derived adhesion factor), mac25 (meningioma-associated cDNA 25), PSF (prostacyclin-stimulating factor) and AGM (angiomodulin), is a special exception of IGFBP-rPs because of its high affinity for insulin and IGFs. Unlike other IGFBPs, IGFBP7 does not act by sequestering insulin and IGFs preventing their binding to receptors, but it acts by increasing the half-life of these factors through direct interactions with them and may promote mitogenic actions depending on the target tissue.<sup>109</sup>

IGFBP7 is a protein that plays an essential role in cell proliferation and has been implicated in the adhesion and migration of different tumor types.<sup>30,110-112</sup> IGFBP7 has been shown to interact with various components of the extracellular matrix, including collagen types II, IV, and V, heparin sulfate, and glycosaminoglycans. It has been

suggested that IGFBP7 contributes to cell/cell adhesion and extracellular cell/matrix adhesion.<sup>108</sup> Additionally, IGFBP7 has been found to accumulate in tumor blood vessels and secondary lymphoid tissues, and it interacts with chemokines such as SLC, CCL21, IP-10, CXCL10, and RANTES.<sup>82,113,114</sup> In the context of cancer, IGFBP7 has been shown to regulate cell proliferation, adhesion, and senescence in various neoplastic tissues.<sup>115-116</sup> Moreover, IGFBP7 has been associated with a poor prognosis in several types of cancer, including inflammatory breast cancer,<sup>117</sup> mesothelioma,<sup>118</sup> prostate cancer<sup>119</sup> and colorectal cancer.<sup>120</sup> In leukemia, IGFBP7 was identified as a negative prognostic factor. High expression of IGFBP7 mRNA is associated with resistance to primary therapy and a worse prognosis in patients with T-ALL,<sup>121</sup> primary acute myeloid leukemia (AML) and Philadelphia negative BCP-ALL samples.<sup>30,122</sup> Therefore, IGFBP7 have been considered a negative prognostic factor in leukemia and is currently being studied as a new therapeutic target.

Despite numerous studies highlighting the varied roles of IGFBP7 in diverse pathological conditions, the underlying molecular mechanisms responsible for these effects remain largely unknown. Elucidating the physiological significance of IGFBP7 could provide crucial insights into various aspects of the IGF system. Since IGFBP7 has been associated with the precise regulation of insulin and IGFs signaling, comprehending its role within this context, particularly regarding the INSR and IGF1R receptors, may uncover novel pathways yet to be explored in biological systems and, therefore, contribute to a greater understanding of complex diseases such as ALL.

In this context, some studies have investigated the effects of IGFBP7 on INSR and IGF1R signaling, however, they generated contradictory results. On the one hand, some authors have demonstrated that IGFBP7 can decrease the signaling of INSR and IGF1R by sequestering insulin and IGFs<sup>103,106,122</sup> or by acting as an antagonist to IGF1R.<sup>123,124</sup> For instance, Evdokimova et al.<sup>123</sup> reported that the N-terminus of IGFBP7 can bind to the extracellular domain of IGF1R, inhibiting its activation. This suggests that IGFBP7 binding to unoccupied IGF1R may hinder the subsequent binding of insulin or IGF1.



IGFBP1	---	QVGVTAGAPWQCAPCSAEKLALCPP-VS-----	ASCSEV----	TRSA	55
IGFBP2	GG-	GGGARAEEVLFRCPPCTPERLAACGP-PPVAPPAAVAAGGARMPCAEL----	VREP	82	
IGFBP3	AG-	ASSAGLGPVVRCEPCDARALAQCAP-PP-----	AVCAEL----	VREP	65
IGFBP4	AG-	PGPSLGDEAIHCPCSEELARCRP-P-----	VGCEEL----	VREP	51
IGFBP5	YA-	GPAQSLGSFVHCEPCDEKALSMCPP-SP-----	LGC-EL----	VKEP	51
IGFBP6	----	ASPGGALARCPGCGQGVQAGCPG-----	GCVEEDGGSPA	55	
IGFBP-rP1/IGFBP7	---	SSSSSDTCGPCEP-----	ASCPP-LPP-----	LGCL----	LGETRD 55
IGFBP-rP2/CCN2/CTGF	---	RPAVGQNC SG--P-----	CRCPDEPAP-----	RC PAG--	VSLVLD 52
IGFBP-rP3/CCN3/NOV	---	QVAATQRCPPQCP-----	GRC PA-TPP-----	TCAPG--	VRAVLD 59
IGFBP-rP4/CCN1/Cyr61	---	RL-ALSTCPA--A-----	CHCPL-EAP-----	KCAPG--	VGLVRD 48
IGFBP-rP5/L56/HtrA	GR-	SAPLAAGCPDRCEP-----	ARCPP--QP-----	EHCE----	GGRRD 60
IGFBP-rP6/ESM-1	AW-	SNNYAVDCPQHCD S-----	SECKS-SP-----	RCKR----	TVLD 49
IGFBP-rP7/CCN5/WISP2	---	KV-RTQLCPT--P-----	CTCPW-PPP-----	RCPLG--	VPLVLD 48
IGFBP-rP8/CCN4/WISP1	---	TSSRPQFCKW--P-----	CECPP-SPP-----	RCPLG--	VSLITD 71
IGFBP-rP9/CCN9/WISP3	---	APQRKQFCHW--P-----	CKCPQ-QKP-----	RCPPG--	VSLVRD 70
IGFBP-rP10/BONO1/KAZALD1	GWMRL	LAEGEGCAPCRP-----	EECA---AP-----	RGCL----	AGVRD 74
GCGCCxxC					
IGFBP1	GCGCC	PMALPLGAAC-----	GVATARCAGLS	CRALPGEQQP-LHAL-----	97
IGFBP2	GCGCC	SVCARLEGEAC-----	GVYTPRCGQLRCYPHPGSELP-LQAL-----	124	
IGFBP3	GCGCC	LTCALSEGQPC-----	GIYTERCGSGLRCQPSDEARP-LQAL-----	107	
IGFBP4	GCGCC	ATCALGLGMP-----	GVYTPRCGSGRLCYPPRGVEKP-LHTL-----	93	
IGFBP5	GCGCC	MTCALAEQSC-----	GVYTERCAQGLRCLPRQDEEKP-LHAL-----	93	
IGFBP6	GCAEA	EGCLRREGQEC-----	GVYTPNCAPGLQCHPPKDDEAP-LRAL-----	97	
IGFBP-rP1/IGFBP7	ACGCC	PMARGEPEPCGGGAGR--	GYCAPGMEC	<b>MSRKRKRGK</b> AGAAAGPGVSGVCVC	113
IGFBP-rP2/CCN2/CTGF	GCGCC	RVCAKQLGELCTERDP---	CDPHKGLFCHFGSPANR-----	KIGVCTA	97
IGFBP-rP3/CCN3/NOV	GCSCC	LVCARQGESCSLEP---	CDESSGLYCDRSADPSN-----	QTGICTA	104
IGFBP-rP4/CCN1/Cyr61	GCGCC	KVCAKQLNEDSKTQP---	CDHTKGLECNFGASSTA-----	LKGICRA	93
IGFBP-rP5/L56/HtrA	ACGCC	CEVCGAPEGAAACGLQE----	GPCGEGLCVVPFGV---	PASATVRRRAQAGLCVC	112
IGFBP-rP6/ESM-1	DCGCC	RVCAAGRGETCYRTVSGMDGMKCGPLRCQPSNGEDPF-GEEF-----	GIC	99	
IGFBP-rP7/CCN5/WISP2	GCGCC	RVCAARRLGEPDQLHV---	CDASQGLVCQPGAGPGG-----	RGALCLL	93
IGFBP-rP8/CCN4/WISP1	GCECC	KCAQQLGDNCTEAAI---	CDPHRGLYCDYSGDRPRY-----	AIGVC-A	116
IGFBP-rP9/CCN9/WISP3	GCGCC	KICAKQGEICNEADL---	CDPHKGLYCDYSVDRPRY-----	ETGVC-A	115
IGFBP-rP10/BONO1/KAZALD1	ACGCC	WECANLEGQLCDLPSAHFYGHGCEQLECRL-----	DTGGDL	SRGEVPEPLCAC	128

**Figure 6.** Amino acid sequence alignment of the N-terminal domains from human IGFBP1 to 6 and human IGFBP-rP1 to 10. Alignment was performed using Align approach by UniProt databases ([www.uniprot.org](http://www.uniprot.org)). Signal peptides were not included in the analysis. Small gaps were introduced to optimize alignment. Consensus amino acid residues are shaded orange. Blue box indicates the IGF-binding domain of IGFBPs (GCGCCxxC sequence, where x is any amino acid residue). Red box shows the heparin-binding site in IGFBP-rP1/IGFBP7.

However, on the other hand, different groups have shown that IGFBP7 can improve insulin signaling through INSR or IGF1R.<sup>30,109,125</sup> Morgantini et al.<sup>125</sup> showed that under insulin-sensitive conditions, IGFBP7 produced by liver macrophages binds to hepatic INSR and enhances the activation of Akt (Ser473) by insulin in hepatocytes, enhancing glycolytic activity. In insulin-resistant conditions where Akt does not respond to insulin, IGFBP7 binds to INSR with lower affinity but still activates the MAPK pathway, leading to gluconeogenesis and lipogenesis. However, this study did not fully

explore the relationship between IGFBP7, insulin and its receptors, but provides concrete evidence that IGFBP7 at physiological levels can contribute to glycolytic metabolism by mediating responses through INSR and downstream pathways such as PI3K-Akt and MAPK.

It is important to consider that the differences in INSR/IGF1R signaling and internalization complexes among the biological models used in these studies should not be overlooked. However, in our own work, we have shown that the amount of IGFBP7 protein available to cells may contribute to the discrepancies in the results. As an example, Evdokimova et al.<sup>123</sup> used a concentration of 20 µg/ml of IGFBP7, while Morgantini et al.<sup>125</sup> used 20 ng/ml. It is plausible that at high concentrations, IGFBP7 may indeed restrict or prevent the binding of IGF1/insulin to IGF1R. Notably, 20 µg/ml exceeds the physiological levels of IGFBP7 in human adult serum (21-35 ng/ml).<sup>126</sup>

Moreover, the findings reported by Morgantini et al.<sup>125</sup> highlight the significance of IGFBP7 as a crucial regulator of the insulin pathway, facilitating metabolic parameters and enhancing sensitivity to this hormone. When considering cancer, specifically ALL, it is well-established that the glycolytic metabolism of leukemic cells profoundly impacts disease treatment and chemotherapy response.<sup>127</sup> Given the potential of IGFBP7 to regulate the activity of insulin and IGFs towards their respective receptors, it is reasonable to consider the potential contribution of IGFBP7 (through the PI3K-Akt pathway) to the glycolytic metabolism in ALL. However, before postulating this hypothesis, it is crucial to comprehend the intricacies of glycolytic metabolism in ALL and the proteins that orchestrate this machinery.

## **1.6 PI3K-Akt pathway and glycolytic metabolism**

Phosphatidylinositol 3-kinase (PI3K)-Akt pathway stands as the most activated pathway in human cancers, exerting significant control over key metabolic processes, such as glucose metabolism. Activation of PI3K-Akt signaling plays a vital role in maintaining systemic metabolic homeostasis and regulating the growth and metabolism of individual cells in response to insulin, growth factors, and cytokines under physiological conditions. However, in cancer cells, especially in ALL, oncogenic activation of this pathway leads to a reprogramming of cellular metabolism, resulting in enhanced activity of nutrient transporters and metabolic enzymes that support the anabolic demands of rapidly proliferating cells.<sup>127</sup>

The PI3K-AKT signaling network occupies a central role in promoting cell survival and growth and is activated downstream of receptor tyrosine kinases (RTKs, main signaling regulator), cytokine receptors, integrins, and G protein-coupled receptors (GPCRs).<sup>128</sup> The class Ia PI3K exists as heterodimers consisting of a catalytic subunit (p110 $\alpha$ , p110 $\beta$ , or p110 $\delta$ ) and a regulatory subunit (p85 $\alpha$ , p85 $\beta$ , or shorter variants). Class Ib, on the other hand, comprises the catalytic subunit p110 $\gamma$  associated with the regulatory subunit p101.<sup>129</sup> Class Ia PI3K is activated when the SH2 domains within the regulatory subunits interact with phospho-tyrosine residues on activated receptors or adaptor proteins, while class Ib is activated by GPCRs.

As previously discussed, activation INSR and IGF1R in ALL is mediated by insulin and IGFs (Figure 7). After ligand coupling, its receptors are auto phosphorylated inducing recruitment of insulin receptor substrate proteins (IRS1-4) and SHC. IRS and SHC proteins are recognized by various signaling molecules that contain a Src homology 2 (SH2) domain, such as Grb2 and PI3K. Activation of PI3K at the plasma membrane leads to the phosphorylation of its phospholipid substrate, phosphatidylinositol 4,5-bisphosphate (PIP2), generating the second messenger, phosphatidylinositol 3,4,5-trisphosphate (PIP3).<sup>127-129</sup> Phosphatase and tensin homologue (PTEN) attenuate PI3K signaling by dephosphorylating PIP3 to regenerate PIP2. Accumulation of PIP3 at the plasma membrane creates docking sites for downstream effector proteins containing a pleckstrin homology (PH) domain that specifically interacts with this lipid species. One of these effector proteins is the serine-threonine kinase Akt. Upon binding to PIP3, Akt is phosphorylated by phosphoinositide-dependent protein kinase 1 (PDK1) at Thr308, which is crucial for its activation, and by mechanistic target of rapamycin (mTOR) complex 2 (mTORC2) at Ser473, further enhancing Akt activity. Activated Akt phosphorylates an extensive array of downstream substrates, many of which are redundantly regulated by the three Akt isoforms (Akt1, Akt2 and Akt3). This phosphorylation cascade influences various cellular functions, including protein synthesis and growth, glucose metabolism, cell cycle, cell proliferation, cell survival, and apoptosis. Akt-mediated phosphorylation of these protein targets exerts a profound impact on cellular metabolism, contributing to the regulation of diverse metabolic pathways, such as glycolytic metabolism.<sup>130-134</sup>

The altered glucose metabolism represents a characteristic metabolic modification that distinguishes cancer cells from their normal counterparts. This metabolic phenotype, commonly referred to as aerobic glycolysis or the Warburg

effect,<sup>136</sup> was initially described by Otto Warburg<sup>137</sup> almost a century ago. It is characterized by an augmented uptake of glucose and its conversion into lactate, even in the presence of sufficient oxygen levels. Glycolysis, besides generating ATP, provides metabolic intermediates that serve as substrates for branching metabolic pathways, supporting the biosynthesis of essential macromolecules such as proteins, lipids, and nucleotides required for cell proliferation and growth.<sup>136</sup>

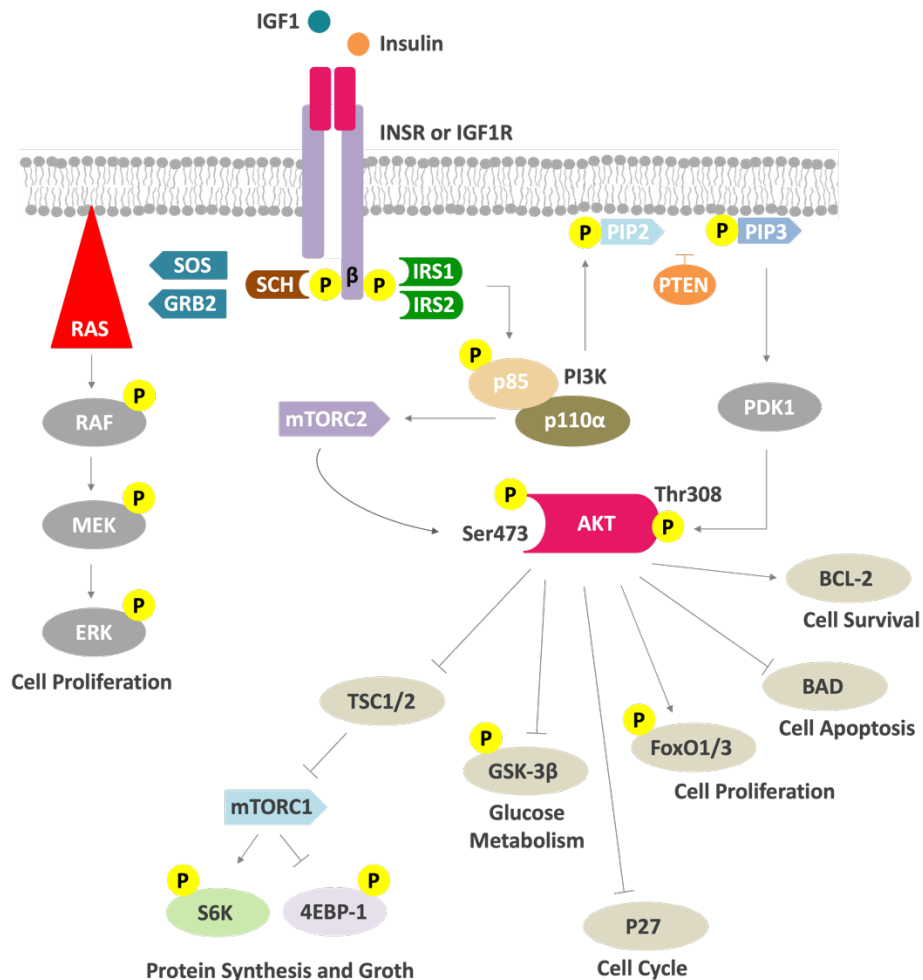


**Figure 7.** PI3K-Akt signaling pathway. Insulin/IGFs functions as a ligand to interact with RTKs in the cellular membrane, which leads to autophosphorylation and recruitment of the adaptor proteins IRS1, IRS2, and Shc. The interaction of IRS1/2 with  $\beta$ -subunit of the cognate receptor induces the activation of PI3K. PI3K converts PIP2 to the lipid second messenger PIP3. Akt family of kinases is activated by PDK1 and by mTORC2 complex resulting in the phosphorylation at Thr308 and Ser473, respectively. Activated Akt then regulates downstream signaling molecules including Tuberous sclerosis protein 1/2 (TSC1/2) which inhibit mTORC1 complex and regulate S6K and 4EB-P1 phosphorylation, FoxO transcription factors, GSK-3 $\beta$ , p27, BAD, and BCL-2. These downstream molecules are involved in several cellular processes

including protein synthesis, glucose metabolism and cell survival. In parallel, SHC activation induces the activation of the MAPK pathway, which results in increased cell proliferation, mediated by RAS activation. Adapted from Jung and Suh.<sup>135</sup>

Akt activation has been demonstrated to be sufficient to stimulate aerobic glycolysis.<sup>138,139</sup> Persistent activation of Akt can trigger a growth factor-independent elevation in glucose uptake in addition to promoting glycolysis. This Akt-mediated induction of aerobic glycolysis renders cancer cells reliant on glucose for their survival, thereby highlighting the glycolytic pathway as a potential therapeutic target for combating cancer. PI3K-Akt signaling exerts control over multiple regulatory checkpoints within glycolysis. This includes acute post-translational modifications as well as longer-term transcriptional effects on key components such as glucose transporters (GLUTs) and glycolytic enzymes.<sup>138-143</sup>

Intracellular glucose uptake dependent on PI3K-Akt pathway signaling is facilitated by a family of transporters known as GLUTs.<sup>144</sup> Among these, GLUT1 exhibits ubiquitous expression and is frequently upregulated in cancer cells. Conversely, GLUT4 is primarily expressed in insulin-responsive muscle and adipose tissue, where it plays a pivotal role in facilitating the clearance of glucose from the bloodstream following food consumption.<sup>144,145</sup>

As anticipated, glucose uptake through both GLUT1 and GLUT4 is attributed to the activation of Akt. Studies investigating insulin-stimulated glucose uptake have demonstrated that Akt2 associates with vesicles containing GLUT4, thereby stimulating the translocation of GLUT4 from these vesicles to the cell's plasma membrane.<sup>146,147</sup> This regulatory process primarily involves the Akt-mediated phosphorylation and inhibition of TBC1D4 (also known as AS160), a GTPase-activating protein (GAP) responsible for facilitating GLUT4 trafficking. However, this mechanism appears to be specific to GLUT4 and is unlikely to significantly impact glucose uptake in cancer cells, which predominantly rely on GLUT1.<sup>148,149</sup>

Recent investigations have highlighted the role of thioredoxin-interacting protein (TXNIP) as a direct substrate of Akt in the regulation of both GLUT1 and GLUT4 trafficking.<sup>150</sup> Notably, TXNIP has been found to promote GLUT1 endocytosis and inhibit glucose uptake. However, Akt phosphorylation of TXNIP leads to its inhibition, resulting in a rapid increase in the presence of GLUT1 and GLUT4 at the plasma membrane and subsequently enhanced glucose uptake across various cell types,

including mouse embryonic fibroblasts, 3T3-L1 adipocytes, and different mouse tissues such as skeletal muscle, white adipose tissue, and liver.<sup>150-152</sup>

In the context of ALL, fine-tuning the glycolytic pathway is a crucial step in the malignant transformation of immune cell progenitors.<sup>153,154</sup> Among immune cells, including those involved in ALL, GLUT1 is primarily responsible for coordinating glucose uptake.<sup>155-157</sup> Transcriptional regulation, increased plasma membrane targeting and recycling of GLUT1 are directly regulated by insulin, growth factors and cytokines. It is well established that in ALL cells, activation of the PI3K-Akt axis by RTKs or oncogenic lesions (gain-of-function mutations) induces GLUT1 accumulation at the cell surface and increases aerobic glycolysis.<sup>127,158,159</sup> These observations underscore the pivotal significance of the PI3K-Akt pathway in governing glucose metabolism in cancer, particularly in ALL.

## 2. JUSTIFICATION

Pediatric ALL is a complex and heterogeneous malignancy characterized by abnormal proliferation and differentiation of lymphoid progenitor cells.<sup>18-22</sup> As anticipated, the dysregulation of growth factor signaling pathways, such as the IGF system, plays a critical role in the pathogenesis and progression of ALL.<sup>77-83</sup> Understanding the IGF system and its associated signaling pathways, particularly the INSR and IGF1R as well as downstream signaling via the PI3K-Akt pathway, hold significant scientific and therapeutic importance in the context of ALL.

IGFBP7, a member of the insulin-like growth factor-binding protein family, has been identified as a key regulator of the IGF system, primarily triggering activation in the majority of instances.<sup>30,110-112</sup> Due to its non-classical nature as a protein associated with the PI3K-Akt pathway, scant evidence exists pertaining to the precise regulation of IGFBP7 within this pathway. Moreover, given the documented capacity of IGFBP7 to enhance glycolytic metabolism in hepatocytes,<sup>125</sup> its interaction with RTKs<sup>123,125</sup> and its association with unfavorable prognosis in ALL<sup>30,121,160</sup> it is reasonable to hypothesize that targeting IGFBP7 could emerge as a novel therapeutic approach for pediatric ALL.

### 3. OBJECTIVES

#### 3.1 General aim

The general aim of this thesis was to examine the involvement of IGFBP7 in the insulin/IGF axis and elucidate the consequences of its modulation in pediatric Acute Lymphoblastic Leukemia.

#### 3.2 Specific aims

*3.2.1 Chapter 1: manuscript "Physiologic IGFBP7 levels prolong IGF1R activation in Acute Lymphoblastic Leukemia."*

- Assess the impact of *IGFBP7* knockdown or protein neutralization utilizing an anti-IGFBP7 monoclonal antibody on ALL survival *in vitro*.
- Investigate the contribution of IGFBP7 in the insulin/IGFs axis through functional assays employing ALL cell lines and primary ALL cells.
- Elucidate the molecular pathways involved in ALL proliferation and progression responses, specifically focusing on the interplay between IGFBP7, the insulin/IGFs axis, and associated signaling pathways.
- Quantify the activity of IGF1R and INSR receptors in ALL, dependent or not on IGFBP7 and its ligands.
- Assess the therapeutic effectiveness of the anti-IGFBP7 monoclonal antibody in ALL by utilizing patient-derived xenograft (PDX) models.

*3.2.2 Chapter 2: manuscript "IGFBP7 fuels the glycolytic metabolism in B-cell Precursor Acute Lymphoblastic Leukemia by sustaining activation of the IGF1R-Akt-GLUT1 axis."*

- Validate IGF1R as a target of IGFBP7 in ALL through loss-of-function assays.
- Identify signature genes in ALL modulated by insulin/IGF1+IGFBP7.
- Establish the contribution of IGFBP7 in stimulating glycolytic metabolism in ALL, particularly through the IGF1R-Akt-GLUT1 axis.



## 4. CHAPTER I - MANUSCRIPT

## REGULAR ARTICLE



## Physiologic IGFBP7 levels prolong IGF1R activation in acute lymphoblastic leukemia

Leonardo Luís Artico,<sup>1,2,\*</sup> Angelo Brunelli Albertoni Laranjeira,<sup>1,\*</sup> Livia Weijenborg Campos,<sup>1,2</sup> Juliana Ronchi Corrêa,<sup>1,2</sup> Priscila Pini Zenatti,<sup>1</sup> José Barreto Campello Carvalheira,<sup>3</sup> Sandra Regina Brambilla,<sup>3</sup> Alexandre Eduardo Nowill,<sup>4</sup> Silvia Regina Brandalise,<sup>1</sup> and José Andrés Yunes<sup>1,5</sup>

<sup>1</sup>Centro Infantil Boldrini, Campinas, Brazil; <sup>2</sup>Graduate Program in Genetics and Molecular Biology, Biology Institute, State University of Campinas; <sup>3</sup>Departamento de Clínica Médica; <sup>4</sup>Centro Integrado de Pesquisas Oncohematológicas na Infância, and <sup>5</sup>Departamento de Genética Médica, Faculty of Medical Sciences, State University of Campinas, Campinas, Brazil

### Key Points

- Physiologic levels of extracellular IGFBP7 prolong the surface expression and activation of IGF1R by insulin/IGF in ALL.
- Knockdown or antibody neutralization of IGFBP7 decrease ALL progression in vivo.

Insulin and insulin-like growth factors (IGFs) are mitogenic and prosurvival factors to many different cell types, including acute lymphoblastic leukemia (ALL). Circulating IGFs are bound by IGF binding proteins (IGFBPs) that regulate their action. IGFBP7 is an IGFBP-related protein (IGFBP-rP) that in contrast to other IGFBPs/IGFBP-rPs features higher affinity for insulin than IGFs and was shown to bind the IGF1 receptor (IGF1R) as well. The role of IGFBP7 in cancer is controversial: on some tumors, it functions as an oncogene, whereas in others, it functions as a tumor suppressor. In childhood ALL, higher *IGFBP7* expression levels were associated with worse prognosis. Here we show that IGFBP7 exerts mitogenic and prosurvival autocrine effects on ALL cells that were dependent on insulin/IGF. *IGFBP7* knockdown or antibody-mediated neutralization resulted in significant attenuation of ALL cell viability in vitro and leukemia progression in vivo. IGFBP7 was shown to prolong the surface retention of the IGF1R under insulin/IGF1 stimulation, resulting in sustained IGF1R, insulin receptor substrate 1 (IRS-1), protein kinase B (AKT), and extracellular signal-regulated kinase (ERK) phosphorylation. Conversely, the insulin receptor was readily internalized and dephosphorylated on insulin stimulation, despite IGFBP7 addition. The affinity of homodimeric IGF1R for insulin is reportedly >100 times lower than for IGF1. In the presence of IGFBP7, however, 25 ng/mL insulin resulted in IGF1R activation levels equivalent to that of 5 ng/mL IGF1. In conclusion, IGFBP7 plays an oncogenic role in ALL by promoting the perdurance of IGF1R at the cell surface, prolonging insulin/IGF stimulation. Preclinical data demonstrate that IGFBP7 is a valid target for antibody-based therapeutic interventions in ALL.

### Introduction

Insulin and insulin-like growth factors (IGF1 and IGF2) are well-known mitogenic and prosurvival factors to many different cell types, including both B-cell precursor (BCP) and T-cell acute lymphoblastic leukemias (ALLs).<sup>1</sup> Insulin/IGFs act by binding to receptor tyrosine kinases made of homo- or heterodimeric insulin receptor (INSR) and IGF1 receptor (IGF1R) chains, that recruit and phosphorylate insulin receptor substrate proteins (IRS1-4), thus initiating the downstream activation of the phosphatidylinositol 3-kinase/protein kinase B/mammalian target of rapamycin (PI3K/AKT/mTOR) and Ras/Raf/MAPK signaling

Submitted 16 October 2020; accepted 6 April 2021; prepublished online on *Blood Advances* First Edition 26 August 2021; final version published online 24 September 2021. DOI 10.1182/bloodadvances.2020003627.

\*L.L.A. and A.B.A.L. contributed equally to this study.

For data sharing, contact the corresponding author at andres@boldrini.org.br. The full-text version of this article contains a data supplement.

© 2021 by The American Society of Hematology

pathways.<sup>2,3</sup> Circulating IGFs are normally bound by 1 of the 6 IGF binding proteins (IGFBPs) that can both inhibit or potentiate IGF action.<sup>4</sup> In ALL, IGFBP1, 3, and 4 were shown to inhibit, whereas IGFBP2, 5, and 6 had no influence on, IGF1-induced proliferation of the NALM16 and RS4;11 cell lines in vitro.<sup>5</sup>

The IGF-binding domain of IGFBPs is shared by some other extracellular proteins, collectively called IGFBP-related proteins (IGFBP-rPs). IGFBP-rPs bind IGFs with low affinity (100-1000 times lower than IGFBPs 1-6) and have multiple IGF-independent roles; therefore, their physiologic significance in the IGFs system remains undefined.<sup>6</sup> However, IGFBP-rP1, best known as IGFBP7, is a special case among IGFBP-rPs or IGFBPs, because it binds insulin with relatively high affinity, although with lower affinity than that exhibited by the INSR.<sup>7</sup> In short-term experiments (3 minutes), IGFBP7 was shown to inhibit insulin-stimulated INSR signaling.<sup>7</sup> In 72-hour cell proliferation assays, on the contrary, IGFBP7 was shown to enhance the mitogenic activities of IGFs and insulin,<sup>8</sup> suggesting that physiologically, it may not compete with the INSR/IGF1R for their ligands but instead may augment the half-life of these growth factors.

We previously reported that ALL cells are the main source of IGFBP7 in the leukemia bone marrow microenvironment. The leukemia-secreted IGFBP7 was shown to stimulate bone marrow stromal cells to produce more asparagine, thus counteracting the effect of the antineoplastic drug L-asparaginase.<sup>9</sup> In that study, we also found that the knockdown of *IGFBP7* in 2 BCP-ALL cell lines (REH and 697) resulted in reduced proliferation,<sup>9</sup> suggesting that *IGFBP7* could play an autocrine role as well. Here we characterize the autocrine effects of IGFBP7 in ALL, performing preclinical studies to validate it as a target for therapeutic intervention.

## Methods

### Cell culture

ALL cell lines were cultured in RPMI-1640 (Cultilab, Campinas, São Paulo, Brazil) with 10% fetal bovine serum (FBS), 50 U/mL penicillin, and 50 µg/mL streptomycin (Cultilab). Cryopreserved mononuclear cells from diagnostic bone marrow samples of children with ALL were thawed, depleted of dead cells by Ficoll-gradient centrifugation, and cultured in AIM-V medium (Thermo Fisher Scientific, Waltham, Massachusetts). The study was approved by the Research Ethics Committee from the State University of Campinas (CAAE: 0014.0.144.146-08 and 0018.0.144.146-08) and was conducted in accordance with the Declaration of Helsinki. Animal experiments were approved by the Animal Experimentation Ethics Committees of the State University of Campinas (CEUA/UNICAMP, protocol 1133/2008) and Centro Infantil Boldrini (CEUA/BOLDRINI, protocol 0006/2020).

### Short hairpin RNA knockdown of *IGFBP7* and *IGF1R*

*IGFBP7* and *IGF1R* were downregulated using pLKO.1 MISSION short hairpin RNA (shRNA; NM\_001553.1-959s1c1 and NM\_001553.1-812s1c1) or the pLKO.1 MISSION LacO shRNA (NM\_000875) lentiviral vectors (Sigma-Aldrich, San Luis, Missouri), respectively, and their corresponding nontarget shRNA control vectors, as previously described.<sup>9</sup>

### Cell viability and proliferation assays

Cell viability was analyzed by the 3-(4,5-dimethylthiazol-2-yl)-2,5-dimethyltetrazolium bromide (MTT) assay. *IGFBP7* knockdown cells were cultured at 30 000 cells per well, in 96-well plates, in RPMI-3% FBS. Antibody neutralization of IGFBP7 was analyzed in 96-well plates at 30 000 cells per well in RPMI-10% FBS with 20 µg/mL anti-IGFBP7 (clone C311) or anti-prostate-specific antigen (PSA; Rheabiotec, Campinas, São Paulo, Brazil) control. The effects of insulin (500 ng/mL; Novo Nordisk, Bagsværd, Denmark), IGF1 (200 ng/mL; R&D Systems, Minneapolis, Minnesota), IGF2 (200 ng/mL; R&D Systems), and/or IGFBP7 (100 ng/mL; R&D Systems) on cell lines or primary ALL cells was assessed in 96-well plates at 30 000 cells per well in RPMI-10% FBS or AIM-V, respectively. Proliferation of *IGFBP7* or *IGF1R* knockdown cells was assayed in 24-well plates at 50 000 cells per well in RPMI-3% FBS or RPMI-10% FBS, respectively. Numbers of living cells were estimated in a Countess II Cell Counter (Thermo Fisher Scientific) after trypan blue staining.

### Apoptosis assays

Cell lines or primary ALL cells were cultured at 50 000 cells per well in 96-well plates in RPMI-3% FBS or RPMI-10% FBS or AIM-V medium alone or supplemented with insulin (500 ng/mL), IGFBP7 (100 ng/mL or 20 µg/mL), anti-IGFBP7 (clone C311; 20 µg/mL), or anti-PSA (20 µg/mL). After 24 or 48 hours, cells were washed with phosphate-buffered saline (PBS), resuspended in Annexin-V binding buffer (Becton Dickinson, Franklin Lakes, New Jersey), and labeled with fluorescein isothiocyanate (FITC)-conjugated Annexin-V (Immuno Tools, Friesoythe, Germany) for 20 minutes and 7-Aminoactinomycin D (7AAD, 5 µg/mL; Thermo Fisher Scientific) for 3 minutes, at room temperature, and immediately analyzed in a LSR Fortessa cytometer (Becton Dickinson) using the FlowJo Software (Becton Dickinson).

### 5-bromo-2'-deoxyuridine cell cycle assay

We used the FITC 5-bromo-2'-deoxyuridine (BrdU) Flow Kit (Becton Dickinson). Cells at 50 000 cells per well in 96-well plates were starved 4 hours in serum-free RPMI medium for synchronization and then were cultured in RPMI-10% FBS for 24 hours and labeled for 4 hours with BrdU. Finally, cells were labeled with 7AAD and analyzed in a LSR Fortessa cytometer using the FlowJo software.

### Migration assay

Thirty thousand cells were seeded in the upper chamber of transwell culture plate inserts with 5-µm pores (Corning, New York) in RPMI-10% FBS. Stromal cell-derived factor 1 (SDF-1, 100 ng/mL; Sigma-Aldrich) or vehicle was added in the lower chamber to stimulate migration. After 4 hours of incubation, cells in the lower chamber were counted in a LSR Fortessa cytometer using the FlowJo software.

### Enzyme-linked immunosorbent assay

Enzyme-linked immunosorbent assay (ELISA) of IGFBP7 in conditioned culture medium was described elsewhere.<sup>9</sup> Cell lines or primary ALL cells were cultured in serum-free RPMI or AIM-V medium, respectively, for 4 hours, at 250,000 cells per well, in 48-well plates. Cells were left untreated or treated with insulin (500 ng/mL) and/or IGFBP7 (100 ng/mL) for 15 minutes or 4 hours, pelleted, and lysed in RIPA-like buffer (50 mM Tris-HCl; 150 mM NaCl; 1% NP-40;

0.5% sodium deoxycholate; 0.1% sodium dodecyl sulfate) supplemented with 1% phosphatase inhibitor cocktail I (Sigma-Aldrich), 1% phosphatase inhibitor cocktail II (Sigma-Aldrich), 1% protease inhibitor cocktail (Sigma-Aldrich), and 1 mM phenylmethylsulfonyl fluoride (Sigma-Aldrich). Lysates were analyzed using the PathScan Sandwich ELISA Antibody Pair Kits for Phospho-IRS-1 (panTyr), Phospho-Akt1 (Ser473), Phospho-IGF1R $\beta$  (Tyr1131), and Phospho-INSR $\beta$  (Tyr1150/1151; Cell Signaling Technology, Danvers, Massachusetts). To quantify IGF1R $\beta$  and INSR $\beta$  proteins, we adapted the Sandwich ELISA Antibody Pair Kit protocols. Briefly, plates were coated overnight at 4°C, using 10  $\mu$ g cell lysate in 100  $\mu$ L/well. The capture antibodies offered in the PathScan kits were used to detect IGF1R $\beta$  and INSR $\beta$ , followed by incubation with a horseradish peroxidase-conjugated anti-mouse immunoglobulin G (IgG; 1:1000, Cell Signaling Technology).

### Anti-IGFBP7 monoclonal antibody production

Balb/c mice were immunized with a IGFBP7-derived peptide antigen (sequence 100% homologous in human and mouse) by standard methods.<sup>10</sup> Hybridomas were selected by ELISA against the native IGFBP7.<sup>9</sup> The detection limit reached by clone C311 in ELISA against the bovine serum albumin (BSA)-conjugated antigen peptide was 0.05 ng (data not shown). Of note, the peptide antigen has no relevant similarity against any other protein as evaluated by BLASTp.

### Western blot

Cell lines or primary ALL cells were cultured for 4 hours in serum-free RPMI or AIM-V medium, respectively, and then left untreated or stimulated with insulin (500 ng/mL), IGFBP7 (100 ng/mL), and/or anti-IGFBP7 (clone C311; 20  $\mu$ g/mL) for 15 minutes or 4 hours and then pelleted and lysed in RIPA-like buffer. Thirty micrograms of protein was electrophoresed in 10% sodium dodecyl sulfate-polyacrylamide gels and electroblotted onto nitrocellulose membranes. Membranes were immunoblotted overnight at 4°C with antibodies (Cell Signaling Technology) against phospho-Akt (Ser473; clone 9271), phospho-p44/42 MAPK (Erk1/2; Thr202/Tyr204; clone 9101), and  $\beta$ -actin (clone 4967) in Tris-buffered saline with Tween 20 (20 mM Tris, 150 mM NaCl, 0.1% Tween-20) with 2% BSA (Sigma-Aldrich). Immunodetection was performed by incubation with horseradish peroxidase-conjugated anti-rabbit IgG (1:5,000; Cell Signaling Technology) in 5% nonfat dry milk in Tris-buffered saline with Tween 20, for 1 hour at room temperature, and developed using the Super Signal West Pico Chemiluminescent Substrate (Thermo Fisher Scientific). Images were acquired with a ChemiDoc equipment (Bio-Rad, Hercules, California).

### INSR and IGF1R internalization assay

ALL cells ( $2.5 \times 10^5$ ) were starved in serum-free medium (RPMI for cell lines and AIM-V for primary cells) for 4 hours and then were left untreated or stimulated with insulin (500 ng/mL) and/or IGFBP7 (100 ng/mL) for 15 minutes or 4 hours. When indicated, the C311 anti-IGFBP7 antibody was added 210 minutes after the beginning of the 4-hour starvation time. After washing with PBS, the surface expression of INSR and IGF1R was analyzed by labeling cells with the anti-hCD220-PE (clone 3B6; Becton Dickinson) and anti-hCD221-BV421 (clone 1H7; Becton Dickinson) antibodies or the corresponding isotype controls (mIgG1k-PE, clone MOPC-21, and mIgG1k-BV421, clone X40; Becton Dickinson) diluted in 0.5%

BSA in PBS for 30 minutes at 4°C. Cells were analyzed in a LSR Fortessa cytometer using the FlowJo Software.

### In vivo experiments

NOD/SCID (NOD.CB17-Prkdc<sup>scid</sup>/J) mice (Jackson Laboratory, Bar Harbor, Maine) were provided by the animal facility at the State University of Campinas (CEMIB, UNICAMP, Brazil). The NSGS (NOD.Cg-Prkdc<sup>scid</sup>Il2rg<sup>tm1Wj</sup>/Tg(CMV-IL3,CSF2,KITLG)1Eav/MloYsZJ) mice (Jackson Laboratory) were provided by the Boldrini's animal facility. Ten million *IGFBP7* knockdown or Scramble ALL cell lines were injected via the tail vein into nonirradiated NOD/SCID mice. Blood from the retro-orbital plexus was collected weekly to monitor by flow cytometry the percentage of leukemia cells (cells positive for hCD45-FITC, clone HI30; Becton Dickinson) in total CD45<sup>+</sup> mononuclear cells: sum of hCD45<sup>+</sup> and mCD45<sup>+</sup> (mCD45-PE, clone 30F-11; Becton Dickinson). After 4 or 6 weeks, mice were killed, and blood, spleen, liver, and bone marrow were collected to evaluate the percentage leukemia cells. For survival analyses, animals were killed in the moribund state, and Kaplan-Meier curves were compared using the log-rank test. The therapeutic efficacy of C311 anti-IGFBP7 vs polyclonal Balb/c, given intraperitoneally, at 25  $\mu$ g 3 times per week for 4 weeks was tested against a T-cell ALL (T-ALL, patient T979) xenograft in nonirradiated NSGS mice. Treatment initiated 24 hours after transplantation. In another experiment, using a BCP-ALL (patient B1421) and nonirradiated NOD/SCID, treatment awaited overt leukemia ( $\geq 0.5\%$  hCD45 cells in the peripheral blood of half of the animals), and consisted of 20  $\mu$ g of the C311 anti-IGFBP7 or an irrelevant anti-PSA (Rheabiotech) antibody, intraperitoneally, 3 times per week for 4 weeks. The percentage of ALL cells in peripheral blood mononuclear cells was monitored weekly. The study was approved by the Animal Experimentation Ethics Committees of the State University of Campinas (CEUA/UNICAMP, protocol 1133/2008) and Centro Infantil Boldrini (CEUA/BOLDRINI, protocol 0006/2020).

## Results

### IGFBP7 knockdown or neutralization decrease the proliferation, survival, and migration of ALL cell lines

To determine whether IGFBP7 has an autocrine role in ALL, different BCP- and T-ALL cell lines were stably transduced with lentiviral particles carrying shRNA constructs directed against IGFBP7 (sh.959 and sh.812) or a noncoding random sequence (sh.Scramble). Downregulation of secreted IGFBP7 levels was confirmed by ELISA and Western blot (supplemental Figure 1A-B). *IGFBP7* knockdown markedly reduced the growth rate of sh.IGFBP7 cells in comparison with sh.Scramble-transduced controls (Figure 1A; supplemental Figure 1C), confirming our previous findings on the mitogenic effect of IGFBP7 in BCP-ALL cell lines.<sup>9</sup> Accordingly, BrdU incorporation assays revealed a decreased rate of nucleotide incorporation during S-phase on *IGFBP7* downregulation, accompanied by rising of the sub-G1/G0 population of apoptotic cells (Figure 1B; supplemental Figure 2A). The deleterious effect of *IGFBP7* knockdown on cell viability was confirmed by culturing sh.959 or control cells with suboptimal (3%) serum concentration (Figure 1C; supplemental Figure 2B-C).



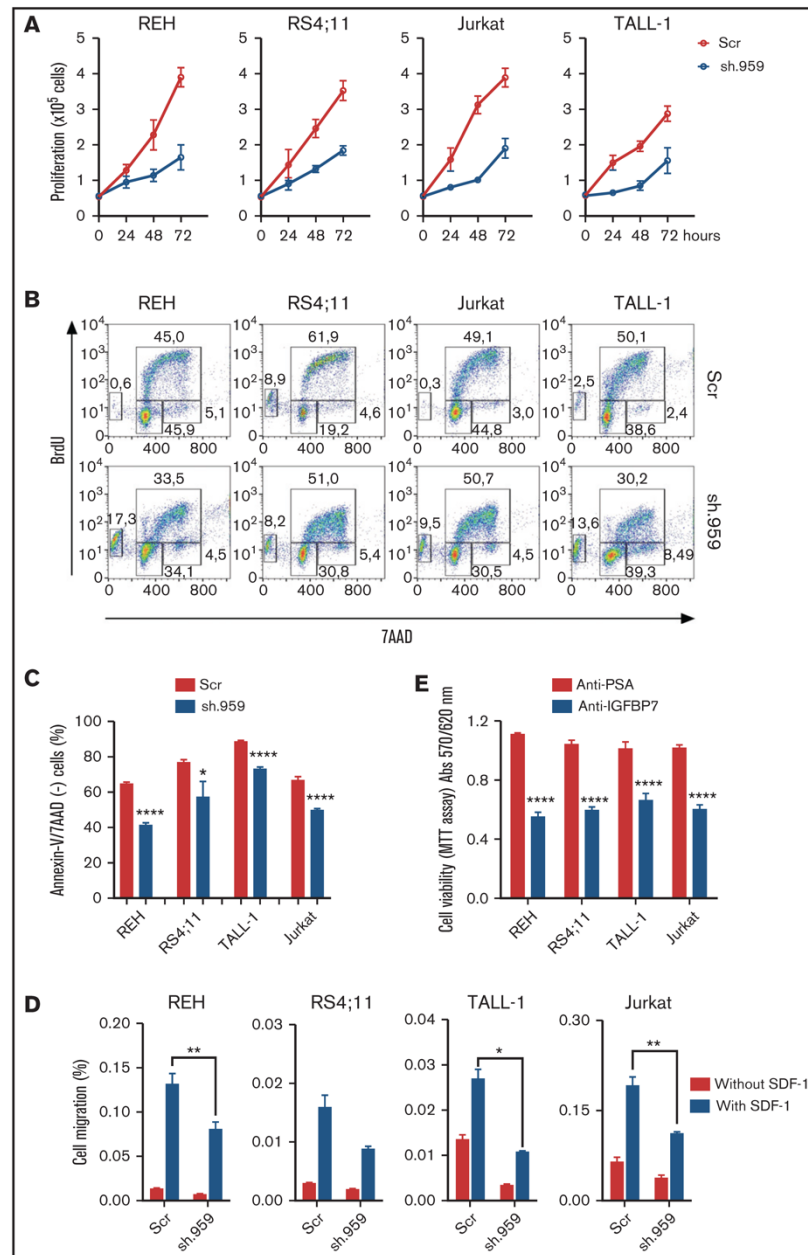


**Figure 1. IGFBP7 knockdown or neutralization decreases ALL cell line proliferation, survival, and migration.** (A) Proliferation of REH, RS4;11 (BCP-ALL), TALL-1, and Jurkat (T-ALL) cell lines stably transduced with lentivirus expressing shRNA against IGFBP7 (sh.959) or scramble control (Scr) analyzed by the trypan blue exclusion technique. Results from 3 independent experiments run in triplicate wells, using RPMI-3% FBS. (B) Cell cycle analysis of cells after 4-hour incubation with BrdU, using RPMI-10% FBS. The percentage of cells in G0/G1, S-phase, G2/M, and in apoptosis (sub-G0/G1) was evaluated by flow cytometry. Results representative of 3 independent experiments run in triplicate wells (see supplemental Figure 2A). (C) Cells were cultured in RPMI-3% FBS for 24 hours, and the percentage of apoptotic cells was

Chemokines and cell migration play a key role in establishing the leukemia bone marrow niche and in organs infiltration on disease progression. *IGFBP7* knockdown significantly reduced the migration of ALL cells in the transwell system toward SDF-1 (Figure 1D). Being an extracellular protein, *IGFBP7* is an attractive target for therapeutic intervention using monoclonal antibodies. We produced an anti-*IGFBP7* antibody (clone C311) and tested its effects on ALL cell viability. Both our own antibody (Figure 1E) and a commercial one (supplemental Figure 2D) significantly reduced ALL cell viability when added to the culture medium, whereas no effect was seen with an anti-PSA control.

### **IGFBP7 potentiates the insulin prosurvival effect on primary ALL cells**

After confirming by orthogonal approaches that *IGFBP7* exerts an autocrine mitogenic and prosurvival effect in ALL, we investigated whether this was dependent on the presence of its ligand insulin. As shown in Figure 2A-B, *IGFBP7* mitogenic action was clearly dependent on the combined addition of insulin. Although *IGFBP7* or insulin alone promoted cell proliferation in half of the samples tested, their effect was clearly higher and more frequent when used in combination (supplemental Figure 3).

Because cell lines are not good surrogates for primary ALL cells, some experiments were repeated using short-term culture of primary BCP- and T-ALL cells. As shown in Figure 2C-D (supplemental Figure 4A), the combined addition of *IGFBP7* and insulin protected primary ALL cells from apoptosis, as visualized by the increased number of Annexin-V/7AAD-negative cells. Likewise, addition of anti-*IGFBP7* antibody (clone C311) resulted in a drastic reduction of cell viability (Figure 2E; supplemental Figure 4B). No clear association could be found between the survival of ALL cells and the corresponding mRNA expression levels of *INSR*, *IGF1R*, or *IGFBP7* (supplemental Figure 5A-B). Of note, these experiments were performed using physiologic levels of *IGFBP7*, which in the diagnostic bone marrow plasma from children with ALL is ~50 ng/mL.<sup>9</sup> When nonphysiologic, much higher concentrations were used (20 µg/mL) to reproduce some of our fellows' contradictory results<sup>11,12</sup> *IGFBP7* caused an inhibitory effect on primary ALL cell viability (Figure 2F; supplemental Figure 4C).

### **IGFBP7 prolongs IGF1R but not INSR activation in primary ALL cells**

Insulin/IGFs act by binding to homo- or heterodimeric INSR and IGF1R cell surface tyrosine kinase receptors that recruit and phosphorylate insulin receptor substrate proteins (IRS1-4), thus initiating the downstream activation of the phosphatidylinositol 3-kinase/Akt/mTOR and Ras/Raf/MAPK signaling pathways.<sup>2</sup> Here we found that *IGFBP7* significantly enhanced IRS-1 (pan-tyrosine) phosphorylation on insulin stimulation (Figure 3A). Interestingly, treatment of ALL cell lines with *IGFBP7* plus insulin resulted in increased IRS-1

phosphorylation for at least 4 hours but not when these factors were added separately. Likewise, *IGFBP7* plus insulin prolonged Akt (S473) and Erk1/2 phosphorylation in *IGFBP7* knockdown cell lines (Figure 3B). Sustained Akt (S473) phosphorylation by the combined stimulation of cells with *IGFBP7* plus insulin was confirmed in 18 primary ALL samples analyzed (Figure 4A; supplemental Figure 6; supplemental Table 1). When the status of IGF1Rβ (Tyr1131) and INSRβ (Tyr1150/1151) was addressed, both showed similar levels of activation at the 15-minute time point and both for the insulin and *IGFBP7* plus insulin treatments. At the 4-hour time point, however, only the IGF1Rβ (Tyr1131) remained phosphorylated and exclusively when primary ALL cells were treated with the *IGFBP7* plus insulin combination. Insulin treatment alone was not sufficient to keep the receptor active (Figure 4B-C; supplemental Figures 7 and 8). Similar results were obtained with the use of IGF1; however, doses 5 times lower than insulin were required, because 5 ng/mL IGF1 resulted in IGF1Rβ (Tyr1131) phosphorylation at levels equal to those obtained with 25 ng/mL of insulin (Figure 4D). Two conclusions could be drawn from these findings: first, *IGFBP7* did not simply increase the half-life of insulin,<sup>2</sup> otherwise both IGF1R and INSR should have been activated at the 4-hour time point; and second, the IGF1R seemed to be the candidate molecule in mediating the *IGFBP7* potentiation of insulin/IGF1 stimulus. To picture the importance of IGF1R in ALL, we silenced the *IGF1R* gene in the REH and Jurkat cell lines using an Isopropyl β-D-1-thiogalactopyranoside (IPTG)-inducible shRNA vector. *IGF1R* knockdown was strongly detrimental in terms of proliferation and survival of both cell lines (Figure 4E-F; supplemental Figure 9A-B).

A previous work has shown that the N-terminal 97-amino-acid portion of *IGFBP7* binds to the extracellular portion of IGF1R and suppresses its internalization in response to IGF1.<sup>11</sup> Here we confirmed these findings both in ALL cell lines and primary ALL cells (Figure 5A-B; supplemental Figure 10). As expected, insulin treatment of serum-starved ALL cells resulted in significant internalization of both the INSR and IGF1R receptors. When insulin was added in conjunction with *IGFBP7*, however, only the INSR was internalized, whereas IGF1R remained at the cell surface for as long as the 4 hours tested. As expected, preincubation of ALL cells with the anti-*IGFBP7* antibody (clone C311) abolished *IGFBP7*-induced IGF1R retention at the cell surface. Treating of ALL cells with primaquine or cycloheximide did not interfere with *IGFBP7*-mediated cell surface retention of IGF1R (Figure 6A-B), suggesting that receptor recycling or synthesis did not contribute to the surface maintenance of IGF1R. Interestingly, treating of *IGFBP7*-silenced cell lines with the endocytosis inhibitor dansylcadaverine partially restored their proliferative response to insulin (Figure 6C-D). These results are consistent with the notion that *IGFBP7* exerts its effects through binding and stabilization of the IGF1R receptor at the surface of ALL cells, thus prolonging its response to insulin.

**Figure 1. (continued)** evaluated by flow cytometry after Annexin-V-FITC/7AAD staining. Bars represent means ± standard error (SE) of 4 independent experiments run in duplicate wells. See also supplemental Figure 2C. (D) Migration of ALL cells in the transwell system toward SDF-1 (100 ng/mL) or PBS 1×, using RPMI-10% FBS. Cells in the lower chamber were counted by flow cytometry after 4-hour migration. Bars represent means ± SE for triplicate wells. (E) Viability of ALL cells measured by the MTT assay after 48-hour culture in RPMI-10% FBS supplemented with an anti-*IGFBP7* (clone C311, 20 µg/mL) or anti-PSA control (20 µg/mL) monoclonal antibody. Bars represent means ± SE for 3 independent experiments run in triplicate wells. Statistical analyses were done by 1- or 2-way analysis of variance (ANOVA) and Bonferroni posttests (\**P* ≤ .05, \*\**P* .01, \*\*\**P* .001, and \*\*\*\**P* .0001).

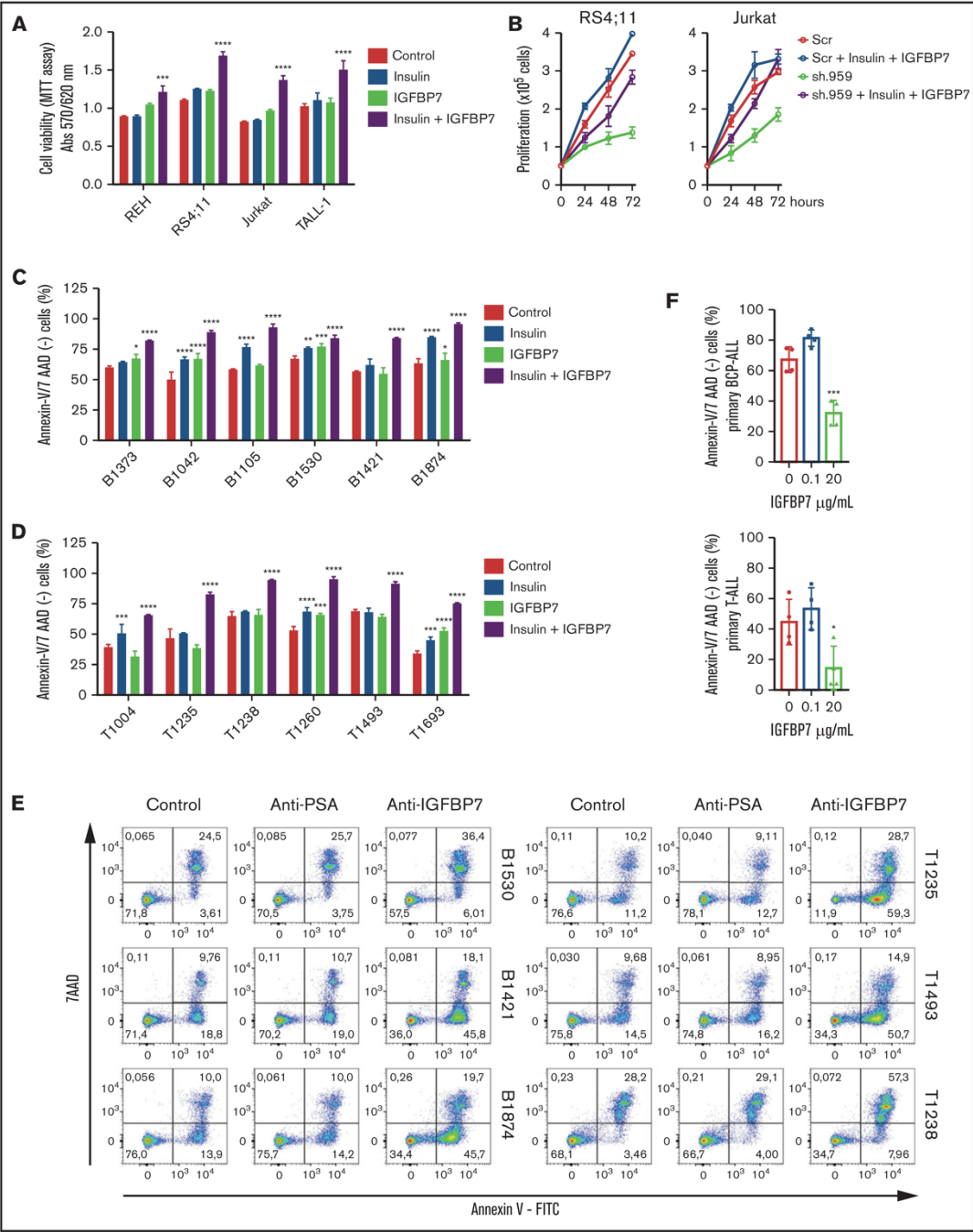
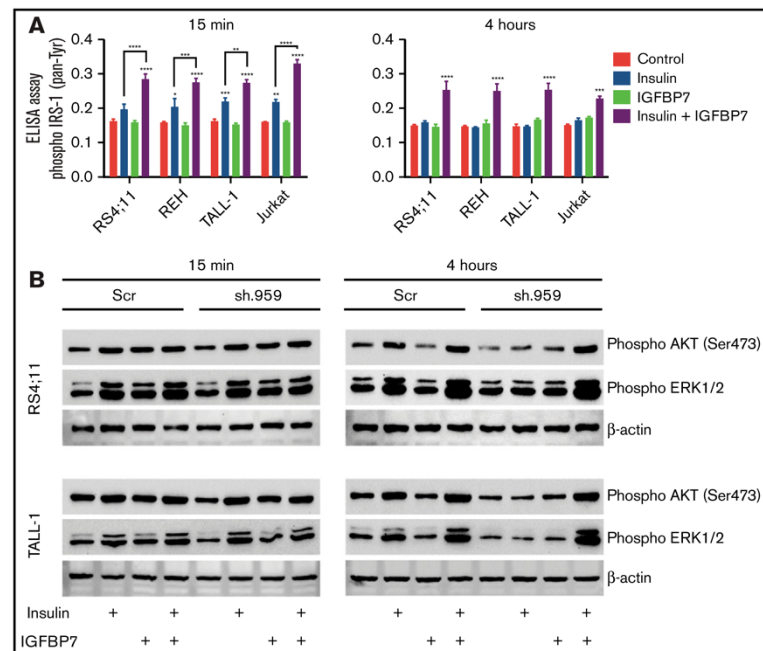


Figure 2.



**Figure 3. IGFBP7 prolongs IRS, AKT, and ERK activation by insulin in ALL cell lines.** (A) ELISA results for Phospho-IRS-1 (pan-Tyrosine; #7133, Cell Signaling Technology) on different ALL cell lines that were starved for 4 hours in serum free RPMI-1640 medium and then left untreated (Control) or stimulated for 15 minutes or 4 hours with insulin (500 ng/mL) and/or IGFBP7 (100 ng/mL). Bars represent means  $\pm$  SE for triplicate wells. (B) Western blot results for Phospho-Akt (Ser473) and Phospho-Erk1/2 on the RS4;11 and TALL-1 ALL cell lines stably expressing a scramble shRNA (Scr) or shRNA against IGFBP7 (sh.959), after 4-hour starvation in serum-free RPMI-1640 and left untreated or stimulated for the indicated time with insulin (500 ng/mL) and/or IGFBP7 (100 ng/mL). The effect of IGFBP7 in prolonging (4 hours) AKT and ERK activation is better visualized in sh.959 cells. Of note, IGFBP7 is not needed for the short-term (15 minutes) stimulation of ALL cells with insulin (supplemental Figure 14). Statistical analysis was done by 2-way ANOVA and Bonferroni posttests (\* $P$ .05, \*\* $P$ .01, \*\*\* $P$ .001, and \*\*\*\* $P$ .0001).

### IGFBP7 knockdown or neutralization decreases the progression of ALL in vivo

Considering the complexity of the insulin/IGF system, in vitro experiments are just a poor approximation for the real situation. For instance, several proteases are known to cleave IGFBPs/IGFBP-rPs, liberating insulin/IGF for INSR/IGF1R binding. In addition, interaction of IGFBPs/IGFBP-rPs with extracellular matrix components can modulate their affinity for insulin/IGFs.<sup>13</sup> To address the leukemogenic potential of autocrine IGFBP7 secreted by ALL cells,

under physiologic paracrine/endocrine IGFBP7 levels and under the interaction/competition with other cells and molecules, we transplanted the sh.959 cell lines into immunocompromised NOD/SCID mice. Silencing of *IGFBP7* resulted in significant attenuation of leukemia progression, as evaluated by the percentage of leukemia cells (human CD45<sup>+</sup>) in the peripheral blood, bone marrow, liver, and spleen, in relation to mice transplanted with Scramble cells (Figure 7A). Moreover, *IGFBP7* knockdown resulted in a significant increase in the Kaplan-Meier survival curves of mice (Figure 7B). Similar results were obtained in mice transplanted with patient-

**Figure 2. The prosurvival effect of IGFBP7 is insulin (IGF) dependent.** (A) ALL cell lines were cultured in RPMI-10% FBS supplemented with insulin (500 ng/mL) and/or IGFBP7 (100 ng/mL) for 48 hours. Cell viability was quantified by the MTT assay. Bars represent means  $\pm$  SE for 2 independent experiments run in triplicate wells. (B) Proliferation of RS4;11 and Jurkat cell lines expressing shRNAs against IGFBP7 (sh.959) or scramble control (Scr) analyzed by the trypan blue exclusion technique after insulin (500 ng/mL) and/or IGFBP7 (100 ng/mL) treatment. Results from a single experiment run in triplicate wells, using RPMI-3% FBS. See also supplemental Figure 3. (C) Primary BCP-ALL cells after 48 hours or (D) primary T-ALL cells after 24 hours cultured in AIM-V serum-free medium supplemented with insulin (500 ng/mL) and/or IGFBP7 (100 ng/mL). Cell viability was measured by Annexin-V/7AAD staining and flow cytometry. Bars represent means  $\pm$  SE of Annexin-V/7AAD negative fraction of 2 independent experiments run in duplicate wells. See also supplemental Figure 4A. (E) Primary BCP or T-ALL cells were cultured in AIM-V serum-free medium (Control) supplemented with an anti-PSA control (20  $\mu$ g/mL) or anti-IGFBP7 antibody (clone C311, 20  $\mu$ g/mL) for 48 or 24 hours, respectively. Apoptosis was measured by Annexin-V/7AAD staining and flow cytometry. See also supplemental Figure 4B. High IGFBP7 concentrations (20  $\mu$ g/mL) are detrimental to primary BCP- and T-ALL (F) cells after 24 hours of treatment in AIM-V serum-free medium supplemented with insulin (500 ng/mL). See also supplemental Figure 4C. Statistical analysis was done by 1- or 2-way ANOVA and Bonferroni posttests (\* $P$ .05, \*\* $P$ .01, \*\*\* $P$ .001, and \*\*\*\* $P$ .0001).

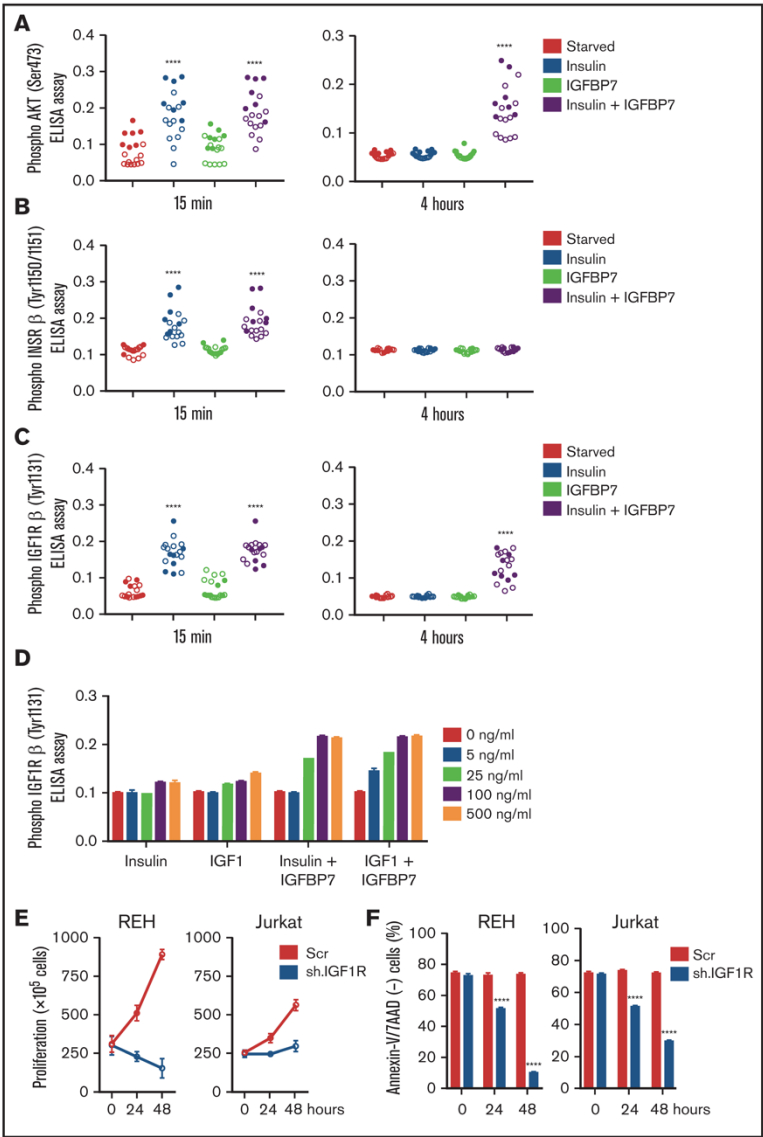


**Figure 4.** IGFBP7 prolongs IGF1R activation by insulin or IGF1 in primary ALL cells. (A) ELISA results for AKT (Ser473) phosphorylation, (B) INSR $\beta$  (Tyr1150/1151) phosphorylation, and (C) IGF1R $\beta$  (Tyr1131) phosphorylation in 11 primary BCP (open circles) and 7 T-ALL (solid circles) cells cultured in AIM-V serum-free medium supplemented with insulin (500 ng/mL), IGFBP7 (100 ng/mL), or a combination of both for 15 minutes and 4 hours. Circles represent means of 2 independent experiments run in duplicate wells. See also supplemental Figures 6, 7, and 8. (D) Dose-response effect for insulin and IGF1, alone or in combination with IGFBP7, on long-term (4 hours) phosphorylation of IGF1R $\beta$  (Tyr1131) as measured by ELISA. Bars represent means  $\pm$  SE for duplicate wells. (E) Proliferation and (F) survival of REH and Jurkat cell lines stably transduced with IPTG-inducible shRNA vectors against *IGF1R* or Scramble control (Scr), after 24 and 48 hours of IPTG (1  $\mu$ g/mL) stimulation, as measured by the trypan blue exclusion technique and Annexin-V/7AAD staining, respectively. Bars represent means  $\pm$  SE for 2 independent experiments run in triplicate wells. See also supplemental Figure 9A-B. Statistical analysis was done by 1- or 2-way ANOVA and Bonferroni posttests (\*\*\*\**P* .0001).



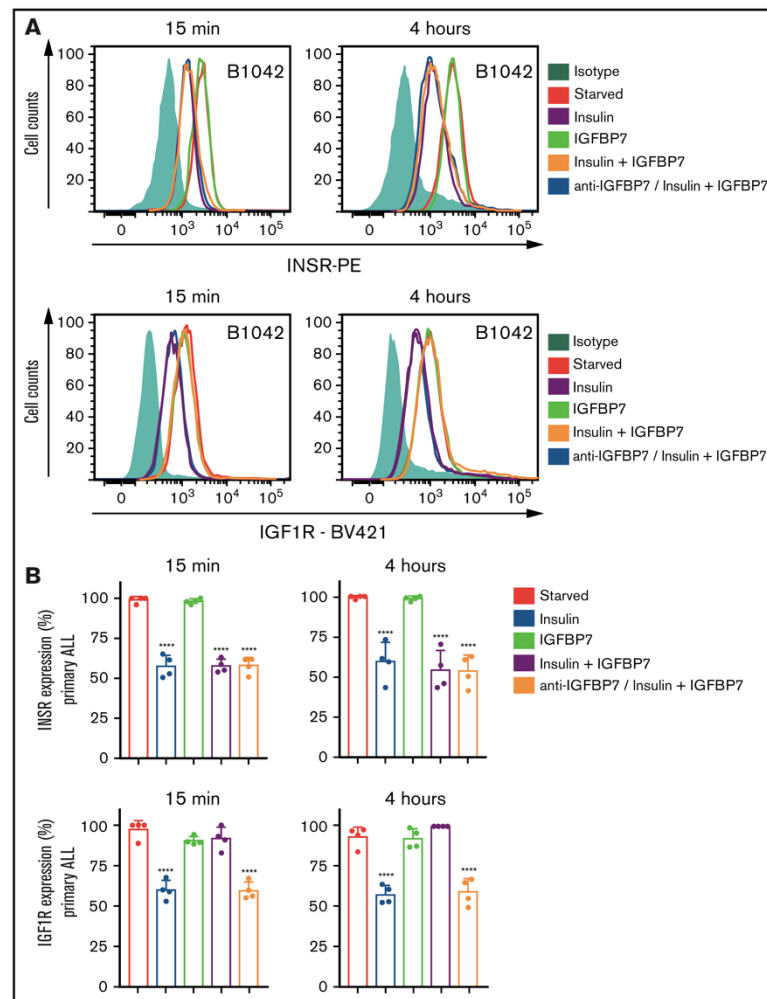


**Figure 5. IGFBP7 inhibits IGF1R internalization on insulin stimulation.** (A) Cell surface expression of the INSR and IGF1R in a representative case of serum-starved primary BCP-ALL (B1042) cells after 15 minutes or 4 hours of treatment with insulin (500 ng/mL), IGFBP7 (100 ng/mL), anti-IGFBP7 (clone C311, 20  $\mu$ g/mL), or associations, as measured by flow cytometry analysis. The anti-IGFBP7 antibody (clone C311) was added 30 minutes before insulin/IGFBP7 addition. (B) Normalized results from 4 different primary BCP-ALL (B1042 and B1421) and T-ALL (T1238 and T1260) cells, according to the times and treatments described above. A histogram overlay was used to calculate the percentage of labeled cells with respect to cells left untreated (Starved). See also supplemental Figure 10. Statistical analysis was done by 1-way ANOVA and Bonferroni posttests (\*\*\*\* $P$  < .0001).

derived xenografts (PDX-ALL; Figure 7C-D) or the RS4;11 cell line (Figure 7E). Mice treated with the anti-IGFBP7 antibody (clone C311) showed decreased leukemic progression and survived longer than animals treated with an isotype or polyclonal antibody controls. Of note, the mouse ortholog of IGFBP7 is functional on human IGF1R (supplemental Figure 11), and our anti-IGFBP7 antibody binds both human and mouse IGFBP7 (supplemental Figure 2E).

## Discussion

Although insulin and IGF1 have been known to enhance ALL survival/proliferation in vitro for decades,<sup>14-16</sup> their role in ALL has not been fully explored, except in T-ALL where IGF1R expression was shown to be under Notch1 control and to play a fundamental role in T-ALL progression and transplantability in mice.<sup>17,18</sup> Interestingly, tumor-associated dendritic cells support T-ALL growth via IGF1R activation.<sup>19</sup> Our gene expression data indicate that primary BCP-

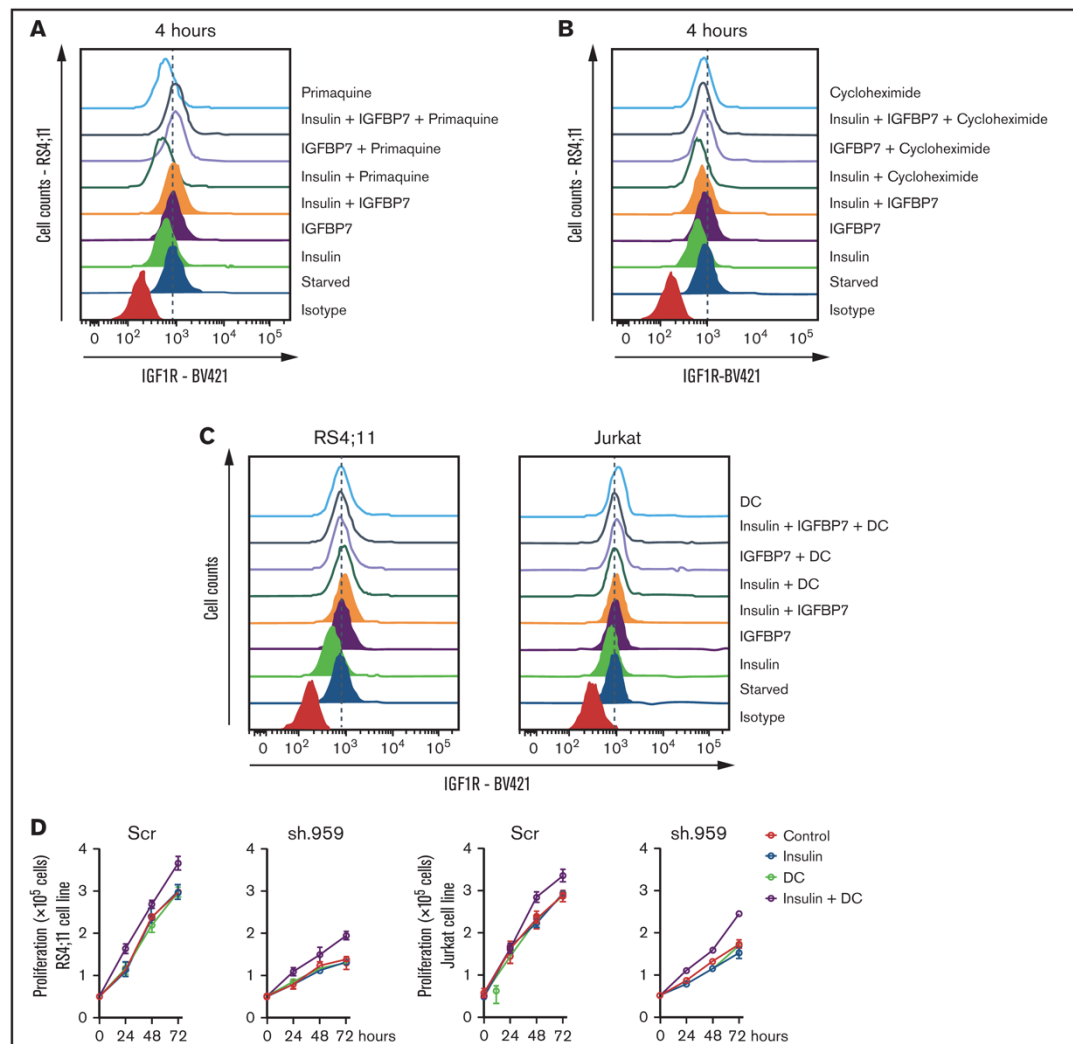


**Figure 6.** Receptor recycling or synthesis do not contribute to IGF1R retention at the cell surface on IGFBP7 treatment. RS4;11 or Jurkat cells were starved for 4 hours in serum-free RPMI medium and then left untreated or stimulated for 4 hours with insulin (500 ng/mL), IGFBP7 (100 ng/mL), and their combination. Receptor recycling, synthesis, and endocytosis were inhibited by concomitant addition of (A) primaquine (100  $\mu$ M), (B) cycloheximide (20  $\mu$ M), or (C) dansylcadaverine (DC; 10  $\mu$ g/mL), respectively. The cell surface expression of IGF1R was measured by flow cytometry. (D) Proliferation of RS4;11 and Jurkat cells expressing shRNAs against IGFBP7 (sh.959) or scramble control (Scr) analyzed by the trypan blue exclusion technique after treatment with insulin (500 ng/mL), dansylcadaverine (DC; 10  $\mu$ g/mL), or their combination. Results from a single experiment run in triplicate wells, using RPMI-3% FBS.

ALL and T-ALL express both the *INSR* and *IGF1R*, although *INSR* seemed lower in T-ALL (supplemental Figure 12B). This was confirmed by us (Figure 5A; supplemental Figure 10) and others<sup>5,18</sup> by flow cytometry analyses. Thus, ALL cells seem ready to respond to insulin/IGFs. However, as we showed here, addition of insulin/IGFs alone has a rather small effect on ALL survival (supplemental Figure 13). Association of IGFBP7 with the insulin/IGF stimulus seemed

mandatory to have any significant effect on primary ALL survival, and this may be the reason why the role of insulin/IGF1 in ALL biology could have been underappreciated in previous studies.

High *IGFBP7* expression has been associated with treatment resistance<sup>20</sup> and/or worse prognosis in ALL.<sup>9,21,22</sup> Here, we demonstrate that IGFBP7 exerts an autocrine prosurvival and mitogenic

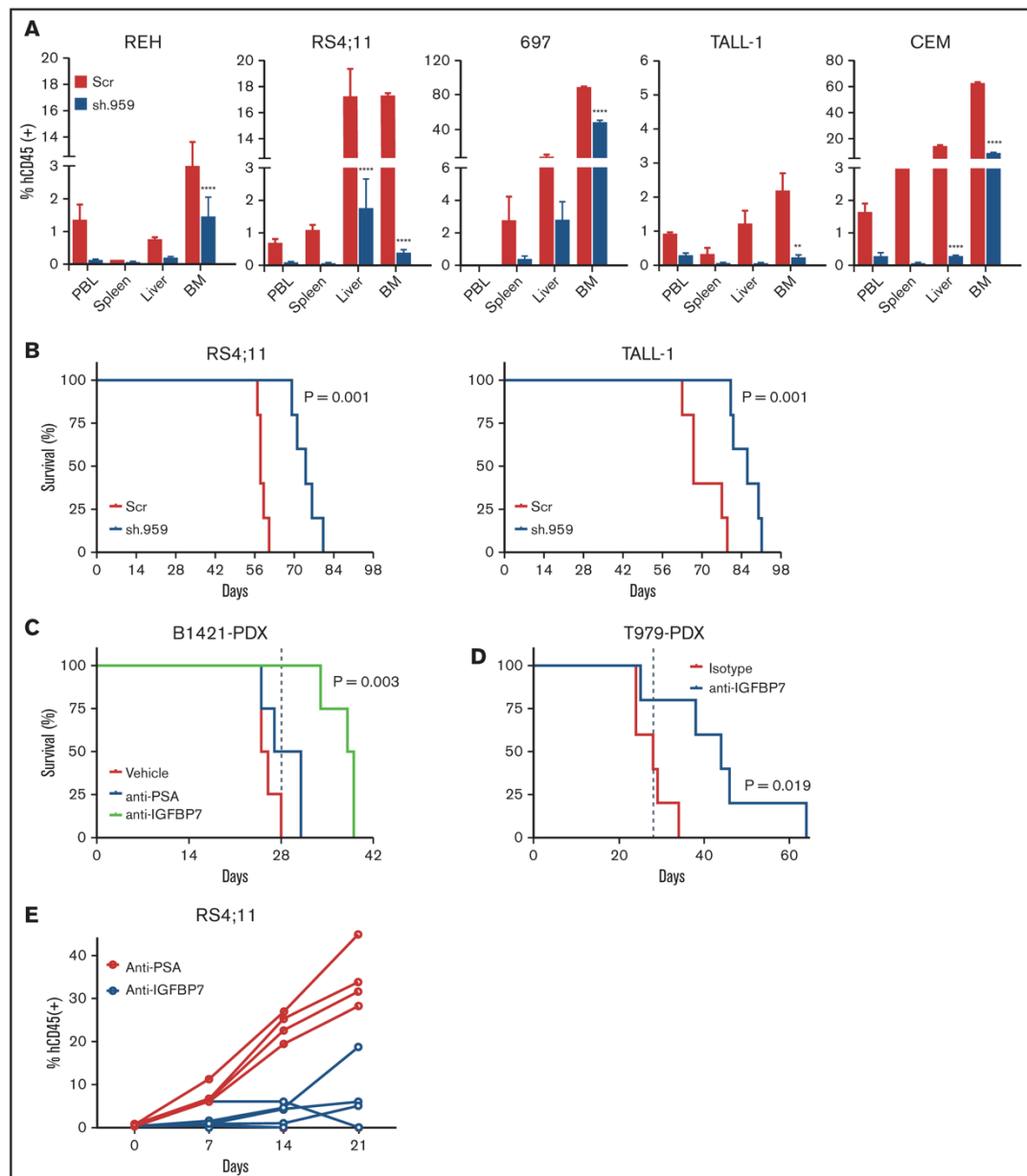


**Figure 7. IGFBP7 knockdown or neutralization decreases the progression of ALL in vivo.** (A) NOD/SCID mice were transplanted with 10 million sh.959 or Scramble (Scr) ALL cell lines. After 4 (REH, RS4;11, and 697) to 6 (TALL-1 and CCRF-CEM) weeks, animals were killed and evaluated for the percentage of leukemia (hCD45<sup>+</sup>) cells in the peripheral blood (PBL), spleen, liver, and bone marrow (BM) by flow cytometry. Bars represent means  $\pm$  SE for 3 animals. Statistical analysis was done by 2-way ANOVA and Bonferroni posttests (\*\* $P \leq .01$  and \*\*\*\* $P \leq .0001$ ). (B) Kaplan-Meier survival curves of NOD/SCID mice (5 animals per group) transplanted with sh.959 or Scramble (Scr) ALL cells. (C) Survival curves of NOD/SCID mice transplanted with a patient-derived BCP-ALL xenograft (B1421-PDX) and treated with the anti-IGFBP7 (clone C311) or anti-PSA antibody, as above, for 4 weeks. Treatment of mice (4 animals per group) started when half of the animals had  $\geq 0.5\%$  of leukemia cells

effect on ALL that is dependent on insulin/IGFs. Results were confirmed *in vivo*. By using *IGFBP7* knockdown ALL cell lines or antibody-mediated neutralization of *IGFBP7* in animals transplanted with primary ALL, we demonstrated the relevance of autocrine or extracellularly available *IGFBP7* levels, respectively, in ALL fitness, at physiologic concentrations of insulin, IGFs, *INSR*, *IGF1R*, *IGFBPs*, extracellular matrix components, and all other factors that modulate insulin/IGF action.<sup>4</sup>

On activation and autophosphorylation, receptor tyrosine kinases undergo rapid internalization, mainly by clathrin-mediated endocytosis.<sup>23</sup> The *INSR* has a C-terminal motif for *MAD2* binding, which in turn recruits *BUBR1* and the clathrin adaptor protein complex *AP2*, which facilitates clathrin coating and endocytosis on receptor activation.<sup>24</sup> Conversely, *IGF1R* has no such *MAD2* binding motif and exhibits prolonged perdurance at the cell surface, apparently mediated by *IRS-1* binding to and blocking of *AP2*.<sup>25</sup> In keeping with previous findings in breast cancer,<sup>11</sup> we found that *IGFBP7* inhibited *IGF1R* internalization despite insulin stimulation. The cell surface retention of *IGF1R* in ALL was found to prolong the insulin-induced phosphorylation of *IGF1R* $\beta$ , *IRS-1*, *ERK*, and *AKT*. In contrast, in breast cancer MCF10A and MCF10CA1a cell lines, the cell surface-retained *IGF1R* was insensitive to *IGF1* or insulin. Hypothetically, *IGFBP7* binding to unoccupied *IGF1R* sterically restricts or allosterically prevents subsequent binding of *IGF1*/insulin.<sup>11</sup> However, this inhibitory effect required preincubation of breast cancer cells for 2 hours with *IGFBP7* before addition of growth factors. Simultaneous addition of *IGFBP7* with insulin/*IGF1* had no effect.<sup>11</sup> Here, *IGFBP7* and insulin or *IGF1* was added simultaneously. Although differences in the *INSR*/*IGF1R* signaling and/or internalization complexes between ALL and breast cancer cells should not be undervalued, we suspect that the amount of *IGFBP7* added to cells likely contributed to the discrepancy. Evdokimova et al<sup>11</sup> used *IGFBP7* at 20  $\mu$ g/mL, whereas we used 100 ng/mL. At 20  $\mu$ g/mL, we also found an inhibitory effect of *IGFBP7* on ALL cells. It is plausible that at this high concentration, *IGFBP7* may indeed restrict or prevent *IGF1*/insulin binding to the *IGF1R*, but 20  $\mu$ g/mL is far above the physiologic levels of *IGFBP7* in adult serum (21–35 ng/mL)<sup>26</sup> or childhood ALL bone marrow plasma (49 ng/mL).<sup>9</sup> Unfortunately, the use of supraphysiologic amounts of *IGFBP7* has been the rule rather than the exception in the literature. As shown here, physiologic levels of *IGFBP7* promoted the perdurance of *IGF1R* at the surface of ALL cells, prolonging insulin/IGFs stimulation. Accordingly, a recent study in mouse hepatocytes showed that *IGFBP7* (20 ng/mL) binds to the *INSR*, potentiating its activation by insulin.<sup>27</sup> Likewise, ectopic expression of *IGFBP7* in the breast cancer MDA-MB468 cell line enhanced *IGF1R* $\beta$ /*INSR* $\beta$  phosphorylation by insulin,<sup>11</sup> an effect probably resulting from *IGF1R* $\beta$  activation because this cell line expresses very low levels of *INSR*.<sup>28</sup>

ALL cells express both the *INSR* (*INSR-A* isoform) and the *IGF1R* (supplemental Figure 12A–B). *INSR* and *IGF1R* form hybrid receptors consisting of one molecule of *INSR* and one molecule of *IGF1R*. Homotypic *INSR* and *IGF1R* have the strongest binding affinity for

insulin and *IGF1*, respectively, whereas *INSR*/*IGF1R* hybrid receptors display high affinity binding for both insulin and *IGF1*.<sup>29</sup> At the supraphysiologic levels (500 ng/mL or 100 nM) used in this study, insulin was expected to bind *INSR*, *IGF1R*, and *INSR*/*IGF1R* receptors. However, only *IGF1R* was retained at the cell surface and showed prolonged phosphorylation on *IGFBP7*/insulin treatment of ALL cells. Previous coimmunoprecipitation assays demonstrated that *IGFBP7* binds the extracellular part of *IGF1R* but not *INSR*.<sup>11</sup> Thus, we deduce that *IGFBP7* exerted its effect by binding to homotypic *IGF1R*. Otherwise, we would expect the *INSR* chain, at least from heterotypic *INSR*/*IGF1R* receptors, to be phosphorylated as well.

Insulin is at least 200-fold less specific for the *IGF1R* than is *IGF1*.<sup>29</sup> Interestingly, monoclonal antibodies directed against the extracellular part of *IGF1R* are able to dramatically increase insulin binding to homotypic *IGF1R* to affinity levels approaching *IGF1* binding. Apparently, these antibodies could promote insulin binding by inducing a conformational change in the *IGF1R*, which results in loss of inhibitory constraints.<sup>30</sup> We speculate whether something similar was produced by *IGFBP7*, because 25 ng/mL insulin was able to activate the *IGF1R* to levels equivalent to those obtained with 5 ng/mL *IGF1* (ie, a fivefold difference only).

Different drugs and antibodies targeting *IGF1R* have been developed, but most did not advance to clinical trials.<sup>31</sup> The similarity between *IGF1R* and *INSR* receptors and their heterodimerization has been a challenge to the design of specific therapeutic drugs targeting *IGF1R*.<sup>3</sup> The SCH 717454 monoclonal antibody against *IGF1R* has shown promising *in vivo* results against 2 of 8 ALL samples tested.<sup>31</sup> Here we present *IGFBP7* as a new target candidate for therapeutic antibodies directed to modulate the insulin/IGF system. We showed that *IGFBP7* neutralization using a monoclonal antibody was safe (in mice) and resulted in significant increments on the survival of mice transplanted with patient-derived xenografts. Although dose-response experiments were not performed, the anti-*IGFBP7* antibody was used at 1 mg/kg, every 3 days, which was compatible to that of a recent preclinical study with an Fc-engineered CD19 antibody.<sup>32</sup>

In conclusion, we confirmed the notion that insulin/IGFs are important mitogenic and pro-survival factors in ALL and revealed *IGFBP7* as a relevant player in this context and as a valid target for therapeutic intervention in the treatment of leukemia and possibly other cancers that involve the IGF system.

## Acknowledgments

The authors thank Maria Carolina Spago and Marcia Cristina Fornazim, from the State University of Campinas, for excellent technical help with cell culture experiments. L.L.A., A.B.A.L., L.W.C., J.R.C., and P.P.Z. received a scholarship from Fundação de Amparo à Pesquisa do Estado de São Paulo (FAPESP). J.A.Y. received a productivity fellowship from the Brazilian National Counsel of Technological and Scientific Development (CNPq, process 305896/2013-0 and 301596/2017-4). This

**Figure 7. (continued)** (hCD45<sup>+</sup>) in the peripheral blood. (D) Survival curves of NSGS mice (5 animals per group) transplanted with a patient-derived T-ALL xenograft (T979-PDX) and treated intraperitoneally with 20  $\mu$ g, 3 times per week, of anti-*IGFBP7* (clone C311) or polyclonal Balb/c antibodies (isotype). Treatment started 1 day after transplantation and lasted for 4 weeks. Survival curves were compared by the log-rank test. (E) Progression of RS4;11 cells into NOD/SCID mice treated with 20  $\mu$ g anti-*IGFBP7* (clone C311) or anti-PSA antibody given intraperitoneally 3 times per week. The percentage of leukemia cells (hCD45<sup>+</sup> cells) in peripheral blood mononuclear cells was evaluated by flow cytometry. Curves are for individual animals.



work was supported by grants to J.A.Y. from CNPq (471003/2013-1) and FAPESP (12/12802-1 and 14/20015-5).

## Authorship

Contribution: L.L.A., A.B.A.L., and J.A.Y. conceived and designed the study; L.L.A. and A.B.A.L. performed all experiments; L.W.C., J.B.C.C., and S.R.B. performed cellular signal transduction analyses by Western blot; J.R.C. performed fluorescence-activated cell sorting analysis; P.P.Z. performed antibody production and PDX animal experiment; A.E.N. contributed analytical tools; S.R.B. contributed patient's samples and the corresponding clinical data; and L.L.A.,

A.B.A.L., and J.A.Y. performed statistical analysis and wrote the manuscript.

Conflict-of-interest disclosure: The authors declare no competing financial interests.

ORCID profiles: J.A.Y., 0000-0002-1316-3525; L.L.A., 0000-0003-4691-2446; L.W.C., 0000-0003-1012-4747; J.R.C., 0000-0003-1502-0293; P.P.Z., 0000-0002-8662-7458; J.B.C.C., 0000-0002-0136-0943; A.E.N., 0000-0003-0648-6913; S.R.B., 0000-0003-3696-9852.

Correspondence: José Andrés Yunes, 1270 Dr. Gabriel Porto St, Campinas, SP 13083-210, Brazil; e-mail: andres@boldrini.org.br.

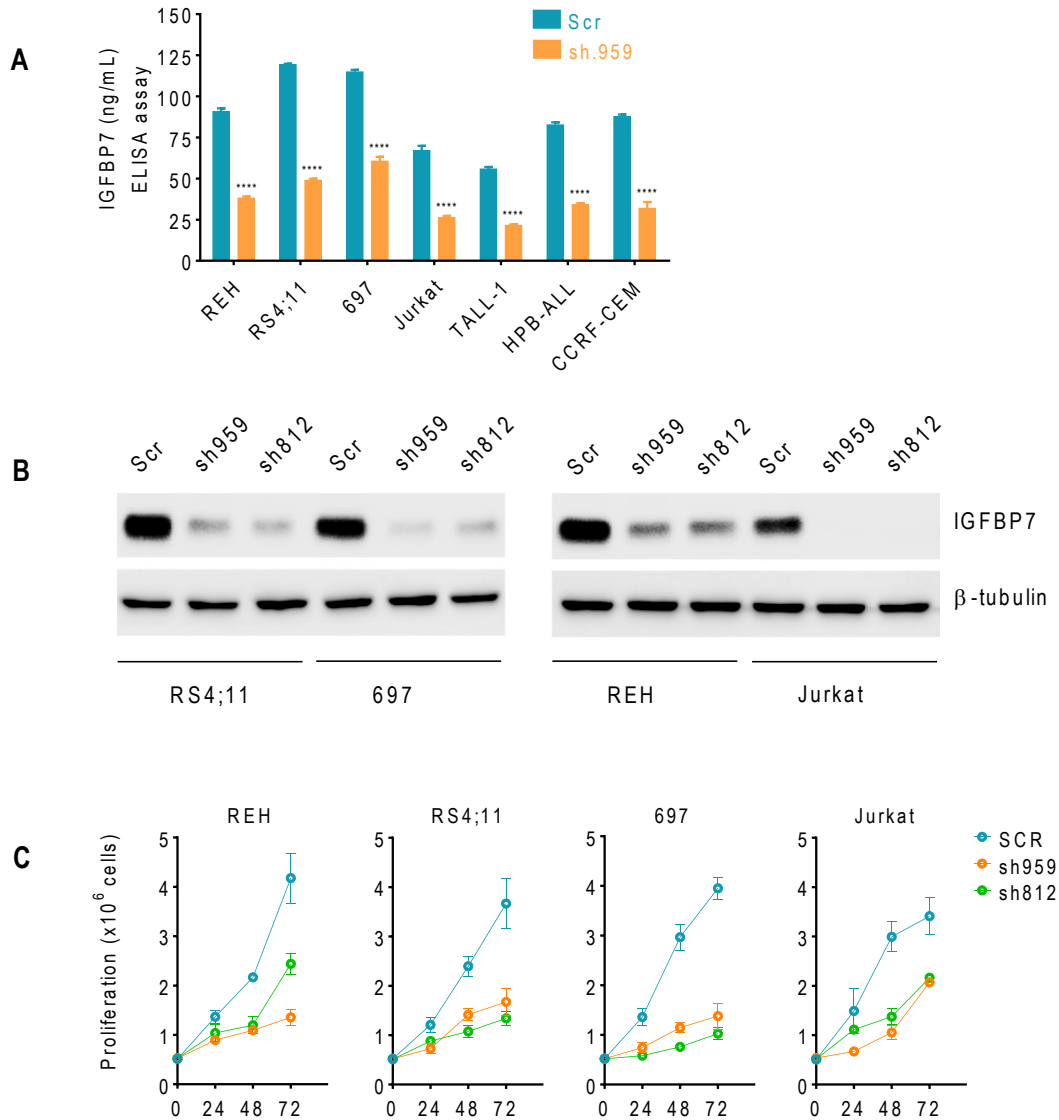
## References

- Gibson LF. Survival of B lineage leukemic cells: signals from the bone marrow microenvironment. *Leuk Lymphoma*. 2002;43(1):19-27.
- Khandwala HM, McCutcheon IE, Flyvbjerg A, Friend KE. The effects of insulin-like growth factors on tumorigenesis and neoplastic growth. *Endocr Rev*. 2000;21(3):215-244.
- Hakuno F, Takahashi SI. IGF1 receptor signaling pathways. *J Mol Endocrinol*. 2018;61(1):T69-T86.
- Jones JL, Clemmons DR. Insulin-like growth factors and their binding proteins: biological actions. *Endocr Rev*. 1995;16(1):3-34.
- Yamada H, Iijima K, Tomita O, et al. Effects of insulin-like growth factor-1 on B-cell precursor acute lymphoblastic leukemia. *Int J Hematol*. 2013;97(1):73-82.
- Hwa V, Oh Y, Rosenfeld RG. The insulin-like growth factor-binding protein (IGFBP) superfamily. *Endocr Rev*. 1999;20(6):761-787.
- Yamanaka Y, Wilson EM, Rosenfeld RG, Oh Y. Inhibition of insulin receptor activation by insulin-like growth factor binding proteins. *J Biol Chem*. 1997;272(49):30729-30734.
- Akagi K, Sato J, Okabe Y, Sakamoto Y, Yasumitsu H, Miyazaki K. Synergistic growth stimulation of mouse fibroblasts by tumor-derived adhesion factor with insulin-like growth factors and insulin. *Cell Growth Differ*. 1996;7(12):1671-1677.
- Laranjeira ABA, de Vasconcellos JF, Sodek L, et al. IGFBP7 participates in the reciprocal interaction between acute lymphoblastic leukemia and BM stromal cells and in leukemia resistance to asparaginase. *Leukemia*. 2012;26(5):1001-1011.
- Grant GA. Synthetic peptides for production of antibodies that recognize intact proteins. *Curr Protoc Mol Biol*. 2002;Chapter 11:16.
- Evdokimova V, Tognon CE, Benatar T, et al. IGFBP7 binds to the IGF-1 receptor and blocks its activation by insulin-like growth factors. *Sci Signal*. 2012;5(255):ra92.
- Heesch S, Schlee C, Neumann M, et al. BAALC-associated gene expression profiles define IGFBP7 as a novel molecular marker in acute leukemia. *Leukemia*. 2010;24(8):1429-1436.
- Bach LA. IGF-binding proteins. *J Mol Endocrinol*. 2018;61(1):T11-T28.
- Estrov Z, Meir R, Barak Y, Zaizov R, Zadik Z. Human growth hormone and insulin-like growth factor-1 enhance the proliferation of human leukemic blasts. *J Clin Oncol*. 1991;9(3):394-399.
- Bird MC, Bosanquet AG, Forskitt S, Gilby ED. Semi-micro adaptation of a 4-day differential staining cytotoxicity (DiSC) assay for determining the in-vitro chemosensitivity of haematological malignancies. *Leuk Res*. 1986;10(4):445-449.
- Pieters R, Loonen AH, Huismans DR, et al. In vitro drug sensitivity of cells from children with leukemia using the MTT assay with improved culture conditions. *Blood*. 1990;76(11):2327-2336.
- Medyouf H, Ghysdael J. The calcineurin/NFAT signaling pathway: a novel therapeutic target in leukemia and solid tumors. *Cell Cycle*. 2008;7(3):297-303.
- Medyouf H, Gusscott S, Wang H, et al. High-level IGF1R expression is required for leukemia-initiating cell activity in T-ALL and is supported by Notch signaling. *J Exp Med*. 2011;208(9):1809-1822.
- Triplett TA, Cardenas KT, Lancaster JN, et al. Endogenous dendritic cells from the tumor microenvironment support T-ALL growth via IGF1R activation. *Proc Natl Acad Sci USA*. 2016;113(8):E1016-E1025.
- Holleman A, Cheok MH, den Boer ML, et al. Gene-expression patterns in drug-resistant acute lymphoblastic leukemia cells and response to treatment. *N Engl J Med*. 2004;351(6):533-542.
- Hu S, Chen R, Man X, et al. Function and expression of insulin-like growth factor-binding protein 7 (IGFBP7) gene in childhood acute myeloid leukemia. *Pediatr Hematol Oncol*. 2011;28(4):279-287.
- Bartram I, Erben U, Ortiz-Tanchez J, et al. Inhibition of IGF1-R overcomes IGFBP7-induced chemotherapy resistance in T-ALL. *BMC Cancer*. 2015;15(1):663.

23. Girmila L, Takahashi SI, Crudden C, et al. When phosphorylation encounters ubiquitination: a balanced perspective on IGF-1R signaling. *Prog Mol Biol Transl Sci*. 2016;141:277-311.
24. Choi E, Zhang X, Xing C, Yu H. Mitotic checkpoint regulators control insulin signaling and metabolic homeostasis. *Cell*. 2016;166(3):567-581.
25. Yoneyama Y, Lanzerstorfer P, Niwa H, et al. IRS-1 acts as an endocytic regulator of IGF-I receptor to facilitate sustained IGF signaling. *eLife*. 2018;7:e32893.
26. López-Bermejo A, Khosravi J, Corless CL, et al. Generation of anti-insulin-like growth factor-binding protein-related protein 1 (IGFBP-rP1/MAC25) monoclonal antibodies and immunoassay: quantification of IGFBP-rP1 in human serum and distribution in human fluids and tissues. *J Clin Endocrinol Metab*. 2003;88(7):3401-3408.
27. Morgantini C, Jager J, Li X, et al. Liver macrophages regulate systemic metabolism through non-inflammatory factors [corrections published in *Nat Metab*. 2021;3:287 and *Nat Metab*. 2019;1:497]. *Nat Metab*. 2019;1(4):445-459.
28. Davison Z, de Blacqui re GE, Westley BR, May FE. Insulin-like growth factor-dependent proliferation and survival of triple-negative breast cancer cells: implications for therapy. *Neoplasia*. 2011;13(6):504-515.
29. Frattali AL, Pessin JE. Relationship between alpha subunit ligand occupancy and beta subunit autophosphorylation in insulin/insulin-like growth factor-1 hybrid receptors. *J Biol Chem*. 1993;268(10):7393-7400.
30. Soos MA, Field CE, Lammers R, et al. A panel of monoclonal antibodies for the type I insulin-like growth factor receptor. Epitope mapping, effects on ligand binding, and biological activity. *J Biol Chem*. 1992;267(18):12955-12963.
31. Pollak M. The insulin receptor/insulin-like growth factor receptor family as a therapeutic target in oncology. *Clin Cancer Res*. 2012;18(1):40-50.
32. Schewe DM, Alsadeq A, Sattler C, et al. An Fc-engineered CD19 antibody eradicates MRD in patient-derived *MLL*-rearranged acute lymphoblastic leukemia xenografts. *Blood*. 2017;130(13):1543-1552.

## 5. SUPPLEMENTARY MATERIAL

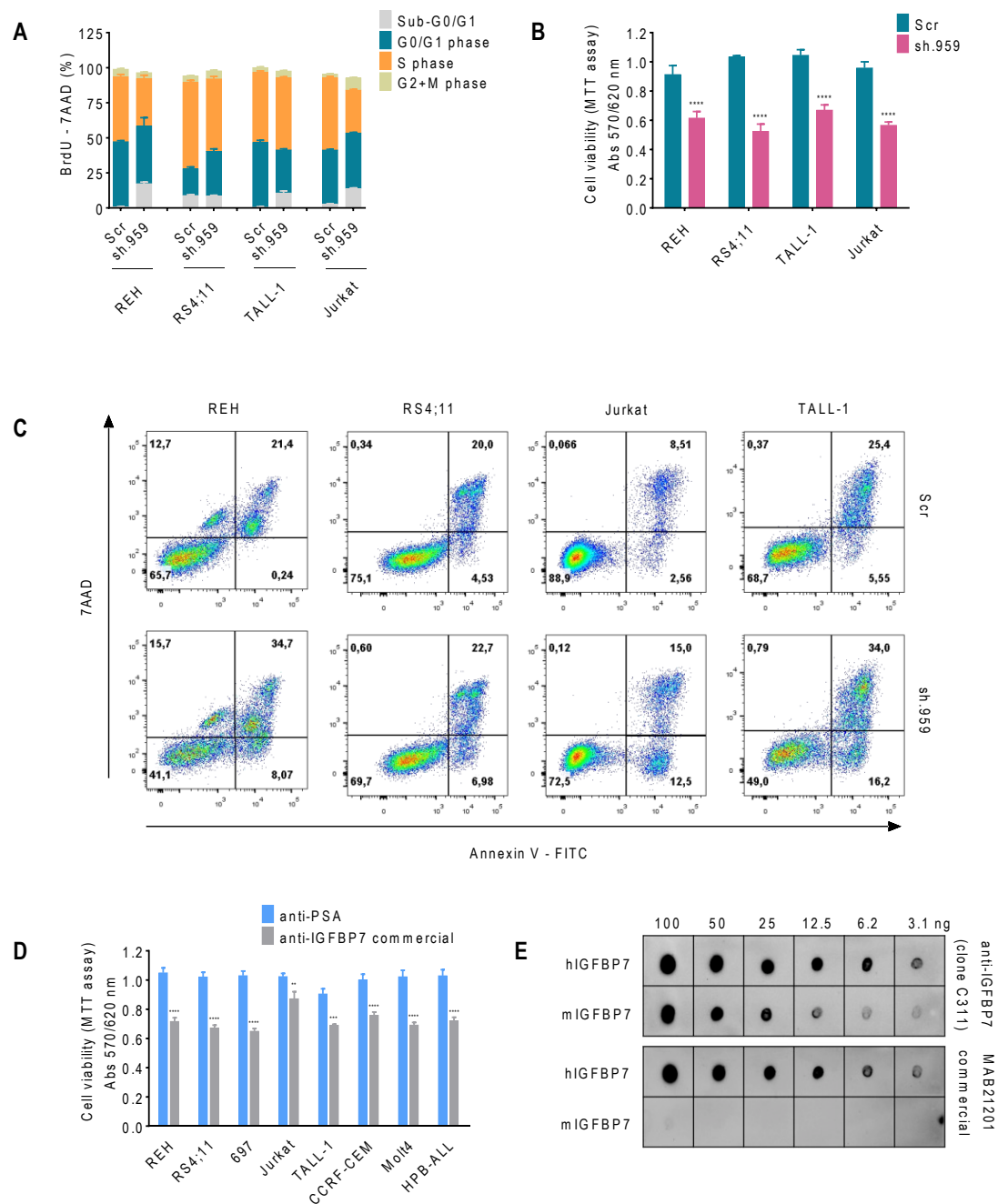
### 5.1 Supplementary figures



**Supplementary Figure 1. Validation of *IGFBP7* knockdown.** (A) Downregulation of IGFBP7 secretion in conditioned culture media of BCP-ALL (REH, RS4;11, 697) and T-ALL (Jurkat, TALL-1, HPB-ALL and CCRF-CEM) cell lines stably transduced with lentiviral shRNA constructs against *IGFBP7* (sh.959) or a non-coding random sequence, Scrambled (Scr). Conditioned media were collected after 24 h of culture in RPMI-10% FBS. IGFBP7 levels were measured by ELISA assay. Bars represent means  $\pm$  SE for triplicate wells. Statistical analysis was done by Two-way ANOVA and Bonferroni post-tests (\*\*\*) =  $P \leq 0.001$ ). (B) Western blot analysis showing lower IGFBP7 protein expression in RS4;11, 697, REH and Jurkat cell lines stably transduced with lentiviral shRNA constructs against *IGFBP7* (sh.959 and sh.812) in

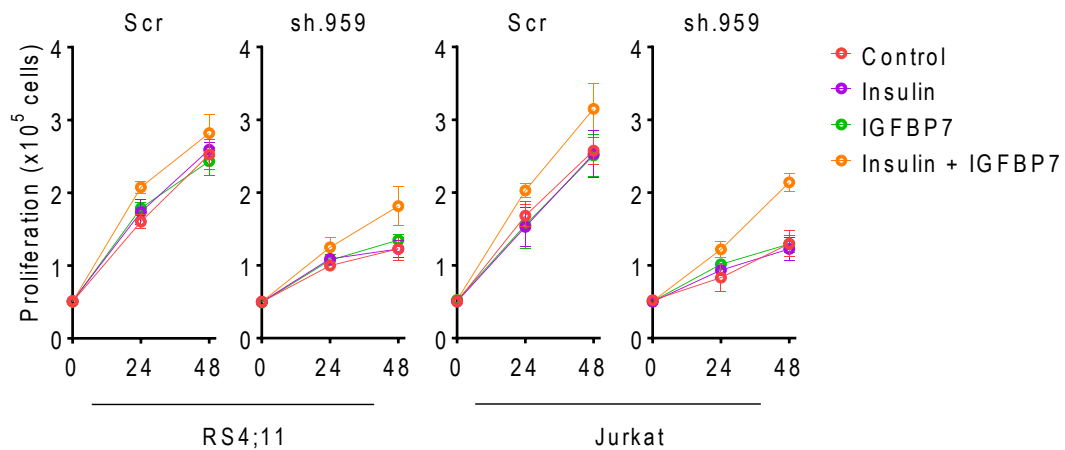
comparison to a non-coding random sequence, Scramble (Scr). The  $\beta$ -tubulin antibody was used as loading control. (C) Proliferation of REH, RS4;11, 697 and Jurkat cell lines stably transduced with lentivirus expressing two different shRNA against IGFBP7 (sh.959 in orange and sh.812 in green) or Scramble control (Scr in blue) analyzed by the trypan blue exclusion technique. Results from a single experiment run in triplicate wells, using RPMI-3%FBS.



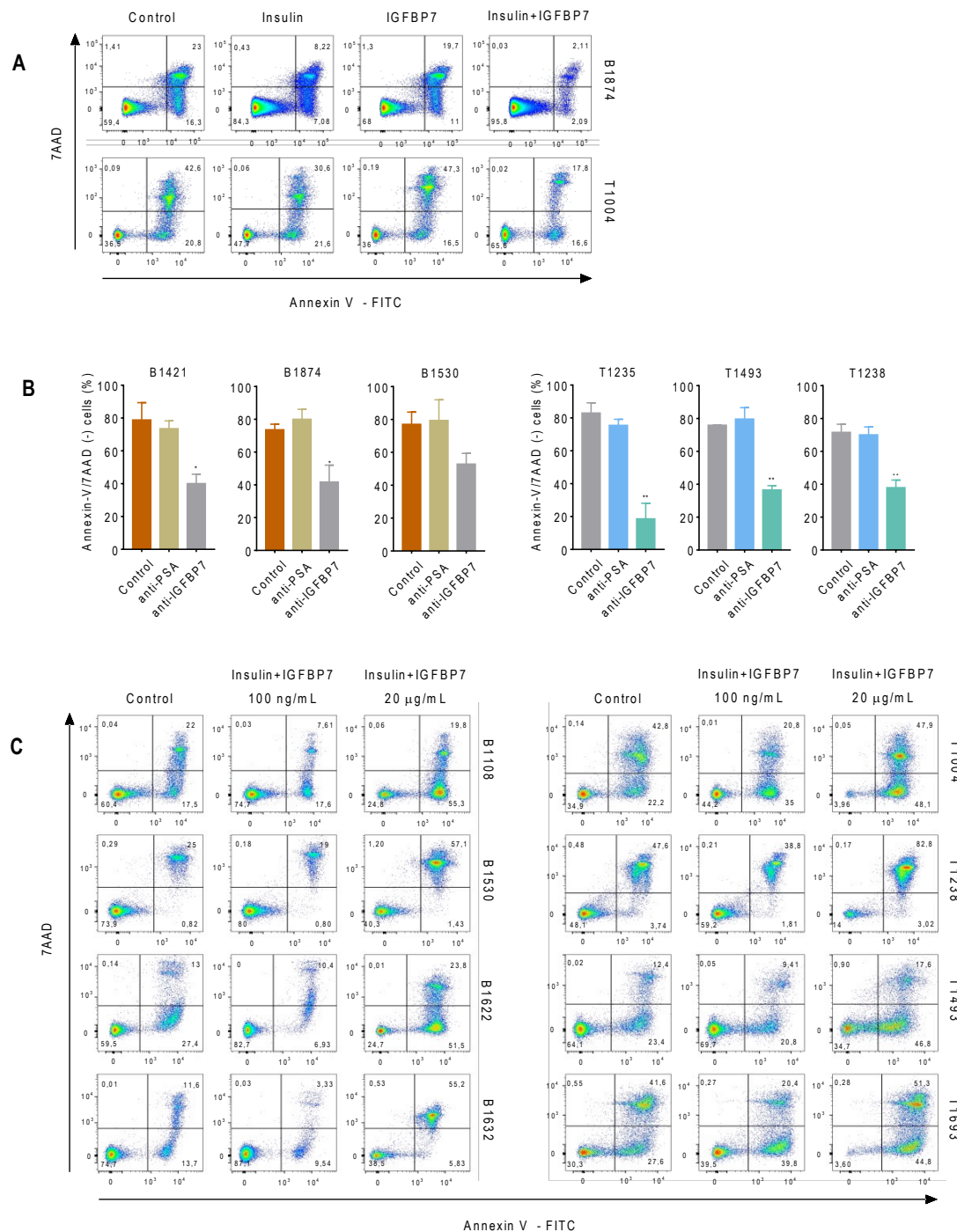


**Supplementary Figure 2. Effect of *IGFBP7* knockdown or neutralization on ALL proliferation and viability.** (A) Cell cycle analysis of sh.959 or Scramble (Scr) ALL cells was evaluated by the BrdU incorporation assay. Percentage means  $\pm$  SE of cells in G0/G1, S-phase, G2/M and in apoptosis (Sub-G0/G1) (see Fig 1B for gates used) are shown for three independent experiments run in triplicate wells. (B) Cell viability of sh.959 or Scr ALL cells cultured in RPMI-3%FBS for 24 h. Viable cells were quantified by the MTT assay. Bars represent means  $\pm$  SE for three independent experiments run in triplicate wells. (C) Apoptosis assay for sh.959 or Scr cells after 24 h of culture in RPMI-3%FBS. Dot plot graphs of a representative experiment are shown. (D) Effect of a commercially available anti-IGFBP7 antibody (20  $\mu$ g/ml) or an anti-PSA control (20  $\mu$ g/ml) against different ALL cell lines cultured

in RPMI-10%FBS for 48 h. Viable cells were quantified by the MTT assay. Bars represent means  $\pm$  SE for two independent experiments run in triplicate wells. (E) Dot blot test carried out with our mouse anti-IGFBP7 antibody (clone C311) produced by hybridoma cell culture and protein G purification. For comparison, we used the mouse IGFBP-rp1/IGFBP-7 antibody MAB21201, obtained from the R&D Systems. Increasing amounts of the recombinant human or mouse IGFBP7 protein were deposited on a nitrocellulose membrane. Membranes were immunoblotted overnight at 4°C with 0.2 mg/ml of antibodies. Immunodetection was performed by incubation with horseradish peroxidase-conjugated anti-mouse IgG (1:1000 – clone 7076, Cell Signaling Technology) in 5% non-fat dry milk in TBST, for 1 h at room temperature, and developed by using the Super Signal West Pico Chemiluminescent Substrate detection reagent (Thermo Fisher Scientific) and images were acquired with an ChemiDoc equipment (Bio-Rad). Statistical analysis was done by Two-way ANOVA and Bonferroni post-tests (\*\* $P \leq 0.01$  \*\*\* $P \leq 0.001$  and \*\*\*\* $P \leq 0.0001$ ).

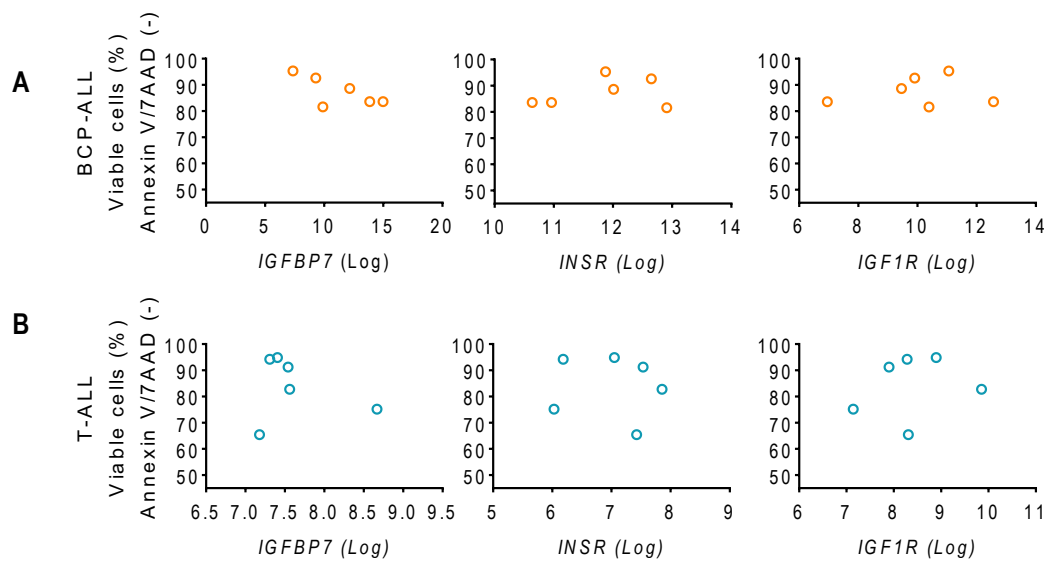


**Supplementary Figure 3. Treatment of IGFBP7 knockdown cell lines with insulin or IGFBP7 alone did not induce proliferation.** Proliferation of RS4;11 and Jurkat cell lines stably transduced with lentivirus expressing shRNA against IGFBP7 (sh.959) or Scramble control (Scr) analyzed by the trypan blue exclusion technique after insulin (500 ng/ml) and/or IGFBP7 (100 ng/ml) treatment. Results from a single experiment run in triplicate wells, using RPMI-3%FBS. Results of the same experiment are shown in Fig. 2B.

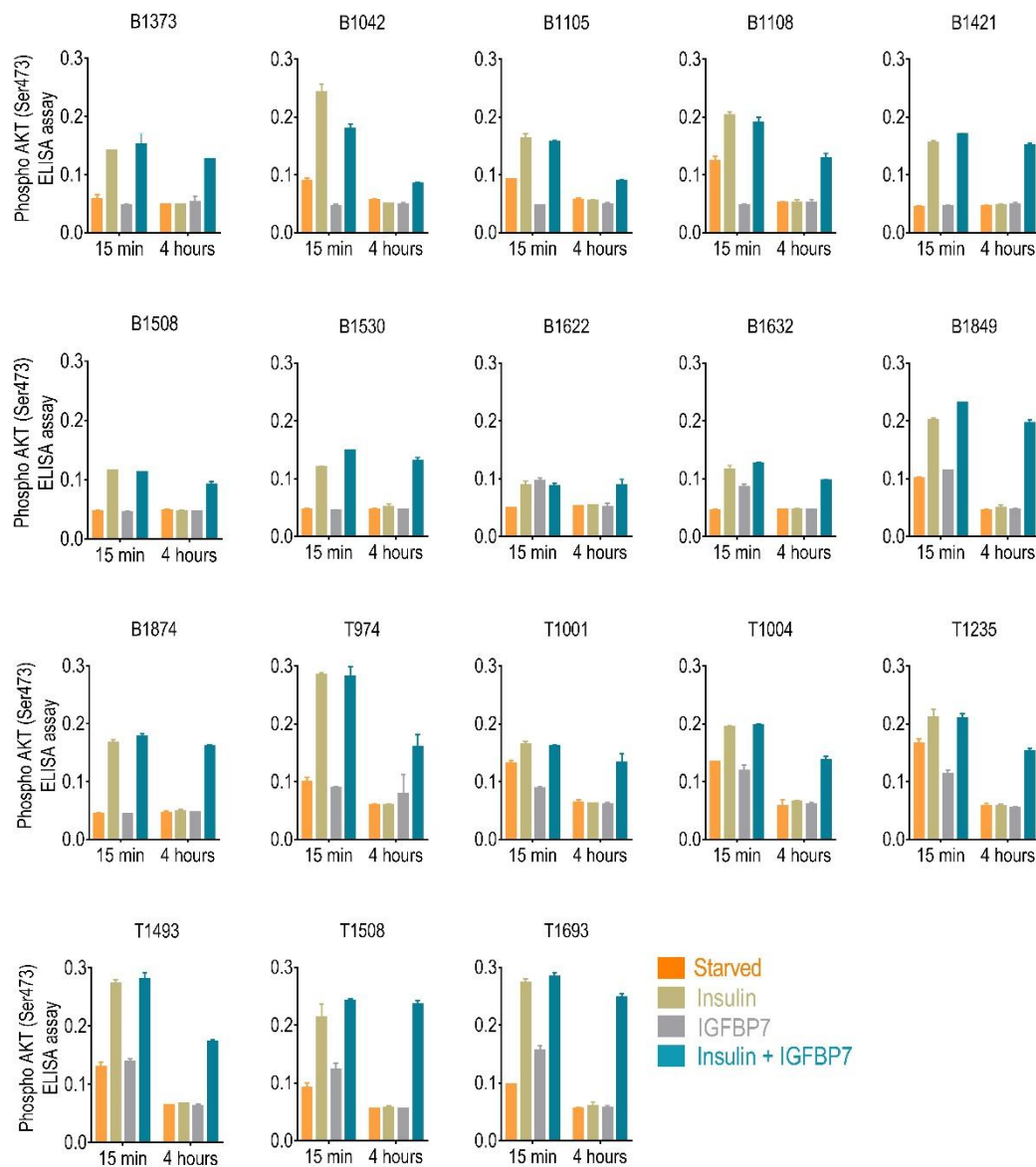


**Supplementary Figure 4. IGFBP7 potentiates the pro-survival effects of insulin on primary ALL cells. (A)** Representative dot plot graphs of apoptosis in primary BCP-ALL (B1874) and T-ALL (T1004) cells at 48 h and 24 h, respectively, after culture in AIM-V serum-free medium alone (control) or with insulin (500 ng/ml) and/or IGFBP7 (100 ng/ml). **(B)** Results from three independent cell viability experiments with primary BCP- (B1421, B1874, B1530) or T-ALL (T1235, T1493, T1238) cells cultured for 48 h or 24 h, respectively, on AIM-V serum-free medium (Control) supplemented with anti-PSA control antibody (20 µg/ml) or anti-IGFBP7 antibody (clone C311, 20 µg/ml). Bars correspond to the mean  $\pm$  SE percentage of viable cells

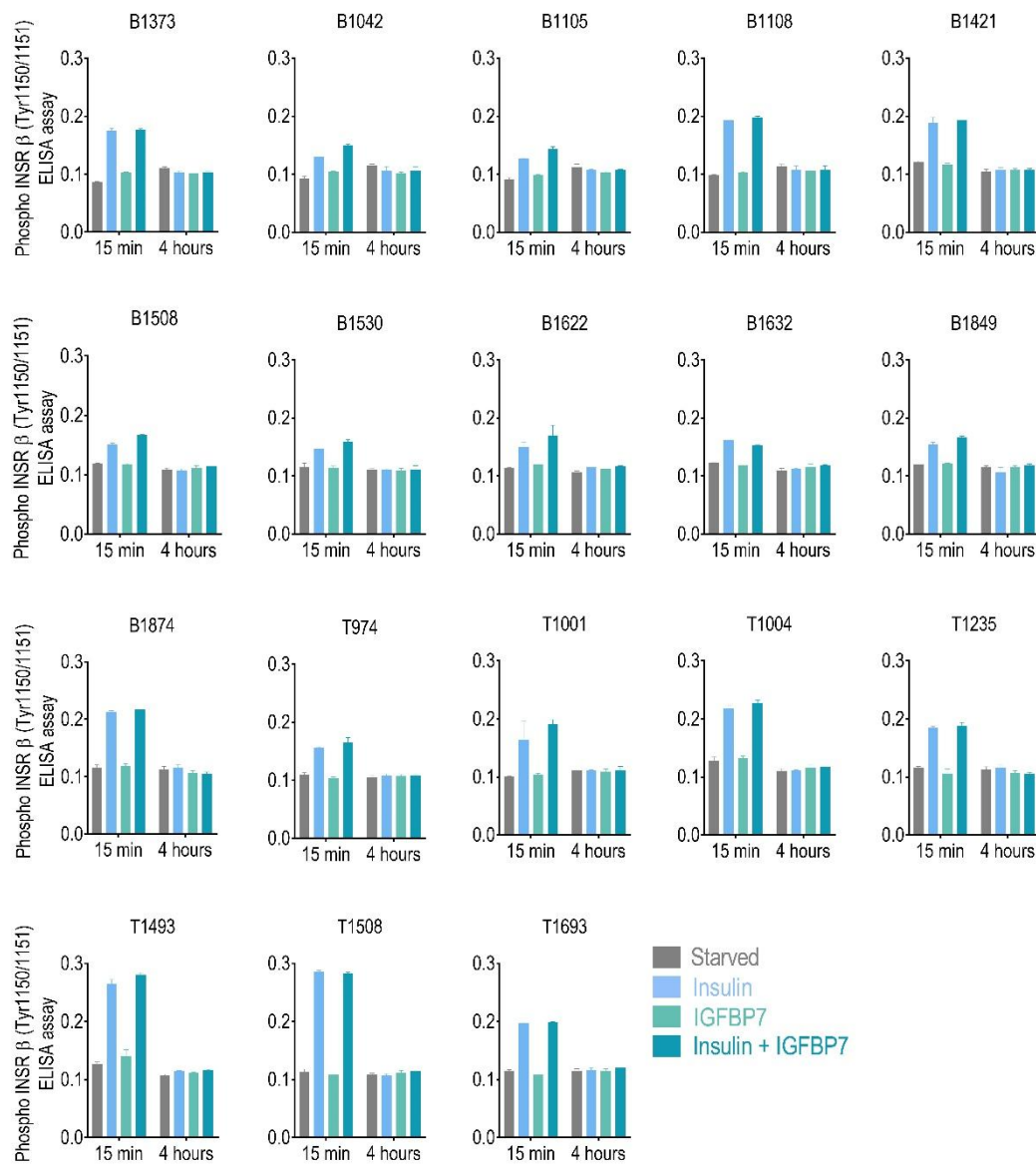
(Annexin-V/7AAD negative cell fraction). **(C)** High IGFBP7 concentrations (20 µg/ml) induce a drastic reduction in the viability of primary BCP- and T-ALL cells after 24 h of culture in AIM-V serum-free medium. The AIM-V medium AIM-V medium is a HEPES-buffered (pH 6.7 to 6.9), low-endotoxin (<0.1 ng/ml) basal medium consisting of an equal volume mixture of Dulbecco's Modified Eagle Medium (DMEM) and Ham's Nutrient Mixture F-12 (F-12). It contains purified human albumin, human transferrin, and human recombinant insulin and is further supplemented with a proprietary mixture of purified noncytokine factors.<sup>1</sup> Statistical analysis was done by One-way ANOVA and Bonferroni post-tests (\* =  $P \leq 0.05$  and \*\* =  $P \leq 0.01$ ).



**Supplementary Figure 5. Expression levels (mRNA) of *IGFBP7*, *INSR*, and *IGF1R* did not correlate with primary ALL cell survival under *IGFBP7*/insulin stimulation.** Gene expressions were measured by microarray (Gene 1.0 ST, Affymetrix) analysis. Expression values were obtained using the Bioconductor platform and the Plier16 algorithm and are expressed in a log2 scale.<sup>2</sup> Each point corresponds to data from one patient sample. Spearman correlation was performed using the average survival percentage (Annexin-V/7AAD negative fraction) of primary cells after 48 h (BCP-ALL; **A**) or 24 h (T-ALL; **B**) of culture in AIM-V serum-free medium supplemented with insulin (500 ng/ml) and *IGFBP7* (100 ng/ml) (See Figure 2A and B). All P-values were nonsignificant ( $P > 0.05$ ).

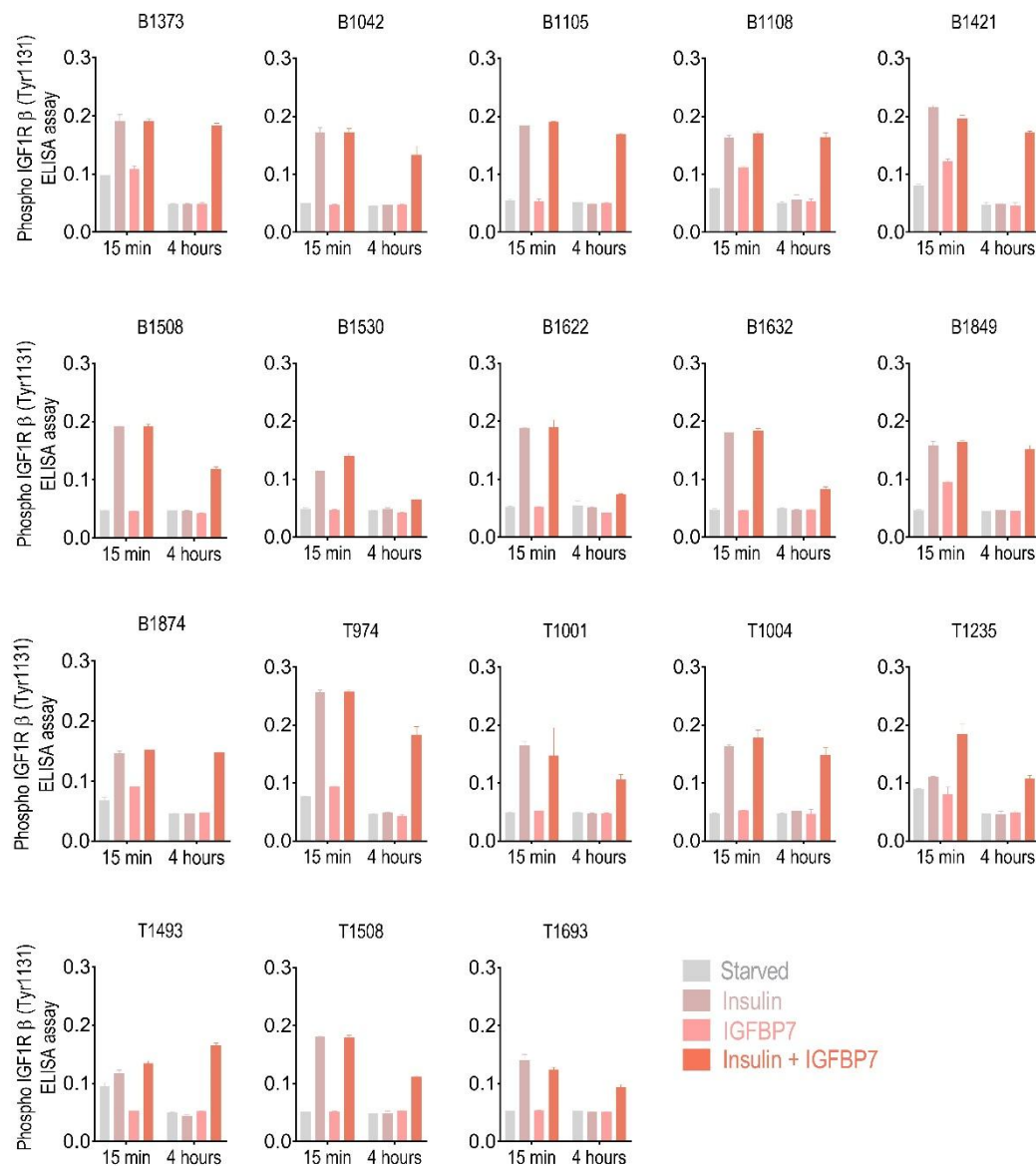


**Supplementary Figure 6. IGFBP7 prolongs AKT activation by insulin in primary ALL cells.** Phospho-AKT (Ser473) ELISA results for the individual primary BCP- and T-ALL samples after treatment with insulin (500 ng/ml), IGFBP7 (100 ng/ml), or a combination of both, for the indicated periods of times. Representative graphs of two independent experiments performed in duplicate wells are shown. These data are shown in Fig 3A.

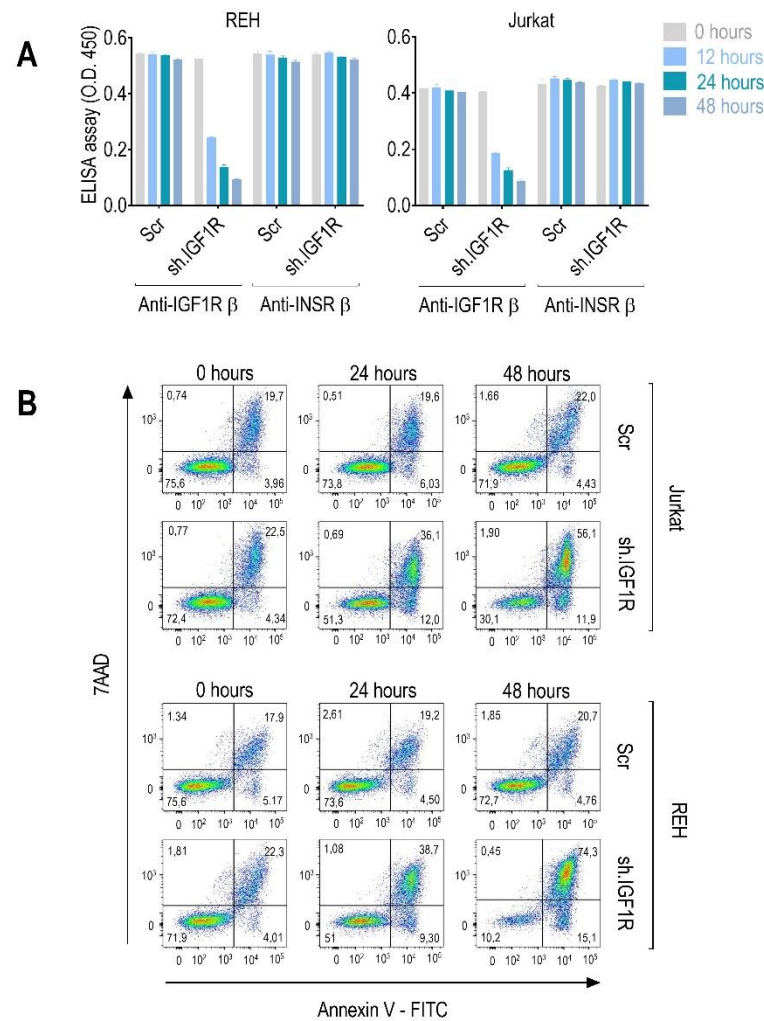


**Supplementary Figure 7. IGFBP7 prolongs INSR activation by insulin in primary ALL cells.** Phospho-INSR $\beta$  (Tyr1150/1151) ELISA results for the individual primary BCP- and T-ALL samples after treatment with insulin (500 ng/ml), IGFBP7 (100 ng/ml), or a combination of both, for the indicated periods of times. Representative graphs of two independent experiments performed in duplicate wells are shown. These data are shown in Fig 3B.

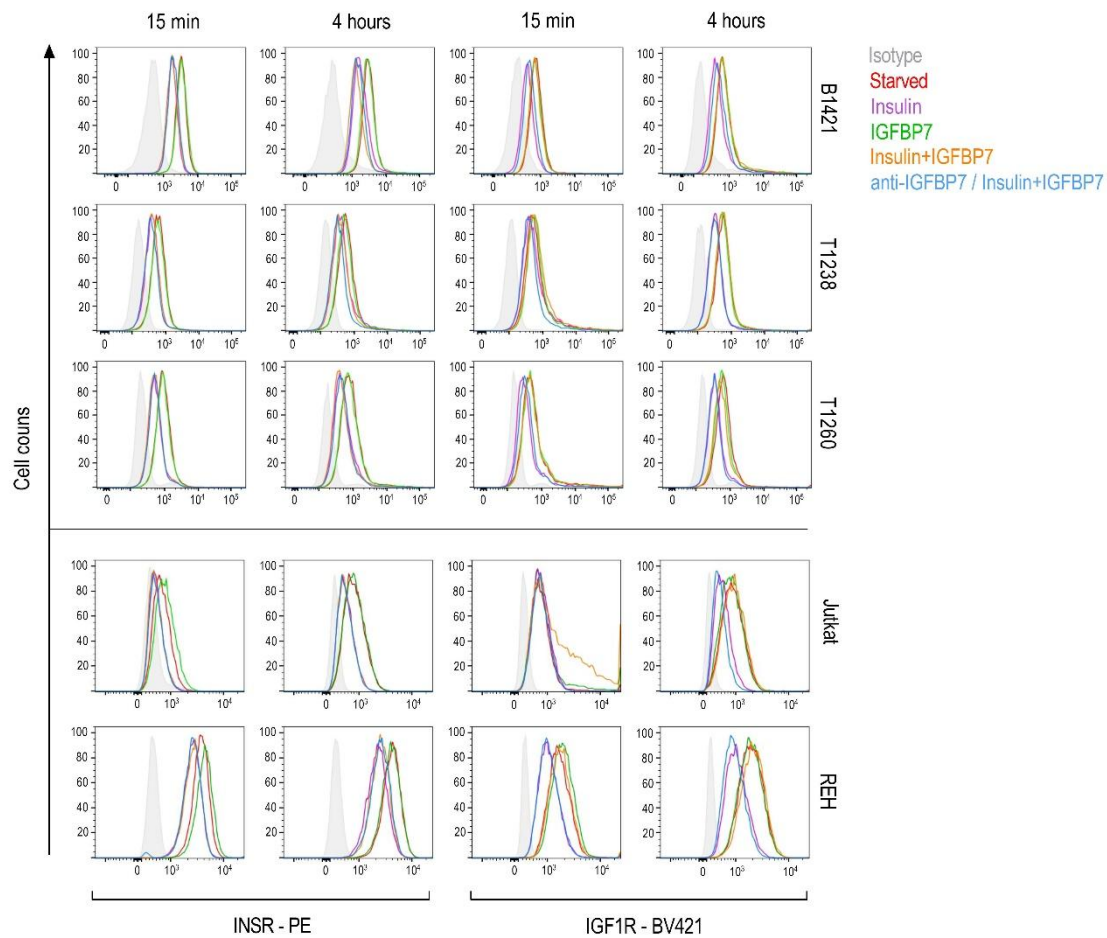




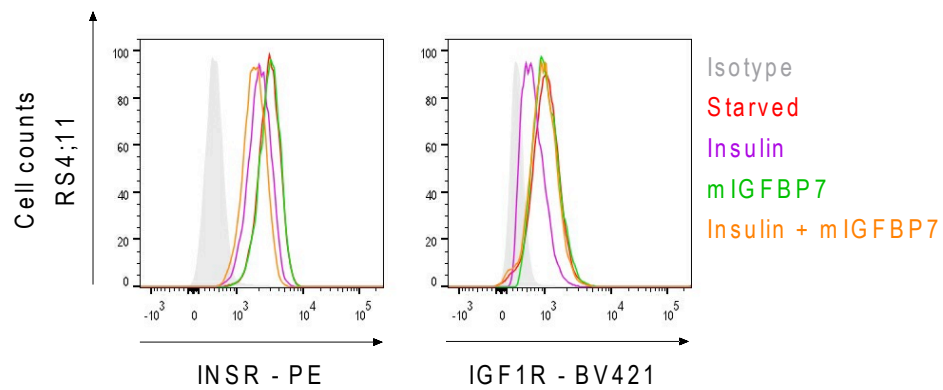
**Supplementary Figure 8. IGFBP7 prolongs IGF1R activation by insulin in primary ALL cells.** Phospho-IGF1R $\beta$  (Tyr1131) ELISA results for the individual primary BCP- and T-ALL samples after treatment with insulin (500 ng/ml), IGFBP7 (100 ng/ml), or a combination of both, for the indicated periods of times. Representative graphs of two independent experiments performed in duplicate wells are shown. These data are shown in Fig 3C.



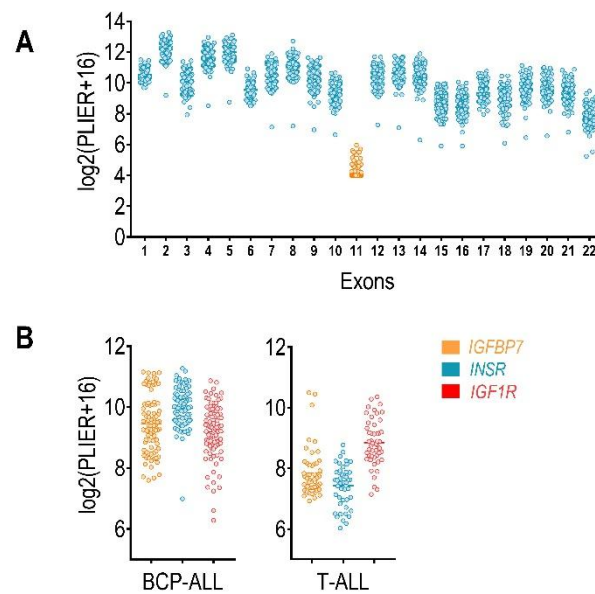
**Supplementary Figure 9. Conditional knockdown of *IGF1R* in the REH and Jurkat cell lines.** The REH and Jurkat cell lines were stably transduced with the pLKO.1 MISSION LacO shRNA lentiviral vector NM\_000208 (Sigma-Aldrich) for inducible expression of a shRNA against *IGF1R* (sh.IGF1R). As negative control, cells were transduced with the MISSION LacO Non-Target shRNA Control Vector (Scr). Transduced cells were cultured under puromycin selection for 10 days. **(A)** Downregulation of *IGF1R* $\beta$ , but not *INSR* $\beta$ , at different time points of IPTG (1  $\mu$ g/ml) treatment, as measured by ELISA of cell extracts. **(B)** Representative dot plots of the apoptosis assay of sh.IGF1R or Scramble (Scr) cells after IPTG (1  $\mu$ g/ml) stimulation. Results are part of those shown in Fig 3E.



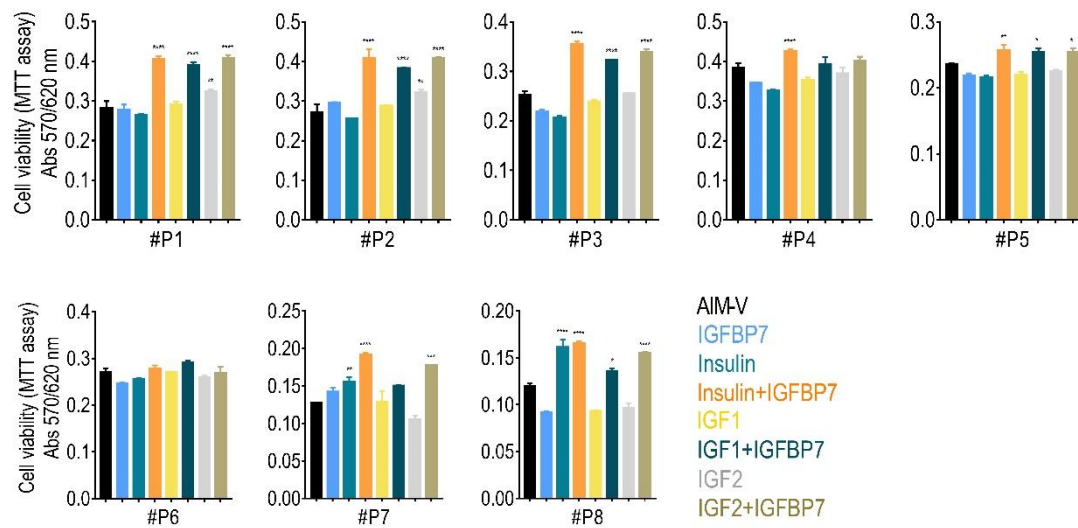
**Supplementary Figure 10. IGFBP7 inhibits IGF1R internalization upon insulin stimulation in cell lines and primary ALL cells.** Cell surface expression of the INSR and IGF1R in serum-starved primary ALLs or the Jurkat and REH cell lines, after 15 min or 4 h of treatment with insulin (500 ng/ml), IGFBP7 (100 ng/ml), anti-IGFBP7 (clone C311, 20 µg/mL) or associations, as measured by flow cytometry analysis. The anti-IGFBP7 antibody (clone C311) was added 30 min before IGFBP7/insulin addition. Histogram graphs for a forth primary BCP-ALL (B1042 ) is shown in Fig 4A. These data are shown in Fig 4B.



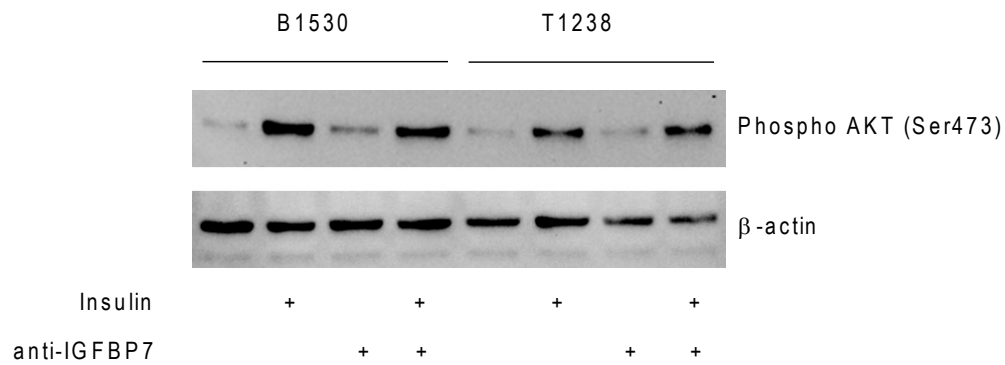
**Supplementary Figure 11. The mouse IGFBP7 is functional on human IGF1R.** Cell surface expression of the INSR and IGF1R in serum starved RS4;11 cell line, after 4 h of treatment with insulin (500 ng/ml), mouse IGFBP7 (mIGFBP7; 100 ng/ml) or both, as measured by flow cytometry analysis. The mIGFBP7 was obtained from R&D Systems (catalog # 2120-B7).



**Supplementary Figure 12. mRNA expression levels of *INSR*, *IGF1R*, and *IGFBP7* in primary ALL.** Gene expressions were measured by microarray (Gene 1.0 ST, Affymetrix) analysis. Expression values were obtained using the Bioconductor platform and the Plier16 algorithm and are expressed in a log2 scale.<sup>2</sup> **(A)** Expression of the different exons of the *INSR* gene in 93 samples of pediatric ALL. Each point corresponds to one patient's ALL. Results demonstrate that ALL cells predominantly express isoform A of the *INSR* (isoform that lacks exon 11). **(B)** Expression of *IGFBP7*, *INSR*, and *IGF1R* transcripts in different BCP- (n=90) and T-ALL (n: 49). T-ALLs seem to express lower levels of *IGFBP7* and *INSR* than BCP-ALLs.



**Supplementary Figure 13. IGFBP7 potentiates the pro-survival effects of both insulin, IGF1, and IGF2 in primary ALL.** Primary BCP-ALL cells were cultured in AIM-V serum-free medium supplemented with different combinations of insulin (500 ng/ml), IGF1 (200 ng/ml), IGF2 (200 ng/ml) and IGFBP7 (100 ng/ml). After 48 h, cell viability was measured by the MTT assay. Bars represent means  $\pm$  SE for duplicate wells. For patient's information please see Supplementary Table 2. Statistical analysis was done by One-way ANOVA and Bonferroni post-tests (\* =  $P \leq 0.05$ , \*\* =  $P \leq 0.01$ , \*\*\* =  $P \leq 0.001$  and \*\*\*\* =  $P \leq 0.0001$ ).



**Supplementary Figure 14. Short term insulin stimulation of ALL cells is independent of IGFBP7.** Western blot results for Phospho-Akt (Ser473) on the B1530 and T1238 primary ALLs (BCP- and T-ALL, respectively) after 15 min of insulin (500 ng/ml) treatment in serum free AIM-V medium. Primary ALL cells were thawed, centrifuged through a Ficoll-Hypaque gradient, and then were incubated at 37°C, 5% CO<sub>2</sub>, during 4 h in AIM-V medium before insulin stimulation. Anti-IGFBP7 (clone C311; 20µg/ml) was added 30 min before insulin stimulation, as a mean of neutralizing the IGFBP7 protein produced and secreted by ALL cells.

## 5.2 Supplementary tables

**Supplementary Table 1.** Clinical and biological features of Primary BCP- ant T-ALL samples used in the functional studies showed in Figure 2A and B.

ID	Gender	Age	WBC per $\mu$ L	CALLA	Chromosome translocation	Follow up (years)	Status at last follow up
<b>B1373</b>	M	11.9	73,400	pos	na	4,1	in remission
<b>B1042</b>	F	5.14	33,200	pos	neg	7,3	in remission
<b>B1105</b>	F	4.12	13,400	pos	neg	13 days	dead
<b>B1108</b>	M	3.30	76,400	pos	neg	6,9	lost to follow up
<b>B1421</b>	M	4.82	10,280	pos	neg	8,1	in remission
<b>B1508</b>	M	4.56	145,810	pos	neg	6,6	in remission
<b>B1530</b>	F	11.24	76,370	pos	neg	13,3	in remission
<b>B1622</b>	M	16.20	47,500	pos	neg	2,11	in remission
<b>B1632</b>	F	7.87	55,707	neg	t(1;12) (p36;q13)	3,5	in remission
<b>B1849</b>	F	11.07	63,277	pos	neg	4,6	in remission
<b>B1874</b>	M	4,28	16,140	pos	neg	2,5	in remission
<b>T974</b>	M	11.12	230,550	pos	t(9;15) (q34;q22)	1,7	lost to follow up
<b>T1001</b>	M	10.05	934,000	neg	neg	0,3	dead
<b>T1004</b>	F	2.62	950,000	neg	neg	7,9	in remission



<b>T1235</b>	M	5,50	196,000	pos	neg	10,11	in remission
<b>T1493</b>	M	12.36	391,200	neg	neg	7,0	in remission
<b>T1508</b>	M	4.30	112,200	neg	neg	0,8	in remission
<b>T1693</b>	F	1.96	63,560	pos	t(7;14) (q11.2;q32)	4,11	in remission
<b>T979</b>	M	9,40	76,400	neg	neg	12,2	in remission

---

ID: patient's identification; F: female; M: male; Age: age in years; na: not available; pos: positive; neg: negative; WBC: white blood cells; CALLA: common acute lymphoblastic leukemia antigen.

**Supplementary Table 2.** Clinical and biological features of Primary BCP-ALL samples used in the functional studies showed in Supplementary Figure 13.

<b>ID</b>	<b>Gender</b>	<b>Age</b>	<b>WBC per <math>\mu</math>L</b>	<b>CALLA</b>	<b>Chromosome translocation</b>	<b>Follow up (years)</b>	<b>Status at last follow up</b>
<b>P1</b>	F	5.39	34,900	pos	na	19.5	in remission
<b>P2</b>	M	9.25	134,000	pos	t(9;22) p190	2.5	died
<b>P3</b>	M	2.44	48,700	pos	na	1.7	lost to follow up
<b>P4</b>	F	6.40	52,000	neg	na	20.8	in remission
<b>P5</b>	F	2.59	77,500	na	na	23.5	in remission
<b>P6</b>	M	10.57	149,600	pos	na	0.7	died
<b>P7</b>	F	10.25	45,000	pos	neg	1.3	died
<b>P8</b>	M	3.92	34,500	pos	na	23.2	in remission

ID: patient's identification; F: female; M: male; Age: age in years; na: not available; pos: positive; neg: negative; WBC: white blood cells; CALLA: common acute lymphoblastic leukemia antigen.

### 5.3 Supplementary references

- 1) Helinski EH, Bielat KL, Ovak GM, Pauly JL. Long-term cultivation of functional human macrophages in Teflon dishes with serum-free media. *J Leukoc Biol.* 1988;44(2):111-121.
- 2) Silveira AB, Laranjeira AB, Rodrigues GO, et al. PI3K inhibition synergizes with glucocorticoids but antagonizes with methotrexate in T-cell acute lymphoblastic leukemia. *Oncotarget.* 2015;6(15):13105-13118.

## 6. CHAPTER II - MANUSCRIPT



International Journal of  
Molecular Sciences



Brief Report

# IGFBP7 Fuels the Glycolytic Metabolism in B-Cell Precursor Acute Lymphoblastic Leukemia by Sustaining Activation of the IGF1R–Akt–GLUT1 Axis

Leonardo Luís Artico <sup>1,2</sup>, Juliana Silveira Ruas <sup>1</sup>, José Ricardo Teixeira Júnior <sup>1,2</sup>, Natacha Azussa Migita <sup>1</sup>, Gustavo Seguchi <sup>1</sup>, Xinghua Shi <sup>3</sup>, Silvia Regina Brandalise <sup>1</sup>, Roger Frigério Castilho <sup>4</sup>, and José Andrés Yunes <sup>1,\*</sup>

- <sup>1</sup> Centro Infantil Boldrini, Campinas 13083-210, SP, Brazil; lla.unicamp2017@gmail.com (L.L.A.); ruasjulianas@gmail.com (J.S.R.); jrteixeira094@gmail.com (J.R.T.J.); azussamigita@gmail.com (N.A.M.); gseguchi@gmail.com (G.S.); silvia@boldrini.org.br (S.R.B.)
- <sup>2</sup> Graduate Program in Genetics and Molecular Biology, Institute of Biology, University of Campinas, Campinas 13083-862, SP, Brazil
- <sup>3</sup> Department of Computer and Information Sciences, Temple University, Philadelphia, PA 19122, USA; mindyshi@temple.edu
- <sup>4</sup> Department of Pathology, School of Medical Sciences, University of Campinas, Campinas 13083-887, SP, Brazil; rogerc@unicamp.br
- \* Correspondence: andres@boldrini.org.br; Tel.: +55-(19)-3787-9096

**Abstract:** Increased glycolytic metabolism plays an important role in B-cell precursor Acute Lymphoblastic Leukemia (BCP-ALL). We previously showed that IGFBP7 exerts mitogenic and pro-survival effects in ALL by promoting IGF1 receptor (IGF1R) permanence on the cell surface, thus prolonging Akt activation upon IGFs/insulin stimulation. Here, we show that sustained activation of the IGF1R–PI3K–Akt axis concurs with GLUT1 upregulation, which enhances energy metabolism and increases glycolytic metabolism in BCP-ALL. IGFBP7 neutralization with a monoclonal antibody or the pharmacological inhibition of the PI3K–Akt pathway was shown to abrogate this effect, restoring the physiological levels of GLUT1 on the cell surface. The metabolic effect described here may offer an additional mechanistic explanation for the strong negative impact seen in ALL cells in vitro and in vivo after the knockdown or antibody neutralization of IGFBP7, while reinforcing the notion that it is a valid target for future therapeutic interventions.

**Keywords:** IGFBP7; IGF1R; GLUT1; PI3K–Akt; Acute Lymphoblastic Leukemia



**Citation:** Artico, L.L.; Ruas, J.S.; Teixeira Júnior, J.R.; Migita, N.A.; Seguchi, G.; Shi, X.; Brandalise, S.R.; Castilho, R.F.; Yunes, J.A. IGFBP7 Fuels the Glycolytic Metabolism in B-Cell Precursor Acute Lymphoblastic Leukemia by Sustaining Activation of the IGF1R–Akt–GLUT1 Axis. *Int. J. Mol. Sci.* **2023**, *24*, 9679. <https://doi.org/10.3390/ijms24119679>

Academic Editor: Spiro Mihaylov Konstantinov

Received: 5 April 2023

Revised: 21 May 2023

Accepted: 30 May 2023

Published: 2 June 2023



**Copyright:** © 2023 by the authors. Licensee MDPI, Basel, Switzerland. This article is an open access article distributed under the terms and conditions of the Creative Commons Attribution (CC BY) license (<https://creativecommons.org/licenses/by/4.0/>).

## 1. Introduction

Acute Lymphoblastic Leukemia (ALL) is the most common childhood cancer. Although survival rates for pediatric ALL have reached around 90% in the last decade, 20% to 30% of patients still relapse [1–3], and some experience long-term sequelae of therapy including a second malignancy [4–6]. Therefore, new drugs and therapeutic strategies are needed.

Fine-tuning of the glycolytic pathway is a critical step in the malignant transformation of B-cells [7,8]. In B-cell precursor Acute Lymphoblastic Leukemia (BCP-ALL), increased glycolytic metabolism plays an important role in ALL [9,10]. In immune cells, including BCP-ALL, Glucose Transporter 1 (GLUT1) coordinates glucose uptake [10,11]. Transcriptional regulation, increased plasma membrane targeting, and the recycling of GLUT1 are directly regulated by insulin, growth factors, and cytokines [12,13]. It is well-established that in leukemia cells, activation of the PI3K–Akt axis by receptor tyrosine kinases or oncogenic lesions (gain-of-function mutations) induces GLUT1 accumulation at the cell surface and increases aerobic glycolysis [14]. Recently, a feedforward loop between glycolytic ATP production and PI3K–Akt pathway activation was reported in T-cells [15,16], highlighting

the importance of this crosstalk for cellular activation and survival. Together, these observations point to an important role for PI3K–Akt in the control of glucose metabolism in immune cells and in the Warburg effect on blood cell disorders, such as BCP-ALL.

We previously showed that IGFBP7 (insulin-like growth factor-binding protein 7) exerts mitogenic and prosurvival autocrine effects in ALL [17]. Under insulin/recombinant insulin-like growth factor 1 (rIGF1) stimulation, recombinant IGFBP7 (rIGFBP7) promotes IGF1 receptor (IGF1R) permanence on the cell surface, fueling the PI3K–Akt pathway and, consequently, increasing cell viability/proliferation. We also demonstrated that IGFBP7 is a valid target for antibody-based therapeutic interventions in ALL [17]. Although the positive regulatory circuitry between PI3K–Akt and glycolytic metabolism is crucial for immune cells' survival, almost nothing is known about the existence of extracellular proteins (e.g., IGFBP7) that are possibly regulating this system, which may also be important in the oncogenic context, including ALL. Here, we show that the rIGFBP7-mediated rIGF1/IGF1R sustained activation of the PI3K–Akt pathway concurs with GLUT1 upregulation and increased glycolytic metabolism in BCP-ALL.

## 2. Results and Discussion

We previously showed that the treatment of ALL cells with insulin+rIGFBP7 prolongs IGF1R signaling (but not the insulin receptor, INSR) and Akt phosphorylation for up to 4 h [17]. Here, we confirmed this finding in a timecourse experiment. Treatment of BCP-ALL cell lines (RS4;11 and 697) with rIGF1+rIGFBP7 resulted in IGF1R signaling and Akt phosphorylation that reached a peak in about 15 min and lasted for 4 h, while phosphorylation of the INSR, after peaking at 15 min, rapidly decreased to low levels in 1 h (Figure S1A). These data indicate that IGFBP7 effects are not restricted to merely extending the half-life of the IGF1 ligand, since in that case both IGF1R and INSR should have been activated at the 4 h point. Overall, these findings confirm that IGF1R is the primary mediator of the IGFBP7 enhancement of IGF1 activity in BCP-ALL.

To test whether IGF1R is indispensable for the transduction of the rIGF1+rIGFBP7 stimulus to downstream effectors such as Akt, we generated two IGF1R knockout cell lines (IGF1Rko—Figure S1B,C). As expected, NTC cells (no target control) maintained detectable levels of IGF1R and Akt phosphorylation (but not INSR) 4 h after rIGF1+rIGFBP7 co-treatment, while no such sustained signaling was seen in IGF1Rko cells nor when rIGF1 or rIGFBP7 were used separately (Figures 1A,B and S1D). A previous study demonstrated that the N-terminal 97 amino acid fragment of IGFBP7 binds to the extracellular domain of IGF1R and prevents its internalization in response to IGF1 [18]. In our previous study, we confirmed this finding by showing that IGFBP7 prevented the internalization of IGF1R in ALL cells after insulin/IGF1 stimulation [17]. Together, these results support the idea that IGFBP7 functions by binding to and stabilizing the IGF1R receptor on the surface of ALL cells, thereby extending its response to IGF1 or insulin. The mechanism responsible for IGF1R retention at the cell surface is not yet known and deserves further investigation.

To better understand the cellular consequences of prolonged IGF1R/Akt signaling in BCP-ALL, we performed a microarray gene expression analysis followed by a Gene Set Enrichment Analysis (GSEA) [19,20]. Hallmark gene sets characteristic of cell growth (PI3K/Akt/mTOR, mTORC1, MYC targets, E2F targets, and mitotic spindle) and metabolism (oxidative phosphorylation-OXPHOS, adipogenesis, fatty acid metabolism, and glycolysis) were upregulated upon rIGF1+rIGFBP7 treatment of BCP-ALL cell lines (Figure 1C). This result is in agreement with reports showing that INSR and IGF1R deliver overlapping transcriptional responses, even though, at the organism level, insulin acts on metabolism, and IGF1 acts on growth [21]. As we know, dysregulation of these pathways was linked to the development and progression of several cancers, including ALL [22]. In general, activation of the PI3K/Akt/mTOR pathway downstream of IGF signaling promotes cell survival, proliferation, and growth by regulating protein translation, ribosome biogenesis, and cell cycle progression [23], which is in agreement with our previous findings on ALL [17]. Insulin and IGFs signaling also impact cellular metabolism

by regulating OXPHOS, adipogenesis, fatty acid metabolism, and glycolysis. Activation of these pathways leads to increased glucose uptake and utilization, lipid synthesis, and mitochondrial biogenesis, ultimately supporting cell growth and proliferation [24]. As IGFBP7 enhances the signaling of these pathways, it might also contribute to the glycolytic metabolism of BCP-ALL.

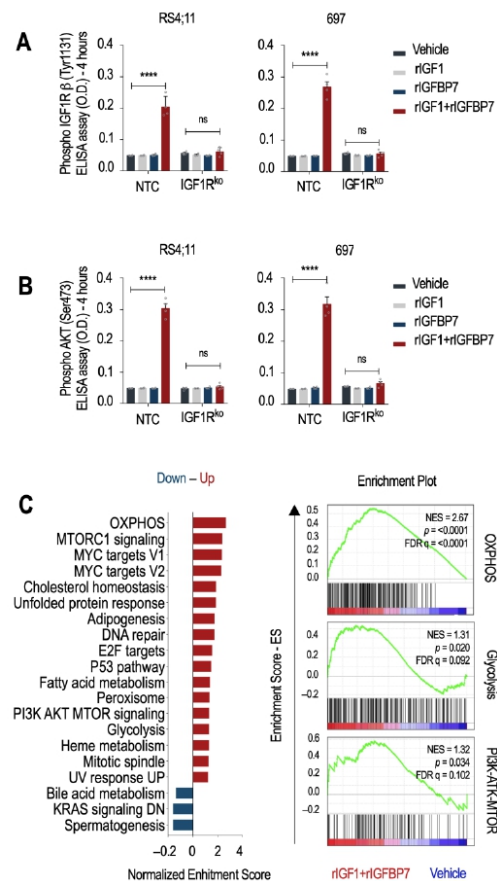


**Figure 1.** IGFBP7 sustains activation of the IGF1R/Akt axis under IGF1 stimulation in an IGF1R-dependent manner in BCP-ALL cells. **(A,B)** ELISA results for **(A)** phospho-IGF1Rβ (Tyr1131) and **(B)** phospho-Akt (Ser473) in RS4;11 and 697 BCP-ALL cell lines (no target control (NTC) and IGF1R knockout) after 4 h of treatment with rIGF1 (50 ng/mL) and/or rIGFBP7 (100 ng/mL). Bars represent means ± SEM for four independent experiments; ns = not significant. **(C)** Left: GSEA analysis results. Statistically significant hallmark gene sets were selected (FDR < 0.25) and distributed by the Normalized Enrichment Score (NES). Red bars indicate upregulated hallmark gene sets in BCP-ALL cell lines after 6 h stimulation with rIGF1+rIGFBP7 (50 ng/mL and 100 ng/mL, respectively) in serum-free medium. Blue bars indicate downregulated hallmark gene sets. Right: GSEA enrichment plots for selected hallmarks. Green curve corresponds to the enrichment score (ES). The normalized enrichment score (NES) represents the strength of the relationship between phenotype and gene signature. Bars represent means ± SEM for three independent experiments. Statistical analyses were completed by 2-way ANOVA and Bonferroni post-tests (\*\*\*\*  $p \leq 0.0001$ ).

In order to check whether IGFBP7 contributes to the improvement of energy metabolism on BCP-ALL, we determined the oxygen consumption rate (OCR) and extracellular acidification rate (ECAR) in BCP-ALL cells upon rIGF1+rIGFBP7 stimulation to assess OXPHOS and glycolysis, respectively. Both the basal and maximal OCR of the 697 cell line increased upon treatment, along with the OCR coupled to ATP synthesis (Figure 2A–C). In addition, when mitochondrial OXPHOS was chemically inhibited, treated 697 cells showed significantly increased glycolytic metabolism (Figure 2D,E). A similar trend toward increased OCR and ECAR following rIGF1+rIGFBP7 treatment was found in the RS4;11 ALL cell line, even though the differences were non-significant at the statistical level (Figures 2F,G and S2).

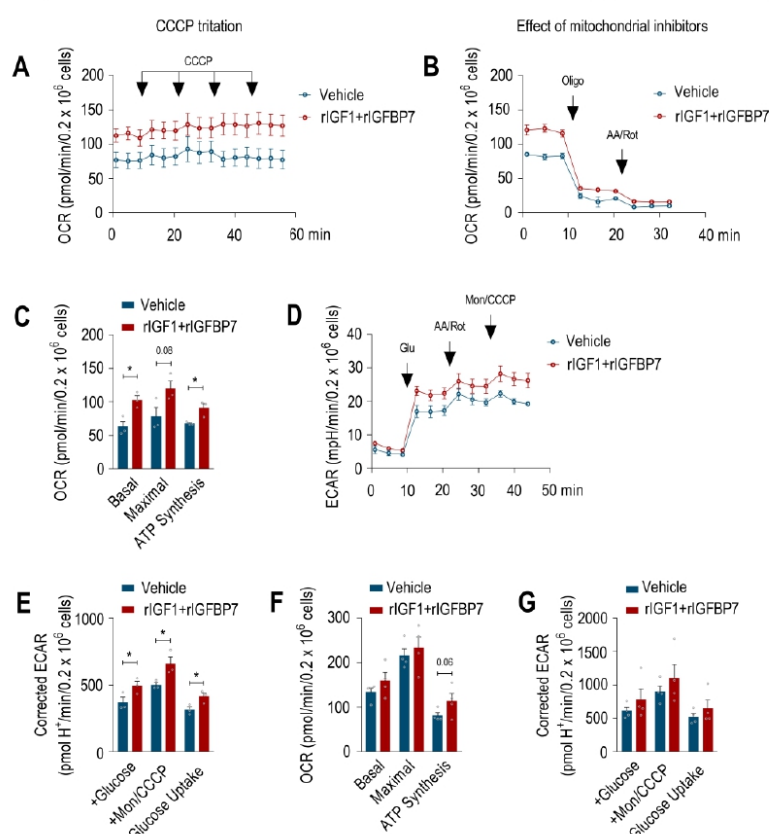


**Figure 2.** IGFBP7 enhances the energy metabolic parameters of BCP-ALL cells after IGF1 stimulation. Oxygen consumption rate (OCR) traces in 697 and RS4;11 cell lines after 4 h of treatment with rIGF1+rIGFBP7 (50 ng/mL and 100 ng/mL, respectively) or control (vehicle). (A) Arrows indicate sequential injections of CCCP (total amount of 1.2  $\mu$ M) to reach maximal OCR in 697 cells. (B) Arrows indicate oligomycin (Oligo, 1  $\mu$ g/mL) and antimycin+rotenone (AA/Rot, 1  $\mu$ M each) injections to evaluate fractions of OCR linked to ATP synthesis and non-mitochondrial OCR, respectively, in 697 cells. (C) OCR rates (basal, maximal, and linked to ATP synthesis) in 697 cell line. Bars or curves represent means  $\pm$  SEM for three independent experiments. (D) Representative extracellular acidification rate (ECAR) traces in 697 cell line after 4 h of treatment with rIGF1+rIGFBP7 (50 ng/mL and 100 ng/mL, respectively) or control (vehicle). Arrows indicate glucose (Glu, 10 mM), antimycin+rotenone (AA/Rot,



1  $\mu$ M each) and monensin+CCCP (Mon, 200  $\mu$ M; CCCP, 1  $\mu$ M) injections. (E) Individual ECAR rates in 697 cell line (basal (+glucose), maximal (Mon+CCCP), and glucose uptake (basal with glucose—basal without glucose)). Bars represent means  $\pm$  SEM for three independent experiments. (F) OCR rates (basal, maximal, and linked to ATP synthesis) in the RS4;11 cell line. Bars or curves represent means  $\pm$  SEM for four independent experiments. (G) Individual ECAR rates in the RS4;11 cell line (basal (+glucose), maximal (Mon+CCCP), and glucose uptake (basal with glucose—basal without glucose)). Bars represent means  $\pm$  SEM for four independent experiments. Statistical analyses were completed by unpaired *t*-test (\*  $p \leq 0.05$ ).

Since Akt activation induces aerobic glycolysis by promoting glucose uptake by the cell [25,26], we tested if the increased glycolytic capacity of rIGF1+rIGFBP7-treated BCP-ALL cells would rely on Akt activation and increased glucose uptake as well. To assess glucose uptake, we cultured cells in medium supplemented with 2-deoxy-D-glucose (2-DG), a glucose analog that induces cell death at high concentrations. In this assay, cell death would indicate higher 2-DG uptake. Sensitivity to lethal 2-DG supplementation was clearly more pronounced when cells were pretreated with rIGF1+rIGFBP7 than by any of these factors individually (Figure 3A,B). No such additive effect was seen with the IGF1Rko cells, indicating that IGF1R was indispensable for the increased glucose uptake triggered by rIGF1+rIGFBP7. Likewise, rIGFBP7 neutralization with an anti-IGFBP7 monoclonal antibody [17] or PI3K inhibition with Ly294002 protected rIGF1+rIGFBP7-stimulated BCP-ALL cells from the lethal effects of 2-DG, highlighting the importance of these two components (IGFBP7 and PI3K) in glucose uptake regulation in BCP-ALL. Similar results were observed in four primary BCP-ALL cells (Table S1 and Figure 3C). The level of sustained Akt phosphorylation upon rIGF1+rIGFBP7 treatment correlated to the degree of 2-DG sensitivity in BCP-ALL cell lines (Figure S3) and in primary BCP-ALL cells (Figure S4). Importantly, similar results were found when rIGF1 was substituted by insulin (Figure S5).

Studies showed that Akt activation results in increased amounts of GLUT1 at the plasma membrane of both normal and malignant hematopoietic cells [25,27,28]. Chronic Akt activation was shown to stabilize GLUT1 at the cell surface by inhibiting the endocytic machinery [29,30]. Accordingly, 24 h after rIGF1+rIGFBP7 treatment, BCP-ALL cells showed ~60% more GLUT1 on their cell surface than untreated cells. As anticipated, this effect was completely abrogated when the cells were pretreated with anti-IGFBP7 antibody or Ly294002. Moreover, IGF1Rko cells showed no changes in GLUT1 surface expression under any tested condition (Figure 4A,B). In addition, compatible results were found in primary BCP-ALL samples (Figure 4C,D). GLUT1 overexpression (*SLC2A1*) had a negative prognostic impact on several types of cancer [12], including BCP-ALL (Figure 4E). The glucose metabolism was implicated in the mechanism of action and resistance to L-asparaginase [31] and glucocorticoids [32–34] in ALL. Therefore, understanding the molecular mechanism that governs GLUT1 expression and glycolysis in ALL seems to be extremely important.

Activation of the PI3K–Akt pathway in immune cells triggers the glycolytic metabolism, primarily by promoting GLUT1 expression and the transport of glucose across the plasma membrane [7–10]. Numerous studies suggested that targeting the PI3K–Akt pathway could be a potential approach to disrupt GLUT1 activity and block glycolytic metabolism in ALL, thereby contributing to disease eradication [25,27–30].

Despite a wealth of knowledge about the pro-survival effects mediated by the PI3K–Akt pathway in cancer, the non-classical physiological mechanisms regulating this pathway remain poorly understood. Previously, we demonstrated a significant activation of the insulin/IGF1–IGF1R–PI3K–Akt axis by IGFBP7 in ALL. Our data showed that the physiological levels of IGFBP7 sustain the surface expression and activation of IGF1R by insulin/IGF1, revealing a new mechanism of ALL survival and chemotherapy resistance [17,35]. We also demonstrated that the genetic knockdown or IGFBP7 neutralization using an anti-IGFBP7 monoclonal antibody significantly decreased ALL progression in vivo, highlighting IGFBP7 as a potential therapeutic target for ALL [17].



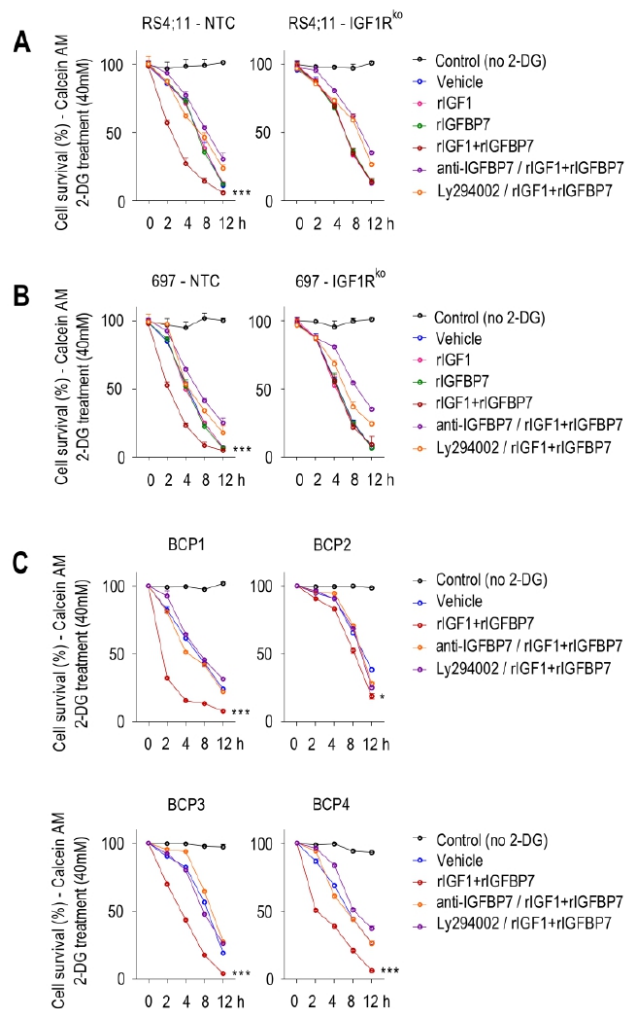


**Figure 3.** IGFBP7 potentiates glucose uptake in BCP-ALL in an IGF1-, IGF1R-, and PI3K-dependent manner, as evaluated by the 2-DG induced cell death assay. **(A–C)** Calcein AM cell viability assay in **(A)** RS4;11 and **(B)** 697 BCP-ALL cell lines (no target control (NTC) and IGF1R knockout) and **(C)** primary BCP-ALL cells. Except for the control (no 2-DG; black lines), in all other conditions cells were pretreated with rIGF1 (50 ng/mL) and/or rIGFBP7 (100 ng/mL) for 4 h and then subjected to 2-DG treatment (40 mM) for up to 12 h. Where indicated, cells were pretreated with an anti-IGFBP7 antibody (clone C311, 20 µg/mL) or Ly294002 (30 µM), which was added 30 min before rIGF1+rIGFBP7 treatment initiation. Viable cells (Calcein +) were measured by flow cytometry at each indicated time point. Curves represent means  $\pm$  SEM for three independent experiments. Statistical analyses correspond to differences between areas under the curves (AUC) (\*  $p \leq 0.05$ ; \*\*\*  $p \leq 0.001$ ).

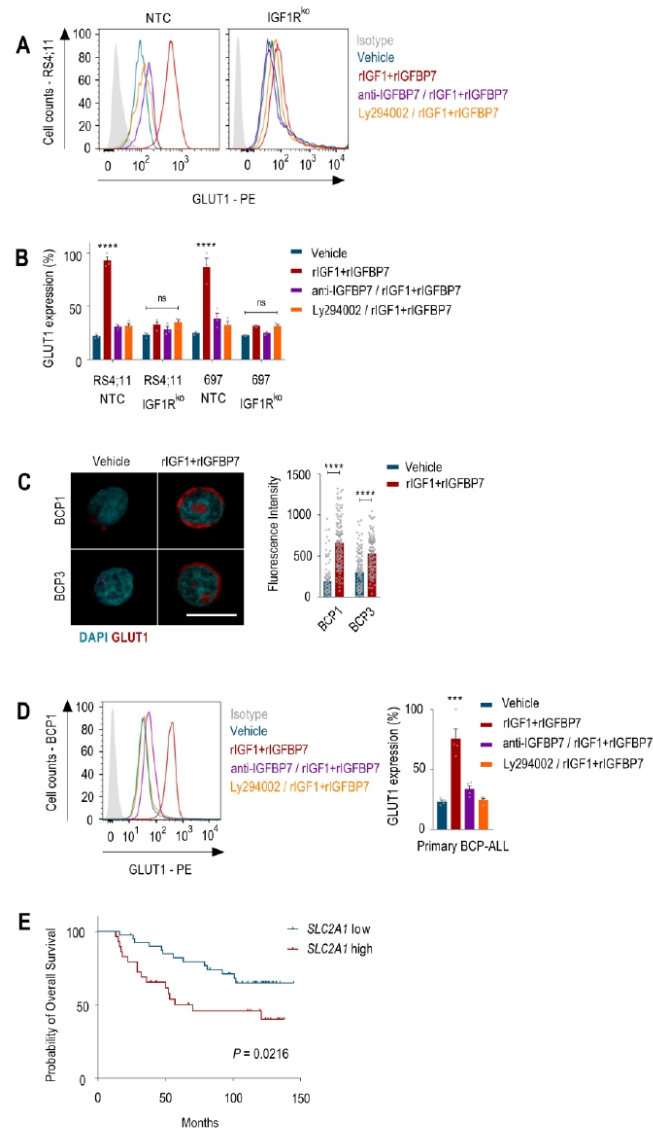


**Figure 4.** IGFBP7 promotes GLUT1 expression at the cell surface of BCP-ALL in an IGF1-, IGF1R-, and PI3K-dependent manner. **(A)** GLUT1 cell surface expression obtained by flow cytometry in the RS4;11 and 697 BCP-ALL cell lines (no target control (NTC) and IGF1R knockout) after 24 h of treatment with rIGF1+rIGFBP7 (50 ng/mL and 100 ng/mL, respectively) or control (vehicle). Where indicated, cells were pretreated with an anti-IGFBP7 antibody (clone C311, 20 µg/mL) or Ly294002 (30 µM), which was added 30 min before rIGF1+rIGFBP7 (30 µM). **(B)** Normalized results of GLUT1 surface expression from three independent experiments. Bars represent means ± SEM; ns = not significant. **(C)** Confocal analysis of GLUT1 expression in two primary BCP-ALL (BCP1 and 3) samples collected

24 h after treatment with rIGF1+rIGFBP7 (50 ng/mL and 100 ng/mL, respectively) or control (vehicle). Scale bar: 10  $\mu$ m. Bars represent means  $\pm$  SEM of the fluorescence intensity of individual cells (symbols). (D) GLUT1 cell surface expression obtained by flow cytometry in primary BCP-ALL cells treated for 24 h with rIGF1+rIGFBP7 (50 ng/mL and 100 ng/mL, respectively) or control (vehicle). Where indicated, cells were pretreated with an anti-IGFBP7 antibody (clone C311, 20  $\mu$ g/mL) or LY294002 (30  $\mu$ M), which was added 30 min before rIGF1+rIGFBP7. Left: GLUT1 cell surface expression in a representative case (BCP1). Right: normalized results for GLUT1 cell surface expression for four different primary BCP-ALL samples. (E) Kaplan–Meier survival curves generated by the cBioPortal (<http://www.cbioportal.org> (accessed on 15 February 2023)). Overall survival curves of BCP-ALL patients according to low ( $n = 40$ ) versus high ( $n = 41$ ) *SLC2A1* expression. Curves were compared by the log-rank test. Bars represent means  $\pm$  SEM. Differences were compared by 1- or 2-way ANOVA and Bonferroni post-tests (\*\* $p \leq 0.001$ ; \*\*\*\* $p \leq 0.0001$ ).

Although we extensively explored and discussed the molecular mechanism underlying these effects in our previous studies [17,35], here, we present a novel avenue for therapeutic interventions targeting the glycolytic metabolism in ALL. Our findings support the involvement of IGFBP7 in GLUT1 expression and in promoting an increased glycolytic metabolism in BCP-ALL. Specifically, we discovered that the rIGF1+rIGFBP7-mediated activation of the PI3K–Akt pathway was mainly dependent on IGF1R, as knocking out this receptor in the BCP-ALL cell lines resulted in signaling abrogation. To confirm the role of both IGFBP7 and PI3K–Akt in enhancing the glycolytic activity of BCP-ALL, we employed two strategies: (1) neutralization of the IGFBP7 protein with a monoclonal antibody and (2) inhibition of PI3K with the LY294002 drug. Both approaches resulted in significant inhibition of the sustained PI3K–Akt–GLUT1 signaling induced by rIGF1+rIGFBP7, thus validating the significance of the IGF1+IGFBP7–IGF1R–Akt–GLUT1 axis in regulating the glycolytic metabolism of BCP-ALL (Figure 5).

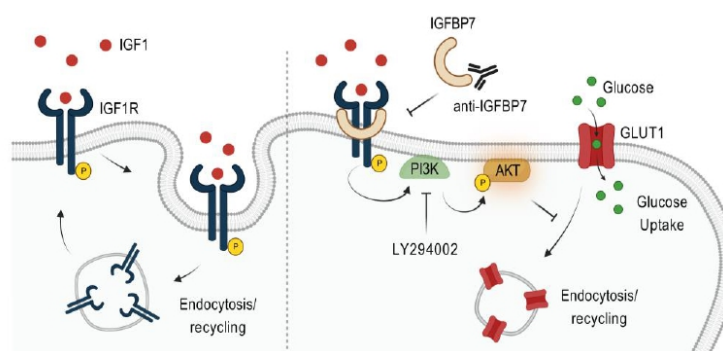


**Figure 5.** Schematic diagram illustrating the proposed mechanism by which IGFBP7 stimulates the glycolytic metabolism of ALL. In presence of IGFBP7, IGF1R remains active on the cell surface and sustains the activation of the PI3K–Akt pathway for a longer time. Active Akt blocks GLUT1 endocytosis/recycling, thus resulting in more GLUT1 at the cell surface and in increased glucose transport to fuel the glycolytic metabolism. IGFBP7 neutralization with a monoclonal antibody or the pharmacological inhibition of PI3K–Akt pathway was shown to abrogate this effect, restoring the physiological levels of GLUT1 on the cell surface. The mechanism by which IGFBP7 retains IGF1R at the cell surface is not known. Figure created with [BioRender.com](https://www.biorender.com).

The metabolic effect described here may offer an additional mechanistic explanation for the strong negative impact seen in ALL cells *in vitro* and *in vivo* after the knockdown or antibody neutralization of IGFBP7 [17], while reinforcing the notion that it is a valid target for future therapeutic interventions. In conclusion, our observations reveal a hitherto

unknown role for IGF1R in the glycolytic metabolism of BCP-ALL, opening doors for future investigations.

### 3. Materials and Methods

#### 3.1. Cell Culture

BCP-ALL cell lines and primary BCP-ALL were cultured as described by Artico et al. [17]. The use of primary BCP-ALL for in vitro experiments was approved by the Research Ethics Committee from the State University of Campinas (CAAE: 0014.0.144.146-08 and 0018.0.144.146-08).

#### 3.2. Knockout of IGF1R in BCP-ALL Cell Lines

Knockout of IGF1R in RS4;11 and 697 cells was performed using the all-in-one doxycycline inducible CRISPR system with lentiviral vector TLCV2 (Ref. #87360, Addgene, Watertown, MA, USA). We designed a guide sequence to knockout IGF1R at exon 3 (IGF1R gRNA: 5'-CACCGGCATAGTAGTAGTGG-3') and a non-targeting sequence as a control (NTC gRNA: 5'-AAATGTGAGATCAGAGTAAT-3'). Guide-sequence oligonucleotides were phosphorylated with T4 PNK (Thermo Fisher Scientific, Waltham, MA, USA) and annealed by incubation in a thermocycler under the following conditions: 30 min at 37 °C, 5 min at 95 °C, ramp down to 25 °C at 5 °C per min. TLCV2 was digested with Esp3I (Thermo Fisher Scientific) and ligated to the phosphorylated and annealed oligonucleotides by incubation at 22 °C for 1 h with T4 DNA ligase. Competent *Stbl3 E. coli* cells were transformed with each ligation reaction, and plasmid DNA was extracted with the NucleoSpin Plasmid Mini kit (Macherey-Nagel, Düren, Germany). For production of lentiviral particles containing each TLCV2 construct, we used the second-generation lentiviral package plasmid psPAX2 (Ref. #12260, Addgene, Watertown, MA, USA) and the VSV-G envelope plasmid pMD2.G (Ref. #12259, Addgene, Watertown, MA, USA). HEK293T cells cultured in DMEM medium containing 10% FBS and 1% penicillin/streptomycin were transfected at 70% confluence with each TLCV2 construct and helper plasmids at a ratio of 3:2:1 TLCV2:psPAX2:pMD2.G, with 1 µg of DNA per mL of culture medium. Transfection was performed using polyethylenimine (PEI; Sigma-Aldrich, St. Louis, MO, USA) at a ratio of 3:1 PEI:DNA (*w/w*), with both PEI and DNA diluted in Opti-MEM (Thermo Fisher Scientific, Waltham, MA, USA) at a volume 1/10 of the total volume of culture medium, followed by incubation for 20 min before being applied to the cells. Transfection medium was replaced with culture medium without antibiotics 16 h after transfection. Supernatant containing lentiviral particles was collected 24 h and 48 h later and filtered through a 0.45 µm PVDF membrane. RS4;11 and 697 cells were transduced by spinfection with Polybrene (Sigma-Aldrich, St. Louis, MO, USA). Polybrene was applied to the supernatant containing lentiviral particles to a final concentration of 8 µg/mL. Next, the supernatant was used to resuspend  $3.0 \times 10^5$  cells in a 24-well plate, which was then centrifuged at  $800 \times g$  for 1 h at room temperature. Transduction medium was replaced with culture medium 6 h after transduction. Two days later, puromycin (Thermo Fisher Scientific, Waltham, MA, USA) was added to the medium at a concentration of 2 µg/mL to select transduced cells. To induce Cas9 expression from the TLCV2 construct, cells were incubated with 1 µg/mL doxycycline (Sigma-Aldrich, St. Louis, MO, USA) for 48 h. Cells were then incubated with anti-IGF1R (anti-hCD221-BV421, clone 1H7) and/or anti-INSR (anti-hCD220-PE, clone 3B6) antibodies (Becton Dickinson, Franklin Lakes, NJ, USA) or the corresponding isotype controls (mIgG1k-BV421, clone X40 and mIgG1k-PE, clone MOPC-21, respectively; Becton Dickinson, Franklin Lakes, NJ, USA) and then analyzed by flow cytometry. Cells transduced with the TLCV2-IGF1R sgRNA construct that were positive for EGFP (indicating induction of Cas9 expression) and negative for surface IGF1R (relative to cells transduced with the TLCV2-NTC sgRNA) were sorted with BD FACSAria™ Fusion (Becton Dickinson, Franklin Lakes, NJ, USA).

### 3.3. Enzyme-Linked Immunosorbent Assay—ELISA

BCP-ALL cells ( $1 \times 10^6$ ) were incubated for 4 h in serum-free medium (RPMI1640 for cell lines and AIM-V for primary cells). Afterwards, cells were treated with rIGF1 (50 ng/mL, R&D Systems Biotechnology, Minneapolis, MI, USA) and/or rIGFBP7 (100 ng/mL, R&D Systems Biotechnology, Minneapolis, MI, USA) for 4 h. Where indicated, cells were pretreated with an anti-IGFBP7 antibody (clone C311, 20 µg/mL [17] or Ly294002 (30 µM, #9901 Cell Signaling Technology, Danvers, MA, USA), which was added 30 min before rIGF1+rIGFBP7 treatment initiation. Enzyme-linked immunosorbent assay (ELISA) for phospho-IGF1R, phospho-INSR, and phospho-Akt in BCP-ALL cell lines and primary BCP-ALL cells was performed as described by Artico et al. [17].

### 3.4. Differential Expression Array Analysis

Gene expression analysis were performed using three different BCP-ALL cell lines (697, RS4;11, and REH), untransformed or transformed with lentiviral MISSION pLKO.1-puro shRNA expression vectors (Sigma-Aldrich, St. Louis, MO, USA) against IGFBP7 (shRNA #812 and shRNA #959) or non-template control (shRNA Scrambled) [11]. The experiments were performed in 6-well plates ( $1 \times 10^6$  cells/well), with all four versions of each of the cell lines (WT, Scrambled, #812, and #959). Cells were starved during 4 h in serum-free RPMI1640 medium, and then two wells for each version were stimulated with rIGF1+rIGFBP7 (50 ng/mL and 100 ng/mL, respectively) and two wells with vehicle (control, PBS) for 6 h. Cells from the duplicate wells were joined, and total RNA was extracted using the Illustra RNA Mini Spin kit (GE Healthcare Life Sciences, Chicago, IL, USA). RNA was quantified using Qubit Fluorometer (Thermo Fisher Scientific, Waltham, MA, USA) and run in agarose gel electrophoresis for quality assessment. The isolated RNA was amplified, labeled, and purified to obtain biotin-labeled cRNA using the reagents and enzymes supplied in the GeneChip® WT Pico Reagent Kit (Affymetrix, Thermo Fisher Scientific, Waltham, MA, USA), in accordance with the instructions of the manufacturer. Array hybridization and washes were performed using GeneChip® Hybridization, Wash, and Stain kit (Affymetrix, Thermo Fisher Scientific, Waltham, MA, USA) on a Hybridization Oven 645 and a Fluidics Station 450 (Affymetrix, Thermo Fisher Scientific, Waltham, MA, USA). Slides were scanned using GeneChip® Scanner 3000 (Affymetrix, Thermo Fisher Scientific, Waltham, MA, USA) and Command Console software 3.1 (Affymetrix, Thermo Fisher Scientific, Waltham, MA, USA) with default settings. CEL files were analyzed using Affymetrix Expression Console software (version 4.0.1). A Principal Component Analysis (PCA) in Affymetrix Expression Console software (version 4.0.1) revealed that the expression values for the RS4;11 #812 cells (both untreated or treated with rIGFBP7+rIGF1) were outliers and were, therefore, discarded from subsequent analysis. Gene expression values were obtained using the Signal Space Transformation-Robust Multi-Chip Analysis (SST-RMA) analysis algorithm. Log2 expression values were used for Gene Set Enrichment Analysis (GSEA) [19,20] against the Hallmark gene sets [36]. As differences between WT/Scrambled versus knockdown cell lines were not strong enough to overcome differences due to the genetic background of the cell lines used, we found it better to simply compare, irrespectively of any genetic modification, rIGF1+rIGFBP7-treated versus -untreated (vehicle). Untreated (vehicle) WT, Scrambled, #812, and #959 cells from the three different cell lines were all together in one group ( $n = 11$ , because RS4;11\_#812 was excluded), whereas rIGF1+rIGFBP7-treated WT, Scrambled, #812, and #959 cells ( $n = 11$ ) were in the other group. By doing so, we increased the sample size and the statistical discrimination of differences among groups under comparison. Significant Hallmark gene sets were selected (nominal  $p$  values  $\leq 0.05$ ) and distributed by the Normalized Enrichment Score (NES).

### 3.5. Extracellular Flux Analysis in 697 and RS4;11 Cell Lines

Oxygen consumption (OCR) and extracellular acidification rate (ECAR) in 697 and RS4;11 cell lines were measured using a Seahorse XF24 Analyzer (Agilent Technologies, Santa Clara, CA, USA). Cells were starved (serum-free) for 4 h and then treated with



rIGF1+rIGFBP7 (50 ng/mL and 100 ng/mL, respectively) or vehicle (PBS) for 4 h. Cells were seeded at  $2 \times 10^5$ /well in plates previously treated with poly-D-lysine (100 µg/mL, Sigma-Aldrich, St. Louis, MO, USA) and then submitted to centrifugation at  $300 \times g$  for 5 min at room temperature to attach the cells to the well surface. Initially, 500 µL of RPMI1640 medium was placed in each well, and each injection consisted of 75 µL of the respective RPMI1640 medium with the target compound, resulting in a final volume of 800 µL. Three protocols were established to analyze oxidative phosphorylation (OXPHOS) and glycolysis. For OXPHOS, two experimental protocols were performed with RPMI1640 (pH 7.4), containing 10 mM glucose, 1 mM pyruvate, and 2 mM glutamine as metabolic substrates. The first protocol was intended to analyze basal oxygen consumption rate (OCR), maximal OCR, and spare respiratory capacity (SRC). Thus, all four injections were performed with protonophore carbonyl cyanide m-chlorophenylhydrazone (CCCP) to reach final concentrations in wells of 400 nM, 800 nM, 1000 nM, and 1200 nM. The second protocol was to evaluate the mitochondrial parameters such as the fraction of OCR linked to ATP synthesis, H<sup>+</sup> leak, and non-mitochondrial OCR. The first addition consisted of 1 µg/mL oligomycin, and the second was of 1 µM antimycin A plus 1 µM rotenone. These two protocols were performed separately in order to avoid underestimation of parameters, maximal OCR and spare respiratory capacity, which can occur in the presence of oligomycin [37,38]. For glycolysis estimation, ECAR was measured, and the protocol was performed with RPMI1640 (pH 7.4) containing 2 mM glutamine. The first addition consisted of 10 mM glucose, the second of 1 µM antimycin A plus 1 µM rotenone, and the third of 200 µM monensin plus 1 µM CCCP [39]. ECAR values were corrected for non-glycolytic acidification [39], considering glutamine as the predominant mitochondrial metabolic substrate. Before the initiation of the three protocols described above, cells were maintained in incubator at 37 °C (without CO<sub>2</sub>) for 1 h to deplete intracellular glucose. At the end of each experiment, the cells were washed twice with PBS, and their viability was determined by the fluorescence of Calcein (200 nM) in a plate reader (Spectra Max M3, Molecular Devices, San Jose, CA, USA). Fluorescence was read at excitation of 492 nm and emission of 518 nm in endpoint mode with an integration time of 1 s. OCR and ECAR values were normalized to cell viability.

### 3.6. 2-DG Treatment and Cell Viability by Calcein-AM Assay

BCP-ALL cells ( $2.5 \times 10^5$ ) were starved for 4 h in serum-free medium (RPMI1640 for cell lines and AIM-V for primary cells). After starvation, cells were treated with rIGF1 (50 ng/mL), insulin (3 nM, Novo Nordisk, Bagsvaerd, Denmark), and/or rIGFBP7 (100 ng/mL) for 4 h. Where indicated, cells were pretreated with an anti-IGFBP7 antibody (clone C311, 20 µg/mL) or Ly294002 (30 µM), which was added 30 min before rIGF1+rIGFBP7 or insulin+rIGFBP7 treatment initiation. 2-DG (40 mM, Sigma-Aldrich, St. Louis, MO, USA) treatment started after 4 h of rIGF1, insulin, and/or rIGFBP7 stimulation. Cellular viability was measured by Calcein-AM (Thermo Fisher Scientific, Waltham, MA, USA). Calcein positive cells were monitored in a timecourse by flow cytometry using a LSR Fortessa cytometer (Becton Dickinson, Franklin Lakes, NJ, USA) 30 min after addition of Calcein-AM (200 nM). Data were analyzed with FlowJo software Version 10 (Becton Dickinson, Franklin Lakes, NJ, USA).

### 3.7. GLUT1 Cell Surface Expression by Flow Cytometry

BCP-ALL cells ( $2.5 \times 10^5$ ) were starved in serum-free medium (RPMI1640 for cell lines and AIM-V for primary cells) for 4 h and then stimulated with rIGF1+rIGFBP7 (50 ng/mL and 100 ng/mL, respectively) for 24 h. Where indicated, cells were pretreated with an anti-IGFBP7 antibody (clone C311, 20 µg/mL) or Ly294002 (30 µM), which was added 30 min before rIGF1+rIGFBP7 treatment initiation. Cells were washed with PBS and fixed with 4% paraformaldehyde without permeabilization. Surface expression of GLUT1 was analyzed by labeling cells with the anti-hGLUT1-PE (NB110-39113PE, Novus Biologicals, Centennial, CO, USA) antibody or the corresponding isotype control (mIgG1k-PE, clone MOPC-21, Becton Dickinson, Franklin Lakes, NJ, USA) diluted in 0.5% BSA in PBS for

30 min at 4 °C. Cells were analyzed in a LSR Fortessa cytometer and with FlowJo Software Version 10 (Becton Dickinson, Franklin Lakes, NJ, USA).

### 3.8. GLUT1 Cell Surface Expression by Confocal Analysis

BCP-ALL primary cells ( $5 \times 10^5$ ) were cultured in a 12-well Millicell glass chamber (Sigma-Aldrich, Merck) previously treated with poly-D-lysine (100 µg/mL) and then submitted to centrifugation at  $300 \times g$  for 5 min at room temperature to attach the cells to the wells' surface. These cells were starved in serum-free medium (AIM-V) for 4 h and then were stimulated with rIGF1+rIGFBP7 (50 ng/mL and 100 ng/mL, respectively) for 24 h. Cells were washed 3 times with PBS, fixed with 4% paraformaldehyde without permeabilization, incubated with the unconjugated monoclonal rabbit anti-GLUT1 antibody (1:100—clone D3J3A, #12939 Cell Signaling Technology) overnight at 4 °C, washed 3 times in PBS, and incubated with anti-Rabbit IgG Fab2 Alexa Fluor (R) 555 (1:500—#4413 Cell Signaling Technology) for 1 h at room temperature. Nuclear staining was completed with DAPI solution (1 µg/mL, Thermo Fisher Scientific) for 10 min. Slides were analyzed using a Zeiss LSM 800 Confocal microscope (63× immersion), and pixel quantification was performed using Image J Fiji Software (Version 1.53t) (Becton Dickinson, Franklin Lakes, NJ, USA) for each individual cell.

### 3.9. Kaplan–Meier Survival Curves

RNA-Seq data on SLC2A1 expression at diagnosis for a series of BCP-ALL samples with overall survival information were generated by the TARGET Initiative (phs000464), which we obtained through cBioPortal (<http://www.cbioportal.org> (accessed on 15 February 2023)), an open-access database for Cancer Genomics [40]. Patients were divided into two groups according to the median SLC2A1 expression: low ( $n = 40$ ) and high ( $n = 41$ ). Survival curves were generated by the Kaplan–Meier method and compared by the log-rank test using GraphPad Prism 8.0 software.

**Supplementary Materials:** The following supporting information can be downloaded at <https://www.mdpi.com/article/10.3390/ijms24119679/s1>.

**Author Contributions:** L.L.A. and J.A.Y. conceived and designed the study; L.L.A. contributed to and coordinated all the experiments. J.S.R. and R.F.C. performed the Seahorse experiments and analyses. N.A.M. and X.S. performed the microarray experiment and analysis. J.R.T.J. generated the knockout of IGF1R in BCP-ALL cells. G.S. performed the confocal microscopy experiment. S.R.B. contributed patients' samples and the corresponding clinical data; L.L.A. and J.A.Y. performed the statistical analysis and wrote the manuscript. All authors have read and agreed to the published version of the manuscript.

**Funding:** L.L.A. received a scholarship from the Fundação de Amparo à Pesquisa do Estado de São Paulo (FAPESP, processes 2019/04943-3 and 2022/04464-0). J.A.Y. received a Research Productivity fellowship from the Brazilian National Council of Technological and Scientific Development (CNPq, processes 305896/2013-0, 301596/2017-4, and 308399/2021-8). This work was supported by grants to J.A.Y. from CNPq (471003/2013-1) and FAPESP (12/12802-1, 14/20015-5) and to R.F.C. from FAPESP (17/17728-8).

**Institutional Review Board Statement:** The study was conducted in accordance with the Declaration of Helsinki and was approved by the Research Ethics Committee from the State University of Campinas (CAAE: 0014.0.144.146-08 and 0018.0.144.146-08).

**Informed Consent Statement:** Informed consent was obtained from all the subjects involved in the study.

**Data Availability Statement:** The data presented in this study are available on request from the corresponding author.

**Acknowledgments:** The authors would like to thank Leticia Grillo Guimarães Pereira, Gabriella Lima dos Reis, and Priscila Pini Zenatti for their excellent technical help with the anti-IGFBP7 monoclonal antibody production/purification.

**Conflicts of Interest:** The authors declare no conflict of interest.

## References

1. Inaba, H.; Mullighan, C.G. Pediatric acute lymphoblastic leukemia. *Haematologica* **2020**, *105*, 2524–2539. [\[CrossRef\]](#) [\[PubMed\]](#)
2. Greaves, M. A causal mechanism for childhood acute lymphoblastic leukaemia. *Nat. Rev. Cancer* **2018**, *18*, 471–484. [\[CrossRef\]](#)
3. Hunger, S.P.; Mullighan, C.G. Acute Lymphoblastic Leukemia in Children. *N. Engl. J. Med.* **2015**, *373*, 1541–1552. [\[CrossRef\]](#)
4. Maule, M.; Scélo, G.; Pastore, G.; Brennan, P.; Hemminki, K.; Tracey, E.; Sankila, R.; Weiderpass, E.; Olsen, J.H.; McBride, M.L.; et al. Risk of second malignant neoplasms after childhood leukemia and lymphoma: An international study. *J. Natl. Cancer Inst.* **2007**, *99*, 790–800. [\[CrossRef\]](#)
5. Yavvari, S.; Makena, Y.; Sukhvasi, S.; Makena, M.R. Large Population Analysis of Secondary Cancers in Pediatric Leukemia Survivors. *Children* **2019**, *6*, 130. [\[CrossRef\]](#)
6. Al-Mahayri, Z.N.; AlAhmad, M.M.; Ali, B.R. Long-Term Effects of Pediatric Acute Lymphoblastic Leukemia Chemotherapy: Can Recent Findings Inform Old Strategies? *Front. Oncol.* **2021**, *11*, 710163. [\[CrossRef\]](#) [\[PubMed\]](#)
7. Chan, L.N.; Chen, Z.; Braas, D.; Lee, J.-W.; Xiao, G.; Geng, H.; Cosgun, K.N.; Hurtz, C.; Shojaaee, S.; Cazzaniga, V.; et al. Metabolic gatekeeper function of B-lymphoid transcription factors. *Nature* **2017**, *542*, 479–483. [\[CrossRef\]](#)
8. Müschen, M. Metabolic gatekeepers to safeguard against autoimmunity and oncogenic B cell transformation. *Nat. Rev. Immunol.* **2019**, *19*, 337–348. [\[CrossRef\]](#)
9. Boag, J.M.; Beesley, A.; Firth, M.J.; Freitas, J.R.; Ford, J.; Hoffmann, K.; Cummings, A.J.; de Klerk, N.; Kees, U.R. Altered glucose metabolism in childhood pre-B acute lymphoblastic leukaemia. *Leukemia* **2006**, *20*, 1731–1737. [\[CrossRef\]](#) [\[PubMed\]](#)
10. Liu, T.; Kishton, R.J.; Macintyre, A.N.; Gerriets, V.A.; Xiang, H.; Liu, X.; Abel, E.D.; Rizzieri, D.; Locasale, J.W.; Rathmell, J.C. Glucose transporter 1-mediated glucose uptake is limiting for B-cell acute lymphoblastic leukemia anabolic metabolism and resistance to apoptosis. *Cell Death Dis.* **2014**, *5*, e1516. [\[CrossRef\]](#)
11. Wofford, J.A.; Wieman, H.L.; Jacobs, S.R.; Zhao, Y.; Rathmell, J.C. IL-7 promotes Glut1 trafficking and glucose uptake via STAT5-mediated activation of Akt to support T-cell survival. *Blood* **2008**, *111*, 2101–2111. [\[CrossRef\]](#)
12. Ancey, P.; Contat, C.; Meylan, E. Glucose transporters in cancer—from tumor cells to the tumor microenvironment. *FEBS J.* **2018**, *285*, 2926–2943. [\[CrossRef\]](#)
13. Chandel, N.S. Signaling and Metabolism. *Cold Spring Harb. Perspect. Biol.* **2021**, *13*, a040600. [\[CrossRef\]](#)
14. Hoxhaj, G.; Manning, B.D. The PI3K–AKT network at the interface of oncogenic signalling and cancer metabolism. *Nat. Rev. Cancer* **2020**, *20*, 74–88. [\[CrossRef\]](#) [\[PubMed\]](#)
15. Xu, K.; Yin, N.; Peng, M.; Stamatiades, E.G.; Chhangawala, S.; Shyu, A.; Li, P.; Zhang, X.; Do, M.H.; Capistrano, K.J.; et al. Glycolytic ATP fuels phosphoinositide 3-kinase signaling to support effector T helper 17 cell responses. *Immunity* **2021**, *54*, 976–987. [\[CrossRef\]](#)
16. Xu, K.; Yin, N.; Peng, M.; Stamatiades, E.G.; Shyu, A.; Li, P.; Zhang, X.; Do, M.H.; Wang, Z.; Capistrano, K.J.; et al. Glycolysis fuels phosphoinositide 3-kinase signaling to bolster T cell immunity. *Science* **2021**, *371*, 405–410. [\[CrossRef\]](#) [\[PubMed\]](#)
17. Artico, L.L.; Laranjeira, A.B.A.; Campos, L.W.; Corrêa, J.R.; Zenatti, P.P.; Carvalheira, J.B.C.; Brambilla, S.R.; Nowill, A.E.; Brandalise, S.R.; Yunes, J.A. Physiologic IGF1R levels prolong IGF1R activation in acute lymphoblastic leukemia. *Blood Adv.* **2021**, *5*, 3633–3646. [\[CrossRef\]](#) [\[PubMed\]](#)
18. Evdokimova, V.; Tognon, C.E.; Benatar, T.; Yang, W.; Krutikov, K.; Pollak, M.; Sorensen, P.H.B.; Seth, A. IGF1R Binds to the IGF-1 Receptor and Blocks Its Activation by Insulin-Like Growth Factors. *Sci. Signal.* **2012**, *5*, ra92. [\[CrossRef\]](#) [\[PubMed\]](#)
19. Mootha, V.K.; Lindgren, C.M.; Eriksson, K.-E.; Subramanian, A.; Sihag, S.; Lehar, J.; Puigserver, P.; Carlsson, E.; Ridderstråle, M.; Laurila, E.; et al. PGC-1 $\alpha$ -responsive genes involved in oxidative phosphorylation are coordinately downregulated in human diabetes. *Nat. Genet.* **2003**, *34*, 267–273. [\[CrossRef\]](#)
20. Subramanian, A.; Tamayo, P.; Mootha, V.K.; Mukherjee, S.; Ebert, B.L.; Gillette, M.A.; Paulovich, A.; Pomeroy, S.L.; Golub, T.R.; Lander, E.S.; et al. Gene set enrichment analysis: A knowledge-based approach for interpreting genome-wide expression profiles. *Proc. Natl. Acad. Sci. USA* **2005**, *102*, 15545–15550. [\[CrossRef\]](#)
21. Boucher, J.; Tseng, Y.-H.; Kahn, C.R. Insulin and Insulin-like Growth Factor-1 Receptors Act as Ligand-specific Amplitude Modulators of a Common Pathway Regulating Gene Transcription. *J. Biol. Chem.* **2010**, *285*, 17235–17245. [\[CrossRef\]](#) [\[PubMed\]](#)
22. Vella, V.; Milluzzo, A.; Scalisi, N.M.; Vigneri, P.; Sciacca, L. Insulin Receptor Isoforms in Cancer. *Int. J. Mol. Sci.* **2018**, *19*, 3615. [\[CrossRef\]](#) [\[PubMed\]](#)
23. Manning, B.D.; Cantley, L.C. AKT/PKB Signaling: Navigating Downstream. *Cell* **2007**, *129*, 1261–1274. [\[CrossRef\]](#) [\[PubMed\]](#)
24. Pollak, M. Insulin and insulin-like growth factor signalling in neoplasia. *Nat. Rev. Cancer* **2008**, *8*, 915–928. [\[CrossRef\]](#)
25. Rathmell, J.C.; Fox, C.J.; Plas, D.R.; Hammerman, P.S.; Cinalli, R.M.; Thompson, C.B. Akt-Directed Glucose Metabolism Can Prevent Bax Conformation Change and Promote Growth Factor-Independent Survival. *Mol. Cell. Biol.* **2003**, *23*, 7315–7328. [\[CrossRef\]](#)
26. Elstrom, R.L.; Bauer, D.E.; Buzzai, M.; Karnauskas, R.; Harris, M.H.; Plas, D.R.; Zhuang, H.; Cinalli, R.M.; Alavi, A.; Rudin, C.M.; et al. Akt Stimulates Aerobic Glycolysis in Cancer Cells. *Cancer Res.* **2004**, *64*, 3892–3899. [\[CrossRef\]](#)
27. Wieman, H.L.; Wofford, J.A.; Rathmell, J.C. Cytokine Stimulation Promotes Glucose Uptake via Phosphatidylinositol-3 Kinase/ Akt Regulation of Glut1 Activity and Trafficking. *Mol. Biol. Cell* **2007**, *18*, 1437–1446. [\[CrossRef\]](#)
28. Siska, P.J.; van der Windt, G.J.W.; Kishton, R.J.; Cohen, S.; Eisner, W.; MacIver, N.J.; Kater, A.P.; Weinberg, J.B.; Rathmell, J.C. Suppression of Glut1 and Glucose Metabolism by Decreased Akt/mTORC1 Signaling Drives T Cell Impairment in B Cell Leukemia. *J. Immunol.* **2016**, *197*, 2532–2540. [\[CrossRef\]](#)



29. Waldhart, A.N.; Dykstra, H.; Peck, A.S.; Boguslawski, E.A.; Madaj, Z.B.; Wen, J.; Veldkamp, K.; Hollowell, M.; Zheng, B.; Cantley, L.C.; et al. Phosphorylation of TXNIP by AKT Mediates Acute Influx of Glucose in Response to Insulin. *Cell Rep.* **2017**, *19*, 2005–2013. [\[CrossRef\]](#)
30. Avanzato, D.; Pupo, E.; Ducano, N.; Isella, C.; Bertalot, G.; Luise, C.; Pece, S.; Bruna, A.; Rueda, O.M.; Caldas, C.; et al. High USP6NL Levels in Breast Cancer Sustain Chronic AKT Phosphorylation and GLUT1 Stability Fueling Aerobic Glycolysis. *Cancer Res.* **2018**, *78*, 3432–3444. [\[CrossRef\]](#)
31. Takahashi, H.; Inoue, J.; Sakaguchi, K.; Takagi, M.; Mizutani, S.; Inazawa, J. Autophagy is required for cell survival under L-asparaginase-induced metabolic stress in acute lymphoblastic leukemia cells. *Oncogene* **2017**, *36*, 4267–4276. [\[CrossRef\]](#) [\[PubMed\]](#)
32. Hulleman, E.; Kazemier, K.M.; Holleman, A.; VanderWeele, D.J.; Rudin, C.M.; Broekhuis, M.J.C.; Evans, W.E.; Pieters, R.; Boer, M.L.D. Inhibition of glycolysis modulates prednisolone resistance in acute lymphoblastic leukemia cells. *Blood* **2009**, *113*, 2014–2021. [\[CrossRef\]](#) [\[PubMed\]](#)
33. Beesley, A.; Firth, M.J.; Ford, J.; Weller, E.R.; Freitas, J.R.; Perera, K.U.; Kees, U.R. Glucocorticoid resistance in T-lineage acute lymphoblastic leukaemia is associated with a proliferative metabolism. *Br. J. Cancer* **2009**, *100*, 1926–1936. [\[CrossRef\]](#) [\[PubMed\]](#)
34. Buentke, E.; Nordström, A.; Lin, H.; Björklund, A.-C.; Laane, E.; Harada, M.; Lu, L.; Tegnebratt, T.; Stone-Elander, S.; Heyman, M.; et al. Glucocorticoid-induced cell death is mediated through reduced glucose metabolism in lymphoid leukemia cells. *Blood Cancer J.* **2011**, *1*, e31. [\[CrossRef\]](#) [\[PubMed\]](#)
35. Laranjeira, A.B.A.; de Vasconcellos, J.F.; Sodek, L.; Spago, M.C.; Fornazim, M.C.; Tone, L.G.; Brandalise, S.R.; Nowill, E.A.; Yunes, J.A. IGFBP7 participates in the reciprocal interaction between acute lymphoblastic leukemia and BM stromal cells and in leukemia resistance to asparaginase. *Leukemia* **2011**, *26*, 1001–1011. [\[CrossRef\]](#)
36. Liberzon, A.; Birger, C.; Thorvaldsdóttir, H.; Ghandi, M.; Mesirov, J.P.; Tamayo, P. The Molecular Signatures Database Hallmark Gene Set Collection. *Cell Syst.* **2015**, *1*, 417–425. [\[CrossRef\]](#) [\[PubMed\]](#)
37. Ruas, J.S.; Siqueira-Santos, E.S.; Amigo, I.; Rodrigues-Silva, E.; Kowaltowski, A.J.; Castilho, R.F. Underestimation of the Maximal Capacity of the Mitochondrial Electron Transport System in Oligomycin-Treated Cells. *PLoS ONE* **2016**, *11*, e0150967. [\[CrossRef\]](#)
38. Ruas, J.S.; Siqueira-Santos, E.S.; Rodrigues-Silva, E.; Castilho, R.F. High glycolytic activity of tumor cells leads to underestimation of electron transport system capacity when mitochondrial ATP synthase is inhibited. *Sci. Rep.* **2018**, *8*, 17383. [\[CrossRef\]](#) [\[PubMed\]](#)
39. Mookerjee, S.A.; Nicholls, D.G.; Brand, M.D. Determining Maximum Glycolytic Capacity Using Extracellular Flux Measurements. *PLoS ONE* **2016**, *11*, e0152016. [\[CrossRef\]](#)
40. Gao, J.; Aksoy, B.A.; Dogrusoz, U.; Dresdner, G.; Gross, B.E.; Sumer, S.O.; Sun, Y.; Jacobsen, A.; Sinha, R.; Larsson, E.; et al. Integrative Analysis of Complex Cancer Genomics and Clinical Profiles Using the cBioPortal. *Sci. Signal.* **2013**, *6*, pl1. [\[CrossRef\]](#)

**Disclaimer/Publisher's Note:** The statements, opinions and data contained in all publications are solely those of the individual author(s) and contributor(s) and not of MDPI and/or the editor(s). MDPI and/or the editor(s) disclaim responsibility for any injury to people or property resulting from any ideas, methods, instructions or products referred to in the content.

## 7. SUPPLEMENTARY MATERIAL

### 7.1 Supplementary figures

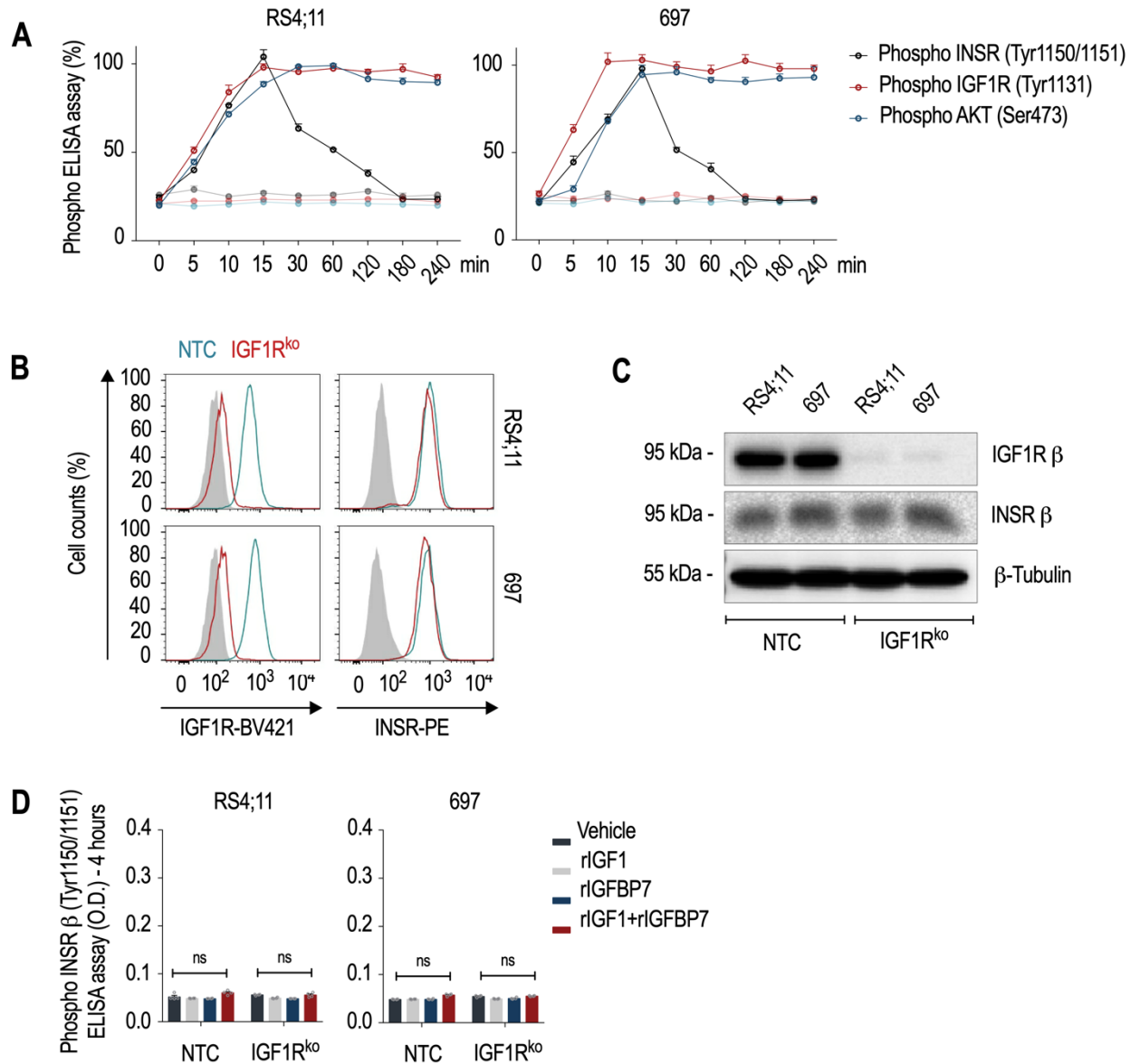


**Figure S1.** Time course of IGF1R/Akt phosphorylation and generation of IGF1R knockout BCP-ALL cell lines. (A) Normalized ELISA results for phospho-INSR $\beta$  (Tyr1150/1151), phospho-IGF1R $\beta$  (Tyr1131) and phospho-Akt (Ser473) in RS4;11 and 697 BCP-ALL cell lines. Time-lapse experiments were performed after treatment with rIGF1+rIGFBP7 (50 and 100 ng/mL, respectively) or vehicle (light lines). Curves represent means  $\pm$  SEM for two independent experiments. (B) IGF1R (left) or INSR (right) surface expression measured by flow cytometry in RS4;11 and 697 BCP-ALL cell lines (NTC, no target control and IGF1R knockout) 48 h after doxycycline activation of the CRISPR-mediated knockout. Gray histograms represents cells staining with respective isotype control antibody. (C) IGF1R, INSR

and  $\beta$ -tubulin expression in total cell lysates measured by western blot in RS4;11 and 697 BCP-ALL cell lines (NTC, no target control and IGF1R knockout) 48 h after doxycycline activation of CRISPR knockout. Western blot protocol has been previously described.<sup>1</sup> Briefly, membranes were immunoblotted overnight at 4 °C with anti-Insulin Receptor  $\beta$  (clone L55B10, #3020 Cell Signaling Technology), anti-IGF1 Receptor  $\beta$  (clone D23H3, #9750 Cell Signaling Technology) and  $\beta$ -tubulin (clone 9F3 #2128 Cell Signaling Technology). Images were acquired with a ChemiDoc equipment (Bio-Rad). (D) ELISA results for phospho-INSR $\beta$  (Tyr1150/1151) in RS4;11 and 697 BCP-ALL cell lines (NTC, no target control and IGF1R knockout) after 4 h of treatment with rIGF1 (50 ng/mL) and/or rIGFBP7 (100 ng/mL). Bars represent means  $\pm$  SEM for four independent experiments; ns = not significant.

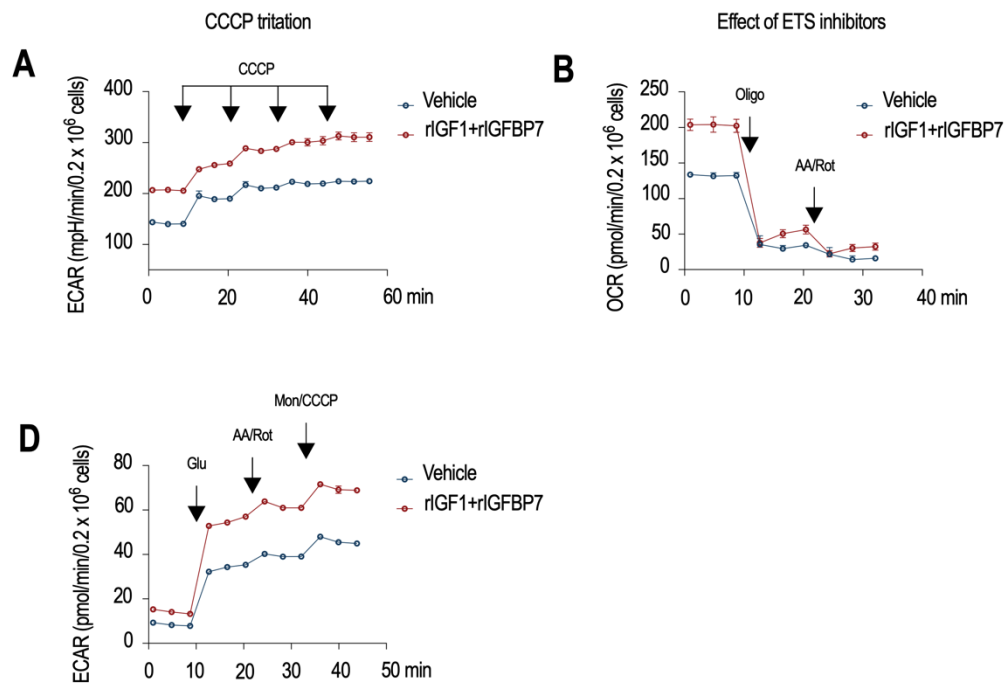


**Figure S2.** (A-B) One representative oxygen consumption rate (OCR) traces in RS4;11 cell line after 4 h of treatment with rIGF1+rIGFBP7 (50 ng/mL and 100 ng/mL, respectively) or control (vehicle). (A) Arrows indicate sequential injections of CCCP (total amount of 1.2  $\mu$ M) to reach maximal OCR. (B) Arrows indicate oligomycin (Oligo, 1  $\mu$ g/mL) and antimycin+rotenone (AA/Rot, 1  $\mu$ M each) injections to evaluate fractions of OCR linked to ATP synthesis and non-mitochondrial OCR, respectively. (C) One representative extracellular acidification rate (ECAR) traces in RS4;11 cell line after 4 h of treatment with rIGF1+rIGFBP7 (50 ng/mL and 100 ng/mL, respectively) or control (vehicle). Arrows indicate glucose (Glu, 10 mM), antimycin+rotenone (AA/Rot, 1  $\mu$ M each) and monensin+CCCP (Mon, 200  $\mu$ M; CCCP, 1  $\mu$ M) injections.

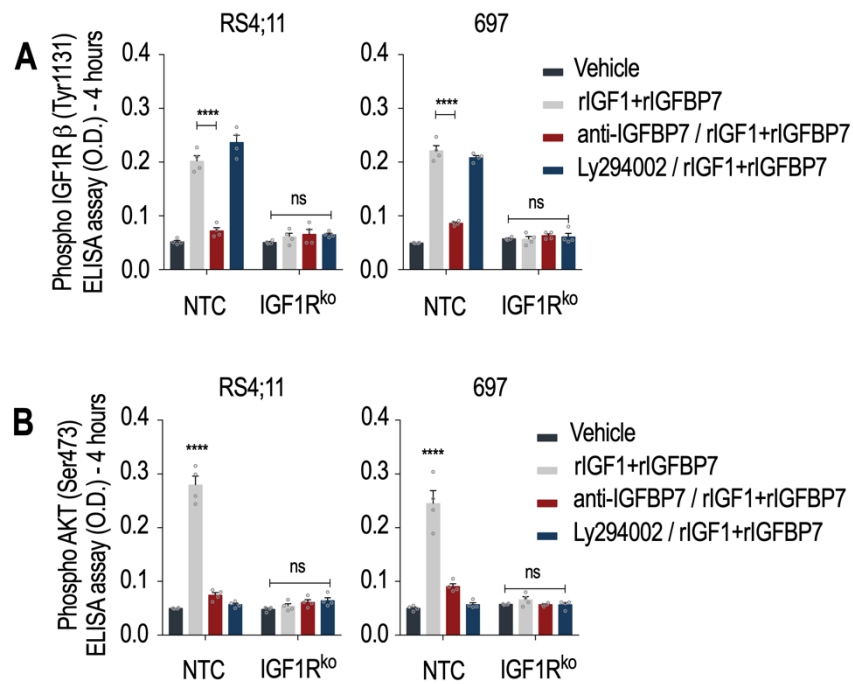


**Figure S3.** Sustained IGF1R/Akt phosphorylation in normal and IGF1R knockout BCP-ALL cells. ELISA results for (A) phospho-IGF1R $\beta$  (Tyr1131) and (B) phospho-Akt (Ser473) in RS4;11 and 697 BCP-ALL cell lines (NTC, no target control and IGF1R knockout) 4 h after rIGF1+ rIGFBP7 treatment (50 and 100 ng/mL, respectively). Where indicated, cells were pretreated with an anti-IGFBP7 antibody (clone C311, 20  $\mu$ g/mL) or Ly294002 (30  $\mu$ M) which were added 30 min before rIGF1+rIGFBP7. Bars represent means  $\pm$  SEM for four wells. Statistical analyses were done by 2-way ANOVA and Bonferroni posttests (\*\*\*\* $P \leq 0.0001$ ); ns = not significant.

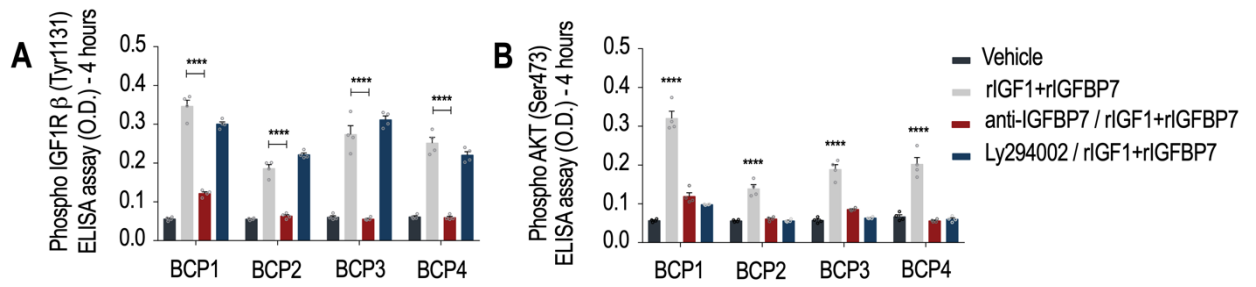


**Figure S4.** Sustained IGF1R/Akt phosphorylation in primary BCP-ALL cells. ELISA results for (A) phospho-IGF1R $\beta$  (Tyr1131) and (B) phospho-Akt (Ser473) in four different primary BCP-ALL samples 4 h after treatment with rIGF1+rIGFBP7 (50 and 100 ng/mL, respectively) or vehicle. Where indicated, cells were also treated with an anti-IGFBP7 antibody (clone C311, 20  $\mu$ g/mL) or Ly294002 (30  $\mu$ M) which were added 30 min before rIGF1+rIGFBP7. Bars represent means  $\pm$  SEM for four wells. Statistical analyses were done by 2-way ANOVA and Bonferroni posttests (\*\*\*\* $P \leq 0.0001$ ).

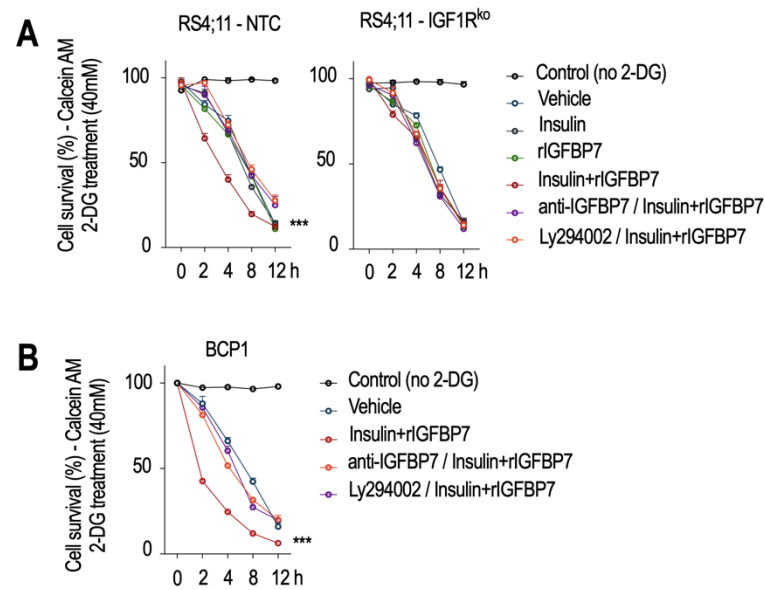


**Figure S5.** Calcein AM cell viability assays on BCP-ALL cells exposed to lethal doses of 2-deoxy-D-glucose (2-DG). Cell viability results for the **(A)** RS4;11 BCP-ALL cell line (NTC: no target control and IGF1R knockout) and **(B)** BCP1 primary BCP-ALL sample. For all conditions (except for the “no 2-DG” control group, black lines) cells were pretreated with rIGF1 (50 ng/mL) and/or rIGFBP7 (100 ng/mL) for 4 h and then subjected to 2-DG treatment (40 mM) for up to 12 h. Where indicated, cells were also pretreated with an anti-IGFBP7 antibody (20 µg/mL) or Ly294002 (30 µM) which were added 30 min before rIGF1+rIGFBP7. Viable cells (Calcein+) were determined by flow cytometry at each indicated time point. Curves represent means  $\pm$  SEM for three independent experiments. Statistical analyses correspond to differences between areas under the curves (AUC) (\*\*P $\leq$ 0.01, \*\*\*P $\leq$ 0.001).

## 7.2 Supplementary Table

Clinical and biological features of primary BCP-ALL samples used in the functional studies.

ID	Gender	Age	WBC per mm <sup>3</sup>	CALLA	Karyotype	Follow up (years)	Status at last follow up
<b>BCP1</b>	M	9.06	4,230	Pos	57, XXYY, +4, +6, +8, +10, +15, +17, +18, +21, +21	6.732	Alive
<b>BCP2</b>	M	15.3 3	37,690	Pos	49, XXY, +17, +22	3.789	Death
<b>BCP3</b>	M	4.10	34,450	Pos	54, XXY, +6, +14, +17, +18, +21, +22	6.590	Alive
<b>BCP4</b>	F	3.78	6,800	Pos	58, XX, der(4) t(1;4) (p13;16), +4,+5,+6,+9,+10,+12,+14,+17,+1 8,+19	5.347	Alive

ID: patient's identification; F: female; M: male; Age: age in years; Pos: positive (>20%); WBC: white blood cells; CALLA: common acute lymphoblastic leukemia antigen (CD10).



## 8. GENERAL DISCUSSION

Insulin and IGFs are well-known as mitogenic and pro-survival factors for various cell types, including those of pediatric ALL.<sup>67-69,73</sup> The actions of circulating insulin and IGFs are carefully regulated by IGFBPs. Among these binding proteins, IGFBP7 stands out as an IGFBP-related protein (IGFBP-rP) that demonstrates high affinity for insulin and moderate affinity for IGFs. Additionally, IGFBP7 has been found to bind to both IGF1R and INSR, further expanding its potential mechanisms of action.<sup>102-104</sup>

In pediatric ALL, elevated levels of *IGFBP7* expression have been linked to a poorer prognosis and resistance to chemotherapy.<sup>30,121,160</sup> A previous research by our group has revealed that ALL cells are the primary source of IGFBP7 within the BM microenvironment, suggesting a paracrine model of action. In that study we demonstrated that association of IGFBP7+insulin/IGF1/IGF2 leads to the upregulation of *ASNS* (asparagine synthetase) expression and increased secretion of asparagine by BMSCs. This observation, made within a co-culture system, indicates that IGFBP7 shields ALL cells from the effects of the L-asparaginase. Furthermore, at that time we discovered that the knockdown of *IGFBP7* in two ALL cell lines resulted in diminished proliferation, suggesting that IGFBP7 may also exert an autocrine influence on leukemia cells. Thus, in this thesis we present important findings that prove and characterize the autocrine role of IGFBP7 in pediatric ALL.

The data presented in the first chapter provides compelling evidence that *IGFBP7* knockdown or protein neutralization using an anti-IGFBP7 monoclonal antibody (clone C311) results in reduced cell viability, migration and proliferation, while simultaneously inducing apoptosis in both cell lines and primary ALL cells. To address the leukemogenic potential of autocrine IGFBP7 secreted by ALL cells under physiologic paracrine/endocrine IGFBP7 levels and under the interaction/competition with other cells and molecules, we transplanted the *IGFBP7* knockdown cell lines (REH, RS4;11, Jurkat and TALL-1) into immunocompromised NOD/SCID mice. Downregulation of *IGFBP7* resulted in significant attenuation of leukemia progression *in vivo* as evaluated by the percentage of leukemia cells (human CD45+) in the peripheral blood, bone marrow, liver, and spleen, in relation to mice transplanted with Scramble (control) cells. Additionally, mice transplanted with two patient-derived xenografts or the RS4;11 cell line and subsequently treated with our anti-IGFBP7

antibody showed decreased leukemic progression and survived longer than animals treated with an isotype antibody control. After confirming by orthogonal approaches that IGFBP7 exerts an autocrine effect in pediatric ALL, we further investigated whether this effect was dependent on the presence of its ligand, insulin/IGFs.

By utilizing approaches such as flow cytometry, ELISA, and western blot, we successfully demonstrated that IGFBP7 exerts a significant effect on the surface retention of IGF1R upon insulin/IGF1 stimulation. This leads to sustained activation of IGF1R, IRS, AKT, and ERK proteins in ALL cell lines, a result that was further validated in 18 primary ALL samples. Our findings also challenge the notion that INSR plays a prolonged action in ALL mediated by IGFBP7, as its activation was limited to 15 min in our experiments. Interestingly, while the affinity of homodimeric IGF1R for insulin is reportedly over 200 times lower compared to IGF1,<sup>161</sup> the presence of IGFBP7 facilitated equivalent levels of IGF1R activation at 25 ng/mL insulin as compared to 5 ng/mL IGF1.

It is worth noting that all of our findings were based on the utilization of physiological doses of IGFBP7, specifically at 100 ng/mL. Previous studies have demonstrated that IGFBP7 possesses anti-cancer properties, as high concentrations of recombinant protein were shown to induce cell death in cancer cell lines.<sup>103,106,122-124</sup> In our experiments, we also observed an inhibitory effect on ALL cells at a concentration of 20 µg/mL. However, it is important to acknowledge that this high concentration of IGFBP7 might potentially hinder or prevent the binding of IGF1/insulin to IGF1R. Nevertheless, it should be noted that 20 µg/mL is significantly higher than the physiological levels of IGFBP7 typically found in adult serum (21-35 ng/mL)<sup>126</sup> or childhood ALL bone marrow plasma (49 ng/mL).<sup>100</sup> Regrettably, the use of supraphysiological amounts of IGFBP7 has been the rule rather than the exception in the literature.

All together, these cumulative findings establish that physiologic IGFBP7 serves as an autocrine oncogenic factor in pediatric ALL by promoting the perdurance of IGF1R at the cell surface, thereby prolonging insulin/IGF1 stimulation and ultimately enhancing signaling pathways such as PI3K-AKT-mTOR and Ras/Raf/MAPK.

To confirm the importance of IGF1R to IGFBP7-mediated pro-survival effects in pediatric ALL, we interrogated whether IGF1R is indispensable for the transduction of the insulin/IGF1+IGFBP7 stimulus to downstream effects such as sustained Akt phosphorylation in chapter two of this thesis. To answer this question, we knocked out

*IGF1R* on two different BCP-ALL cell lines (RS4;11 and 697). As expected, NTC cells (no target control) maintained detectable levels of IGF1R and Akt phosphorylation after prolonged exposure (4 h) to rIGF1+rIGFBP7 co-treatment, while no such sustained signaling was seen in IGF1R-KO cells or when rIGF1 or rIGFBP7 were used separately. This data provides confirmation that IGF1R serves as the primary mediator of the signaling pathway facilitated by IGFBP7 and its ligands in BCP-ALL.

To better understand the cellular consequences of prolonged IGF1R/Akt signaling in BCP-ALL, we performed microarray gene expression analysis followed by Gene Set Enrichment Analysis (GSEA). Hallmark gene sets characteristic of cell growth (PI3K/Akt/mTOR, mTORC1, MYC targets, E2F targets, and mitotic spindle) and metabolism (oxidative phosphorylation-OXPHOS, adipogenesis, fatty acid metabolism, and glycolysis) were upregulated upon rIGF1+rIGFBP7 treatment in BCP-ALL cell lines. We confirmed the impact of rIGF1+rIGFBP7 co-treatment on energy metabolism by Seahorse analysis. Both the basal and maximal OCR were increased upon rIGF1+rIGFBP7 treatment, along with the OCR coupled to ATP synthesis. When mitochondrial OXPHOS was chemically inhibited, treated BCP-ALL cells showed a significantly increased glycolytic metabolism, supporting the notion that IGFBP7 can improve metabolism through IGF1R-Akt signaling in pediatric BCP-ALL.

To evaluate the effects of IGFBP7 on glycolytic metabolism by orthogonal methods, we cultured BCP-ALL cells in medium supplemented with 2-deoxy-D-glucose (2-DG). Sensitivity to lethal 2-DG supplementation was markedly more pronounced when cells were pretreated with rIGF1+rIGFBP7 than by these factors individually. No such additive effect was seen with the IGF1R-KO cells, indicating that IGF1R is indispensable for increasing glucose uptake triggered by IGFBP7. Likewise, IGFBP7 neutralization with an anti-IGFBP7 monoclonal antibody or PI3K inhibition with Ly294002 protected rIGF1+rIGFBP7-stimulated BCP-ALL cells from the lethal effects of 2-DG.

As anticipated, chronic Akt activation has been shown to improve glycolytic metabolism in ALL by stabilizing GLUT1 at the cell surface. This effect is caused by blocking the GLUT1 endocytic machinery.<sup>139,150,162-164</sup> Accordingly, 24 h after rIGF1+rIGFBP7 treatment (which promotes sustained activation of Akt), BCP-ALL cells showed ~60% more GLUT1 on their cell surface compared to untreated cells. This effect was completely abrogated when the cells were pretreated with anti-IGFBP7 antibody or Ly294002. Moreover, IGF1R-KO cells showed no changes in GLUT1

surface expression under any conditions tested, confirming the role of IGFBP7 in enhancing glycolytic metabolism in ALL through the IGF1R-Akt-GLUT1 axis.

In general, the cellular and metabolic effect described here may offer an additional mechanistic explanation for the strong negative impact seen in ALL cells *in vitro* and *in vivo* after the knockdown or antibody neutralization of IGFBP7, while reinforcing the notion that it is a valid target for future therapeutic interventions. In conclusion, our observations reveal a hitherto unknown role for IGFBP7 in pediatric ALL, opening doors for future investigations.

## 9. CONCLUSIONS

- *IGFBP7* knockdown or protein neutralization leads to reduced proliferation, migration and survival of cell lines and primary ALL cells *in vitro*.
- Physiologic IGFBP7 potentiates insulin/IGF1-mediated molecular signaling via IGF1R in pediatric ALL, by prolonging the phosphorylation of IRS-1 (Ser302 and pan-Tyr), Akt (Ser473) and Erk1/2, which activates the downstream PI3K/Akt/mTOR and Ras/Raf/MAPK pathways responsible for mitogenic effects.
- The sustained activation of the PI3K-AKT-mTOR and Ras/Raf/MAPK pathways by IGFBP7 was found to be associated with the retention of IGF1R on the cell surface.
- *IGFBP7* knockdown or protein neutralization using an anti-IGFBP7 monoclonal antibody (clone C311) attenuates ALL progression *in vivo*, improving the survival of NOD/SCID mice transplanted with cell lines (*IGFBP7* knockdown) or primary ALL cells.
- IGF1R is the target of IGFBP7 action in ALL cells, as IGF1R knockout completely abolished the cell signaling triggered by insulin/IGF1+IGFBP7 stimulus
- IGFBP7 enhances the glycolytic metabolism of BCP-ALL cells in an insulin/IGF1-dependent manner by upregulating GLUT1 on the cell surface.

## 10. FINAL CONSIDERATIONS AND FUTURE DIRECTIONS

Providing a general overview of the data and information shared in this thesis, we propose two distinct areas that warrant further investigation due to the limited understanding surrounding them. Considering the role of IGFBP7 in ALL progression and, in turn, the important effects mediated by IGFBP7 in the glycolytic pathway, we hypothesize that IGFBP7 could (1) serve as a vital target for studying leukemogenesis process in the BM microenvironment and, in the other hand, (2) IGFBP7 may also hold potential as a strong candidate in the context of metabolic syndromes, which commonly exhibit insulin resistance.

*IGFBP7 and BM microenvironment - implications for leukemogenesis:* as previously established, the distinguishing characteristic of ALL is the abnormal proliferation and accumulation of hematopoietic progenitor cells within the BM.<sup>41,47</sup> However, it is now recognized that the initiation of the leukemogenic process is mediated by leukemia-initiating cells (LICs).<sup>62</sup> These LICs possessing stem-like properties are capable of initiating and sustaining leukemia.<sup>63,64</sup> The molecular mechanisms that induce LICs outgrowth in the BM are not fully understood, but several factors have been implicated. BMSCs play a vital role in providing growth factors, including IGFs and IGFBPs, as well as cytokines to support normal hematopoiesis. In the presence of LICs, BMSCs can create a supportive niche facilitating LICs proliferation and the establishment of ALL. Therefore, characterizing the growth factors secreted by the various cell types comprising the BM microenvironment, with specific emphasis on IGFBP7 and IGFs, holds immense value in comprehending the early stages of ALL development, since the PI3K/Akt/mTOR, IGFs, Wnt, and Notch have recently been reported as relevant pathways that functionally modulate LICs activity and may have a direct impact on disease maintenance.<sup>62</sup>

*IGFBP7 signaling in metabolic diseases:* in the context of oncogenesis, downstream signaling of IGF1R/INSR, facilitated by insulin/IGF1+IGFBP7 contributes to the activation of the PI3K and MAPK pathways, promoting cell proliferation and survival - a counterproductive dynamic against cancer eradication. However, in metabolic diseases, particularly obesity and type 2 diabetes, insulin/IGF1 signaling is compromised. The sustained signaling of the IGF1R-PI3K-Akt-GLUT1 axis mediated by insulin/IGF1+IGFBP7, could yield favorable metabolic outcomes and offer therapeutic prospects for managing these diseases. The pathogenesis of insulin

resistance and hyperinsulinemia in obesity is complex and multifactorial. But, it is known that a key factor underlying the development of insulin resistance and metabolic dysregulation in obesity is closely related to the dysfunction of hepatic and adipose tissue, leading to disruption of the endocrine function of these tissues.<sup>165,166</sup> Given the role of IGFBP7 on the potentiation of INSR<sup>125</sup> and IGF1R signaling,<sup>167,168</sup> we have raised the hypothesis that IGFBP7 could exert a positive impact on hepatocyte/adipocyte insulin/IGF signaling, resulting in an improvement of function and intracellular homeostasis. To address this hypothesis, an investigation was initiated under the BEPE-FAPESP fellowship conducted at the University of California-Berkeley in collaboration with Dr Ana Paula Arruda from the Department of Nutritional Sciences and Toxicology. The preliminary data of this speculation are presented in this thesis as an attachment.

## 11. REFERENCES

1. Stratton MR, Campbell PJ, Futreal PA. The cancer genome. *Nature*. 2009 Apr 9;458(7239):719-24. doi: 10.1038/nature07943.
2. Stratton MR. Exploring the genomes of cancer cells: progress and promise. *Science*. 2011 Mar 25;331(6024):1553-8. doi: 10.1126/science.1204040.
3. World Health Organization (WHO). Global Health Estimates 2020: Deaths by Cause, Age, Sex, by Country and by Region, 2000-2019. WHO; 2020. Accessed April 09, 2023. Website: [who.int/data/gho/data/themes/mortality-and-global-health-estimates/ghe-leading-causes-of-death](https://www.who.int/data/gho/data/themes/mortality-and-global-health-estimates/ghe-leading-causes-of-death)
4. Ferlay J., Ervik M.L.F., Colombet M., Mery L., Piñeros M. Global Cancer Observatory: Cancer Today. International Agency for Research on Cancer; Lyon, France: 2021
5. Bissell MJ, Radisky D. Putting tumours in context. *Nat Rev Cancer*. 2001 Oct;1(1):46-54. doi: 10.1038/35094059.
6. Davidoff AM. Pediatric oncology. *Semin Pediatr Surg*. 2010 Aug;19(3):225-33. doi: 10.1053/j.sempedsurg.2010.03.007.
7. Hanahan D, Weinberg RA. The hallmarks of cancer. *Cell*. 2000 Jan 7;100(1):57-70. doi: 10.1016/s0092-8674(00)81683-9.
8. Hanahan D, Weinberg RA. Hallmarks of cancer: the next generation. *Cell*. 2011 Mar 4;144(5):646-74. doi: 10.1016/j.cell.2011.02.013.
9. Hanahan D. Hallmarks of Cancer: New Dimensions. *Cancer Discov*. 2022 Jan;12(1):31-46. doi: 10.1158/2159-8290.CD-21-1059.
10. Vogelstein B, Papadopoulos N, Velculescu VE, Zhou S, Diaz LA Jr, Kinzler KW. Cancer genome landscapes. *Science*. 2013 Mar 29;339(6127):1546-58. doi: 10.1126/science.1235122.
11. National Cancer Institute. Childhood Cancers. NIH; 2020. Accessed April 09, 2023. Website: <https://www.cancer.gov/types/childhood-cancers>
12. Ma X, Liu Y, Liu Y, Alexandrov LB, Edmonson MN, Gawad C, Zhou X, Li Y, Rusch MC, Easton J, Huether R, Gonzalez-Pena V, Wilkinson MR, Hermida LC, Davis S, Sioson E, Pounds S, Cao X, Ries RE, Wang Z, Chen X, Dong L, Diskin SJ, Smith MA, Guidry Auvil JM, Meltzer PS, Lau CC, Perlman EJ, Maris JM, Meshinchi S, Hunger SP, Gerhard DS, Zhang J. Pan-cancer genome and transcriptome analyses of 1,699 paediatric leukaemias and solid tumours. *Nature*. 2018 Mar 15;555(7696):371-376. doi: 10.1038/nature25795.



13. Gröbner SN, Worst BC, Weischenfeldt J, Buchhalter I, Kleinheinz K, Rudneva VA, Johann PD, Balasubramanian GP, Segura-Wang M, Brabetz S, Bender S, Hutter B, Sturm D, Pfaff E, Hübschmann D, Zipprich G, Heinold M, Eils J, Lawerenz C, Erkek S, Lambo S, Waszak S, Blattmann C, Borkhardt A, Kuhlen M, Eggert A, Fulda S, Gessler M, Wegert J, Kappler R, Baumhoer D, Burdach S, Kirschner-Schwabe R, Kontny U, Kulozik AE, Lohmann D, Hettmer S, Eckert C, Bielack S, Nathrath M, Niemeyer C, Richter GH, Schulte J, Siebert R, Westermann F, Molenaar JJ, Vassal G, Witt H; ICGC PedBrain-Seq Project; ICGC MMML-Seq Project; Burkhardt B, Kratz CP, Witt O, van Tilburg CM, Kramm CM, Fleischhack G, Dirksen U, Rutkowski S, Frühwald M, von Hoff K, Wolf S, Klingebiel T, Koscielniak E, Landgraf P, Koster J, Resnick AC, Zhang J, Liu Y, Zhou X, Waanders AJ, Zwijnenburg DA, Raman P, Brors B, Weber UD, Northcott PA, Pajtler KW, Kool M, Piro RM, Korbel JO, Schlesner M, Eils R, Jones DTW, Lichter P, Chavez L, Zapatka M, Pfister SM. The landscape of genomic alterations across childhood cancers. *Nature*. 2018 Mar 15;555(7696):321-327. doi: 10.1038/nature25480.
14. Sweet-Cordero EA, Biegel JA. The genomic landscape of pediatric cancers: Implications for diagnosis and treatment. *Science*. 2019 Mar 15;363(6432):1170-1175. doi: 10.1126/science.aaw3535. PMID: 30872516; PMCID: PMC7757338.
15. ICGC/TCGA Pan-Cancer Analysis of Whole Genomes Consortium. Pan-cancer analysis of whole genomes. *Nature*. 2020 Feb;578(7793):82-93. doi: 10.1038/s41586-020-1969-6.
16. INCA, 2019. Estimativa 2020: incidência de câncer no Brasil. Instituto Nacional de Câncer José Alencar Gomes da Silva. Coordenação de Prevenção e Vigilância, Rio de Janeiro, p. 122.
17. Steliarova-Foucher E, Colombet M, Ries LAG, Moreno F, Dolya A, Bray F, Hesselting P, Shin HY, Stiller CA; IICC-3 contributors. International incidence of childhood cancer, 2001-10: a population-based registry study. *Lancet Oncol*. 2017 Jun;18(6):719-731. doi: 10.1016/S1470-2045(17)30186-9.
18. Pui CH, Mullighan CG, Evans WE, Relling MV. Pediatric acute lymphoblastic leukemia: where are we going and how do we get there? *Blood*. 2012 Aug 9;120(6):1165-74. doi: 10.1182/blood-2012-05-378943.
19. Inaba H, Greaves M, Mullighan CG. Acute lymphoblastic leukaemia. *Lancet*. 2013 Jun 1;381(9881):1943-55. doi: 10.1016/S0140-6736(12)62187-4.

20. Hunger SP, Mullighan CG. Acute Lymphoblastic Leukemia in Children. *N Engl J Med*. 2015 Oct 15;373(16):1541-52. doi: 10.1056/NEJMra1400972.
21. Greaves M. A causal mechanism for childhood acute lymphoblastic leukaemia. *Nat Rev Cancer*. 2018 Aug;18(8):471-484. doi: 10.1038/s41568-018-0015-6.
22. Inaba H, Mullighan CG. Pediatric acute lymphoblastic leukemia. *Haematologica*. 2020 Nov 1;105(11):2524-2539. doi: 10.3324/haematol.2020.247031.
23. Pillozzi S, Masselli M, De Lorenzo E, Accordi B, Cilia E, Crociani O, Amedei A, Veltroni M, D'Amico M, Basso G, Becchetti A, Campana D, Arcangeli A. Chemotherapy resistance in acute lymphoblastic leukemia requires hERG1 channels and is overcome by hERG1 blockers. *Blood*. 2011 Jan 20;117(3):902-14. doi: 10.1182/blood-2010-01-262691.
24. Pui CH, Robison LL, Look AT. Acute lymphoblastic leukaemia. *Lancet*. 2008 Mar 22;371(9617):1030-43. doi: 10.1016/S0140-6736(08)60457-2. PMID: 18358930.
25. Pui CH, Sandlund JT, Pei D, Campana D, Rivera GK, Ribeiro RC, Rubnitz JE, Razzouk BI, Howard SC, Hudson MM, Cheng C, Kun LE, Raimondi SC, Behm FG, Downing JR, Relling MV, Evans WE; Total Therapy Study XIIIB at St Jude Children's Research Hospital. Improved outcome for children with acute lymphoblastic leukemia: results of Total Therapy Study XIIIB at St Jude Children's Research Hospital. *Blood*. 2004 Nov 1;104(9):2690-6. doi: 10.1182/blood-2004-04-1616.
26. Migita NA, Jotta PY, do Nascimento NP, Vasconcelos VS, Lopes Centoducatte G, Massirer KB, de Azevedo AC, Brandalise SR, Yunes JA. Classification and genetics of pediatric B-other Acute Lymphoblastic Leukemia by targeted RNA-sequencing. *Blood Adv*. 2023 Feb 27;bloodadvances.2022009179. doi: 10.1182/bloodadvances.2022009179.
27. Hjort MA, Abdollahi P, Vandsemb EN, Fenstad MH, Lund B, Slørdahl TS, Børset M, Rø TB. Phosphatase of regenerating liver-3 is expressed in acute lymphoblastic leukemia and mediates leukemic cell adhesion, migration and drug resistance. *Oncotarget*. 2017 Dec 13;9(3):3549-3561. doi: 10.18632/oncotarget.23186.
28. Mraz M, Zent CS, Church AK, Jelinek DF, Wu X, Pospisilova S, Ansell SM, Novak AJ, Kay NE, Witzig TE, Nowakowski GS. Bone marrow stromal cells protect lymphoma B-cells from rituximab-induced apoptosis and targeting integrin  $\alpha$ -4- $\beta$ -1 (VLA-4) with natalizumab can overcome this resistance. *Br J Haematol*. 2011 Oct;155(1):53-64. doi: 10.1111/j.1365-2141.2011.08794.x.

29. Sison EA, Brown P. The bone marrow microenvironment and leukemia: biology and therapeutic targeting. *Expert Rev Hematol.* 2011 Jun;4(3):271-83. doi: 10.1586/ehm.11.30.
30. Laranjeira AB, de Vasconcellos JF, Sodek L, Spago MC, Fornazim MC, Tone LG, Brandalise SR, Nowill AE, Yunes JA. IGFBP7 participates in the reciprocal interaction between acute lymphoblastic leukemia and BM stromal cells and in leukemia resistance to asparaginase. *Leukemia.* 2012 May;26(5):1001-11. doi: 10.1038/leu.2011.289.
31. Ma Z, Zhao X, Deng M, Huang Z, Wang J, Wu Y, Cui D, Liu Y, Liu R, Ouyang G. Bone Marrow Mesenchymal Stromal Cell-Derived Periostin Promotes B-ALL Progression by Modulating CCL2 in Leukemia Cells. *Cell Rep.* 2019 Feb 5;26(6):1533-1543.e4. doi: 10.1016/j.celrep.2019.01.034.
32. Hou D, Wang B, You R, Wang X, Liu J, Zhan W, Chen P, Qin T, Zhang X, Huang H. Stromal cells promote chemoresistance of acute myeloid leukemia cells via activation of the IL-6/STAT3/OXPHOS axis. *Ann Transl Med.* 2020 Nov;8(21):1346. doi: 10.21037/atm-20-3191.
33. Sporn MB, Roberts AB. Autocrine growth factors and cancer. *Nature.* 1985 Feb 28-Mar 6;313(6005):745-7. doi: 10.1038/313745a0.
34. Jasmin C, Georgoulas V, Smadja-Joffe F, Boucheix C, Le Bousse-Kerdiles C, Allouche M, Cibert C, Azzarone B. Autocrine growth of leukemic cells. *Leuk Res.* 1990;14(8):689-93. doi: 10.1016/0145-2126(90)90095-q.
35. Mori N, Shirakawa F, Murakami S, Oda S, Eto S. Interleukin-1 alpha as an autocrine growth factor for acute lymphoblastic leukaemia cells. *Br J Haematol.* 1994 Feb;86(2):386-8. doi: 10.1111/j.1365-2141.1994.tb04746.x.
36. Buffière A, Uzan B, Aucagne R, Hermetet F, Mas M, Nassurdine S, Aznague A, Carmignac V, Tournier B, Bouchot O, Ballerini P, Barata JT, Bastie JN, Delva L, Pflumio F, Quéré R. T-cell acute lymphoblastic leukemia displays autocrine production of Interleukin-7. *Oncogene.* 2019 Nov;38(48):7357-7365. doi: 10.1038/s41388-019-0921-4.
37. Simioni C, Conti I, Varano G, Brenna C, Costanzi E, Neri LM. The Complexity of the Tumor Microenvironment and Its Role in Acute Lymphoblastic Leukemia: Implications for Therapies. *Front Oncol.* 2021 May 5;11:673506. doi: 10.3389/fonc.2021.673506.

38. Knight T, Irving JA. Ras/Raf/MEK/ERK Pathway Activation in Childhood Acute Lymphoblastic Leukemia and Its Therapeutic Targeting. *Front Oncol.* 2014 Jun 24;4:160. doi: 10.3389/fonc.2014.00160.
39. Sanchez VE, Nichols C, Kim HN, Gang EJ, Kim YM. Targeting PI3K Signaling in Acute Lymphoblastic Leukemia. *Int J Mol Sci.* 2019 Jan 18;20(2):412. doi: 10.3390/ijms20020412.
40. Fasouli ES, Katsantoni E. JAK-STAT in Early Hematopoiesis and Leukemia. *Front Cell Dev Biol.* 2021 May 14;9:669363. doi: 10.3389/fcell.2021.669363.
41. Dander E, Palmi C, D'Amico G, Cazzaniga G. The Bone Marrow Niche in B-Cell Acute Lymphoblastic Leukemia: The Role of Microenvironment from Pre-Leukemia to Overt Leukemia. *Int J Mol Sci.* 2021 Apr 23;22(9):4426. doi: 10.3390/ijms22094426.
42. Chen D, Yoo BK, Santhekadur PK, Gredler R, Bhutia SK, Das SK, Fuller C, Su ZZ, Fisher PB, Sarkar D. Insulin-like growth factor-binding protein-7 functions as a potential tumor suppressor in hepatocellular carcinoma. *Clin Cancer Res.* 2011 Nov 1;17(21):6693-701. doi: 10.1158/1078-0432.CCR-10-2774.
43. Cobaleda C, Sánchez-García I. B-cell acute lymphoblastic leukaemia: towards understanding its cellular origin. *Bioessays.* 2009 Jun;31(6):600-9. doi: 10.1002/bies.200800234.
44. Chiarini F, Lonetti A, Evangelisti C, Buontempo F, Orsini E, Evangelisti C, Cappellini A, Neri LM, McCubrey JA, Martelli AM. Advances in understanding the acute lymphoblastic leukemia bone marrow microenvironment: From biology to therapeutic targeting. *Biochim Biophys Acta.* 2016 Mar;1863(3):449-463. doi: 10.1016/j.bbamcr.2015.08.015.
45. Schofield R. The relationship between the spleen colony-forming cell and the haemopoietic stem cell. *Blood Cells.* 1978;4(1-2):7-25.
46. Shafat MS, Gnaneswaran B, Bowles KM, Rushworth SA. The bone marrow microenvironment - Home of the leukemic blasts. *Blood Rev.* 2017 Sep;31(5):277-286. doi: 10.1016/j.blre.2017.03.004.
47. Congrains A, Bianco J, Rosa RG, Mancuso RI, Saad STO. 3D Scaffolds to Model the Hematopoietic Stem Cell Niche: Applications and Perspectives. *Materials (Basel).* 2021 Jan 26;14(3):569. doi: 10.3390/ma14030569.
48. Taichman RS, Reilly MJ, Emerson SG. Human osteoblasts support human hematopoietic progenitor cells in vitro bone marrow cultures. *Blood.* 1996 Jan 15;87(2):518-24.

49. Kiel MJ, Radice GL, Morrison SJ. Lack of evidence that hematopoietic stem cells depend on N-cadherin-mediated adhesion to osteoblasts for their maintenance. *Cell Stem Cell*. 2007 Aug 16;1(2):204-17. doi: 10.1016/j.stem.2007.06.001.
50. Kunisaki Y, Bruns I, Scheiermann C, Ahmed J, Pinho S, Zhang D, Mizoguchi T, Wei Q, Lucas D, Ito K, Mar JC, Bergman A, Frenette PS. Arteriolar niches maintain haematopoietic stem cell quiescence. *Nature*. 2013 Oct 31;502(7473):637-43. doi: 10.1038/nature12612.
51. Ding L, Morrison SJ. Haematopoietic stem cells and early lymphoid progenitors occupy distinct bone marrow niches. *Nature*. 2013 Mar 14;495(7440):231-5. doi: 10.1038/nature11885.
52. Stier S, Ko Y, Forkert R, Lutz C, Neuhaus T, Grünewald E, Cheng T, Dombkowski D, Calvi LM, Rittling SR, Scadden DT. Osteopontin is a hematopoietic stem cell niche component that negatively regulates stem cell pool size. *J Exp Med*. 2005 Jun 6;201(11):1781-91. doi: 10.1084/jem.20041992.
53. Rankin EB, Wu C, Khatri R, Wilson TL, Andersen R, Araldi E, Rankin AL, Yuan J, Kuo CJ, Schipani E, Giaccia AJ. The HIF signaling pathway in osteoblasts directly modulates erythropoiesis through the production of EPO. *Cell*. 2012 Mar 30;149(1):63-74. doi: 10.1016/j.cell.2012.01.051.
54. Chen JY, Miyanishi M, Wang SK, Yamazaki S, Sinha R, Kao KS, Seita J, Sahoo D, Nakauchi H, Weissman IL. Hoxb5 marks long-term haematopoietic stem cells and reveals a homogenous perivascular niche. *Nature*. 2016 Feb 11;530(7589):223-7. doi: 10.1038/nature16943.
55. Nombela-Arrieta C, Pivarnik G, Winkel B, Canty KJ, Harley B, Mahoney JE, Park SY, Lu J, Protopopov A, Silberstein LE. Quantitative imaging of haematopoietic stem and progenitor cell localization and hypoxic status in the bone marrow microenvironment. *Nat Cell Biol*. 2013 May;15(5):533-43. doi: 10.1038/ncb2730.
56. Day RB, Link DC. Megakaryocytes in the hematopoietic stem cell niche. *Nat Med*. 2014 Nov;20(11):1233-4. doi: 10.1038/nm.3745.
57. Sugiyama T, Kohara H, Noda M, Nagasawa T. Maintenance of the hematopoietic stem cell pool by CXCL12-CXCR4 chemokine signaling in bone marrow stromal cell niches. *Immunity*. 2006 Dec;25(6):977-88. doi: 10.1016/j.immuni.2006.10.016.
58. Yamazaki S, Ema H, Karlsson G, Yamaguchi T, Miyoshi H, Shioda S, Taketo MM, Karlsson S, Iwama A, Nakauchi H. Nonmyelinating Schwann cells maintain

- hematopoietic stem cell hibernation in the bone marrow niche. *Cell*. 2011 Nov 23;147(5):1146-58. doi: 10.1016/j.cell.2011.09.053.
59. Pinho S, Marchand T, Yang E, Wei Q, Nerlov C, Frenette PS. Lineage-Biased Hematopoietic Stem Cells Are Regulated by Distinct Niches. *Dev Cell*. 2018 Mar 12;44(5):634-641.e4. doi: 10.1016/j.devcel.2018.01.016.
  60. Bruns I, Lucas D, Pinho S, Ahmed J, Lambert MP, Kunisaki Y, Scheiermann C, Schiff L, Poncz M, Bergman A, Frenette PS. Megakaryocytes regulate hematopoietic stem cell quiescence through CXCL4 secretion. *Nat Med*. 2014 Nov;20(11):1315-20. doi: 10.1038/nm.3707.
  61. Zhao M, Perry JM, Marshall H, Venkatraman A, Qian P, He XC, Ahamed J, Li L. Megakaryocytes maintain homeostatic quiescence and promote post-injury regeneration of hematopoietic stem cells. *Nat Med*. 2014 Nov;20(11):1321-6. doi: 10.1038/nm.3706.
  62. Tamiro F, Weng AP, Giambra V. Targeting Leukemia-Initiating Cells in Acute Lymphoblastic Leukemia. *Cancer Res*. 2021 Aug 15;81(16):4165-4173. doi: 10.1158/0008-5472.CAN-20-2571.
  63. Lapidot T, Sirard C, Vormoor J, Murdoch B, Hoang T, Caceres-Cortes J, Minden M, Paterson B, Caligiuri MA, Dick JE. A cell initiating human acute myeloid leukaemia after transplantation into SCID mice. *Nature*. 1994 Feb 17;367(6464):645-8. doi: 10.1038/367645a0.
  64. Bonnet D, Dick JE. Human acute myeloid leukemia is organized as a hierarchy that originates from a primitive hematopoietic cell. *Nat Med*. 1997 Jul;3(7):730-7. doi: 10.1038/nm0797-730.
  65. Shastri A, Choudhary G, Teixeira M, Gordon-Mitchell S, Ramachandra N, Bernard L, Bhattacharyya S, Lopez R, Pradhan K, Giricz O, Ravipati G, Wong LF, Cole S, Bhagat
  66. Tan Y, Wu Q, Zhou F. Targeting acute myeloid leukemia stem cells: Current therapies in development and potential strategies with new dimensions. *Crit Rev Oncol Hematol*. 2020 Aug;152:102993. doi: 10.1016/j.critrevonc.2020.102993.
  67. Pollak M. The insulin receptor/insulin-like growth factor receptor family as a therapeutic target in oncology. *Clin Cancer Res*. 2012 Jan 1;18(1):40-50. doi: 10.1158/1078-0432.CCR-11-0998.
  68. Mazerbourg S, Monget P. Insulin-Like Growth Factor Binding Proteins and IGFBP Proteases: A Dynamic System Regulating the Ovarian Folliculogenesis. *Front Endocrinol (Lausanne)*. 2018 Mar 29;9:134. doi: 10.3389/fendo.2018.00134.

69. Gibson LF. Survival of B lineage leukemic cells: signals from the bone marrow microenvironment. *Leuk Lymphoma*. 2002 Jan;43(1):19-27. doi: 10.1080/10428190210188.
70. Girnita L, Takahashi SI, Crudden C, Fukushima T, Worrall C, Furuta H, Yoshihara H, Hakuno F, Girnita A. Chapter Seven - When Phosphorylation Encounters Ubiquitination: A Balanced Perspective on IGF-1R Signaling. *Prog Mol Biol Transl Sci*. 2016;141:277-311. doi: 10.1016/bs.pmbts.2016.04.001.
71. Choi E, Zhang X, Xing C, Yu H. Mitotic Checkpoint Regulators Control Insulin Signaling and Metabolic Homeostasis. *Cell*. 2016 Jul 28;166(3):567-581. doi: 10.1016/j.cell.2016.05.074.
72. Yoneyama Y, Lanzerstorfer P, Niwa H, Umehara T, Shibano T, Yokoyama S, Chida K, Weghuber J, Hakuno F, Takahashi SI. IRS-1 acts as an endocytic regulator of IGF-I receptor to facilitate sustained IGF signaling. *Elife*. 2018 Apr 11;7:e32893. doi: 10.7554/eLife.32893.
73. Pollak MN, Schernhammer ES, Hankinson SE. Insulin-like growth factors and neoplasia. *Nat Rev Cancer*. 2004 Jul;4(7):505-18. doi: 10.1038/nrc1387.
74. Blatt J. IGF1 and leukemia. *Pediatr Hematol Oncol*. 2000 Apr-May;17(3):199-201. doi: 10.1080/088800100276361.
75. El-Shewy HM, Luttrell LM. Insulin-like growth factor-2/mannose-6 phosphate receptors. *Vitam Horm*. 2009;80:667-97. doi: 10.1016/S0083-6729(08)00624-9.
76. Ross JA, Perentesis JP, Robison LL, Davies SM. Big babies and infant leukemia: a role for insulin-like growth factor-1? *Cancer Causes Control*. 1996 Sep;7(5):553-9. doi: 10.1007/BF00051889.
77. Estrov Z, Meir R, Barak Y, Zaizov R, Zadik Z. Human growth hormone and insulin-like growth factor-1 enhance the proliferation of human leukemic blasts. *J Clin Oncol*. 1991 Mar;9(3):394-9. doi: 10.1200/JCO.1991.9.3.394.
78. Baier TG, Ludwig WD, Schönberg D, Hartmann KK. Characterisation of insulin-like growth factor I receptors of human acute lymphoblastic leukaemia (ALL) cell lines and primary ALL cells. *Eur J Cancer*. 1992;28A(6-7):1105-10. doi: 10.1016/0959-8049(92)90466-f.
79. Neely EK, Rosenfeld RG, Illescas A, Smith SD. Mitogenic effects of human recombinant insulin on B-cell precursor acute lymphoblastic leukemia cells. *Leukemia*. 1992 Nov;6(11):1134-42.

80. Leverrier Y, Thomas J, Mathieu AL, Low W, Blanquier B, Marvel J. Role of PI3-kinase in Bcl-X induction and apoptosis inhibition mediated by IL-3 or IGF-1 in Baf-3 cells. *Cell Death Differ*. 1999 Mar;6(3):290-6. doi: 10.1038/sj.cdd.4400492.
81. Ogawa M, Nishiura T, Oritani K, Yoshida H, Yoshimura M, Okajima Y, Ishikawa J, Hashimoto K, Matsumura I, Tomiyama Y, Matsuzawa Y. Cytokines prevent dexamethasone-induced apoptosis via the activation of mitogen-activated protein kinase and phosphatidylinositol 3-kinase pathways in a new multiple myeloma cell line. *Cancer Res*. 2000 Aug 1;60(15):4262-9.
82. Tu W, Cheung PT, Lau YL. Insulin-like growth factor 1 promotes cord blood T cell maturation and inhibits its spontaneous and phytohemagglutinin-induced apoptosis through different mechanisms. *J Immunol*. 2000 Aug 1;165(3):1331-6. doi: 10.4049/jimmunol.165.3.1331.
83. Medyouf H, Gusscott S, Wang H, Tseng JC, Wai C, Nemirovsky O, Trumpp A, Pflumio F, Carboni J, Gottardis M, Pollak M, Kung AL, Aster JC, Holzenberger M, Weng AP. High-level IGF1R expression is required for leukemia-initiating cell activity in T-ALL and is supported by Notch signaling. *J Exp Med*. 2011 Aug 29;208(9):1809-22. doi: 10.1084/jem.20110121.
84. Khandwala HM, McCutcheon IE, Flyvbjerg A, Friend KE. The effects of insulin-like growth factors on tumorigenesis and neoplastic growth. *Endocr Rev*. 2000 Jun;21(3):215-44. doi: 10.1210/edrv.21.3.0399.
85. Baserga R, Peruzzi F, Reiss K. The IGF-1 receptor in cancer biology. *Int J Cancer*. 2003 Dec 20;107(6):873-7. doi: 10.1002/ijc.11487.
86. Hernández-Sánchez C, Mansilla A, de Pablo F, Zardoya R. Evolution of the insulin receptor family and receptor isoform expression in vertebrates. *Mol Biol Evol*. 2008 Jun;25(6):1043-53. doi: 10.1093/molbev/msn036.
87. Whittaker J, Groth AV, Mynarcik DC, Pluzek L, Gadsbøll VL, Whittaker LJ. Alanine scanning mutagenesis of a type 1 insulin-like growth factor receptor ligand binding site. *J Biol Chem*. 2001 Nov 23;276(47):43980-6. doi: 10.1074/jbc.M102863200.
88. Westermeier F, Sáez T, Arroyo P, Toledo F, Gutiérrez J, Sanhueza C, Pardo F, Leiva A, Sobrevia L. Insulin receptor isoforms: an integrated view focused on gestational diabetes mellitus. *Diabetes Metab Res Rev*. 2016 May;32(4):350-65. doi: 10.1002/dmrr.2729.



89. Belfiore A, Malaguarnera R, Vella V, Lawrence MC, Sciacca L, Frasca F, Morrione A, Vigneri R. Insulin Receptor Isoforms in Physiology and Disease: An Updated View. *Endocr Rev.* 2017 Oct 1;38(5):379-431. doi: 10.1210/er.2017-00073.
90. Denley A, Wallace JC, Cosgrove LJ, Forbes BE. The insulin receptor isoform exon 11- (IR-A) in cancer and other diseases: a review. *Horm Metab Res.* 2003 Nov-Dec;35(11-12):778-85. doi: 10.1055/s-2004-814157.
91. Belfiore A, Frasca F, Pandini G, Sciacca L, Vigneri R. Insulin receptor isoforms and insulin receptor/insulin-like growth factor receptor hybrids in physiology and disease. *Endocr Rev.* 2009 Oct;30(6):586-623. doi: 10.1210/er.2008-0047.
92. Vella V, Milluzzo A, Scalisi NM, Vigneri P, Sciacca L. Insulin Receptor Isoforms in Cancer. *Int J Mol Sci.* 2018 Nov 16;19(11):3615. doi: 10.3390/ijms19113615.
93. Sciacca L, Cassarino MF, Genua M, Pandini G, Le Moli R, Squatrito S, Vigneri R. Insulin analogues differently activate insulin receptor isoforms and post-receptor signalling. *Diabetologia.* 2010 Aug;53(8):1743-53. doi: 10.1007/s00125-010-1760-6.
94. Morcavallo A, Gaspari M, Pandini G, Palummo A, Cuda G, Larsen MR, Vigneri R, Belfiore A. Research resource: New and diverse substrates for the insulin receptor isoform A revealed by quantitative proteomics after stimulation with IGF-II or insulin. *Mol Endocrinol.* 2011 Aug;25(8):1456-68. doi: 10.1210/me.2010-0484.
95. Genua M, Pandini G, Cassarino MF, Messina RL, Frasca F. c-Abl and insulin receptor signalling. *Vitam Horm.* 2009;80:77-105. doi: 10.1016/S0083-6729(08)00604-3.
96. Benyoucef S, Surinya KH, Hadaschik D, Siddle K. Characterization of insulin/IGF hybrid receptors: contributions of the insulin receptor L2 and Fn1 domains and the alternatively spliced exon 11 sequence to ligand binding and receptor activation. *Biochem J.* 2007 May 1;403(3):603-13. doi: 10.1042/BJ20061709.
97. Blanquart C, Achi J, Issad T. Characterization of IRA/IRB hybrid insulin receptors using bioluminescence resonance energy transfer. *Biochem Pharmacol.* 2008 Oct 1;76(7):873-83. doi: 10.1016/j.bcp.2008.07.027.
98. Pandini G, Medico E, Conte E, Sciacca L, Vigneri R, Belfiore A. Differential gene expression induced by insulin and insulin-like growth factor-II through the insulin receptor isoform A. *J Biol Chem.* 2003 Oct 24;278(43):42178-89. doi: 10.1074/jbc.M304980200.
99. Malaguarnera R, Belfiore A. The emerging role of insulin and insulin-like growth factor signaling in cancer stem cells. *Front Endocrinol (Lausanne).* 2014 Feb 4;5:10. doi: 10.3389/fendo.2014.00010.

100. Laranjeira, A. Participação do IGFBP7 na interação leucemia-estroma e na resistência a quimioterapia. 2012. Tese (doutorado) - Universidade Estadual de Campinas, Instituto de Biologia, Campinas, SP. Disponível em: <<http://www.repositorio.unicamp.br/handle/REPOSIP/316896>>. Access in 05/29/2023.
101. Baxter RC. IGF binding proteins in cancer: mechanistic and clinical insights. *Nat Rev Cancer*. 2014 May;14(5):329-41. doi: 10.1038/nrc3720.
102. Jones JI, Clemmons DR. Insulin-like growth factors and their binding proteins: biological actions. *Endocr Rev*. 1995 Feb;16(1):3-34. doi: 10.1210/edrv-16-1-3.
103. Hwa V, Oh Y, Rosenfeld RG. The insulin-like growth factor-binding protein (IGFBP) superfamily. *Endocr Rev*. 1999 Dec;20(6):761-87. doi: 10.1210/edrv.20.6.0382.
104. Bach LA. IGF-binding proteins. *J Mol Endocrinol*. 2018 Jul;61(1):T11-T28. doi: 10.1530/JME-17-0254.
105. Oh Y, Nagalla SR, Yamanaka Y, Kim HS, Wilson E, Rosenfeld RG. Synthesis and characterization of insulin-like growth factor-binding protein (IGFBP)-7. Recombinant human mac25 protein specifically binds IGF-I and -II. *J Biol Chem*. 1996 Nov 29;271(48):30322-5. doi: 10.1074/jbc.271.48.30322.
106. Yamanaka Y, Wilson EM, Rosenfeld RG, Oh Y. Inhibition of insulin receptor activation by insulin-like growth factor binding proteins. *J Biol Chem*. 1997 Dec 5;272(49):30729-34. doi: 10.1074/jbc.272.49.30729.
107. Kim HS, Nagalla SR, Oh Y, Wilson E, Roberts CT Jr, Rosenfeld RG. Identification of a family of low-affinity insulin-like growth factor binding proteins (IGFBPs): characterization of connective tissue growth factor as a member of the IGFBP superfamily. *Proc Natl Acad Sci U S A*. 1997 Nov 25;94(24):12981-6. doi: 10.1073/pnas.94.24.12981.
108. Sato J, Hasegawa S, Akaogi K, Yasumitsu H, Yamada S, Sugahara K, Miyazaki K. Identification of cell-binding site of angiomodulin (AGM/TAF/Mac25) that interacts with heparan sulfates on cell surface. *J Cell Biochem*. 1999 Nov 1;75(2):187-95.
109. Akaogi K, Sato J, Okabe Y, Sakamoto Y, Yasumitsu H, Miyazaki K. Synergistic growth stimulation of mouse fibroblasts by tumor-derived adhesion factor with insulin-like growth factors and insulin. *Cell Growth Differ*. 1996 Dec;7(12):1671-7.
110. Jiang W, Xiang C, Cazacu S, Brodie C, Mikkelsen T. Insulin-like growth factor binding protein 7 mediates glioma cell growth and migration. *Neoplasia*. 2008 Dec;10(12):1335-42. doi: 10.1593/neo.08694.

111. Georges RB, Adwan H, Hamdi H, Hielscher T, Linnemann U, Berger MR. The insulin-like growth factor binding proteins 3 and 7 are associated with colorectal cancer and liver metastasis. *Cancer Biol Ther.* 2011 Jul 1;12(1):69-79. doi: 10.4161/cbt.12.1.15719.
112. Hu S, Chen R, Man X, Feng X, Cen J, Gu W, He H, Li J, Chai Y, Chen Z. Function and expression of insulin-like growth factor-binding protein 7 (IGFBP7) gene in childhood acute myeloid leukemia. *Pediatr Hematol Oncol.* 2011 May;28(4):279-87. doi: 10.3109/08880018.2011.557852.
113. Girard JP, Baekkevold ES, Yamanaka T, Haraldsen G, Brandtzaeg P, Amalric F. Heterogeneity of endothelial cells: the specialized phenotype of human high endothelial venules characterized by suppression subtractive hybridization. *Am J Pathol.* 1999 Dec;155(6):2043-55. doi: 10.1016/S0002-9440(10)65523-X.
114. Nagakubo D, Murai T, Tanaka T, Usui T, Matsumoto M, Sekiguchi K, Miyasaka M. A high endothelial venule secretory protein, mac25/angiomodulin, interacts with multiple high endothelial venule-associated molecules including chemokines. *J Immunol.* 2003 Jul 15;171(2):553-61. doi: 10.4049/jimmunol.171.2.553.
115. Subramanian A, Sharma A, Mokbel K. Insulin-like growth factor binding proteins and breast cancer. *Breast Cancer Res Treat.* 2008 Jan;107(2):181-94. doi: 10.1007/s10549-007-9549-0.
116. Pollak M. Insulin and insulin-like growth factor signalling in neoplasia. *Nat Rev Cancer.* 2008 Dec;8(12):915-28. doi: 10.1038/nrc2536.
117. Bièche I, Lerebours F, Tozlu S, Espie M, Marty M, Lidereau R. Molecular profiling of inflammatory breast cancer: identification of a poor-prognosis gene expression signature. *Clin Cancer Res.* 2004 Oct 15;10(20):6789-95. doi: 10.1158/1078-0432.CCR-04-0306.
118. Sun X, Wei L, Lidén J, Hui G, Dahlman-Wright K, Hjerpe A, Dobra K. Molecular characterization of tumour heterogeneity and malignant mesothelioma cell differentiation by gene profiling. *J Pathol.* 2005 Sep;207(1):91-101. doi: 10.1002/path.1810.
119. Osman I, Bajorin DF, Sun TT, Zhong H, Douglas D, Scattergood J, Zheng R, Han M, Marshall KW, Liew CC. Novel blood biomarkers of human urinary bladder cancer. *Clin Cancer Res.* 2006 Jun 1;12(11 Pt 1):3374-80. doi: 10.1158/1078-0432.CCR-05-2081.

120. Rupp C, Scherzer M, Rudisch A, Unger C, Haslinger C, Schweifer N, Artaker M, Nivarthi H, Moriggl R, Hengstschläger M, Kerjaschki D, Sommergruber W, Dolznig H, Garin-Chesa P. IGFBP7, a novel tumor stroma marker, with growth-promoting effects in colon cancer through a paracrine tumor-stroma interaction. *Oncogene*. 2015 Feb 12;34(7):815-25. doi: 10.1038/onc.2014.18.
121. Heesch S, Schlee C, Neumann M, Stroux A, Kühnl A, Schwartz S, Haferlach T, Goekbuget N, Hoelzer D, Thiel E, Hofmann WK, Baldus CD. BAALC-associated gene expression profiles define IGFBP7 as a novel molecular marker in acute leukemia. *Leukemia*. 2010 Aug;24(8):1429-36. doi: 10.1038/leu.2010.130.
122. Akiel M, Guo C, Li X, Rajasekaran D, Mendoza RG, Robertson CL, Jariwala N, Yuan F, Subler MA, Windle J, Garcia DK, Lai Z, Chen HH, Chen Y, Giashuddin S, Fisher PB, Wang XY, Sarkar D. IGFBP7 Deletion Promotes Hepatocellular Carcinoma. *Cancer Res*. 2017 Aug 1;77(15):4014-4025. doi: 10.1158/0008-5472.CAN-16-2885.
123. Evdokimova V, Tognon CE, Benatar T, Yang W, Krutikov K, Pollak M, Sorensen PH, Seth A. IGFBP7 binds to the IGF-1 receptor and blocks its activation by insulin-like growth factors. *Sci Signal*. 2012 Dec 18;5(255):ra92. doi: 10.1126/scisignal.2003184.
124. Bartram I, Erben U, Ortiz-Tanchez J, Blunert K, Schlee C, Neumann M, Heesch S, Baldus CD. Inhibition of IGF1-R overcomes IGFBP7-induced chemotherapy resistance in T-ALL. *BMC Cancer*. 2015 Oct 8;15:663. doi: 10.1186/s12885-015-1677-z.
125. Morgantini C, Jager J, Li X, Levi L, Azzimato V, Sulen A, Barreby E, Xu C, Tencerova M, Näslund E, Kumar C, Verdeguer F, Straniero S, Hultenby K, Björkström NK, Ellis E, Rydén M, Kutter C, Hurrell T, Lauschke VM, Boucher J, Tomčala A, Krejčová G, Bajgar A, Aouadi M. Liver macrophages regulate systemic metabolism through non-inflammatory factors. *Nat Metab*. 2019 Apr;1(4):445-459. doi: 10.1038/s42255-019-0044-9.
126. López-Bermejo A, Khosravi J, Corless CL, Krishna RG, Diamandi A, Bodani U, Kofoed EM, Graham DL, Hwa V, Rosenfeld RG. Generation of anti-insulin-like growth factor-binding protein-related protein 1 (IGFBP-rP1/MAC25) monoclonal antibodies and immunoassay: quantification of IGFBP-rP1 in human serum and distribution in human fluids and tissues. *J Clin Endocrinol Metab*. 2003 Jul;88(7):3401-8. doi: 10.1210/jc.2002-021315.

127. Hoxhaj G, Manning BD. The PI3K-AKT network at the interface of oncogenic signalling and cancer metabolism. *Nat Rev Cancer*. 2020 Feb;20(2):74-88. doi: 10.1038/s41568-019-0216-7.
128. Fruman DA, Chiu H, Hopkins BD, Bagrodia S, Cantley LC, Abraham RT. The PI3K Pathway in Human Disease. *Cell*. 2017 Aug 10;170(4):605-635. doi: 10.1016/j.cell.2017.07.029.
129. Thorpe LM, Yuzugullu H, Zhao JJ. PI3K in cancer: divergent roles of isoforms, modes of activation and therapeutic targeting. *Nat Rev Cancer*. 2015 Jan;15(1):7-24. doi: 10.1038/nrc3860.
130. Alessi DR, Andjelkovic M, Caudwell B, Cron P, Morrice N, Cohen P, Hemmings BA. Mechanism of activation of protein kinase B by insulin and IGF-1. *EMBO J*. 1996 Dec 2;15(23):6541-51.
131. Alessi DR, James SR, Downes CP, Holmes AB, Gaffney PR, Reese CB, Cohen P. Characterization of a 3-phosphoinositide-dependent protein kinase which phosphorylates and activates protein kinase B $\alpha$ . *Curr Biol*. 1997 Apr 1;7(4):261-9. doi: 10.1016/s0960-9822(06)00122-9.
132. Sarbassov DD, Guertin DA, Ali SM, Sabatini DM. Phosphorylation and regulation of Akt/PKB by the rictor-mTOR complex. *Science*. 2005 Feb 18;307(5712):1098-101. doi: 10.1126/science.1106148.
133. Dummler B, Hemmings BA. Physiological roles of PKB/Akt isoforms in development and disease. *Biochem Soc Trans*. 2007 Apr;35(Pt 2):231-5. doi: 10.1042/BST0350231.
134. Manning BD, Toker A. AKT/PKB Signaling: Navigating the Network. *Cell*. 2017 Apr 20;169(3):381-405. doi: 10.1016/j.cell.2017.04.001.
135. Jung HJ, Suh Y. Regulation of IGF -1 signaling by microRNAs. *Front Genet*. 2015 Jan 13;5:472. doi: 10.3389/fgene.2014.00472.
136. Lunt SY, Vander Heiden MG. Aerobic glycolysis: meeting the metabolic requirements of cell proliferation. *Annu Rev Cell Dev Biol*. 2011;27:441-64. doi: 10.1146/annurev-cellbio-092910-154237.
137. Warburg O, Wind F, Negelein E. THE METABOLISM OF TUMORS IN THE BODY. *J Gen Physiol*. 1927 Mar 7;8(6):519-30. doi: 10.1085/jgp.8.6.519.
138. Rathmell JC, Fox CJ, Plas DR, Hammerman PS, Cinalli RM, Thompson CB. Akt-directed glucose metabolism can prevent Bax conformation change and promote

- growth factor-independent survival. *Mol Cell Biol.* 2003 Oct;23(20):7315-28. doi: 10.1128/MCB.23.20.7315-7328.2003.
139. Elstrom RL, Bauer DE, Buzzai M, Karnauskas R, Harris MH, Plas DR, Zhuang H, Cinalli RM, Alavi A, Rudin CM, Thompson CB. Akt stimulates aerobic glycolysis in cancer cells. *Cancer Res.* 2004 Jun 1;64(11):3892-9. doi: 10.1158/0008-5472.CAN-03-2904.
  140. Gottlob K, Majewski N, Kennedy S, Kandel E, Robey RB, Hay N. Inhibition of early apoptotic events by Akt/PKB is dependent on the first committed step of glycolysis and mitochondrial hexokinase. *Genes Dev.* 2001 Jun 1;15(11):1406-18. doi: 10.1101/gad.889901.
  141. Plas DR, Talapatra S, Edinger AL, Rathmell JC, Thompson CB. Akt and Bcl-xL promote growth factor-independent survival through distinct effects on mitochondrial physiology. *J Biol Chem.* 2001 Apr 13;276(15):12041-8. doi: 10.1074/jbc.M010551200.
  142. Edinger AL, Thompson CB. Antigen-presenting cells control T cell proliferation by regulating amino acid availability. *Proc Natl Acad Sci U S A.* 2002 Feb 5;99(3):1107-9. doi: 10.1073/pnas.042707999.
  143. Buzzai M, Bauer DE, Jones RG, Deberardinis RJ, Hatzivassiliou G, Elstrom RL, Thompson CB. The glucose dependence of Akt-transformed cells can be reversed by pharmacologic activation of fatty acid beta-oxidation. *Oncogene.* 2005 Jun 16;24(26):4165-73. doi: 10.1038/sj.onc.1208622.
  144. Augustin R. The protein family of glucose transport facilitators: It's not only about glucose after all. *IUBMB Life.* 2010 May;62(5):315-33. doi: 10.1002/iub.315.
  145. Adekola K, Rosen ST, Shanmugam M. Glucose transporters in cancer metabolism. *Curr Opin Oncol.* 2012 Nov;24(6):650-4. doi: 10.1097/CCO.0b013e328356da72.
  146. Calera MR, Martinez C, Liu H, Jack AK, Birnbaum MJ, Pilch PF. Insulin increases the association of Akt-2 with Glut4-containing vesicles. *J Biol Chem.* 1998 Mar 27;273(13):7201-4. doi: 10.1074/jbc.273.13.7201.
  147. Ng Y, Ramm G, Lopez JA, James DE. Rapid activation of Akt2 is sufficient to stimulate GLUT4 translocation in 3T3-L1 adipocytes. *Cell Metab.* 2008 Apr;7(4):348-56. doi: 10.1016/j.cmet.2008.02.008.
  148. Sano H, Kane S, Sano E, Mîinea CP, Asara JM, Lane WS, Garner CW, Lienhard GE. Insulin-stimulated phosphorylation of a Rab GTPase-activating protein regulates

- GLUT4 translocation. *J Biol Chem.* 2003 Apr 25;278(17):14599-602. doi: 10.1074/jbc.C300063200.
149. Eguez L, Lee A, Chavez JA, Miinea CP, Kane S, Lienhard GE, McGraw TE. Full intracellular retention of GLUT4 requires AS160 Rab GTPase activating protein. *Cell Metab.* 2005 Oct;2(4):263-72. doi: 10.1016/j.cmet.2005.09.005.
  150. Waldhart AN, Dykstra H, Peck AS, Boguslawski EA, Madaj ZB, Wen J, Veldkamp K, Hollowell M, Zheng B, Cantley LC, McGraw TE, Wu N. Phosphorylation of TXNIP by AKT Mediates Acute Influx of Glucose in Response to Insulin. *Cell Rep.* 2017 Jun 6;19(10):2005-2013. doi: 10.1016/j.celrep.2017.05.041.
  151. Parikh H, Carlsson E, Chutkow WA, Johansson LE, Storgaard H, Poulsen P, Saxena R, Ladd C, Schulze PC, Mazzini MJ, Jensen CB, Krook A, Björnholm M, Tornqvist H, Zierath JR, Ridderstråle M, Altshuler D, Lee RT, Vaag A, Groop LC, Mootha VK. TXNIP regulates peripheral glucose metabolism in humans. *PLoS Med.* 2007 May;4(5):e158. doi: 10.1371/journal.pmed.0040158.
  152. Wu N, Zheng B, Shaywitz A, Dagon Y, Tower C, Bellinger G, Shen CH, Wen J, Asara J, McGraw TE, Kahn BB, Cantley LC. AMPK-dependent degradation of TXNIP upon energy stress leads to enhanced glucose uptake via GLUT1. *Mol Cell.* 2013 Mar 28;49(6):1167-75. doi: 10.1016/j.molcel.2013.01.035.
  153. Chan LN, Chen Z, Braas D, Lee JW, Xiao G, Geng H, Cosgun KN, Hurtz C, Shojaee S, Cazzaniga V, Schjerven H, Ernst T, Hochhaus A, Kornblau SM, Konopleva M, Pufall MA, Cazzaniga G, Liu GJ, Milne TA, Koeffler HP, Ross TS, Sánchez-García I, Borkhardt A, Yamamoto KR, Dickins RA, Graeber TG, Müschen M. Metabolic gatekeeper function of B-lymphoid transcription factors. *Nature.* 2017 Feb 23;542(7642):479-483. doi: 10.1038/nature21076.
  154. Müschen M. Metabolic gatekeepers to safeguard against autoimmunity and oncogenic B cell transformation. *Nat Rev Immunol.* 2019 May;19(5):337-348. doi: 10.1038/s41577-019-0154-3.
  155. Boag JM, Beesley AH, Firth MJ, Freitas JR, Ford J, Hoffmann K, Cummings AJ, de Klerk NH, Kees UR. Altered glucose metabolism in childhood pre-B acute lymphoblastic leukaemia. *Leukemia.* 2006 Oct;20(10):1731-7. doi: 10.1038/sj.leu.2404365.
  156. Wofford JA, Wieman HL, Jacobs SR, Zhao Y, Rathmell JC. IL-7 promotes Glut1 trafficking and glucose uptake via STAT5-mediated activation of Akt to support T-cell survival. *Blood.* 2008 Feb 15;111(4):2101-11. doi: 10.1182/blood-2007-06-096297.

157. Liu T, Kishton RJ, Macintyre AN, Gerriets VA, Xiang H, Liu X, Abel ED, Rizzieri D, Locasale JW, Rathmell JC. Glucose transporter 1-mediated glucose uptake is limiting for B-cell acute lymphoblastic leukemia anabolic metabolism and re-sistance to apoptosis. *Cell Death Dis.* 2014 Nov;5(11):e1516–. doi: 10.1038/cddis.2014.493.
158. Ancey PB, Contat C, Meylan E. Glucose transporters in cancer - from tumor cells to the tumor microenvironment. *FEBS J.* 2018 Aug;285(16):2926-2943. doi: 10.1111/febs.14577.
159. Chandel NS. Signaling and Metabolism. *Cold Spring Harb Perspect Biol.* 2021 Feb 1;13(2):a040600. doi: 10.1101/cshperspect.a040600.
160. Holleman A, Cheok MH, den Boer ML, Yang W, Veerman AJ, Kazemier KM, Pei D, Cheng C, Pui CH, Relling MV, Janka-Schaub GE, Pieters R, Evans WE. Gene-expression patterns in drug-resistant acute lymphoblastic leukemia cells and response to treatment. *N Engl J Med.* 2004 Aug 5;351(6):533-42. doi: 10.1056/NEJMoa033513.
161. Frattali AL, Pessin JE. Relationship between alpha subunit ligand occupancy and beta subunit autophosphorylation in insulin/insulin-like growth factor-1 hybrid receptors. *J Biol Chem.* 1993 Apr 5;268(10):7393-400.
162. Wieman HL, Wofford JA, Rathmell JC. Cytokine stimulation promotes glucose uptake via phosphatidylinositol-3 kinase/Akt regulation of Glut1 activity and trafficking. *Mol Biol Cell.* 2007 Apr;18(4):1437-46. doi: 10.1091/mbc.e06-07-0593.
163. Siska PJ, van der Windt GJ, Kishton RJ, Cohen S, Eisner W, MacIver NJ, Kater AP, Weinberg JB, Rathmell JC. Suppression of Glut1 and Glucose Metabolism by Decreased Akt/mTORC1 Signaling Drives T Cell Impairment in B Cell Leukemia. *J Immunol.* 2016 Sep 15;197(6):2532-40. doi: 10.4049/jimmunol.1502464.
164. Avanzato D, Pupo E, Ducano N, Isella C, Bertalot G, Luise C, Pece S, Bruna A, Rueda OM, Caldas C, Di Fiore PP, Sapino A, Lanzetti L. High USP6NL Levels in Breast Cancer Sustain Chronic AKT Phosphorylation and GLUT1 Stability Fueling Aerobic Glycolysis. *Cancer Res.* 2018 Jul 1;78(13):3432-3444. doi: 10.1158/0008-5472.CAN-17-3018.
165. Hotamisligil GS. Inflammation and metabolic disorders. *Nature.* 2006 Dec 14;444(7121):860-7. doi: 10.1038/nature05485.
166. Poloz Y, Stambolic V. Obesity and cancer, a case for insulin signaling. *Cell Death Dis.* 2015 Dec 31;6(12):e2037. doi: 10.1038/cddis.2015.381.
167. Artico LL, Laranjeira ABA, Campos LW, Corrêa JR, Zenatti PP, Carvalheira JBC, Brambilla SR, Nowill AE, Brandalise SR, Yunes JA. Physiologic IGF1 levels



prolong IGF1R activation in acute lymphoblastic leukemia. *Blood Adv.* 2021 Sep 28;5(18):3633-3646. doi: 10.1182/bloodadvances.2020003627.

- 168.** Artico LL, Ruas JS, Teixeira Júnior JR, Migita NA, Seguchi G, Shi X, Brandalise SR, Castilho RF, Yunes JA. IGFBP7 Fuels the Glycolytic Metabolism in B-Cell Precursor Acute Lymphoblastic Leukemia by Sustaining Activation of the IGF1R-Akt-GLUT1 Axis. *Int J Mol Sci.* 2023 Jun 2;24(11):9679. doi: 10.3390/ijms24119679.

## 12. ATTACHMENTS

### 12.1 Activities Report BEPE – FAPESP 2019/4943-3

**Re:** Activities Report BEPE – FAPESP 2019/4943-3

**Candidate:** Leonardo Luís Artico

**Local Principal Investigator:** Dr José Andres Yunes, Centro Infantil Boldrini

**Hosting Principal Investigator:** Dr Ana Paula Arruda, Department of Nutritional Sciences and Toxicology, University of California – Berkeley

**Insulin signaling in metabolic diseases: the role of IGFBP7 in hepatic and adipose tissue metabolic function**

#### 1. Background

Insulin and insulin-like growth factors (IGF1 and IGF2) are well-known mitogenic and pro-survival factors in many different cell types.<sup>1</sup> Insulin has a very similar structure to IGFs (mainly IGF1), but its functions/actions have substantial differences in cellular physiology. Insulin predominantly regulates metabolic activity, such as anabolic pathways, including glucose and amino acid transport, induction of glycogen, lipid and protein biosynthesis and inhibition of gluconeogenesis, lipolysis, and protein degradation.<sup>2</sup> In short-term, metabolic effect of IGFs is insulin-like. However, in the long term, IGFs may also control cell growth, differentiation, and cell death.<sup>3,4</sup>

In general, insulin and IGF1 act by binding to receptors formed by homo- or heterodimeric insulin receptor (INSR) and IGF1 receptor (IGF1R) chains, on a target cell membrane, followed by activation of tyrosine kinase in the  $\beta$ -subunit of the cognate receptor. After activation, INSR and IGF1R recruit and phosphorylate insulin receptor substrate proteins (IRS1-4) and SHC. IRS1, IRS2 and SHC are recognized by various signaling molecules that contain a Src homology 2 (SH2) domain, such as Grb2 and the 85kDa regulatory subunit of phosphatidylinositol 3-kinase (PI3K), thus initiating the downstream activation of PI3K (PI3K/Akt/mTOR) and MAP kinase (Ras/Raf/Mek/Erk) pathways (Figure 1).<sup>2,5</sup>

Circulating IGFs are normally bound by 1 of the 6 IGF binding proteins (IGFBPs) that can both inhibit or potentiate IGF signaling pathway.<sup>7</sup> IGFBPs bind IGFs with high affinity, but do not bind to insulin; they also have a better affinity for IGFs than for IGF1R (~100 times higher).<sup>8</sup> In most circumstances, IGFBPs inhibit IGF actions by

preventing its binding to IGF receptors and, consequently, promoting downregulation of cellular proliferation, survival, differentiation, and metabolism. However, IGFBPs can also increase IGF signaling, which occurs through proteolytic cleavage, one of the main mechanisms involved in the IGF release from IGFBPs.<sup>9</sup>

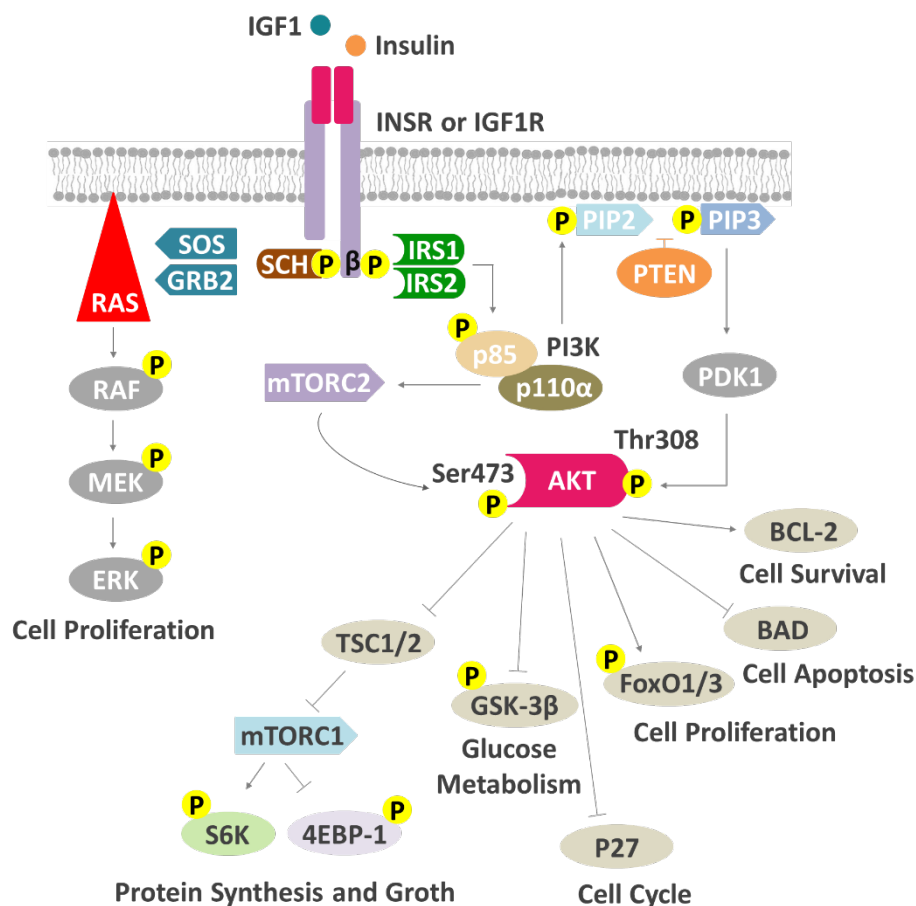


**Figure 1: The insulin/IGFs signaling pathway.** Insulin/IGF1 functions as a ligand to interact with INSR or IGF1R in the cellular membrane, which leads to autophosphorylation and recruitment of the adaptor proteins IRS1, IRS2, and Shc. The interaction of IRS1/2 with  $\beta$ -subunit of the cognate receptor induces the activation of PI3K. PI3K converts PIP2 to the lipid second messenger PIP3. Akt family of kinases is activated by PDK1 and by mTORC2 complex resulting in the phosphorylation at Threonine 308 (Thr308) and Serine 473 (Ser473), respectively. Activated Akt then regulates downstream signaling molecules including Tuberous sclerosis protein 1/2 (TSC1/2) which inhibit mTORC1 complex and regulate S6K and 4EBP-1 phosphorylation, FoxO transcription factors, GSK-3 $\beta$ , p27, BAD, and BCL-2. These downstream molecules are involved in several cellular processes including protein synthesis, glucose metabolism and cell survival., In parallel, SHC activation induces the activation of the

MAPK pathway, which results in increased cell proliferation, mediated by RAS activation. Adapted from Jung and Suh.<sup>6</sup>

IGFBPs are cysteine-rich proteins sharing high similarity in their primary amino acid sequences. Structurally, the cysteines are clustered at the conserved N-terminal third (12 cysteines in IGFBP1 to 5; and 10 in IGFBP6) and at the conserved C-terminal third (6 cysteines) of the proteins. In addition, the IGF-binding domain of IGFBPs (GCGCCxxC sequence, where x is any amino acid residue) is also shared by other 10 extracellular proteins, collectively called IGFBP-related proteins (IGFBP-rP1 - 10) superfamily. IGFBP-rPs carry the N-terminal domain of IGFBPs (Figure 2 – blue box) but discern from the common IGFBP structure mostly in the C-terminus region. Functionally, these proteins can bind IGFs, albeit with lower affinity (100-1000 times) than that observed with IGFBPs and have multiple IGF-independent roles. Therefore, their physiologic significance in the IGFs pathway remains undefined.<sup>8,10</sup>

IGFBP1	---QVGVTAGAPWQCAPCSAEKLALCPP-VS-----ASCSEV---TRSA 55
IGFBP2	GG-GGGARAEVLFRCPPCTPERLAACGP-PPVAPPAAVAAGGARMPCAEEL---VREP 82
IGFBP3	AG-ASSAGLGPVVRCEPCDARALAQCAP-PP-----AVCAEL---VREP 65
IGFBP4	AG-PGPSLGDEAIHCPPCSEKRLARCP-P-----VGCEEL---VREP 51
IGFBP5	YA-GPAQSLGSEFVHCEPCDEKALSMCPP-SP-----LGC-EL---VKEP 51
IGFBP6	----ASPGGALARCPGCGQGVQAGCPG-----GCVEEEDGGSPAE 55
IGFBP-rP1/IGFBP7	---SSSSSDTCGCPCEP-----ASCPP-LPP-----LGCL---LGETRD 55
IGFBP-rP2/CCN2/CTGF	---RPAVGQNCSG--P-----CRCPDEPAP-----RCPAG--VSLVLD 52
IGFBP-rP3/CCN3/NOV	---QVAATQRCPPQCP-----GRCPA-TTP-----TCAPG--VRAVLD 59
IGFBP-rP4/CCN1/Cyr61	---RL-ALSTCPA--A-----CHCPL-EAP-----KCAPG--VGLVRD 48
IGFBP-rP5/L56/HtrA	GR-SAPLAAGCPDRCEP-----ARCPP--QP-----EHCE---GGRARD 60
IGFBP-rP6/ESM-1	AW-SNNYAVDCPQHCDSE-----SECKS-SP-----RCKR---TVLD 49
IGFBP-rP7/CCN5/WISP2	---KV-RTQLCPT--P-----CTCPW-PPP-----RCPLG--VPLVLD 48
IGFBP-rP8/CCN4/WISP1	---TSSRPQFCKW--P-----CECPP-SPP-----RCPLG--VSLITD 71
IGFBP-rP9/CCN9/WISP3	---APQRKQFCHW--P-----CKCPQ-QKP-----RCPPG--VSLVRD 70
IGFBP-rP10/BONO1/KAZALD1	GWMRLLAEGEGCAPCRP-----EECA--AP-----RGCL---AGRVRD 74
	<b>GCGCCxxC</b>
IGFBP1	GCGCCPMCALPLGAAC-----GVATARCARGLSRALPGEQQP-LHAL----- 97
IGFBP2	GCGCCSVCARLEGEAC-----GVYTPRCGQGLRCYPHPGSELP-LQAL----- 124
IGFBP3	GCGCCLTALSEGQPC-----GIYTERCGSGLRCQSPDEARP-LQAL----- 107
IGFBP4	GCGCCATCALGLGMPC-----GVYTPRCGSGLRCPYPRGVEKP-LHTL----- 93
IGFBP5	GCGCMTCALAEGQSC-----GVYTERCAQGLRCLPRQDEEK-LHAL----- 93
IGFBP6	GCAEAEGCLRREGQEC-----GVYTPNCAPGLQCHPPKDDEAP-LRAL----- 97
IGFBP-rP1/IGFBP7	ACGCCPMCARGEPEPCGGGGAGR--GYCAPGMECV <b>KSRKRRKGK</b> AGAAAGPGVSGVCVC 113
IGFBP-rP2/CCN2/CTGF	GCGCCRVCAQLGELCTERDP---CDPHKGLFCHFGSPANR-----KIGVCTA 97
IGFBP-rP3/CCN3/NOV	GCSCCLVCARQGESCSLDLEP---CDESSGLYCDRSADPSN-----QTGICTA 104
IGFBP-rP4/CCN1/Cyr61	GCGCKVCAKQLNEDCSKTQP---CDHTKGLECNFGASSTA-----LKGICRA 93
IGFBP-rP5/L56/HtrA	ACGCCVCGAPEGAAACGLQE-----GPCGEGLCQVVPFGV--PASATVRRRAQAGLCVC 112
IGFBP-rP6/ESM-1	DCGCCRVCAAGRGETCYRTVSGMDGMKCGPLRCQPSNGEDPF-GEEF-----GIC 99
IGFBP-rP7/CCN5/WISP2	GCGCCRVCAARRLGEPCDQLHV---CDASQGLVCQPGAGPGG-----RGALCLL 93
IGFBP-rP8/CCN4/WISP1	GCECCKMCAQLGDNCTEAAI---CDPHRGLYCDYSGDRPRY-----AIGVC-A 116
IGFBP-rP9/CCN9/WISP3	GCGCKICAKQPGEICNEADL---CDPHKGLYCDYSVDRPRY-----ETGVC-A 115
IGFBP-rP10/BONO1/KAZALD1	ACGCCWECANLEGQLCDLPSSAHFYGHCGEQLCRL-----DTGGDLRGEVPEPLCAC 128

**Figure 2. Amino acid sequence alignment of the N-terminal domains from human IGFBP1 to 6 and human IGFBP-rP1 to 10.** Alignment was performed using Align approach by UniProt databases ([www.uniprot.org](http://www.uniprot.org)). Signal peptides were not included in the analysis. Small gaps were introduced to optimize alignment. Consensus amino acid residues are shaded orange. Blue box indicates the IGF-binding domain of IGFBPs (GCGCCxxC sequence, where x is any amino acid residue). Red box shows the heparin-binding site in IGFBP-rP1/IGFBP7.

IGFBP-rP1, best known as IGFBP7, is a special case among IGFBP-rPs or IGFBPs. IGFBP7 was the first member of the IGFBP-rPs superfamily to be identified (Figure 3). Structurally, at the N-terminus of the IGFBP7 molecule there is an IGFBP motif (A<sup>30</sup>CGCCPMCA<sup>38</sup>) in a domain including 12 conserved amino acids (cysteines)<sup>11</sup> followed by a heparin-binding site K<sup>89</sup>SRKRRKGK<sup>97</sup>, which interacts with heparin sulfates on the cell surface<sup>12</sup> (Figures 2 and 3). The C-terminus of IGFBP7 differs substantially from the other IGFBPs because it lacks the conserved cysteines and in fact has only one cysteine. Also, while it has a 200-fold lower affinity for IGF-1 than the other IGFBPs, it binds insulin with relatively high affinity, although with lower affinity than that exhibited by the INSR.<sup>13</sup>

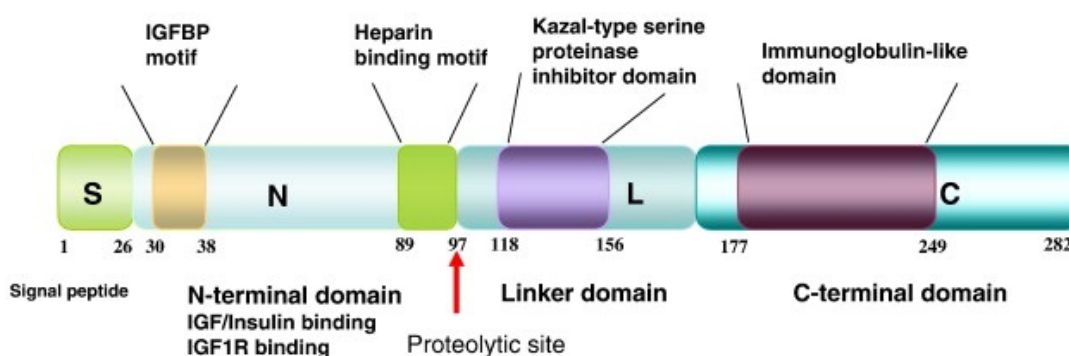


**Figure 3. Structure of IGFBP7.** IGFBP7 showing the three distinct domains: a N-terminal domain, a C-terminal domain and a linker domain. The N-terminal domain is responsible for binding to IGFs/insulin/IGF1R. The C-terminal domain has a lesser similarity to other members of the IGFBP superfamily. The motifs and domains are shown in the figure (from left to right): IGFBP motif; heparin binding motif; Kazal-type serine proteinase inhibitor domain; and immunoglobulin-like domain. The red arrow indicates the proteolytic site at K(Lys)97 and A(Ala)98. Adapted from Zhu et al.<sup>14</sup>

Some studies have shown that IGFBP7 decreases INSR and IGF1R signaling by sequestering insulin and IGFs,<sup>8,13,15</sup> or being an IGF1R antagonist.<sup>16,17</sup> For example,

Evdokimova et al.<sup>16</sup> reported that N-terminus of the IGFBP7 molecule can bind to the extracellular domain of IGF1R and inhibit its activation. Hypothetically, the authors argue that IGFBP7 binding to unoccupied IGF1R sterically restricts or allosterically prevents subsequent binding of insulin/IGF1. However, other studies have shown that IGFBP7 enhance insulin/IGF1 activities.<sup>18,19</sup> For example, an important study published by Morgantini et al.<sup>20</sup> shows that in mice under insulin-sensitive conditions, the IGFBP7 produced by liver macrophages binds to the hepatic INSR and enhances Akt (Ser473) activation by insulin. Under insulin-resistant conditions, in which Akt does not respond to insulin, IGFBP7 binds to the INSR with lower affinity but can still activate the MAPK pathway and induce gluconeogenesis and lipogenesis.<sup>20</sup> However, the relationship between IGFBP7, insulin and IGF1R signaling in hepatocyte metabolism was not fully addressed in this study.

Although differences in the INSR/IGF1R signaling and/or internalization complexes between the biological models used in the studies mentioned above should not be undervalued, we suspect that the amount of IGFBP7 protein available to cells likely contributes to the discrepancy of the results presented in these studies. Evdokimova et al.<sup>16</sup> used IGFBP7 at 20 µg/ml, while Morgantini et al.<sup>20</sup> used 20 ng/ml. It is plausible that in high concentrations, IGFBP7 may indeed restrict or prevent IGF1/insulin binding to the IGF1R. In fact, 20 µg/ml is far above the physiologic levels of IGFBP7 in adult serum (21-35 ng/ml)<sup>21</sup> or childhood ALL bone marrow plasma (49 ng/ml).<sup>19</sup>

Using ALL models, we recently reported that insulin and IGF1 trigger mitogenic action in leukemia, which is prolonged by the addition of physiological levels of IGFBP7.<sup>22</sup> Association of insulin/IGF1 plus IGFBP7 boosts the primary ALL survival *in vitro*. For example, the treatment of ALL cells with insulin plus IGFBP7 (100 ng/ml), sustains the IGF1Rβ (Tyr1131) phosphorylation, but not INSRβ (Tyr1151/1151), for up to 4 h. Besides IGF1Rβ, sustained Akt (Ser473) phosphorylation was also confirmed in 18 retrospective primary ALL samples. Mechanistically, we demonstrated that IGFBP7 inhibits IGF1R internalization (but not INSR), and this effect appears to be insulin/IGF1 dependent. Cell surface retention of IGF1R has been linked to sustained activation of IRS1, Akt and Erk in ALL, mediated by insulin/IGF1 plus IGFBP7 treatment. IGFBP7 neutralization by anti-IGFBP7 monoclonal antibody (clone C311) restored IGF1R signaling and attenuated ALL progression *in vivo*. Interestingly, using IGFBP7 at 20 µg/ml we also found an inhibitory effect on ALL cells, like Evdokimova

et al.<sup>16</sup> found in breast cancer. Therefore, at supraphysiological concentrations, IGFBP7 may have adverse effects when compared to physiological levels, which could justify the inconsistent data present in the literature (To read more about this discussion, access: Artico et al.).<sup>22</sup> We also confirm the significance of IGF1R in the pro-survival effects mediated by IGFBP7 in pediatric ALL, while highlighting the impact of IGFBP7 on glycolytic metabolism through the IGF1R-Akt-GLUT1 axis.<sup>23</sup> Our findings demonstrate that IGFBP7 enhances glycolytic metabolism by stabilizing glucose transporter 1 (GLUT1) on the cell surface, leading to increased glucose uptake. This effect is achieved through sustained Akt activation, which is a downstream target of IGF1R. Gene expression analysis and metabolic assays further support the idea that IGFBP7 promotes energy metabolism by activating signaling pathways associated with cell growth and proliferation. In summary, our studies shed light on the significant role of IGFBP7 in pediatric ALL. It influences the response to chemotherapy, activates IGF1R signaling, modulates glucose metabolism, and impacts leukemia progression.

In the oncogenic context, downstream signaling of IGF1R/INSR, supported by insulin/IGF1 plus IGFBP7, is unfavorable because it contributes to the activation of the PI3K and MAPK pathways, and induction of cell proliferation and survival, creating a opposite dynamic to cancer eradication. However, in metabolic diseases (especially obesity and type 2 diabetes), insulin/IGF1 signaling are defective. The enhanced IGF1R/INSR signaling by IGFBP7 could have beneficial metabolic outcomes and offer therapeutical opportunities to treat those diseases.

The pathogenesis of insulin resistance and hyperinsulinemia in obesity is complex and multifactorial. But, it is known that a key factor underlying the development of insulin resistance and metabolic dysregulation in obesity is closely related to the dysfunction of hepatic and adipose tissue, leading to disruption of the endocrine function of these tissues.<sup>24,25</sup> Given the role of IGFBP7 on the potentiation of INSR<sup>20</sup> and IGF1R signaling,<sup>22,23</sup> we have raised the hypothesis that IGFBP7 could exert a positive impact on hepatocyte/adipocyte insulin/IGF signaling, resulting in an improvement of function and intracellular homeostasis. In order to answer this hypothesis, we performed a series of experiments in different models of insulin resistance in hepatocytes and adipocytes from lean and obese mice. Below, we will present the key findings obtained in this project. Overall, we obtained significant evidence that IGFBP7 potentiate insulin signaling increasing insulin sensitivity in different models of insulin resistance.

## 2. Data presentation

### 2.1 Mice liver perfusion and primary hepatocytes isolation

In the field of oncology, genetically modified or altered biological models are commonly used, where these genetic alterations typically promote cell proliferation, activation of oncogenes, secretion of growth factors, and activation of molecular pathways associated with cell division and invasiveness.<sup>26,27</sup> Together, these characteristics promotes lifelong cell multiplication capacity and immortality. However, when studying metabolic diseases such as obesity and type 2 diabetes, it is crucial to work with biological models that closely reflect physiological scenarios with minimal genetic disturbances related to oncogenes. This approach enhances the reliability of the data and ensures a more accurate representation of the study environment.

In the past, it was common and sufficient to use cell lines and less complex biological models to study metabolic diseases. However, contradictory results often arise when these models are compared to more physiological scenarios involving primary cells and *in vivo* models.<sup>28</sup> In light of these discrepancies, we have chosen to initiate our investigation using primary hepatocytes isolated from mice, which offer a more physiologically relevant model compared to cell lines.<sup>29</sup>

However, obtaining primary hepatocytes is challenging due to the intricate nature of these cells and their limited lifespan in cell culture. Furthermore, the quality of the cells obtained is closely tied to the liver perfusion process and the handling of the organ during the primary hepatocyte isolation procedure. Therefore, I invested a significant amount of time to perfect the protocol to isolate high quality primary hepatocytes from lean and obese mice. Briefly, primary hepatocytes were obtained by perfusing the liver of mice through the portal vein with digestive enzymes. This method allows for the removal of blood cells and contaminants while preserving the structural and functional integrity of the hepatocytes (Figure 4). The following description outlines the steps involved in the perfusion process:

- 1) Surgical preparation: the mouse is anesthetized and placed in a supine position. The abdominal region is carefully sterilized, and a midline incision is made to expose the peritoneal cavity (Figure 4A).
- 2) Catheterization of the portal vein: the portal vein, which carries blood from the digestive organs to the liver, is located. A catheter is inserted into the



portal vein and secured in place using super glue or clamp. The catheter serves as an access point for the perfusion solution (Figure 4A).

- 3) Perfusion solution: typically, the liver is perfused with two different solutions, the first consisting of a buffered saline solution supplemented with calcium and magnesium ions to maintain cell viability and functionality. The second contains enzymes such as collagenase or liberase to help digest liver tissue and release hepatocytes from the hepatic extracellular matrix (Figure 4B).
- 4) Initiation of perfusion: the perfusion solution is then introduced into the portal vein through the catheter. The solution is delivered using a peristaltic pump. The flow rate is carefully controlled to ensure efficient and uniform distribution throughout the liver (Figure 4B).
- 5) Hepatocyte disruption and collection: as the perfusion solution circulates through the liver, it enzymatically digests the extracellular matrix and breaks down the liver tissue. This process facilitates the release of individual hepatocytes. The digested liver tissue containing the released hepatocytes are collected and filtered to separate the hepatocytes from the remaining tissue debris (Figure 4C, D).
- 6) Hepatocyte purification: the collected hepatocytes are then subjected to additional purification steps to eliminate non-hepatocyte cell types and further enhance the purity of the isolated hepatocyte population. This may involve density gradient centrifugation or differential plating techniques to separate hepatocytes from non-parenchymal cells (Figure 4E).

In summary, liver perfusion through the portal vein provides an efficient method for the isolation of primary hepatocytes from mice livers. The detailed protocol can be requested through the website: <https://arrudalab.org/contact-arruda-lab/>

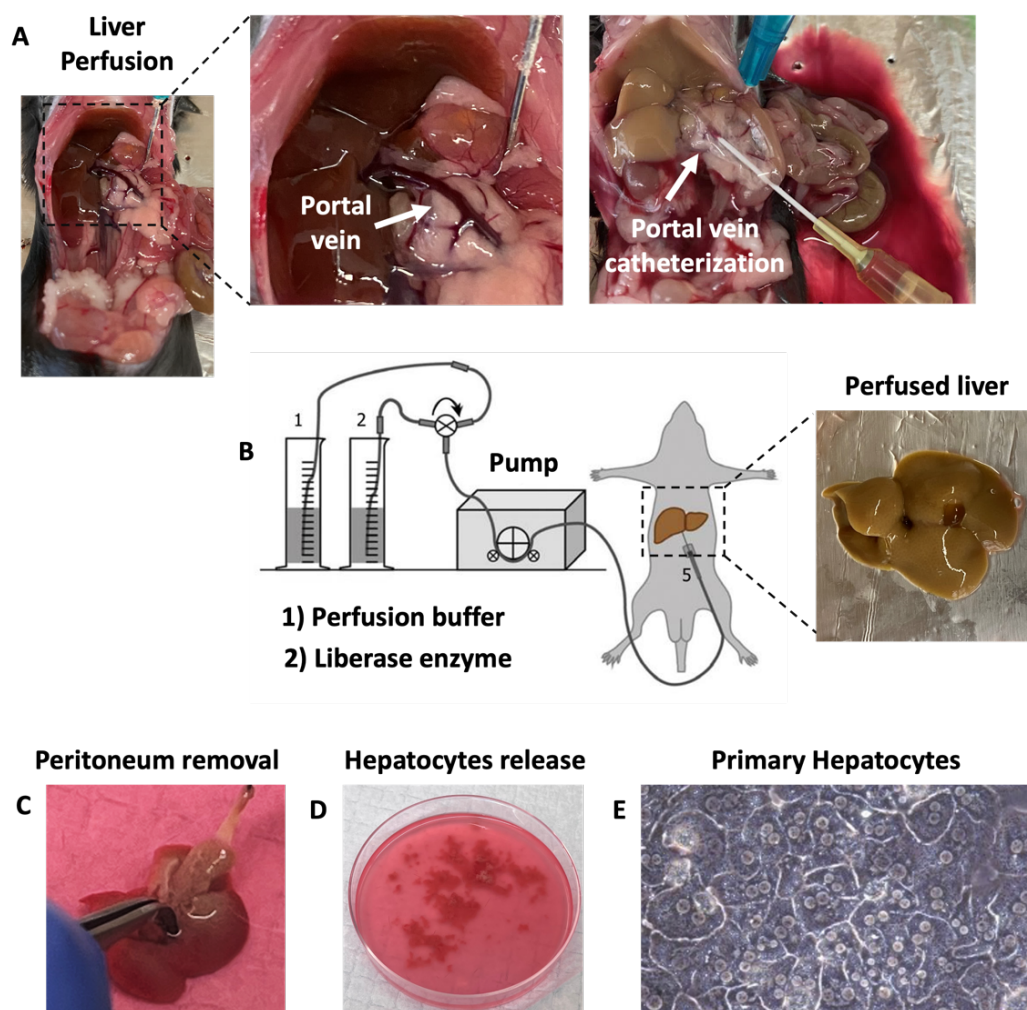


**Figure 4. Mice liver perfusion and primary hepatocytes isolation.** (A) Mouse is anesthetized and placed in a supine position. The abdominal area is sterilized, and a midline incision is made to expose the peritoneal cavity. A catheter is then inserted into the portal vein. The catheter is securely held in place using super glue or clamp, providing an entry point for the perfusion solution. (B) The liver is perfused with two solutions. The first is a buffered saline solution and the second solution contain liberase enzyme to aid in the digestion of liver tissue and release hepatocytes from the extracellular matrix. The perfusion solution is introduced into the portal vein through the cannula using a peristaltic pump. After perfusion, the hepatic peritoneum is removed (C) to release the primary hepatocytes in the culture medium (D). After cell purification and percoll gradient centrifugation, primary hepatocytes are distributed in culture plates (collagenase coating) for future analysis and treatment (E).

## 2.2 IGFBP7 potentiates insulin signaling in primary hepatocytes

As mentioned earlier, IGFBP7 (at physiological levels) plays a significant role in ALL by stimulating the PI3K-Akt pathway and the glycolytic pathway regulated by

insulin/IGF1.<sup>22</sup> In the context of ALL, these effects are specifically mediated through IGF1R.<sup>23</sup> This is evident from the fact that when the IGF1R is knocked out in ALL cell lines, these cells become insensitive to treatment with insulin/IGF1+IGFBP7.

The combination of insulin/IGF1+IGFBP7 in ALL leads to sustained phosphorylation of IGF1R and Akt (Ser473), lasting up to 4 h post-stimulation. Consequently, our initial objective was to determine whether primary hepatocytes would similarly exhibit prolonged activation of the PI3K-Akt pathway following treatment with insulin (3nM), IGFBP7 (100 ng/mL), or their combination. To replicate the findings observed in ALL, we added the treatments to primary hepatocytes at two distinct time points: 3 min and 4 h. Additionally, in order to minimize interference from physiological factors (such as food intake) on insulin signaling, we conducted the experiments under two separate conditions: FED (with freely available food) and FAST state (following a 16-hour fast). In both conditions, after isolating the primary hepatocytes, cells were cultured in serum-free William's medium for 12 h prior to initiating the stimulation with insulin, IGFBP7, or associations (Figure 5A).

The western blot analyses presented in Figure 5B and 5C indicate that the association of insulin+IGFBP7 did not contribute to the sustained phosphorylation of Akt (Ser473) and S6 (Ser 235/236) in primary hepatocytes isolated from fasted mice. However, when primary hepatocytes isolated from fed mouse were stimulated, they exhibited enhanced phosphorylation of both Akt (Ser473) and S6 (Ser235/236) (Figure 5D). Distinct differences in phosphorylation levels were observed after 3 min of stimulation, indicating a potentiation of the insulin effect. Similar to previous findings in ALL, even after 4 h of stimulation, the signaling of these proteins remained higher compared to cells stimulated with insulin alone, as demonstrated by the statistical analyses (Figure 5E). Together, these data suggest that IGFBP7 may potentiate insulin effects on primary hepatocytes, which is in line with Morgantini's findings<sup>20</sup>.

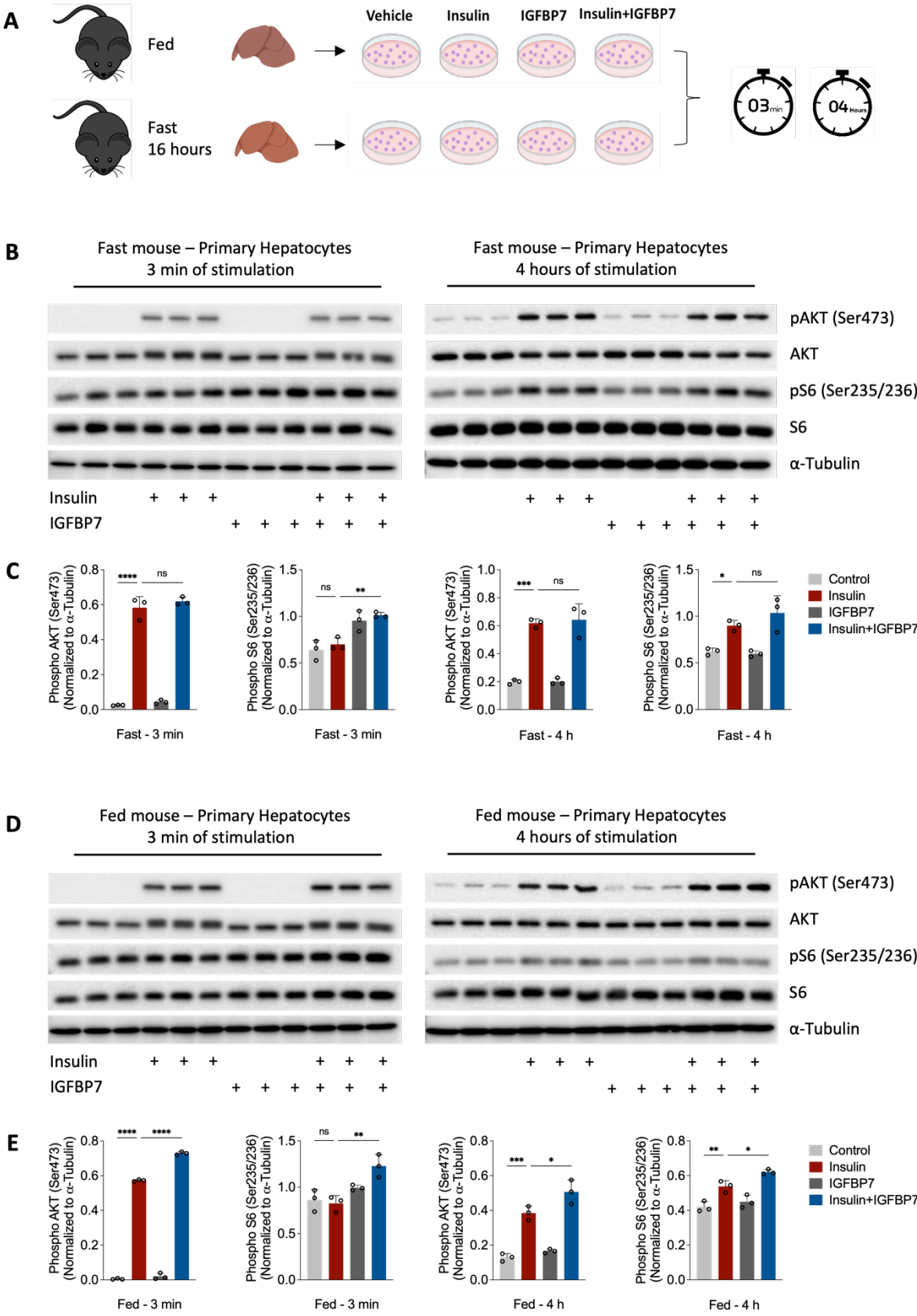


**Figure 5. IGFBP7 potentiates insulin signaling in primary hepatocytes isolated from fed state mouse. (A)** The schematic diagram illustrates the experimental treatments conducted.

Primary hepatocytes were isolated following the procedure described in Figure 4. Two mice, one in a fasted state (16 h) and another in a fed state, were utilized. Once isolated, primary hepatocytes were plated on collagen-coated plates and cultured overnight in serum-free William's medium. Subsequently, cells were stimulated with insulin (3nM), recombinant mouse IGFBP7 protein (100 ng/mL), or associations for 3 min and 4 h. Following stimulation, the plates were rapidly frozen in liquid nitrogen and stored at -80°C. Subsequently, the cells were lysed using NP-40 lysis buffer, the proteins concentration were normalized using BCA kit, and the lysates were subjected to western blot analysis. Western blot analysis for primary hepatocytes isolated from fasting (**B**) or fed mouse (**D**) after 3 min (left) and 4 h (right) of stimulation with insulin, IGFBP7, or their combinations. For each experimental condition, three wells containing primary hepatocytes were treated separately and loaded onto the gels. (**C-E**) Band densitometries were quantified using Image J software and statistical analysis were performed using GraphPad Prism 9.0. (\* $p \geq 0.05$ ; \*\* $p \geq 0.01$ ; \*\*\* $p \geq 0.001$ ; \*\*\*\* $p \geq 0.0001$ ).

We subsequently conducted a second independent experiment to validate our findings, however from now on, using only the 4 h time point (Figure 6A-C). It is important to note that primary hepatocytes do not express IGF1R, despite the liver being a major source of IGF1 secretion.<sup>30</sup> Instead, the INSR is the predominant receptor of the IGF system in hepatocytes and liver tissue. The expression of IGF1R in hepatocytes is limited to the fetal liver, where it plays a critical role in fetal development and growth. However, following birth, hepatocytes undergo a transition and cease to express IGF1R, favoring the presence of INSR.<sup>30-32</sup> Accordingly, in primary hepatocytes isolated from the liver of fed mouse, the endogenous levels of IGF1R are undetectable, in contrast to the abundant expression of INSR (Figure 6D).

To confirm the importance of INSR for the sustained signaling of the PI3K-Akt pathway mediated by insulin+IGFBP7 in primary hepatocytes, we chose to use the "liver-specific insulin receptor knockout (LIRKO) mice model.<sup>33</sup> To obtain mice with hepatocyte specific deletion of insulin receptor we used transgenic mice where the *INSR* gene was flanked by the lox P system. Deletion of the insulin receptor in this model were obtained by administering an adeno-associated virus (AAV) encoding the enzyme Cre recombinase (AAV Cre) under the control of albumin promoter.<sup>33</sup> The Cre recombinase enzyme recognizes and interacts with the lox P sites triggering a recombination event, resulting in the removal of the lox P-flanked region containing *INSR*. Consequently, the insulin receptor gene in hepatocytes undergoes permanent deletion or inactivation after 25 days of injection. As a negative control, we inject AAV

LacZ in another group of LIRKO mice. After 25 days of injection, primary hepatocytes from LIRKO mice (AAV Cre vs. AAV LacZ) were isolated and treated with insulin or insulin+IGFBP7 for 4 h (Figure 7A).

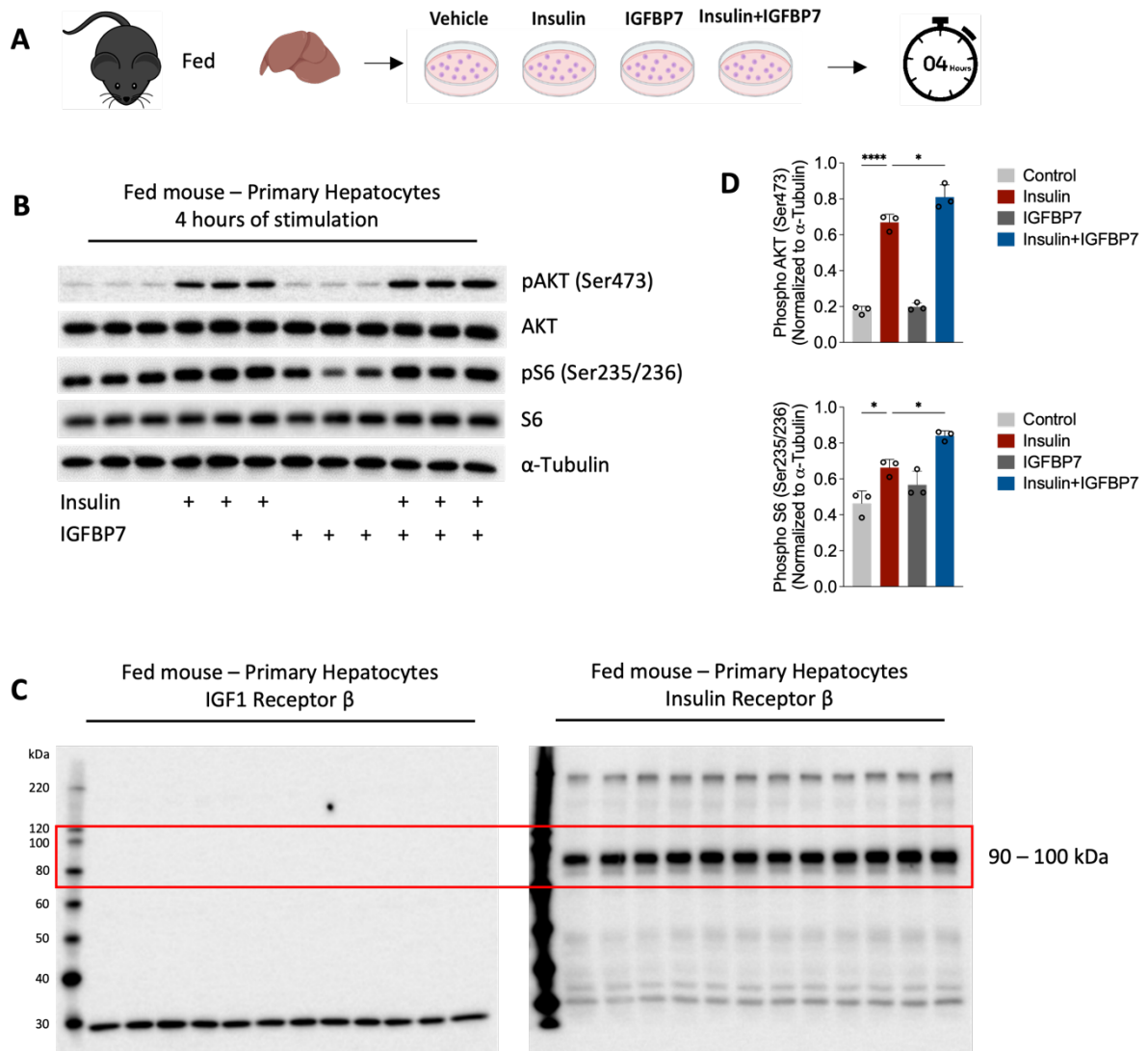


**Figure 6. Confirming the role of IGFBP7 in insulin signaling on primary hepatocytes via INSR.** (A) The schematic diagram illustrates the experimental treatments conducted. Primary hepatocytes were isolated following the procedure described in Figure 4 from fed state mouse. Once isolated, primary hepatocytes were plated on collagen-coated plates and cultured overnight in serum-free William's medium. Afterwards, cells were stimulated with insulin (3nM), recombinant mouse IGFBP7 protein (100 ng/mL), or associations for 4 h. Following stimulation, the plates were rapidly frozen in liquid nitrogen and stored at -80°C. Subsequently, the cells were lysed using NP-40 lysis buffer, the proteins concentration were normalized using BCA kit, and the lysates were subjected to western blot analysis. (B-C) Western blot analysis for primary hepatocytes isolated from fed mouse after 4 h of stimulation with insulin, IGFBP7,



or associations. For each experimental condition, three wells containing primary hepatocytes were treated separately and loaded onto the gels. (D) Band densitometries were quantified using Image J software and statistical analysis were performed using GraphPad Prism 9.0. (\* $p \geq 0.05$ ; \*\*\*\* $p \geq 0.0001$ ). Red square indicates correct molecular weight for INSR and IGF1R (between 90 and 100kDa).

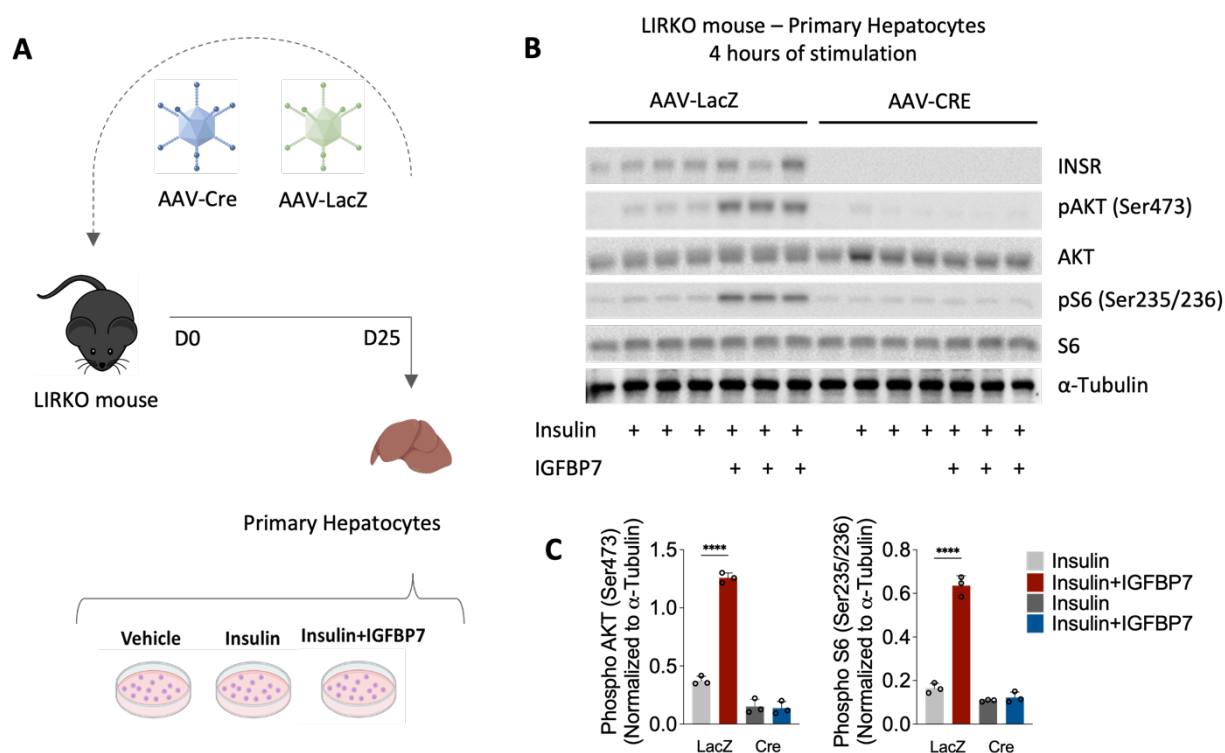


**Figure 7. Knockout of *INSR* on primary hepatocytes suppresses the improvement of insulin signaling mediated by IGFBP7.** (A) The schematic diagram illustrates the experimental treatments conducted. LIRKO mice (8 weeks old) were injected with AAV Cre (Addgene 107787) or AAV LacZ (Addgene CS1164L) ( $1.5 \times 10^{11}$  genome particles per mouse) at day zero (D0). After 25 days (D25) of injection, primary hepatocytes were isolated following the procedure described in Figure 4. Once isolated, primary hepatocytes were plated on collagen-coated plates and cultured overnight in serum-free William's medium. Afterwards, cells were stimulated with insulin (3nM) and/or recombinant mouse IGFBP7 protein (100 ng/mL) for 4 h. Following stimulation, the plates were rapidly frozen in liquid nitrogen and stored at  $-80^{\circ}\text{C}$ . Subsequently, the cells were lysed using NP-40 lysis buffer, the proteins concentration were normalized using BCA kit, and the lysates were subjected to western blot analysis. (B) Western blot analysis for primary hepatocytes isolated from LIRKO mice (AAV Cre vs. AAV LacZ) after 4 h of stimulation with insulin and/or IGFBP7. (C) Band densitometries were quantified using Image J software and statistical analysis were performed using GraphPad Prism 9.0. (\*\*\*\* $p \geq 0.0001$ ).

As depicted in Figure 7B, primary hepatocytes expressing AAV Cre lack INSR expression, confirming the successful deletion of *INSR* gene. In contrast, primary hepatocytes expressing AAV LacZ displayed abundant levels of INSR, aligning with our expectations. Notably, the combination of insulin+IGFBP7 demonstrated a significant ability to sustain phosphorylation of Akt (Ser473) and S6 (Ser235/236) compared to treatment with insulin alone (Figure 7C) or the negative control (no treatment). Importantly, the knockout of *INSR* completely abolished all the observed effects in hepatocytes overexpressing LacZ. Together, these findings provide strong evidence that IGFBP7 enhance insulin signaling in primary hepatocytes and that this effect is dependent on the presence of INSR.

### ***2.3 IGFBP7 improves insulin response in primary hepatocytes from obese mice.***

To explore the broader implications of the data presented above, we investigated whether the combination of insulin+IGFBP7 could enhance insulin response in cellular models of insulin resistance. Prior to addressing this question, we determined the physiologic levels of circulating IGFBP7 in obese mice compared to lean counterparts. To achieve this, we employed two different approaches. The first involved the use of ob/ob mice, while the second involved lean mice maintained on a high-fat diet (HFD) for 9 weeks. IGFBP7 levels of lean, ob/ob and mice on HFD were measured using the Mouse IGFBP7 ELISA Kit (Abcam - ab245712) following the manufacturer's recommendations (Figure 8A).

The results illustrated in Figure 8B demonstrate that the serum levels of IGFBP7 in lean mice are approximately 14 ng/mL. Intriguingly, the circulating levels of IGFBP7 in obese mice, including ob/ob mice and those maintained on a HFD were significantly reduced (Figure 8B).

Both diet induced and genetic induced obesity leads to heightened susceptibility to insulin resistance. Hepatocytes derived from these mice demonstrate impaired insulin signaling pathways and dysregulated glucose metabolism. Insulin resistance in obesity is caused at least in part by elevated levels of circulating free fatty acids and proinflammatory cytokines. Perturbations in critical molecular mediators, including insulin receptor substrate-1 (IRS-1), PI3K-Akt, and peroxisome proliferator-activated receptor gamma coactivator-1 alpha (PGC-1 $\alpha$ ), disrupt insulin signaling cascades,



resulting in decreased glucose uptake, impaired glycogen synthesis, and augmented hepatic gluconeogenesis.<sup>34</sup>

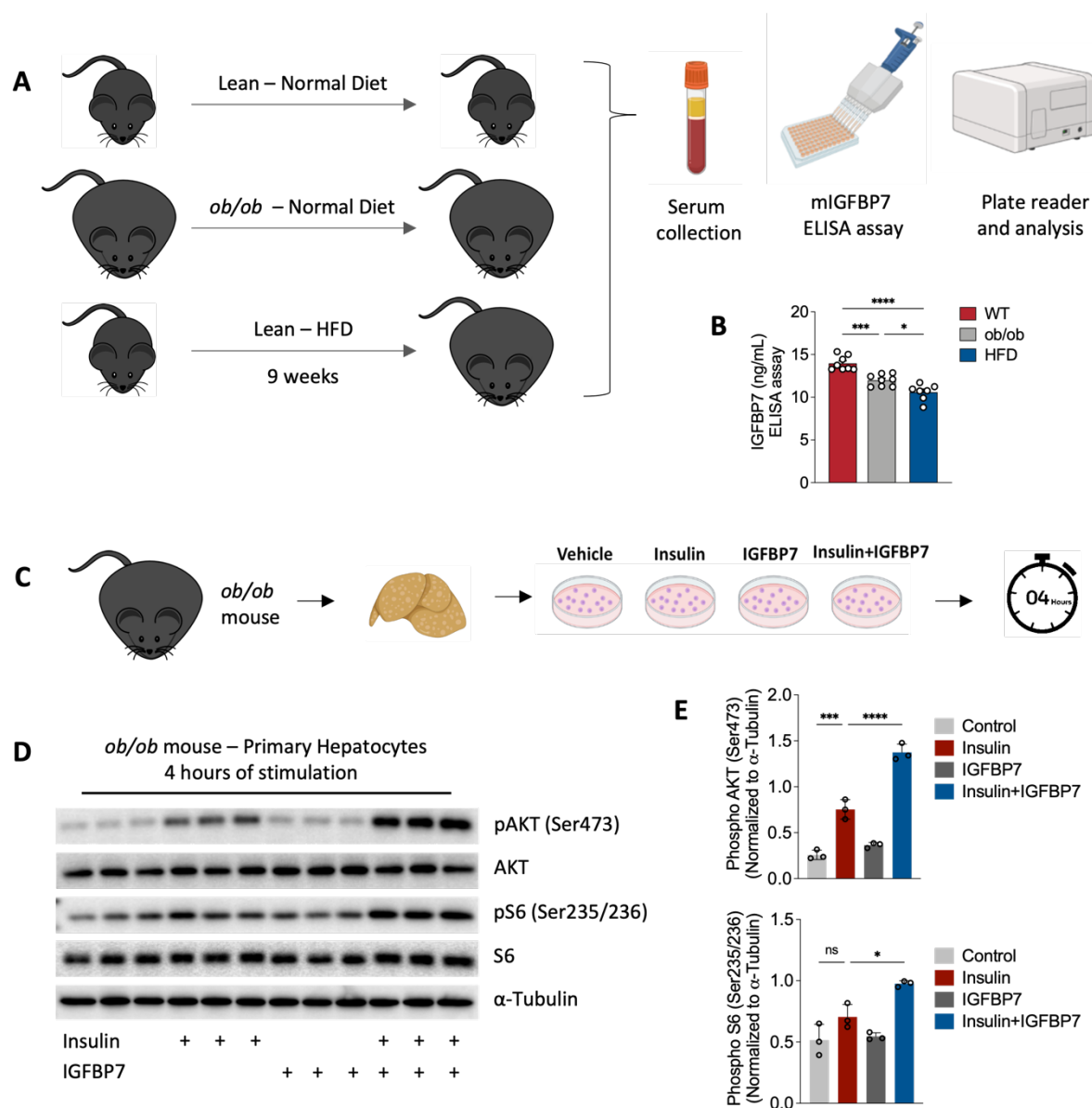


**Figure 8. IGFBP7 improves insulin response in primary hepatocytes from obese mice** (A) The schematic diagram illustrates the experimental procedure conducted to collect blood serum and measurements of the levels of IGFBP7 using mouse IGFBP7 ELISA kit (Abcam - ab245712), following the manufacturer's recommendations. (B) ELISA results for IGFBP7 levels in the serum of lean (n=8), *ob/ob* (n=8) and mice on a HFD for 9 weeks (n=7). (C) The schematic diagram illustrates the experimental treatments conducted to isolate primary hepatocytes from *ob/ob* mouse (8 weeks old). Once isolated, primary hepatocytes were plated on collagen-coated plates and cultured overnight in serum-free William's medium. Afterwards, cells were stimulated with insulin (3nM) and/or recombinant mouse IGFBP7 protein (100

ng/mL) for 4 h. Following stimulation, the plates were rapidly frozen in liquid nitrogen and stored at  $-80^{\circ}\text{C}$ . Subsequently, the cells were lysed using NP-40 lysis buffer, the proteins concentration were normalized using BCA kit, and the lysates were subjected to western blot analysis. **(D)** Western blot analysis for primary hepatocytes isolated from ob/ob mouse after 4 h of stimulation with insulin and/or IGFBP7. **(E)** Band densitometries were quantified using Image J software and statistical analysis were performed using GraphPad Prism 9.0. (\* $p \geq 0.05$ ; \*\*\* $p \geq 0.001$ ; \*\*\*\* $p \geq 0.0001$ ).

Based on the well-documented insulin resistance observed in hepatocytes from ob/ob mice, we sought to investigate the impact of the insulin+IGFBP7 association on these cells and how it would influence downstream signaling mediated by INSR. To achieve this, we isolated primary hepatocytes from an 8-week-old ob/ob mouse and subjected them to insulin and/or IGFBP7 treatment (Figure 8C). Surprisingly, we observed a strong increase in the phosphorylation of Akt (Ser473) and S6 (Ser 235/236) in cells treated with both insulin+IGFBP7 after 4 h of stimulation (Figure 8D-E). In summary, this finding highlights the activation of a sustained signaling axis involving INSR, PI3K-Akt and S6, suggesting that even in models of insulin resistance such as obesity, IGFBP7 is able to increase insulin sensitivity and improve insulin signaling.

### ***2.5 IGFBP7 enhance IGF1R>PI3K-Akt axis in 3T3L1 pre-adipocytes and sustain insulin signaling after TNF- $\alpha$ treatment***

As established in the literature and demonstrated by our data, it is known that mouse hepatocytes lack the expression of IGF1R,<sup>30-32</sup> thereby directing the effects of insulin+IGFBP7 towards INSR. Conversely, in ALL, which expresses both INSR and IGF1R, the signaling support of the PI3K-Akt pathway occurs through IGF1R. This is evident from the fact that the disruption of IGF1R hampers the signaling induced by insulin/IGF1+IGFBP7. Based on this information, we formulated a hypothesis that utilizing a biological model that plays a crucial role in metabolic homeostasis and possesses both receptors (INSR and IGF1R) would provide a more comprehensive understanding of the effects of insulin+IGFBP7 on the signaling of the PI3K-Akt pathway.

Additionally, we sought to investigate a model that could replicate the scenario of insulin resistance and metabolic syndrome. To achieve this, we opted to employ the 3T3L1 cell line differentiated into pre-adipocytes. To induce insulin resistance, we used

a widely accepted and validated protocol that involves the pre-treatment of these differentiated cells with tumor necrosis factor  $\alpha$  (TNF- $\alpha$ ).<sup>36</sup>

Initially, our objective was to investigate whether the combination of insulin+IGFBP7 could activate the PI3K-Akt pathway signaling in 3T3L1 pre-adipocytes. The process of cell differentiation is briefly depicted in Figure 9A. For a comprehensive understanding of the differentiation protocol and the reagents used, please refer to Guney et al.<sup>36</sup> Following the completion of cell differentiation, the cells were subjected to treatment with insulin, IGFBP7, or their combination, as also illustrated in Figure 9A. In general, our findings indicate that the combined treatment of insulin+IGFBP7 sustains the phosphorylation of Akt (Ser473) and S6 (Ser235/236) as anticipated in primary hepatocytes and ALL cells (Figure 9B and C). However, after 4 h of insulin+IGFBP7 treatment, only IGF1R exhibited phosphorylation, suggesting a preference for this receptor (similar to the observed pattern in ALL cells), since we did not detect sustained INSR phosphorylation (Figure 9B and D).

To investigate the potential role of IGFBP7 in mitigating insulin resistance in adipocytes, we examined the effects of combining insulin+IGFBP7 in insulin-resistant adipocytes. Insulin resistance was induced using the *in vitro* system described by Guney et al.<sup>36</sup> In brief, insulin resistance was induced in 3T3L1 pre-adipocytes by exposing them to a low dose (4 ng/mL) of TNF- $\alpha$ , a pro-inflammatory cytokine known to promote insulin resistance in both mice and humans in the context of obesity.<sup>37</sup> After 96 h of TNF- $\alpha$  exposition, the adipocytes were subsequently treated with insulin alone or in combination with IGFBP7 (Figure 10A). The results showed in Figure 10B and C points to an increased insulin resistance, as indicated by reduced phosphorylation of IGF1R after 4 h of insulin treatment. Interestingly, the combined treatment of insulin+IGFBP7 demonstrated a previously unidentified ability of IGFBP7 to enhance IGF1R phosphorylation compared to insulin treatment alone, suggesting a potential role for IGFBP7 in reversing insulin resistance in adipocytes.

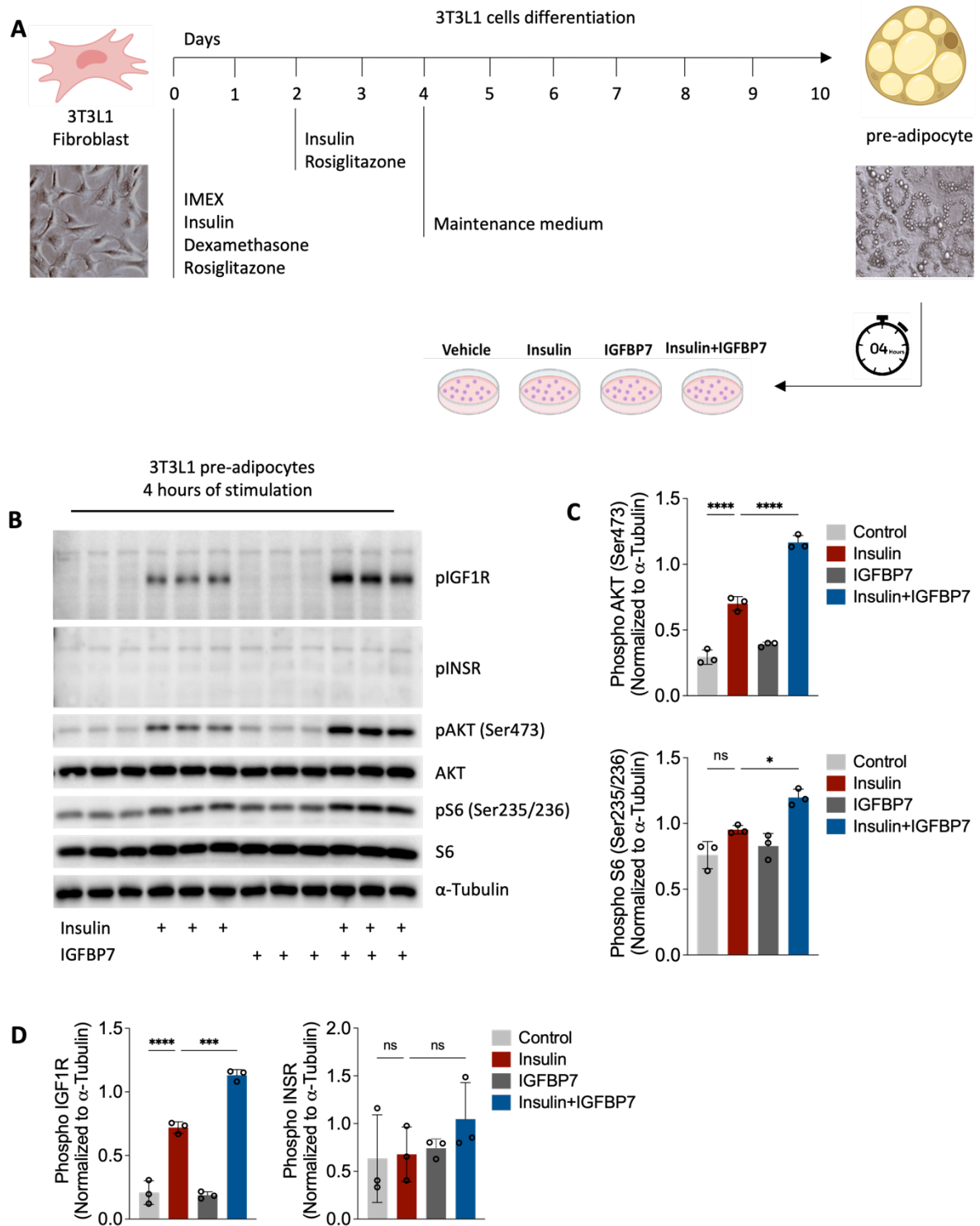


**Figure 9: IGFBP7 enhance IGF1R>PI3K-Akt axis in 3T3L1 pre-adipocytes.** (A) 3T3L1 cell line differentiation was induced by the addition of 500  $\mu$ M 3-isobutyl-1-methylxanthine (IMEX), insulin (5  $\mu$ g/mL), 10  $\mu$ M dexamethasone, and 10  $\mu$ M rosiglitazone. On day 2, the medium was switched to DMEM with 10% FBS and 1% penicillin/streptomycin, insulin (5  $\mu$ g/ml), and 10  $\mu$ M rosiglitazone. On day 4, the medium was switched to DMEM with 10% FBS and 1% penicillin/streptomycin (maintenance medium), which was replaced every other day until day

10, when the adipocytes were fully differentiated. Experiments were performed on day 10.<sup>36</sup> After, cells were stimulated with insulin (3nM) and/or recombinant mouse IGFBP7 protein (100 ng/mL) for 4 h. Following stimulation, the plates were rapidly frozen in liquid nitrogen and stored at -80°C. Subsequently, the cells were lysed using NP-40 lysis buffer, the proteins concentration were normalized using BCA kit, and the lysates were subjected to western blot analysis. **(B)** Western blot analysis for 3T3L1 pre-adipocytes after 4 h of stimulation with insulin and/or IGFBP7. **(C-D)** Band densitometries were quantified using Image J software and statistical analysis were performed using GraphPad Prism 9.0. (\* $p \geq 0.05$ ; \*\*\* $p \geq 0.001$ ; \*\*\*\* $p \geq 0.0001$ ).

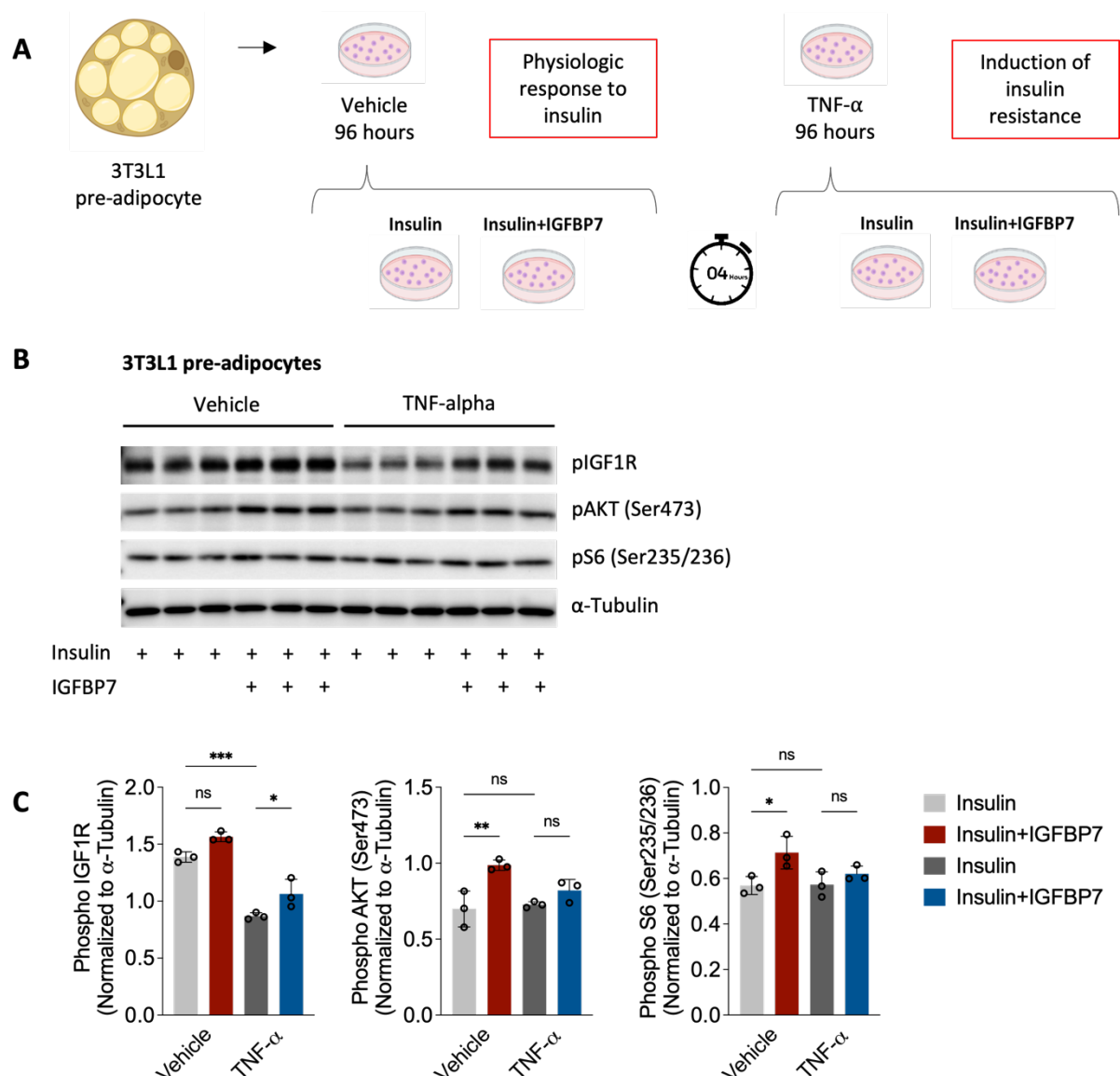


**Figure 10. IGFBP7 sustain insulin signaling in 3T3L1 pre-adipocytes after TNF-α treatment.** **(A)** 3T3L1 cell line differentiation was induced following Figure 9A. Experiments were performed on day 10 after differentiation. Insulin resistance was induced in 3T3L1 pre-adipocytes by exposing them to a low dose (4 ng/mL) of TNF-α for 96 h. Afterwards, pre-

adipocytes were subsequently treated with insulin alone or in combination with IGFBP7 for 4 h. Following stimulation, the plates were rapidly frozen in liquid nitrogen and stored at -80°C. Subsequently, the cells were lysed using NP-40 lysis buffer, the proteins concentration were normalized using BCA kit, and the lysates were subjected to western blot analysis. **(B)** Western blot analysis for 3T3L1 pre-adipocytes after 4 h of stimulation with insulin and/or IGFBP7. **(C)** Band densitometries were quantified using Image J software and statistical analysis were performed using GraphPad Prism 9.0. (\* $p \geq 0.05$ ; \*\* $p \geq 0.01$ ).

In conclusion, the preliminary findings presented in this report unveil the significant involvement of IGFBP7 in insulin signaling within metabolic syndrome models, mirroring the observed effects in ALL.<sup>22,23</sup> Nonetheless, the ongoing challenge we face is comprehending how IGFBP7 distinguishes its affinity for the diverse receptors comprising the IGFs system. Our primary discovery resides in the impact of insulin+IGFBP7 on insulin signaling in obesity models, such as ob/ob and TNF- $\alpha$ -treated 3T3L1 pre-adipocytes. Moving forward, the next phase of this project will delve into the assessment of these effects *in vivo*, employing obese mice exhibiting insulin resistance. This endeavor aims to deepen our understanding of the intricate interplay between IGFBP7 and insulin signaling within the complex milieu of obesity and type 2 diabetes.

### 3.0 Additional activities

Throughout the duration of this project, I had the privilege of contributing to an ongoing research endeavor taking place in Professor Ana Paula Arruda's laboratory. This project has recently been submitted for publication to Nature Communication and is presently undergoing the review process. Title, authors and abstract of this study are described below:

#### **Spatial mapping of zonated subcellular liver architecture in fasting and obesity**

Parlakgul G<sup>1,2</sup>, Pang S<sup>3,4</sup>, Min N<sup>1</sup>, Cagampan E<sup>1</sup>, Artico LL<sup>2</sup>, Villa R<sup>2</sup>, Goncalves RLS<sup>1</sup>, Lee Y<sup>1</sup>, Xu CS<sup>3,5</sup>, Hotamisligil GS<sup>1,6\*</sup> and Arruda AP<sup>2,7\*</sup>

<sup>1</sup>Department of Molecular Metabolism and Sabri Ülker Center, Harvard T.H. Chan School of Public Health, Boston, MA 02115.

<sup>2</sup>Department of Nutritional Sciences and Toxicology, University of California, Berkeley, Berkeley, CA 94720.

<sup>3</sup>HHMI Janelia Research Campus, Ashburn, VA 20147.

<sup>4</sup>Current address: Yale School of Medicine, New Haven, CT 06510.

<sup>5</sup>Current address: Department of Cellular & Molecular Physiology, Yale School of Medicine, New Haven, CT 06510.

<sup>6</sup>Broad Institute of MIT and Harvard, Cambridge, MA 02142.

<sup>7</sup>Chan Zuckerberg Biohub, San Francisco, CA 94158.

\*Co-corresponding authors: [gnotamis@hsph.harvard.edu](mailto:gnotamis@hsph.harvard.edu) & [aarruda@berkeley.edu](mailto:aarruda@berkeley.edu)

## Abstract

The hepatocytes within the liver tissue present an immense capacity to adapt to fluctuations in nutrient availability. Using FIB-SEM and automated segmentation, we extensively explored how the hepatocyte subcellular architecture is regulated during nutritional fluctuations and as a function of liver zonation. We identified a global remodeling of spatial organization of ER sheets in hepatocytes during fasting, characterized by the induction of single rough ER sheet enveloping the mitochondria, which becomes fused and elongated. These alterations are present in periportal and mid-lobular but not in pericentral hepatocytes. In obesity, ER-mitochondria interactions are distinct and fasting fails to induce ER sheets to envelop the mitochondrion due to defective expression of RRB1 protein. Finally, gain- and loss-of-function in vivo models demonstrated RRB1 is necessary and sufficient to enable fasting-induced ER sheet-mitochondria interactions and to regulate fatty acid oxidation. These findings illustrate the importance of a regulated molecular architecture for hepatocyte metabolic flexibility.

## 4.0 References

- 1) Gibson LF. Survival of B lineage leukemic cells: signals from the bone marrow microenvironment. *Leuk Lymphoma*. 2002 Jan;43(1):19-27. doi: 10.1080/10428190210188.

- 2) Hakuno F, Takahashi SI. IGF1 receptor signaling pathways. *J Mol Endocrinol*. 2018 Jul;61(1):T69-T86. doi: 10.1530/JME-17-0311.
- 3) AsghariHanjani N, Vafa M. The role of IGF-1 in obesity, cardiovascular disease, and cancer. *Med J Islam Repub Iran*. 2019 Jun 17;33:56. doi: 10.34171/mjiri.33.56.
- 4) Werner H, Laron Z. Role of the GH-IGF1 system in progression of cancer. *Mol Cell Endocrinol*. 2020 Dec 1;518:111003. doi: 10.1016/j.mce.2020.111003.
- 5) Khandwala HM, McCutcheon IE, Flyvbjerg A, Friend KE. The effects of insulin-like growth factors on tumorigenesis and neoplastic growth. *Endocr Rev*. 2000 Jun;21(3):215-44. doi: 10.1210/edrv.21.3.0399.
- 6) Jung HJ, Suh Y. Regulation of IGF -1 signaling by microRNAs. *Front Genet*. 2015 Jan 13;5:472. doi: 10.3389/fgene.2014.00472.
- 7) Jones JI, Clemmons DR. Insulin-like growth factors and their binding proteins: biological actions. *Endocr Rev*. 1995 Feb;16(1):3-34. doi: 10.1210/edrv-16-1-3.
- 8) Hwa V, Oh Y, Rosenfeld RG. The insulin-like growth factor-binding protein (IGFBP) superfamily. *Endocr Rev*. 1999 Dec;20(6):761-87. doi: 10.1210/edrv.20.6.0382.
- 9) Bach LA. IGF-binding proteins. *J Mol Endocrinol*. 2018 Jul;61(1):T11-T28. doi: 10.1530/JME-17-0254.
- 10) Kim HS, Nagalla SR, Oh Y, Wilson E, Roberts CT Jr, Rosenfeld RG. Identification of a family of low-affinity insulin-like growth factor binding proteins (IGFBPs): characterization of connective tissue growth factor as a member of the IGFBP superfamily. *Proc Natl Acad Sci U S A*. 1997 Nov 25;94(24):12981-6. doi: 10.1073/pnas.94.24.12981.
- 11) Oh Y, Nagalla SR, Yamanaka Y, Kim HS, Wilson E, Rosenfeld RG. Synthesis and characterization of insulin-like growth factor-binding protein (IGFBP)-7. Recombinant human mac25 protein specifically binds IGF-I and -II. *J Biol Chem*. 1996 Nov 29;271(48):30322-5. doi: 10.1074/jbc.271.48.30322.
- 12) Sato J, Hasegawa S, Akaogi K, Yasumitsu H, Yamada S, Sugahara K, Miyazaki K. Identification of cell-binding site of angiomodulin (AGM/TAF/Mac25) that interacts with heparan sulfates on cell surface. *J Cell Biochem*. 1999 Nov 1;75(2):187-95.
- 13) Yamanaka Y, Wilson EM, Rosenfeld RG, Oh Y. Inhibition of insulin receptor activation by insulin-like growth factor binding proteins. *J Biol Chem*. 1997 Dec 5;272(49):30729-34. doi: 10.1074/jbc.272.49.30729.
- 14) Zhu S, Xu F, Zhang J, Ruan W, Lai M. Insulin-like growth factor binding protein-related protein 1 and cancer. *Clin Chim Acta*. 2014 Apr 20;431:23-32. doi: 10.1016/j.cca.2014.01.037.
- 15) Akiel M, Guo C, Li X, Rajasekaran D, Mendoza RG, Robertson CL, Jariwala N, Yuan F, Subler MA, Windle J, Garcia DK, Lai Z, Chen HH, Chen Y, Giashuddin S, Fisher PB, Wang XY, Sarkar D. IGFBP7 Deletion Promotes Hepatocellular Carcinoma. *Cancer Res*. 2017 Aug 1;77(15):4014-4025. doi: 10.1158/0008-5472.CAN-16-2885.



- 16)Evdokimova V, Tognon CE, Benatar T, Yang W, Krutikov K, Pollak M, Sorensen PH, Seth A. IGFBP7 binds to the IGF-1 receptor and blocks its activation by insulin-like growth factors. *Sci Signal*. 2012 Dec 18;5(255):ra92. doi: 10.1126/scisignal.2003184.
- 17)Bartram I, Erben U, Ortiz-Tanchez J, Blunert K, Schlee C, Neumann M, Heesch S, Baldus CD. Inhibition of IGF1-R overcomes IGFBP7-induced chemotherapy resistance in T-ALL. *BMC Cancer*. 2015 Oct 8;15:663. doi: 10.1186/s12885-015-1677-z.
- 18)Akaogi K, Sato J, Okabe Y, Sakamoto Y, Yasumitsu H, Miyazaki K. Synergistic growth stimulation of mouse fibroblasts by tumor-derived adhesion factor with insulin-like growth factors and insulin. *Cell Growth Differ*. 1996 Dec;7(12):1671-7.
- 19)Laranjeira AB, de Vasconcellos JF, Sodek L, Spago MC, Fornazim MC, Tone LG, Brandalise SR, Nowill AE, Yunes JA. IGFBP7 participates in the reciprocal interaction between acute lymphoblastic leukemia and BM stromal cells and in leukemia resistance to asparaginase. *Leukemia*. 2012 May;26(5):1001-11. doi: 10.1038/leu.2011.289.
- 20)Morgantini C, Jager J, Li X, Levi L, Azzimato V, Sulen A, Barreby E, Xu C, Tencerova M, Näslund E, Kumar C, Verdeguer F, Straniero S, Hultenby K, Björkström NK, Ellis E, Rydén M, Kutter C, Hurrell T, Lauschke VM, Boucher J, Tomčala A, Krejčová G, Bajgar A, Aouadi M. Liver macrophages regulate systemic metabolism through non-inflammatory factors. *Nat Metab*. 2019 Apr;1(4):445-459. doi: 10.1038/s42255-019-0044-9.
- 21)López-Bermejo A, Khosravi J, Corless CL, Krishna RG, Diamandi A, Bodani U, Kofoed EM, Graham DL, Hwa V, Rosenfeld RG. Generation of anti-insulin-like growth factor-binding protein-related protein 1 (IGFBP-rP1/MAC25) monoclonal antibodies and immunoassay: quantification of IGFBP-rP1 in human serum and distribution in human fluids and tissues. *J Clin Endocrinol Metab*. 2003 Jul;88(7):3401-8. doi: 10.1210/jc.2002-021315.
- 22)Artico LL, Laranjeira ABA, Campos LW, Corrêa JR, Zenatti PP, Carnevalheira JBC, Brambilla SR, Nowill AE, Brandalise SR, Yunes JA. Physiologic IGFBP7 levels prolong IGF1R activation in acute lymphoblastic leukemia. *Blood Adv*. 2021 Sep 28;5(18):3633-3646. doi: 10.1182/bloodadvances.2020003627.
- 23)Artico LL, Ruas JS, Teixeira Júnior JR, Migita NA, Seguchi G, Shi X, Brandalise SR, Castilho RF, Yunes JA. IGFBP7 Fuels the Glycolytic Metabolism in B-Cell Precursor Acute Lymphoblastic Leukemia by Sustaining Activation of the IGF1R-Akt-GLUT1 Axis. *Int J Mol Sci*. 2023 Jun 2;24(11):9679. doi: 10.3390/ijms24119679.
- 24)Hotamisligil GS. Inflammation and metabolic disorders. *Nature*. 2006 Dec 14;444(7121):860-7. doi: 10.1038/nature05485.
- 25)Poloz Y, Stambolic V. Obesity and cancer, a case for insulin signaling. *Cell Death Dis*. 2015 Dec 31;6(12):e2037. doi: 10.1038/cddis.2015.381.
- 26)Tentler JJ, Tan AC, Weekes CD, Jimeno A, Leong S, Pitts TM, Arcaroli JJ, Messersmith WA, Eckhardt SG. Patient-derived tumour xenografts as models


- for oncology drug development. *Nat Rev Clin Oncol*. 2012 Apr 17;9(6):338-50. doi: 10.1038/nrclinonc.2012.61.
- 27) Kersten K, de Visser KE, van Miltenburg MH, Jonkers J. Genetically engineered mouse models in oncology research and cancer medicine. *EMBO Mol Med*. 2017 Feb;9(2):137-153. doi: 10.15252/emmm.201606857.
  - 28) Lorian V. Differences between in vitro and in vivo studies. *Antimicrob Agents Chemother*. 1988 Oct;32(10):1600-1. doi: 10.1128/AAC.32.10.1600.
  - 29) Guo L, Dial S, Shi L, Branham W, Liu J, Fang JL, Green B, Deng H, Kaput J, Ning B. Similarities and differences in the expression of drug-metabolizing enzymes between human hepatic cell lines and primary human hepatocytes. *Drug Metab Dispos*. 2011 Mar;39(3):528-38. doi: 10.1124/dmd.110.035873.
  - 30) Adamek A, Kasprzak A. Insulin-Like Growth Factor (IGF) System in Liver Diseases. *Int J Mol Sci*. 2018 Apr 27;19(5):1308. doi: 10.3390/ijms19051308.
  - 31) Kineman RD, Del Rio-Moreno M, Sarmiento-Cabral A. 40 YEARS of IGF1: Understanding the tissue-specific roles of IGF1/IGF1R in regulating metabolism using the Cre/loxP system. *J Mol Endocrinol*. 2018 Jul;61(1):T187-T198. doi: 10.1530/JME-18-0076.
  - 32) Waraky A, Aleem E, Larsson O. Downregulation of IGF-1 receptor occurs after hepatic lineage commitment during hepatocyte differentiation from human embryonic stem cells. *Biochem Biophys Res Commun*. 2016 Sep 30;478(4):1575-81. doi: 10.1016/j.bbrc.2016.08.157. .
  - 33) Michael MD, Kulkarni RN, Postic C, Previs SF, Shulman GI, Magnuson MA, Kahn CR. Loss of insulin signaling in hepatocytes leads to severe insulin resistance and progressive hepatic dysfunction. *Mol Cell*. 2000 Jul;6(1):87-97.
  - 34) Collins S, Martin TL, Surwit RS, Robidoux J. Genetic vulnerability to diet-induced obesity in the C57BL/6J mouse: physiological and molecular characteristics. *Physiol Behav*. 2004 Apr;81(2):243-8. doi: 10.1016/j.physbeh.2004.02.006.
  - 35) Zhang Y, Proenca R, Maffei M, Barone M, Leopold L, Friedman JM. Positional cloning of the mouse obese gene and its human homologue. *Nature*. 1994 Dec 1;372(6505):425-32. doi: 10.1038/372425a0.
  - 36) Guney E, Arruda AP, Parlakgul G, Cagampan E, Min N, Lee GY, Greene L, Tsaousidou E, Inouye K, Han MS, Davis RJ, Hotamisligil GS. Aberrant Ca<sup>2+</sup> signaling by IP3Rs in adipocytes links inflammation to metabolic dysregulation in obesity. *Sci Signal*. 2021 Dec 14;14(713):eabf2059. doi: 10.1126/scisignal.abf2059.
  - 37) Hotamisligil GS. Inflammation, metaflammation and immunometabolic disorders. *Nature*. 2017 Feb 8;542(7640):177-185. doi: 10.1038/nature21363.

## 12.2 List of publications (during PhD fellowship)

- 1) Parlakgul G, Pang S, Min N, Cagampan E, **Artico LL**, Villa R, Goncalves RLS, Lee Y, Xu CS, Hotamisligil GS, Arruda AP. Spatial mapping of zonated subcellular liver architecture in fasting and obesity. *In press*.
- 2) **Artico LL**, Ruas JS, Teixeira Júnior JR, Migita NA, Seguchi G, Shi X, Brandalise SR, Castilho RF, Yunes JA. IGFBP7 Fuels the Glycolytic Metabolism in B-Cell Precursor Acute Lymphoblastic Leukemia by Sustaining Activation of the IGF1R-Akt-GLUT1 Axis. *Int J Mol Sci*. 2023 Jun 2;24(11):9679. doi: 10.3390/ijms24119679.
- 3) Canevarolo RR, Melo CPS, Cury NM, **Artico LL**, Corrêa JR, Tonhasca Lau Y, Mariano SS, Sudalagunta PR, Brandalise SR, Zeri ACM, Yunes JA. Glutathione levels are associated with methotrexate resistance in acute lymphoblastic leukemia cell lines. *Front Oncol*. 2022 Dec 1;12:1032336. doi: 10.3389/fonc.2022.1032336.
- 4) Cemin F, **Artico LL**, Piroli V, Yunes JA, Figueroa CA, Alvarez F. Superior in vitro biocompatibility in NbTaTiVZr(O) high-entropy metallic glass coatings for biomedical applications. *Applied Surface Science*, v. 1, p. 153615, 2022.
- 5) **Artico LL**, Laranjeira ABA, Campos LW, Corrêa JR, Zenatti PP, Carvalheira JBC, Brambilla SR, Nowill AE, Brandalise SR, Yunes JA. Physiologic IGF1R levels prolong IGF1R activation in acute lymphoblastic leukemia. *Blood Adv*. 2021 Sep 28;5(18):3633-3646. doi: 10.1182/bloodadvances.2020003627.
- 6) Meneghetti D, Cezarotto VS, do Nascimento NP, Migita NA, Corrêa JR, Riccio MF, Zambaldi LG, Yunes JA, **Artico LL**. Hydroalcoholic leaves extract of *Vaccinium ashei* Reade promotes cell cycle arrest and apoptosis on T-cell acute lymphoblastic leukemia. *Nat Prod Res*. 2022 Sep;36(17):4520-4524. doi: 10.1080/14786419.2021.1990281.

- 7) **Artico LL**, Kömmling G, Clarindo WR, Simões-Menezes AP. Cytotoxic, Genotoxic, Mutagenic, and Phytotoxic Effects of the Extracts from *Eragrostis plana* Nees, 1841 (Poaceae), Grown in a Coal-Contaminated Region. *Water Air Soil Pollut* 231, 81 (2020). <https://doi.org/10.1007/s11270-020-4457-6>
- 8) Artico M, Firpo BA, **Artico LL**, Tubino RMC. Integrated use of sewage sludge and basalt mine waste as soil substitute for environmental restoration. *REM - International Engineering Journal*, v. 73, p. 225-232, 2020.
- 9) Cury NM, Capitão RM, Almeida RDCB, **Artico LL**, Corrêa JR, Simão Dos Santos EF, Yunes JA, Correia CRD. Synthesis and evaluation of 2-carboxy indole derivatives as potent and selective anti-leukemic agents. *Eur J Med Chem*. 2019 Nov 1;181:111570. doi: 10.1016/j.ejmech.2019.111570.

## 12.3 Ethics committee approval 1



UNICAMP

**FACULDADE DE CIÊNCIAS MÉDICAS**  
**COMITÊ DE ÉTICA EM PESQUISA**

[www.fcm.unicamp.br/pesquisa/etica/index.html](http://www.fcm.unicamp.br/pesquisa/etica/index.html)

CEP, 16/12/08.  
(Grupo III)

**PARECER CEP:** Nº 1133/2008 (Este nº deve ser citado nas correspondências referente a este projeto)  
**CAAE:** 0018.0.144.146-08

**I - IDENTIFICAÇÃO:**

**PROJETO:** "IGFBP7 E A QUIMIORESISTÊNCIA DA LEUCEMIA LINFÓIDE AGUDA PEDIÁTRICA".  
**PESQUISADOR RESPONSÁVEL:** Ângelo Brunelli Albertoni Laranjeira  
**INSTITUIÇÃO:** Centro Infantil de Investigações Hematológicas Dr. Domingos A. Boldrini.  
**APRESENTAÇÃO AO CEP:** 12/12/2008  
**APRESENTAR RELATÓRIO EM:** 16/12/09 (O formulário encontra-se no site acima)

**II - OBJETIVOS**

Averiguar se o IGFBP7 exerce um efeito direto sobre as células de LLA, bem como caracterizar outros de seus ligantes além da insulina. Estudar o efeito do IGFBP7 sobre a expressão de genes implicados na biossíntese de asparagina e transportadores de aminoácidos, bem como moléculas implicadas na resistência a apoptose. Pretende-se também a quantificação da expressão de IGFBP7 e ligantes em amostras diagnósticas de LLA e estabelecer uma relação com fatores clínico-biológicos dos pacientes.

**III - SUMÁRIO**

Serão avaliadas amostras de medula óssea de 200 pacientes com LLA, cujo material encontra-se no Banco de células do I. Boldrini. Para os testes com células estromais será utilizado uma linhagem de células imortalizadas, obtidas em centro de pesquisa. Será realizada análise da viabilidade celular (ensaio MTT), PCR em tempo real, análise de aminoácidos por RMN, citometria de fluxo e Western Blot.

**IV - COMENTÁRIOS DOS RELATORES**

O estudo está bem estruturado. Todos os documentos estão corretamente anexados. O Termo de Consentimento Livre e Esclarecido pode ser dispensado por utilizar material biológico de banco.

**V - PARECER DO CEP**

O Comitê de Ética em Pesquisa da Faculdade de Ciências Médicas da UNICAMP, após acatar os pareceres dos membros-relatores previamente designados para o presente caso e atendendo todos os dispositivos das Resoluções 196/96 e complementares, resolve aprovar sem restrições o Protocolo de Pesquisa, bem como ter aprovado a dispensa do Termo do

---

Comitê de Ética em Pesquisa - UNICAMP  
Rua: Tróvão Vieira da Cunha, 126  
Caixa Postal 6111  
13084-971 Campinas - SP

FONE (019) 3521-8936  
FAX (019) 3521-7187  
cep@fcm.unicamp.br

- 1 -



Consentimento Livre e Esclarecido, assim como todos os anexos incluídos na Pesquisa supracitada.

O conteúdo e as conclusões aqui apresentados são de responsabilidade exclusiva do CEP/FCM/UNICAMP e não representam a opinião da Universidade Estadual de Campinas nem a comprometem.

#### VI - INFORMAÇÕES COMPLEMENTARES

O sujeito da pesquisa tem a liberdade de recusar-se a participar ou de retirar seu consentimento em qualquer fase da pesquisa, sem penalização alguma e sem prejuízo ao seu cuidado (Res. CNS 196/96 – Item IV.1.f) e deve receber uma cópia do Termo de Consentimento Livre e Esclarecido, na íntegra, por ele assinado (Item IV.2.d).

Pesquisador deve desenvolver a pesquisa conforme delineada no protocolo aprovado e descontinuar o estudo somente após análise das razões da descontinuidade pelo CEP que o aprovou (Res. CNS Item III.1.z), exceto quando perceber risco ou dano não previsto ao sujeito participante ou quando constatar a superioridade do regime oferecido a um dos grupos de pesquisa (Item V.3.).

O CEP deve ser informado de todos os efeitos adversos ou fatos relevantes que alterem o curso normal do estudo (Res. CNS Item V.4.). É papel do pesquisador assegurar medidas imediatas adequadas frente a evento adverso grave ocorrido (mesmo que tenha sido em outro centro) e enviar notificação ao CEP e à Agência Nacional de Vigilância Sanitária – ANVISA – junto com seu posicionamento.

Eventuais modificações ou emendas ao protocolo devem ser apresentadas ao CEP de forma clara e sucinta, identificando a parte do protocolo a ser modificada e suas justificativas. Em caso de projeto do Grupo I ou II apresentados anteriormente à ANVISA, o pesquisador ou patrocinador deve enviá-las também à mesma junto com o parecer aprovatório do CEP, para serem juntadas ao protocolo inicial (Res. 251/97, Item III.2.e)

Relatórios parciais e final devem ser apresentados ao CEP, de acordo com os prazos estabelecidos na Resolução CNS-MS 196/96.

#### VII - DATA DA REUNIÃO

Homologado na XII Reunião Ordinária do CEP/FCM, em 16 de dezembro de 2008.

*Prof. Dra. Carmen Sílvia Bertuzzo*  
PRESIDENTE DO COMITÊ DE ÉTICA EM PESQUISA  
FCM / UNICAMP

## 12.4 Ethics committee approval 2



FACULDADE DE CIÊNCIAS MÉDICAS  
COMITÊ DE ÉTICA EM PESQUISA

[www.fcm.unicamp.br/pesquisa/etica/index.html](http://www.fcm.unicamp.br/pesquisa/etica/index.html)

CEP, 12/02/09.  
(Grupo II)

**PARECER CEP:** Nº 1105/2008 (Este nº deve ser citado nas correspondências referente a este projeto)  
**CAAE:** 0014.0.144.146-08

### I - IDENTIFICAÇÃO:

**PROJETO:** "MICROAMBIENTE DA MEDULA ÓSSEA E PI3K NA RESISTÊNCIA A DROGAS DA LEUCEMIA LINFÓIDE AGUDA PEDIÁTRICA".

**PESQUISADOR RESPONSÁVEL:** José Andrés Yunes.

**INSTITUIÇÃO:** Centro Infantil de Investigações Hematológicas Dr. Domingos A. Boldrini

**APRESENTAÇÃO AO CEP:** 11/12/2008

**APRESENTAR RELATÓRIO EM:** 12/02/10 (O formulário encontra-se no site acima)

### II - OBJETIVOS

1- Quantificar aminoácidos no meio de cultura de células de estroma da medula óssea tratadas com IGFBP7 + ligantes (insulina, IGF-1, IGF-2); 2- Avaliar efeito de IGFBP7+ligantes (insulina, IGF-1, IGF-2) na sobrevivência de células primárias de LEUCEMIA LINFÓIDE AGUDA (LLA) frente à aspariginase, quando em cultura de curta duração, sem estroma; 3- Avaliar efeito de IGFBP7+ligantes (insulina, IGF-1, IGF-2) na expressão de mRNA de ASNS, glutamina sintetase (GS) e de transportadores de aminoácidos nas células de LLA e do estroma; 4- Tratar células de LLA com diferentes doses de EBIO e verificar viabilidade celular frente a diferentes doses de daunorubicina, quantificando a incorporação intracelular da droga através de citometria de fluxo; 5- Desvendar o mecanismo de fluxo intracelular ligado ao KCNN4, usando substratos e inibidores específicos para os diferentes transportadores; 6- Analisar distribuição intracelular da daunorubicina em células de LLA tratadas ou não com EBIO, por microscopia de fluorescência e co-marcação de lisossomos com LysoTracker blue, do Golgi com NBD-C6-Ceramide e do retículo endoplasmático com DiOC6; 7- avaliar uso do clotrimazol (ou TRAM-34) na sensibilização das células de LLA aos agentes quimioterápicos, in vitro e in vivo (em camundongos); 8- Quantificar níveis de mRNA de GPR56 em amostras de 150 pacientes com LLA e buscar associações com características biológico-clínicas dos pacientes; 9- Confirmar a expressão da proteína GPR56 na superfície das células de LLA, por imunocitoquímica; 10- Sequenciar os exons 3,5,8 e 9 de GPR56 em 30 amostras de DNA ou cDNA de blastos de pacientes e de linhagens de LLA. Serão analisados 3 grupos de pacientes: (i) com doença extramedular ao diagnóstico, (ii) com baixa expressão de GPR56 (<0,05 moléculas de GPR56/ABL), (iii) grupo de pacientes com expressão de GPR56 na mediana; 11- silenciar o GPR56 por iRNA em uma linhagem de LLA e analisar resistência das células a aspariginase quando em cultura com ou sem estroma de medula óssea.

### III - SUMÁRIO

O autor relata que 20% a 30% das crianças com leucemia linfóide aguda (LLA) sofrem recaídas da doença e apresentam maior resistência aos quimioterápicos. Métodos modernos de

Comitê de Ética em Pesquisa - UNICAMP  
Rua: Tessália Vieira de Camargo, 126  
Cajuru Postal 6111  
13083-887 Campinas - SP

PHONE (019) 3521-8936  
FAX (019) 3521-7187  
cep@fcm.unicamp.br



análise de expressão gênica possibilitam a identificação de genes relacionados ao processo de resistência à drogas. Segundo referências apresentadas pelo autor, as células da recaída são altamente proliferativas e mesmo assim mais resistente à quimioterapia, esse processo pode estar relacionado com a maior expressão de genes de reparo do DNA e de anti-apoptose, que compensariam os efeitos da quimioterapia. A interação de blastos leucêmicos com as células estromais da medula óssea (obs: o estroma é o tecido conjuntivo de sustentação de um órgão) aumenta a resistência da LLA à leucemia.

Dois sub-projetos fazem parte do projeto maior. No primeiro a proposta é estudar a função dos genes IGFBP7, KCNN4 e GPR56 na resistência à drogas para o tratamento de LLA, no contexto da interação leucemia-estroma. Para realização desses sub-projetos serão incluídas amostras de sangue/medula óssea de crianças portadoras de leucemia linfóide aguda, sem tratamento prévio, atendidas integralmente no Centro Infantil Boldrini, a pesquisa será feita com o restante do material colhido para diagnóstico e não acarretará em nenhum procedimento ao paciente. É prevista a utilização de 150 amostras retrospectivas. São descritos os procedimentos para obtenção de amostras com, pelo menos, 85% de blastos leucêmicos, basicamente centrifugação diferencial e filtração. As amostras são preservadas em nitrogênio líquido. O controle será feito com amostras provenientes de doadores normais e de pacientes com resultado negativo após exame. O DNA de indivíduos normais será obtido de cartões de triagem neonatal (CIPOI-UNICAMP). Os testes laboratoriais serão realizados com amostras não identificadas e descartadas após seu uso. Segundo o autor a pesquisa com o DNA de tecido estocado não precisa de autorização, desde que seja mantido o anonimato do depositante. O teste de viabilidade e apoptose celular será realizado em cultura em placa, sendo adicionados os produtos de estudo (IGFBP7, insulina, IGF-1, IGF-2, EBIO, clotrimazol, AS605240, daunorubicina, vincristina, asparaginase, corticóide) e avaliação final será colorimétrica.

A quantificação da expressão gênica será por extração total de RNA e síntese de DNA e os mesmos primers utilizados para o PCR também serão usados no sequenciamento.

No segundo sub-projeto existe a proposta de seqüenciar o cDNA de IL-7R, e o domínio JH2 de Jak1 e Jak3, dos blastos leucêmicos de 50 casos de LLA-T (linhagem linfocitária - T). Os dados de polimorfismos do IL-7R serão comparados com frequências publicadas da população caucasiana. Além disso, pretende-se analisar a frequência dos mesmos polimorfismos em amostras de 40 indivíduos saudáveis da nossa população. Caso seja encontrada alguma mutação no IL-7R ou Jak, o cDNA mutante será clonado, assim como o receptor IL-2R, e ambos serão transfectados em células HEK293 e uma série de testes será realizada.

#### IV - COMENTÁRIOS DOS RELATORES

Após respostas às pendências, o projeto encontra-se adequadamente redigido e de acordo com a Resolução CNS/MS 196/96 e suas complementares, bem como o Termo de Consentimento Livre e Esclarecido.

#### V - PARECER DO CEP

O Comitê de Ética em Pesquisa da Faculdade de Ciências Médicas da UNICAMP, após acatar os pareceres dos membros-relatores previamente designados para o presente caso e atendendo todos os dispositivos das Resoluções 196/96 e complementares, resolve aprovar sem





restrições o Protocolo de Pesquisa, bem como ter aprovado o Termo do Consentimento Livre e Esclarecido, assim como todos os anexos incluídos na Pesquisa supracitada.

O conteúdo e as conclusões aqui apresentados são de responsabilidade exclusiva do CEP/FCM/UNICAMP e não representam a opinião da Universidade Estadual de Campinas nem a comprometem.

## VI - INFORMAÇÕES COMPLEMENTARES

O sujeito da pesquisa tem a liberdade de recusar-se a participar ou de retirar seu consentimento em qualquer fase da pesquisa, sem penalização alguma e sem prejuízo ao seu cuidado (Res. CNS 196/96 – Item IV.1.f) e deve receber uma cópia do Termo de Consentimento Livre e Esclarecido, na íntegra, por ele assinado (Item IV.2.d).

Pesquisador deve desenvolver a pesquisa conforme delineada no protocolo aprovado e descontinuar o estudo somente após análise das razões da descontinuidade pelo CEP que o aprovou (Res. CNS Item III.1.z), exceto quando perceber risco ou dano não previsto ao sujeito participante ou quando constatar a superioridade do regime oferecido a um dos grupos de pesquisa (Item V.3.).

O CEP deve ser informado de todos os efeitos adversos ou fatos relevantes que alterem o curso normal do estudo (Res. CNS Item V.4.). É papel do pesquisador assegurar medidas imediatas adequadas frente a evento adverso grave ocorrido (mesmo que tenha sido em outro centro) e enviar notificação ao CEP e à Agência Nacional de Vigilância Sanitária – ANVISA – junto com seu posicionamento.

Eventuais modificações ou emendas ao protocolo devem ser apresentadas ao CEP de forma clara e sucinta, identificando a parte do protocolo a ser modificada e suas justificativas. Em caso de projeto do Grupo I ou II apresentados anteriormente à ANVISA, o pesquisador ou patrocinador deve enviá-las também à mesma junto com o parecer aprovatório do CEP, para serem juntadas ao protocolo inicial (Res. 251/97, Item III.2.e)

Relatórios parciais e final devem ser apresentados ao CEP, de acordo com os prazos estabelecidos na Resolução CNS-MS 196/96.

## VII - DATA DA REUNIÃO

Homologado na I Reunião Ordinária do CEP/FCM, em 20 de janeiro de 2009.

*Profa. Dra. Carmem Sílvia Bertuzzo*  
PRESIDENTE DO COMITÊ DE ÉTICA EM PESQUISA  
FCM/UNICAMP

## 12.5 Animal ethics committee approval 1



CEEA/Unicamp

### Comissão de Ética na Experimentação Animal CEEA/Unicamp

#### CERTIFICADO

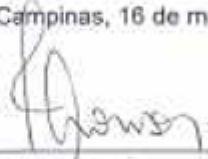
Certificamos que o Protocolo nº 1766-1, sobre "Estudo da via PI3K/AKT/mTOR na Leucemia Linfóide Aguda Pediátrica", sob a responsabilidade de Prof. Dr. José Andrés Yunes / Gilberto C. Franchi Jr., está de acordo com os Princípios Éticos na Experimentação Animal adotados pelo Colégio Brasileiro de Experimentação Animal (COBEA), tendo sido aprovado pela Comissão de Ética na Experimentação Animal – CEEA/Unicamp em 16 de março de 2009.

#### CERTIFICATE

We certify that the protocol nº 1766-1, entitled "Studies of PI3K/AKT/mTOR pathway in Pediatric Acute Lymphoblastic Leukemia", is in agreement with the Ethical Principles for Animal Research established by the Brazilian College for Animal Experimentation (COBEA). This project was approved by the institutional Committee for Ethics in Animal Research (State University of Campinas - Unicamp) on March 16, 2009.

Campinas, 16 de março de 2009.

  
Prof. Dra. Ana Maria A. Guaraldo  
Presidente

  
Fátima Alonso  
Secretária Executiva

CEEA – Unicamp  
Caixa Postal 6106  
13083-970 Campinas, SP – Brasil

Telefone: (19) 3821-6599  
E-mail: [comisa@unicamp.br](mailto:comisa@unicamp.br)  
<http://www.ib.unicamp.br/ceea/>

## 12.6 Animal ethics committee approval 2



Centro Infantil Boldrini  
CNPJ 50.046.887.0001/27  
Telefone 55 (19) 3787-5000

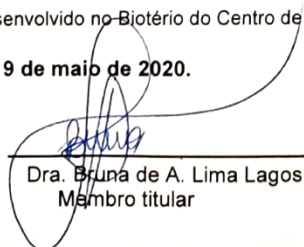
### CERTIFICADO


Certificamos que a proposta intitulada "**Ação de IGFBP7 sobre as vias TGF $\beta$ /p53 e a resistência aos corticoides na Leucemia Linfóide Aguda**", registrada com o n. **0006/2020**, sob a responsabilidade de **Prof Dr José Andres Yunes**, sendo como executores Leonardo Luís Artico, Juliana Ronchi Corrêa, Priscila Pini Zenatti e Ana Clara Lisi – que envolve a produção, manutenção ou utilização de animais pertencentes ao filo Chordata, subfilo Vertebrata (exceto humanos), para fins de pesquisa científica (ou ensino) – encontra-se de acordo com os preceitos da **Lei n. 11.794, de 8 de outubro de 2008, do Decreto n. 6.899, de 15 de julho de 2009**, e com as normas editadas pelo **Conselho Nacional de Controle de Experimentação Animal (CONCEA)**, foi aprovada pela **COMISSÃO DE ÉTICA NO USO DE ANIMAIS (CEUA – Boldrini) DO Centro de Pesquisa Boldrini**, em reunião de **18 de maio de 2020**.

Finalidade:	( ) Ensino (X) Pesquisa Científica	
Vigência do projeto:	20/05/2020 a 01/03/2024	
Vigência da autorização para manipulação de animal:	20/05/2020 a 01/03/2024	
Espécie/linhagem/raça	Espécie: <i>Mus musculus</i>	Quantidade de animais solicitados
	Linhagens:	
	STOCK Smad2 <sup>tm1.1Epb/J</sup>	30 fêmeas
	C57BL/6-J17 <sup>tm1(CPT)/J</sup>	15 machos
	B6.Cg-Commd10 <sup>Tg(Vav1-icre)A2Klo/J</sup>	30 machos
	C57BL/6J	50 machos ; 50 fêmeas
	NOD.Cg-Prkdc <sup>scid</sup> Il2rg <sup>tm1Wj/SzJ</sup>	100 fêmeas
Nº de animais:	695 (estima-se que 420 animais serão gerados nas proles G1 e G2)	
Peso / Idade:	20g / 60 dias	
Sexo:	Informado acima o número das respectivas linhagens	
Origem:	CEMIB / Unicamp e CPB	

A aprovação pela CEUA/Boldrini não dispensa autorização prévia junto ao IBAMA, SISBIO ou CIBio e é restrita a protocolos desenvolvidos no Biotério do Centro de Pesquisa Boldrini.

Campinas, 19 de maio de 2020.

  
Dra. Bruna de A. Lima Lagos  
Membro titular

  
Dr. Pedro de Campos Lima  
Suplente

Importante: Pedimos atenção ao prazo para envio do relatório final de atividades referente a este protocolo: até 30 dias o encerramento da sua vigência. O formulário encontra-se disponível na secretaria da CEUA-Boldrini. A não apresentação de relatório no prazo estabelecido impedirá que novos protocolos sejam submetidos.

## 12.7 Authorization to reproduce chapter 1

6/27/23, 10:19 PM



This is a License Agreement between LEONARDO LUIS ARTICO ("User") and Copyright Clearance Center, Inc. ("CCC") on behalf of the Rightsholder identified in the order details below. The license consists of the order details, the Marketplace Permissions General Terms and Conditions below, and any Rightsholder Terms and Conditions which are included below.

All payments must be made in full to CCC in accordance with the Marketplace Permissions General Terms and Conditions below.

<b>Order Date</b>	27-Jun-2023	<b>Type of Use</b>	Republish in a thesis/dissertation
<b>Order License ID</b>	1369944-1	<b>Publisher</b>	American Society of Hematology
<b>ISSN</b>	2473-9529	<b>Portion</b>	Main product

### LICENSED CONTENT

<b>Publication Title</b>	Blood Advances	<b>Country</b>	United States of America
<b>Author/Editor</b>	American Society of Hematology.	<b>Rightsholder</b>	Elsevier Science & Technology Journals
<b>Date</b>	12/01/2016	<b>Publication Type</b>	Journal
<b>Language</b>	English		

### REQUEST DETAILS

<b>Portion Type</b>	Main product	<b>Distribution</b>	Worldwide
<b>Number of Images / Photos / Illustrations</b>	N/A	<b>Translation</b>	Original language of publication
<b>Format (select all that apply)</b>	Electronic	<b>Copies for the Disabled?</b>	Yes
<b>Who Will Republish the Content?</b>	Academic institution	<b>Minor Editing Privileges?</b>	No
<b>Duration of Use</b>	Life of current edition	<b>Incidental Promotional Use?</b>	No
<b>Lifetime Unit Quantity</b>	Up to 499	<b>Currency</b>	USD
<b>Rights Requested</b>	Main product		

### NEW WORK DETAILS

<b>Title</b>	MECHANISTIC INSIGHTS INTO IGF1R-MEDIATED IGF1R ACTIVATION AND GLYCOLYTIC METABOLISM IN ACUTE LYMPHOBLASTIC LEUKEMIA	<b>Produced by</b>	UNICAMP
		<b>Expected Publication Date</b>	2023-08-18

6/27/23, 10:19 PM

Author LEONARDO LUIS Artico

## ADDITIONAL DETAILS

Order Reference Number	N/A	The Requesting Person/Organization to Appear on the License	LEONARDO LUIS ARTICO
------------------------	-----	---	----------------------

## REQUESTED CONTENT DETAILS

Title, Description or Numeric Reference of the Portion(s)	Main product	Title of the Article/Chapter the Portion Is From	Physiologic IGFBP7 levels prolong IGF1R activation in acute lymphoblastic leukemia
Editor of Portion(s)	N/A	Author of Portion(s)	American Society of Hematology.
Volume / Edition	5 (18)	Issue, if Republishing an Article From a Serial	N/A
Page or Page Range of Portion	3633–3646	Publication Date of Portion	2021-07-28

## RIGHTSHOLDER TERMS AND CONDITIONS

Elsevier publishes Open Access articles in both its Open Access journals and via its Open Access articles option in subscription journals, for which an author selects a user license permitting certain types of reuse without permission. Before proceeding please check if the article is Open Access on <http://www.sciencedirect.com> and refer to the user license for the individual article. Any reuse not included in the user license terms will require permission. You must always fully and appropriately credit the author and source. If any part of the material to be used (for example, figures) has appeared in the Elsevier publication for which you are seeking permission, with credit or acknowledgement to another source it is the responsibility of the user to ensure their reuse complies with the terms and conditions determined by the rights holder. Please contact [permissions@elsevier.com](mailto:permissions@elsevier.com) with any queries.

## Marketplace Permissions General Terms and Conditions

The following terms and conditions ("General Terms"), together with any applicable Publisher Terms and Conditions, govern User's use of Works pursuant to the Licenses granted by Copyright Clearance Center, Inc. ("CCC") on behalf of the applicable Rightsholders of such Works through CCC's applicable Marketplace transactional licensing services (each, a "Service").

1) **Definitions.** For purposes of these General Terms, the following definitions apply:

"License" is the licensed use the User obtains via the Marketplace platform in a particular licensing transaction, as set forth in the Order Confirmation.

"Order Confirmation" is the confirmation CCC provides to the User at the conclusion of each Marketplace transaction. "Order Confirmation Terms" are additional terms set forth on specific Order Confirmations not set forth in the General Terms that can include terms applicable to a particular CCC transactional licensing service and/or any Rightsholder-specific terms.

"Rightsholder(s)" are the holders of copyright rights in the Works for which a User obtains licenses via the Marketplace platform, which are displayed on specific Order Confirmations.



6/27/23, 10:19 PM

"Terms" means the terms and conditions set forth in these General Terms and any additional Order Confirmation Terms collectively.

"User" or "you" is the person or entity making the use granted under the relevant License. Where the person accepting the Terms on behalf of a User is a freelancer or other third party who the User authorized to accept the General Terms on the User's behalf, such person shall be deemed jointly a User for purposes of such Terms.

"Work(s)" are the copyright protected works described in relevant Order Confirmations.

**2)Description of Service.** CCC's Marketplace enables Users to obtain Licenses to use one or more Works in accordance with all relevant Terms. CCC grants Licenses as an agent on behalf of the copyright rightsholder identified in the relevant Order Confirmation.

**3)Applicability of Terms.** The Terms govern User's use of Works in connection with the relevant License. In the event of any conflict between General Terms and Order Confirmation Terms, the latter shall govern. User acknowledges that Rightsholders have complete discretion whether to grant any permission, and whether to place any limitations on any grant, and that CCC has no right to supersede or to modify any such discretionary act by a Rightsholder.

**4)Representations; Acceptance.** By using the Service, User represents and warrants that User has been duly authorized by the User to accept, and hereby does accept, all Terms.

**5)Scope of License; Limitations and Obligations.** All Works and all rights therein, including copyright rights, remain the sole and exclusive property of the Rightsholder. The License provides only those rights expressly set forth in the terms and conveys no other rights in any Works

**6)General Payment Terms.** User may pay at time of checkout by credit card or choose to be invoiced. If the User chooses to be invoiced, the User shall: (i) remit payments in the manner identified on specific invoices, (ii) unless otherwise specifically stated in an Order Confirmation or separate written agreement, Users shall remit payments upon receipt of the relevant invoice from CCC, either by delivery or notification of availability of the invoice via the Marketplace platform, and (iii) if the User does not pay the invoice within 30 days of receipt, the User may incur a service charge of 1.5% per month or the maximum rate allowed by applicable law, whichever is less. While User may exercise the rights in the License immediately upon receiving the Order Confirmation, the License is automatically revoked and is null and void, as if it had never been issued, if CCC does not receive complete payment on a timely basis.

**7)General Limits on Use.** Unless otherwise provided in the Order Confirmation, any grant of rights to User (i) involves only the rights set forth in the Terms and does not include subsequent or additional uses, (ii) is non-exclusive and non-transferable, and (iii) is subject to any and all limitations and restrictions (such as, but not limited to, limitations on duration of use or circulation) included in the Terms. Upon completion of the licensed use as set forth in the Order Confirmation, User shall either secure a new permission for further use of the Work(s) or immediately cease any new use of the Work(s) and shall render inaccessible (such as by deleting or by removing or severing links or other locators) any further copies of the Work. User may only make alterations to the Work if and as expressly set forth in the Order Confirmation. No Work may be used in any way that is unlawful, including without limitation if such use would violate applicable sanctions laws or regulations, would be defamatory, violate the rights of third parties (including such third parties' rights of copyright, privacy, publicity, or other tangible or intangible property), or is otherwise illegal, sexually explicit, or obscene. In addition, User may not conjoin a Work with any other material that may result in damage to the reputation of the Rightsholder. Any unlawful use will render any licenses hereunder null and void. User agrees to inform CCC if it becomes aware of any infringement of any rights in a Work and to cooperate with any reasonable request of CCC or the Rightsholder in connection therewith.

**8)Third Party Materials.** In the event that the material for which a License is sought includes third party materials (such as photographs, illustrations, graphs, inserts and similar materials) that are identified in such material as having been used by permission (or a similar indicator), User is responsible for identifying, and seeking separate licenses (under this Service, if available, or otherwise) for any of such third party materials; without a separate license, User may not use such third party materials via the License.

6/27/23, 10:19 PM

**9)Copyright Notice.** Use of proper copyright notice for a Work is required as a condition of any License granted under the Service. Unless otherwise provided in the Order Confirmation, a proper copyright notice will read substantially as follows: "Used with permission of [Rightsholder's name], from [Work's title, author, volume, edition number and year of copyright]; permission conveyed through Copyright Clearance Center, Inc." Such notice must be provided in a reasonably legible font size and must be placed either on a cover page or in another location that any person, upon gaining access to the material which is the subject of a permission, shall see, or in the case of republication Licenses, immediately adjacent to the Work as used (for example, as part of a by-line or footnote) or in the place where substantially all other credits or notices for the new work containing the republished Work are located. Failure to include the required notice results in loss to the Rightsholder and CCC, and the User shall be liable to pay liquidated damages for each such failure equal to twice the use fee specified in the Order Confirmation, in addition to the use fee itself and any other fees and charges specified.

**10)Indemnity.** User hereby indemnifies and agrees to defend the Rightsholder and CCC, and their respective employees and directors, against all claims, liability, damages, costs, and expenses, including legal fees and expenses, arising out of any use of a Work beyond the scope of the rights granted herein and in the Order Confirmation, or any use of a Work which has been altered in any unauthorized way by User, including claims of defamation or infringement of rights of copyright, publicity, privacy, or other tangible or intangible property.

**11)Limitation of Liability.** UNDER NO CIRCUMSTANCES WILL CCC OR THE RIGHTSHOLDER BE LIABLE FOR ANY DIRECT, INDIRECT, CONSEQUENTIAL, OR INCIDENTAL DAMAGES (INCLUDING WITHOUT LIMITATION DAMAGES FOR LOSS OF BUSINESS PROFITS OR INFORMATION, OR FOR BUSINESS INTERRUPTION) ARISING OUT OF THE USE OR INABILITY TO USE A WORK, EVEN IF ONE OR BOTH OF THEM HAS BEEN ADVISED OF THE POSSIBILITY OF SUCH DAMAGES. In any event, the total liability of the Rightsholder and CCC (including their respective employees and directors) shall not exceed the total amount actually paid by User for the relevant License. User assumes full liability for the actions and omissions of its principals, employees, agents, affiliates, successors, and assigns.

**12)Limited Warranties.** THE WORK(S) AND RIGHT(S) ARE PROVIDED "AS IS." CCC HAS THE RIGHT TO GRANT TO USER THE RIGHTS GRANTED IN THE ORDER CONFIRMATION DOCUMENT. CCC AND THE RIGHTSHOLDER DISCLAIM ALL OTHER WARRANTIES RELATING TO THE WORK(S) AND RIGHT(S), EITHER EXPRESS OR IMPLIED, INCLUDING WITHOUT LIMITATION IMPLIED WARRANTIES OF MERCHANTABILITY OR FITNESS FOR A PARTICULAR PURPOSE. ADDITIONAL RIGHTS MAY BE REQUIRED TO USE ILLUSTRATIONS, GRAPHS, PHOTOGRAPHS, ABSTRACTS, INSERTS, OR OTHER PORTIONS OF THE WORK (AS OPPOSED TO THE ENTIRE WORK) IN A MANNER CONTEMPLATED BY USER; USER UNDERSTANDS AND AGREES THAT NEITHER CCC NOR THE RIGHTSHOLDER MAY HAVE SUCH ADDITIONAL RIGHTS TO GRANT.

**13)Effect of Breach.** Any failure by User to pay any amount when due, or any use by User of a Work beyond the scope of the License set forth in the Order Confirmation and/or the Terms, shall be a material breach of such License. Any breach not cured within 10 days of written notice thereof shall result in immediate termination of such License without further notice. Any unauthorized (but licensable) use of a Work that is terminated immediately upon notice thereof may be liquidated by payment of the Rightsholder's ordinary license price therefor; any unauthorized (and unlicensable) use that is not terminated immediately for any reason (including, for example, because materials containing the Work cannot reasonably be recalled) will be subject to all remedies available at law or in equity, but in no event to a payment of less than three times the Rightsholder's ordinary license price for the most closely analogous licensable use plus Rightsholder's and/or CCC's costs and expenses incurred in collecting such payment.

**14)Additional Terms for Specific Products and Services.** If a User is making one of the uses described in this Section 14, the additional terms and conditions apply:

**a)Print Uses of Academic Course Content and Materials (photocopies for academic coursepacks or classroom handouts).** For photocopies for academic coursepacks or classroom handouts the following additional terms apply:

i)The copies and anthologies created under this License may be made and assembled by faculty members individually or at their request by on-campus bookstores or copy centers, or by off-campus copy shops and other similar entities.

ii)No License granted shall in any way: (i) include any right by User to create a substantively non-identical copy of



6/27/23, 10:19 PM

the Work or to edit or in any other way modify the Work (except by means of deleting material immediately preceding or following the entire portion of the Work copied) (ii) permit "publishing ventures" where any particular anthology would be systematically marketed at multiple institutions.

iii) Subject to any Publisher Terms (and notwithstanding any apparent contradiction in the Order Confirmation arising from data provided by User), any use authorized under the academic pay-per-use service is limited as follows:

A) any License granted shall apply to only one class (bearing a unique identifier as assigned by the institution, and thereby including all sections or other subparts of the class) at one institution;

B) use is limited to not more than 25% of the text of a book or of the items in a published collection of essays, poems or articles;

C) use is limited to no more than the greater of (a) 25% of the text of an issue of a journal or other periodical or (b) two articles from such an issue;

D) no User may sell or distribute any particular anthology, whether photocopied or electronic, at more than one institution of learning;

E) in the case of a photocopy permission, no materials may be entered into electronic memory by User except in order to produce an identical copy of a Work before or during the academic term (or analogous period) as to which any particular permission is granted. In the event that User shall choose to retain materials that are the subject of a photocopy permission in electronic memory for purposes of producing identical copies more than one day after such retention (but still within the scope of any permission granted), User must notify CCC of such fact in the applicable permission request and such retention shall constitute one copy actually sold for purposes of calculating permission fees due; and

F) any permission granted shall expire at the end of the class. No permission granted shall in any way include any right by User to create a substantively non-identical copy of the Work or to edit or in any other way modify the Work (except by means of deleting material immediately preceding or following the entire portion of the Work copied).

iv) Books and Records; Right to Audit. As to each permission granted under the academic pay-per-use Service, User shall maintain for at least four full calendar years books and records sufficient for CCC to determine the numbers of copies made by User under such permission. CCC and any representatives it may designate shall have the right to audit such books and records at any time during User's ordinary business hours, upon two days' prior notice. If any such audit shall determine that User shall have underpaid for, or underreported, any photocopies sold or by three percent (3%) or more, then User shall bear all the costs of any such audit; otherwise, CCC shall bear the costs of any such audit. Any amount determined by such audit to have been underpaid by User shall immediately be paid to CCC by User, together with interest thereon at the rate of 10% per annum from the date such amount was originally due. The provisions of this paragraph shall survive the termination of this License for any reason.

**b) Digital Pay-Per-Uses of Academic Course Content and Materials (e-coursepacks, electronic reserves, learning management systems, academic institution intranets).** For uses in e-coursepacks, posts in electronic reserves, posts in learning management systems, or posts on academic institution intranets, the following additional terms apply:

i) The pay-per-uses subject to this Section 14(b) include:

**A) Posting e-reserves, course management systems, e-coursepacks for text-based content,** which grants authorizations to import requested material in electronic format, and allows electronic access to this material to members of a designated college or university class, under the direction of an instructor designated by the college or university, accessible only under appropriate electronic controls (e.g., password);



**B)Posting e-reserves, course management systems, e-coursepacks for material consisting of photographs or other still images not embedded in text**, which grants not only the authorizations described in Section 14(b)(i)(A) above, but also the following authorization: to include the requested material in course materials for use consistent with Section 14(b)(i)(A) above, including any necessary resizing, reformatting or modification of the resolution of such requested material (provided that such modification does not alter the underlying editorial content or meaning of the requested material, and provided that the resulting modified content is used solely within the scope of, and in a manner consistent with, the particular authorization described in the Order Confirmation and the Terms), but not including any other form of manipulation, alteration or editing of the requested material;

**C)Posting e-reserves, course management systems, e-coursepacks or other academic distribution for audiovisual content**, which grants not only the authorizations described in Section 14(b)(i)(A) above, but also the following authorizations: (i) to include the requested material in course materials for use consistent with Section 14(b)(i)(A) above; (ii) to display and perform the requested material to such members of such class in the physical classroom or remotely by means of streaming media or other video formats; and (iii) to "clip" or reformat the requested material for purposes of time or content management or ease of delivery, provided that such "clipping" or reformatting does not alter the underlying editorial content or meaning of the requested material and that the resulting material is used solely within the scope of, and in a manner consistent with, the particular authorization described in the Order Confirmation and the Terms. Unless expressly set forth in the relevant Order Confirmation, the License does not authorize any other form of manipulation, alteration or editing of the requested material.

ii)Unless expressly set forth in the relevant Order Confirmation, no License granted shall in any way: (i) include any right by User to create a substantively non-identical copy of the Work or to edit or in any other way modify the Work (except by means of deleting material immediately preceding or following the entire portion of the Work copied or, in the case of Works subject to Sections 14(b)(1)(B) or (C) above, as described in such Sections) (ii) permit "publishing ventures" where any particular course materials would be systematically marketed at multiple institutions.

iii)Subject to any further limitations determined in the Rightsholder Terms (and notwithstanding any apparent contradiction in the Order Confirmation arising from data provided by User), any use authorized under the electronic course content pay-per-use service is limited as follows:

A)any License granted shall apply to only one class (bearing a unique identifier as assigned by the institution, and thereby including all sections or other subparts of the class) at one institution;

B)use is limited to not more than 25% of the text of a book or of the items in a published collection of essays, poems or articles;

C)use is limited to not more than the greater of (a) 25% of the text of an issue of a journal or other periodical or (b) two articles from such an issue;

D)no User may sell or distribute any particular materials, whether photocopied or electronic, at more than one institution of learning;

E)electronic access to material which is the subject of an electronic-use permission must be limited by means of electronic password, student identification or other control permitting access solely to students and instructors in the class;

F)User must ensure (through use of an electronic cover page or other appropriate means) that any person, upon gaining electronic access to the material, which is the subject of a permission, shall see:

- a proper copyright notice, identifying the Rightsholder in whose name CCC has granted permission,
- a statement to the effect that such copy was made pursuant to permission,

6/27/23, 10:19 PM

- o a statement identifying the class to which the material applies and notifying the reader that the material has been made available electronically solely for use in the class, and
- o a statement to the effect that the material may not be further distributed to any person outside the class, whether by copying or by transmission and whether electronically or in paper form, and User must also ensure that such cover page or other means will print out in the event that the person accessing the material chooses to print out the material or any part thereof.

G) any permission granted shall expire at the end of the class and, absent some other form of authorization, User is thereupon required to delete the applicable material from any electronic storage or to block electronic access to the applicable material.

iv) Uses of separate portions of a Work, even if they are to be included in the same course material or the same university or college class, require separate permissions under the electronic course content pay-per-use Service. Unless otherwise provided in the Order Confirmation, any grant of rights to User is limited to use completed no later than the end of the academic term (or analogous period) as to which any particular permission is granted.

v) Books and Records; Right to Audit. As to each permission granted under the electronic course content Service, User shall maintain for at least four full calendar years books and records sufficient for CCC to determine the numbers of copies made by User under such permission. CCC and any representatives it may designate shall have the right to audit such books and records at any time during User's ordinary business hours, upon two days' prior notice. If any such audit shall determine that User shall have underpaid for, or underreported, any electronic copies used by three percent (3%) or more, then User shall bear all the costs of any such audit; otherwise, CCC shall bear the costs of any such audit. Any amount determined by such audit to have been underpaid by User shall immediately be paid to CCC by User, together with interest thereon at the rate of 10% per annum from the date such amount was originally due. The provisions of this paragraph shall survive the termination of this license for any reason.

**c) Pay-Per-Use Permissions for Certain Reproductions (Academic photocopies for library reserves and interlibrary loan reporting) (Non-academic internal/external business uses and commercial document delivery).** The License expressly excludes the uses listed in Section (c)(i)-(v) below (which must be subject to separate license from the applicable Rightsholder) for: academic photocopies for library reserves and interlibrary loan reporting; and non-academic internal/external business uses and commercial document delivery.

- i) electronic storage of any reproduction (whether in plain-text, PDF, or any other format) other than on a transitory basis;
- ii) the input of Works or reproductions thereof into any computerized database;
- iii) reproduction of an entire Work (cover-to-cover copying) except where the Work is a single article;
- iv) reproduction for resale to anyone other than a specific customer of User;
- v) republication in any different form. Please obtain authorizations for these uses through other CCC services or directly from the rightsholder.

Any license granted is further limited as set forth in any restrictions included in the Order Confirmation and/or in these Terms.

**d) Electronic Reproductions in Online Environments (Non-Academic-email, intranet, internet and extranet).** For "electronic reproductions", which generally includes e-mail use (including instant messaging or other electronic transmission to a defined group of recipients) or posting on an intranet, extranet or Intranet site (including any display or performance incidental thereto), the following additional terms apply:

- i) Unless otherwise set forth in the Order Confirmation, the License is limited to use completed within 30 days for

6/27/23, 10:19 PM

any use on the Internet, 60 days for any use on an intranet or extranet and one year for any other use, all as measured from the "republishing date" as identified in the Order Confirmation, if any, and otherwise from the date of the Order Confirmation.

ii) User may not make or permit any alterations to the Work, unless expressly set forth in the Order Confirmation (after request by User and approval by Rightsholder); provided, however, that a Work consisting of photographs or other still images not embedded in text may, if necessary, be resized, reformatted or have its resolution modified without additional express permission, and a Work consisting of audiovisual content may, if necessary, be "clipped" or reformatted for purposes of time or content management or ease of delivery (provided that any such resizing, reformatting, resolution modification or "clipping" does not alter the underlying editorial content or meaning of the Work used, and that the resulting material is used solely within the scope of, and in a manner consistent with, the particular License described in the Order Confirmation and the Terms.

#### 15) Miscellaneous.

a) User acknowledges that CCC may, from time to time, make changes or additions to the Service or to the Terms, and that Rightsholder may make changes or additions to the Rightsholder Terms. Such updated Terms will replace the prior terms and conditions in the order workflow and shall be effective as to any subsequent Licenses but shall not apply to Licenses already granted and paid for under a prior set of terms.

b) Use of User-related information collected through the Service is governed by CCC's privacy policy, available online at [www.copyright.com/about/privacy-policy/](http://www.copyright.com/about/privacy-policy/).

c) The License is personal to User. Therefore, User may not assign or transfer to any other person (whether a natural person or an organization of any kind) the License or any rights granted thereunder; provided, however, that, where applicable, User may assign such License in its entirety on written notice to CCC in the event of a transfer of all or substantially all of User's rights in any new material which includes the Work(s) licensed under this Service.

d) No amendment or waiver of any Terms is binding unless set forth in writing and signed by the appropriate parties, including, where applicable, the Rightsholder. The Rightsholder and CCC hereby object to any terms contained in any writing prepared by or on behalf of the User or its principals, employees, agents or affiliates and purporting to govern or otherwise relate to the License described in the Order Confirmation, which terms are in any way inconsistent with any Terms set forth in the Order Confirmation, and/or in CCC's standard operating procedures, whether such writing is prepared prior to, simultaneously with or subsequent to the Order Confirmation, and whether such writing appears on a copy of the Order Confirmation or in a separate instrument.

e) The License described in the Order Confirmation shall be governed by and construed under the law of the State of New York, USA, without regard to the principles thereof of conflicts of law. Any case, controversy, suit, action, or proceeding arising out of, in connection with, or related to such License shall be brought, at CCC's sole discretion, in any federal or state court located in the County of New York, State of New York, USA, or in any federal or state court whose geographical jurisdiction covers the location of the Rightsholder set forth in the Order Confirmation. The parties expressly submit to the personal jurisdiction and venue of each such federal or state court.

*Last updated October 2022*

## 12.8 Authorization to reproduce chapter 2

Gmail - [IJMS] Manuscript ID: ijms-2357332 - Accepted for Publication

6/25/23, 4:04 PM



Leonardo Artico <lla.unicamp2017@gmail.com>

---

### [IJMS] Manuscript ID: ijms-2357332 - Accepted for Publication

---

Ms. Andreea Margareta Sinka <sinka@mdpi.com>

Tue, Jun 20, 2023 at 5:45 AM

To: Leonardo Artico <lla.unicamp2017@gmail.com>, IJMS Editorial Office <ijms@mdpi.com>

Dear Dr. Artico,

Thank you very much for your email.

MDPI is an Open-Access Publisher, which means that everyone is free to re-use the published material if proper accreditation/citation of the original publication is given.

No special permission is required to reuse all or part of article published by MDPI, including figures and tables. For articles published under an open access Creative Common CC BY license, any part of the article may be reused without permission provided that the original article is clearly cited. Reuse of an article does not imply endorsement by the authors or MDPI.

Please feel free to use the published data in your PhD thesis, just make sure to cite the paper appropriately (see citation recommended on the webpage of the published paper).

Kind regards,

Ms. Andreea Sinka  
Assistant Editor

MDPI Open Access Publishing Romania SRL  
Str. Avram Iancu 454  
407280 Floresti, Cluj  
Romania  
Tel. +40 364 150 134  
[www.mdpi.com](http://www.mdpi.com)

## 12.9 Copyright statement

### Statement

The copies of scientific articles authored by me or co-authored by me, already published or submitted for publication in peer-reviewed scientific journals or conference proceedings, which are included in my doctoral thesis titled "MECHANISTIC INSIGHTS INTO IGFBP7-MEDIATED IGF1R ACTIVATION AND GLYCOLYTIC METABOLISM IN ACUTE LYMPHOBLASTIC LEUKEMIA," do not infringe upon the provisions of Law No. 9,610/98, nor the copyright of any publisher.

Campinas, August 18, 2023

Signature: 

Author's name: Leonardo Luís Artico

ID: 6090474633

Signature: 

Advisor name: José Andrés Yunes

ID: 541346374